



SCHOOL of
GRADUATE STUDIES
EAST TENNESSEE STATE UNIVERSITY

East Tennessee State University
Digital Commons @ East
Tennessee State University

Electronic Theses and Dissertations

Student Works

5-2012

Prelamin A Influences a Program of Gene Expression In Regulation of Cell Cycle Control

Christina N. Bridges

East Tennessee State University

Follow this and additional works at: <https://dc.etsu.edu/etd>



Part of the [Biological Phenomena, Cell Phenomena, and Immunity Commons](#)

Recommended Citation

Bridges, Christina N., "Prelamin A Influences a Program of Gene Expression In Regulation of Cell Cycle Control" (2012). *Electronic Theses and Dissertations*. Paper 1213. <https://dc.etsu.edu/etd/1213>

This Dissertation - Open Access is brought to you for free and open access by the Student Works at Digital Commons @ East Tennessee State University. It has been accepted for inclusion in Electronic Theses and Dissertations by an authorized administrator of Digital Commons @ East Tennessee State University. For more information, please contact digilib@etsu.edu.

Prelamin A Influences a Program of Gene Expression
in the Regulation of Cell Cycle Control

A dissertation

presented to

the faculty of the Department of Biochemistry & Molecular Biology
East Tennessee State University

In partial fulfillment

of the requirements for the degree

Doctor of Philosophy in Biomedical Sciences

by

Christina Norton Bridges

May 2012

Antonio E. Rusiñol, Chair

Douglas P. Thewke

Sharon E. Campbell

Deling Yin

Robert V. Schoborg

Keywords: Prelamin A, Lamin A, Cell Cycle, Quiescence, Senescence, FoxO, p27,
Progeria, Pin1

ABSTRACT

Prelamin A Influences a Program of Gene Expression

In Regulation of Cell Cycle Control

by

Christina Norton Bridges

The A-type lamins are intermediate filament proteins that constitute a major part of the eukaryotic nuclear lamina—a tough, polymerized, mesh lining of the inner nuclear membrane, providing shape and structural integrity to the nucleus. Lamin A (LA) filaments also permeate the nucleoplasm, providing additional structural support, but also scaffolding numerous tethered molecules to stabilize, organize, and facilitate molecular interactions to accomplish critical functions of cellular metabolism. Over the past 2 decades, much attention has been focused on roles of LA in maintenance of nuclear structural integrity. Only since the late 1990s have scientists discovered the devastating effects of LA gene (LMNA) mutations, as they have associated hundreds of LMNA mutations to a large group of diseases, called laminopathies, with a broad spectrum of phenotypes, ranging from skeletal, muscular, and neurological defects, to defective lipid storage, to accelerated aging phenotypes in diseases called progerias. Recent advances demonstrate LA regulatory functions include cell signaling, cell cycle regulation, transcription, chromatin organization, viral egress, and DNA damage repair. Amidst the flurry of fascinating research, only recently have researchers begun to focus attention on the different isoforms that exist for LA, a precursor form among them. LA is initially synthesized as Prelamin A (PreA), and undergoes a series of modifications that

truncate the protein to produce “mature” LA. Existence of the precursor form, and its complex maturation pathway, have puzzled researchers since their realization. With a pattern of expression related to cell cycle phase, we hypothesized a role for PreA in cell cycle control. To investigate, we have performed array studies to assess gene expression effects at the levels of transcript expression, protein expression, and phosphorylation modification status. Here, we present evidence for a PreA-mediated program of cell cycle regulatory gene and protein expression modulation. Implicated pathways include RB-E2F, p53, p27^{Kip1}, FoxOs, p300, and the Cyclins, with additional evidence indicating a role for the Pin1 prolyl isomerase in mediating PreA regulation of the cell cycle.

Copyright 2012 by Christina N. Bridges, All Rights Reserved

DEDICATION

Dedicated to Doris Worley Norton and Mary Jane Charlson

To my mother Doris and to Mary Jane, both so beloved to me:

Being the recipient of the love, support, and guidance of two such strong, nurturing, beautiful, kind, generous women has been a blessing in my life beyond imagination. The two of you have made me the person that I am, each by showing me the person I want to become. Thank you both, so much, for everything.

In memoriam: Doris Worley Norton (September 1, 1955 - August 19, 1992)

And as I humbly dedicate everything in my life to God, without headlines or banners, this goes, as well, and I give Him thanks for His many blessings upon me, not the least of which is the gift of the love of my soulmate and husband, Andy, who, by some miracle, has managed to stay with me through these years of the insanity that have been graduate school. *Here's to getting on with life and love...*

ACKNOWLEDGEMENTS

This work was supported by grants from the NIH (1R15HL091502-01A1), East Tennessee State University, and the Progeria Foundation to Antonio Rusiñol and Michael Sinensky. I wish to express my gratitude to Dr. Rusiñol and Dr. Sinensky and these organizations for funding of this work. I would also like to thank the ETSU Biomedical Sciences Graduate Program for funding and support to me. I appreciate Dr. Yaping Zong at Fullmoon Biosciences for providing helpful analysis of data from antibody arrays. Also, I would like to thank Dr. Francis Collins, Director, NIH, and Dr. Robert Goldman, Northwestern University, for providing plasmids used in this project.

Grateful Acknowledgement Goes to:

Michael Stephan Sinensky: For starting this project, for funding, for amazing pioneering work in the field, and finally, for inspiration. Thank you, Dr. Sinensky!

For patience and guidance:

My Graduate Committee: Antonio E. Rusiñol, Douglas P. Thewke, Sharon E. Campbell, Robert V. Schoborg, and Deling Yin

For thoughtful academic discussion, assistance, and expertise:

Michael Sinensky, Philip Musich, and Yue Zou

For endless moral support along the way:

Mitchell Robinson, Beverly Sherwood, Angela Thompson, Karen Ford, Judy Branson, Brian Rowe, Barbara Turner, Scott Champney, David Johnson, and Jack Rary

And for technical assistance and discussions, with a big dose of friendship:

Lia Lerner,* Jessica Keasler,* Courtney Netherland, Ben Hilton, Rhesa Dykes, Jaime Parman-Ryans, Theresa Pickle, and Hui Tang

**Lia & Jessica performed essential laboratory experiments for this project*

And finally, my thanks to the Fullerton Genetics Laboratory, Asheville, NC, for allowing me to perform a multitude of sequencing experiments there and for providing me with unbelievable flexibility as an employee while I have pursued this degree, not to mention the compassion and moral support of a wonderful group of friends.

CONTENTS

	Page
ABSTRACT	2
DEDICATION	5
ACKNOWLEDGEMENTS	6
LIST OF TABLES	13
LIST OF FIGURES	14
LIST OF ABBREVIATIONS	17
Chapter	
1. INTRODUCTION	23
The Nuclear Lamins	23
Posttranslational Lamin Processing	24
The Laminopathies	26
Lamin A Structural Functions	29
Lamin A Nonstructural Functions	31
Lamin A Functions in Cell Cycle Regulation	31
Aims of this Study	34
2. MATERIALS AND METHODS	36
Materials	36
General Laboratory Chemicals, Buffers, Reagents	36
Enzymes, Kits	37
General Laboratory Supplies and Equipment	38
Materials Used in Cloning/Subcloning and Bacterial Cell Culture	39
Plasmids and Oligonucleotides	39
Transfection Reagents	41
Antibodies	41
Mammalian Cell Culture	42

Chapter	Page
Buffers.....	42
Software.....	43
Methods I.: Molecular Biology Methods.....	43
Preparation and Purification of Plasmid DNA from Bacteria.....	43
Digestion of DNA with Restriction Endonucleases.....	44
Polymerase Chain Reaction (PCR).....	44
Automated DNA Cycle Sequencing.....	44
Site-Directed Mutagenesis of DNA.....	45
DNA Gel Electrophoresis.....	47
Purification of DNA Fragments from Agarose.....	47
Precipitation of DNA.....	48
Cloning and Subcloning of DNA.....	48
Restriction Enzyme-Based Subcloning.....	48
PCR-Based Cloning/Subcloning.....	49
DNA Ligation.....	49
Transfection of Mammalian Cells.....	50
Transient Transfections.....	50
Stable Transfections.....	51
Cotransfection.....	51
Methods II.: Protein Chemistry and Biochemistry Methods.....	52
Preparation of Mammalian Cell Lysates.....	52
Cellular Compartment Lysate Fraction Preparation.....	53
Electrophoretic Separation of Proteins.....	53
Protein Blotting.....	54
Immunodetection (Western Blotting).....	54
Zmpste24 Protease Activity Assay.....	55

Chapter	Page
Peptide Phosphorylation Residue Mapping by Edman Degradation	56
Preparation of Cell Extracts for Mass Spectrophotometry	57
Methods III.: Cell Biology Methods	57
Cell Culture-General Cell Culture Techniques	57
Induction of RheoSwitch Expression System	59
Indirect Immunofluorescence and Protein-Protein Co-Localization in Mammalian Cells	59
Cell Cycle Manipulation.....	60
Cell Cycle Analysis Methods	60
Cell Cycle Analysis by Flow Cytometry	60
Assay of Cellular Proliferation by BrdU Incorporation	61
Assay of Cellular Proliferation by Incorporation of [³ H]-Thymidine.....	62
Assay of Cellular Proliferation by Detection of Ki-67.....	62
Methods IV.: Gene Expression Analysis Methods	62
Whole Genome Exon Transcript Microarray	62
Cell Cycle Pathway-Focused RT-qPCR Array	65
Cell Cycle Control Pathway-Specific Antibody Array (Protein Array)	69
Peptidyl Prolyl Isomerase (Pin1) Inhibition with Juglone	71
Lamin A Multi-Isoform Motif Analysis	71
3. RESULTS	73
Prelamin A Expression is Detected In Cell Cycle Arrest.....	73
Accumulated Prelamin A is Farnesylated and Carboxymethylated	75
Zmpste24 Expression Level Does Not Parallel Activity Levels in Quiescent Cells	76
Overexpression of Zmpste24 Leads to Bypass of Quiescence	80
Development of Uncleavable PreA Expression Construct.....	82

Chapter	Page
Effects of Accumulated PreA on Global Gene Expression by Microarray Analysis	83
Ingenuity Pathways™ Analysis: Physiological Function Analysis	84
Ingenuity Pathways™ Analysis: Canonical Pathways Analysis.....	86
Ingenuity Pathways™ Analysis: Integrated Pathway/Network Analysis ..	91
Development of a Model System of Inducible, Stable Lamin Isoform Expression Cell Lines	95
Effects of Uncleavable PreA (L647R PreA) Expression on Cell Cycle Progression	104
Effects of Accumulated PreA on Cell Cycle Pathway-Specific Gene- Expression (by RT-qPCR Array)	107
Cyclins, Cyclin Dependent Kinases (CDKs), Cyclin Dependent Kinase Inhibitors (CKIs)	111
Kinases (Non-Cyclin-Dependent) and Phosphatases	115
Transcription Factors and Associated Genes.....	121
DNA Damage-Related Genes	127
Genes Associated with Cell Structure and Integrity/Chromatin/ Chromosome Organization and Maintenance/Mitotic Assembly	129
Effects of Accumulated PreA on Cell Cycle Control-Specific Protein Expression and Phosphorylation Assay by Antibody Array	131
Cross Referencing Transcript Expression and Protein Expression	137
Significantly Altered Expression of Key Cell Cycle Proteins	138
Motif Analysis of LA Isoforms	144
Kinase Substrate Motifs in PreA.....	145
Phosphorylation of the PreA C-Terminus.....	149
Phosphorylation-Dependent Protein Binding Motifs in the PreA C-Terminus	152

Chapter	Page
Cross-Reference of Kinase Substrate Sites and Kinase-Dependent Protein Motif-Binding Sites	156
Cross-Reference of Genes/Proteins with Altered Expression vs. Motif Analysis Findings	157
WW Domain Proteins (Pin1)	158
Colmunoprecipitation of Pin1 with L647R PreA	162
Pin1 Target Expression in Cells Expressing L647R PreA (FoxOs/p27 ^{Kip1}) ..	165
Nuclear Localization of FoxO3a and p27 ^{Kip1} with L647R PreA Expression..	169
Pin1 Inhibition Mimics L647R PreA Effect on FoxOs p27 ^{Kip1} in Uninduced Cells	172
Pin1 Overexpression Reverses L647R PreA Effect on FoxOs and p27 ^{Kip1} .	175
Senescence Develops in L647R PreA Expressing Cells	177
Results Summary	179
4. DISCUSSION	180
Cell Cycle Related Expression of PreA	180
Prelamin A Expression is Cell Cycle Stage-Specific, Related to Arrest ..	180
Accumulated PreA is Related to Decreased Zmpste24 Activity	181
Overexpression of PreA Inhibits Cell Cycle Progression	182
Motif Analysis Suggests Modes of PreA Interaction with Cell Cycle Regulators.....	182
Pin1 as a Lamin-Binding Protein	184
PreA Expression Alters the Cellular Gene Expression Profile	187
Investigation Using Uncleavable Prelamin A Expression Construct.....	187
Cell Cycle Control-Related Pathways Affected by L647R Expression	189
AHR Pathway	189
RB-E2F Pathway.....	193

Chapter	Page
p300 and Cyclin E Pathway	197
FoxO Pathway.....	200
p53 Pathway	204
mTOR Pathway & p53	207
Conclusions.....	214
REFERENCES.....	217
APPENDICES	263
Appendix A: Full SABiosciences RT-qPCR Gene List/Array Data.....	263
Appendix B: Volcano Plot of RT-qPCR Data	267
Appendix C: Supplemental Motif Analysis Data: HPRD Survey of Kinase Substrate Sites in Lamin A Peptide Sequence.....	268
Appendix D: Supplemental Motif Analysis Data: HPRD Survey of Kinase Dependent Protein Motif-Binding Sites in Lamin A Peptide Sequence ...	278
Appendix E: WW Domain-Containing Nuclear Proteins (HPRD)	279
VITA	283

LIST OF TABLES

Table	Page
1. The Canonical Pathway Analysis™	87
2. Cell Cycle-Related Genes Demonstrating Statistically Significant Altered Expression in Response to L647R PreA Induction	110
3. Results of Antibody Array: Changes in Protein Expression and Phosphorylation	134
4. Prelamin A C-terminus Serine/Threonine Kinase Substrate Motif Analysis..	148
5. Serine/Threonine Kinase Dependent Protein Domain Binding Motifs Within the PreA C-Terminal Fragment	153

LIST OF FIGURES

Figure	Page
1. Maturation of Lamin A Protein by Proteolytic PostTranslational Processing	25
2. Structure and Domain Arrangement of Lamin A Protein	28
3. Lamin A at Nuclear Envelope and throughout Nucleoplasm	30
4. Accumulation of Prelamin A as Cells Enter Quiescence	74
5. Mass Spectrometry Analysis Reveals Accumulated Prelamin A is Farnesyl-Carboxymethylated (FC'd).....	75
6. Zmpste24 Activity Decreases Parallel to the Rate of Cellular Proliferation as Serum Starvation Induces Quiescence.....	77
7. Zmpste24 Expression and Proteolytic Activity Do Not Decrease at the Same Rate with Induction of Quiescence	78
8. Zmpste24-Overexpressing Cells Bypass Cell Cycle Exit under Quiescence-Inducing Conditions	81
9. Cells Overexpressing Zmpste24 Bypass Quiescence	82
10. Ingenuity Pathways Analysis™ “Functional Analysis”	85
11. Ingenuity Pathways Analysis™ Pathways Demonstrating Statistically Significant Gene Expression Regulation.....	88
12. Ingenuity Pathways Analysis™ Pathways Demonstrating the Highest Level of Impact from L647R PreA Expression	90
13. Ingenuity Pathways Analysis™ GeneNetwork1 (with L647R PreA Expression): G1/S Checkpoint Regulation Part 1	92
14. Ingenuity Pathways Analysis™ GeneNetwork2 (with L647R PreA Expression): G1/S Checkpoint Regulation Part 2	93
15. Ingenuity Pathways Analysis™ GeneNetwork 3 (with L647R PreA Expression): p53 Signaling Regulation	94
16. Ingenuity Pathways Analysis™ GeneNetwork 4 (with L647R PreA Expression): AHR-RB-p300 Control of E2F Transcription	95

17.	The RheoSwitch® Mammalian Dual Vector Inducible Expression System.	96
18.	Evaluation of Induced Recombinant Protein Expression in the Rheoswitch® Lamin Isoform-Construct Expression Model System (GFP)	100
19.	Immunostaining of EGFP-L647R Lamin A (PreA) with Antibody to GFP ...	101
20.	Immunoblotting of Expressed Lamin Isoforms Using the Rheoswitch Inducible Expression System	102
21.	Mass Spectroscopy Demonstrates RheoSwitch® Model L647R PreA Recombinant Protein Expressed is FC-PreA.....	103
22.	Decreased Rate of Cellular Proliferation in L647R PreA-Expressing Cells (BrdU Incorporation Assay)	104
23.	Decreased Rate of Cellular Proliferation in L647R PreA-Expressing Cells (Flow Cytometry and Ki67 Immunofluorescent Stain Assay)	106
24.	L647R Effects on Gene Expression (RT-qPCR Assay of Transcript Expression): Cyclins, CDKs, CKIs	113
25.	L647R Effects on Gene Expression (RT-qPCR Assay of Transcript Expression): Kinases & Phosphatases	116
26.	L647R Effects on Gene Expression (RT-qPCR Assay of Transcript Expression): Transcription Factors & Related Genes.....	122
27.	L647R Effects on Gene Expression (RT-qPCR Assay of Transcript Expression): DNA Damage-Related Genes	128
28.	L647R Effects on Gene Expression (RT-qPCR Assay of Transcript Expression): Genes Involved in Chromosomal/Nuclear/Cellular Integrity or Microtubule/Mitotic Assembly.....	130
29.	Lamin A C-terminal 66 Amino Acid Fragment Considered In Motif Analysis	147
30.	Phosphorylation Sites on Lamin A Protein (Compilation Graphic) with Functional Indications	150
31.	Radiolabeled Phosphorylated Peptide Mapping of Lamin A C-Terminus..	151
32.	Arrangement of Phosphorylation-Dependent Protein Motif Binding Sites in the PreA C-Terminal 66 Residue Fragment	155

33.	Combined Graphic of Kinase Substrate Motifs/Protein Motif Binding Sites in PreA C-Terminus.....	157
34.	Pin1 Targets and Molecular Mechanisms	160
35.	Colmunoprecipitation of Pin1 Protein with EGFP-L647R PreA	162
36.	Immunostaining of Pin1 Protein in L647R PreA-Expressing Cells	164
37.	Immunstaining of FoxO3a Protein in EGFP-L647R PreA-Expressing Cells and Colocalization with GFP	170
38.	Increased Expression and Nuclear Translocation of FoxO3a and p27 ^{Kip1} with L647R PreA Expression	171
39.	Pin1 Inhibition by Juglone Treatment Mimics L647R PreA Effects in Uninduced Cells, Leads to FoxO3a Nuclear Localization	173
40.	Pin1 Inhibition By Juglone Treatment Mimics L647R PreA Effects in Uninduced Cells, Results in Increased P27 ^{Kip1} Expression and Nuclear Localization	174
41.	Overexpression Of GST-Pin1 in Induced L647R PreA-Expressing Cells Reverses L647R PreA-Mediated Nuclear of Localization FoxO3	176
42.	Diminished p27 Expression is Evident upon Overexpression of GST-Pin1	177
43.	Senescence Assay of L647R PreA-Expressing Cells (β -galactosidase Assay)	183
44.	Discussion Graphic: mTOR Pathway and Proposed Pathway Inhibitory Effects of PreA Expression and Putative Pin Sequestration	213

LIST OF ABBREVIATIONS*

1°	Primary
2°	Secondary
ANOVA	Analysis of Variance
A-WS	Atypical Werner Syndrome
BJ	Human foreskin fibroblast cells
BNPS	3-bromo-3-methyl-2-l(2-nitrophenyl)thiol-3H indole (BNPS-skatole)
BCA	Bicinchoninic acid
bp	Base pair
BrdU	Bromo-deoxy-Uridine
BSA	Bovine serum albumin
¹⁴ C	Carbon-14 radioisotope
°C	Degrees Celsius
C _t	Threshold cycle
CCD	Charge coupled device
CaaX	Peptide Motif with Cysteine-aliphatic amino acid residue(x2)-X(a Serine, Glutamine, or Methionine)
CDK	Cyclin dependent kinase
Ci/mCi	Curies/milliCuries
CKI	Cyclin dependent kinase inhibitor
CMD1A	Dilated Cardiomyopathy type 1A
CMT-AR	Autosomal Recessive Charcot-Marie-Tooth syndrome
CO ₂	Carbon dioxide

CS	Calf serum
C-Terminus/-Term/ -Terminal	Carboxyl terminus
DAPI	4',6-diamidino-2-phenylindole
DI	Deionized
del50	Lamin A mutant with 50 amino acid residues deleted (Progerin)
DMEM	Dulbecco's modified eagle medium
DMSO	Dimethyl Sulfoxide
DNA	Deoxyribonucleic acid
cDNA	Complementary Deoxyribonucleic acid
dsDNA	Double strand deoxyribonucleic acid
ssDNA	Single strand deoxyribonucleic acid
DNase	Deoxyribonuclease
DPLD	Dunnigan's Partial Lipodystrophy
DTT	Dithiothreitol
ECL	Enhanced Chemiluminescence
<i>E. coli</i>	<i>Escherichia coli</i>
EDMD	Emery Dreyfus Muscular Dystrophy
EDTA	Ethylenediaminetetraacetic acid
EtBr	Ethidium bromide
EtOH	Ethanol
FBS	Fetal Bovine Serum
FCS	Fetal Calf serum
FPLD2	Familial Partial Lipodystrophy type 2

FTase	Farnesyl Transferase
g/mg/μg	Gram/milligram/microgram
GST	Glutathione S Transferase
HTLE	Hunter Thin Layer Electrophoresis
ICMT	Isoprenyl Carboxy Methyltransferase
IF	Immunofluorescence
IP	Immunoprecipitation
GFP/EGFP	Green fluorescent protein/Enhanced Green fluorescent protein
³ H	Tritium, Hydrogen-3 radioisotope
HCl	Hydrochloric acid
HeLa	Human cervical epithelial adenocarcinoma fibroblast cells
HGPS	Hutchinson Gilford Progeria Syndrome
HRP	Horseradish peroxidase
Ig	Immunoglobulin
Kb	Kilobase
KDa	KiloDaltons
KOAc	Potassium acetate
L/ml/μl	Liter/milliliter/microliter
L647R PreA	Leucine→Arginine mutation in Lamin A at amino acid residue #647
LA	Lamin A
mLA	mature Lamin A
wtLA	wild type Lamin A

LGMD1B	Limb-Girdle Muscular Dystrophy type 1B
LMNA	Lamin A gene
LMNB1/2	Lamin B genes
LB	Luria Bertani
LDS	Lithium dodecyl sulfate
L/Leu	Leucine
cm/mm	Centimeter/millimeter
M/mM/ μ M	Molar/millimolar/micromolar
MAD	Mandibuloacral Dysplasia
MALDI-TOF	Matrix-assisted laser desorption/ionization-Time of Flight
2-ME/BME	2/ β - Mercaptoethanol
MES (buffer)	2-N-Morpholino ethanesulfonic acid buffer
MgCl ₂	Magnesium chloride
Min	Minutes
MOPS (buffer)	3-N-Morpholino propanesulfonic acid buffer
MWM	Molecular Weight Marker
NaCl	Sodium chloride
NI	Not Induced
NP-40	Nonidet P-40 detergent
dNTP	Deoxyribonucleotide triphosphates
NLS	nuclear localization signal
N-Terminus/-Term/ -Terminal	Amino terminus

³² P	Orthophosphate, Phosphorus-32, radioisotope
PAGE	Polyacrylamide gel electrophoresis
PBS	Phosphate buffered saline
PCR	Polymerase chain reaction
PI	Propidium iodide
PVDF	Polyvinylidene fluoride
PreA	Prelamin A
Psg(s)	Passages, in cell culture
R/Arg	Arginine
RIPA (buffer)	Radio-immunoprecipitation Assay buffer
Rce1	Ras converting enzyme 1
RD	Restrictive Dermopathy
RNA	Ribonucleic acid
cRNA	Complementary Ribonucleic acid
RNase	Ribonuclease
RT qPCR	Quantitative reverse transcription polymerase chain reaction
S/Ser	Serine
SAP	Shrimp alkaline phosphatase
SDS	Sodium dodecyl sulphate
3T3/NIH 3T3	Swiss mouse embryo fibroblasts
TBE(buffer)	Tris-Borate-EDTA buffer
TBS (buffer)	Tris buffered saline
TBST (buffer)	Tris buffered saline + 0.1% Tween 20

TCA	Trichloroacetic acid
TCEP	Tris(2-carboxyethyl)phosphine
TMB	3,3', 5,5"-Tetramethyl-benzidine
UV	Ultraviolet
Vol	Volume
WB	Western Blot
WI-38	Human lung adherent fibroblast cells
Y/Tyr	Tyrosine
Zmpste24	Zinc Metalloprotease Sterol 24 (yeast) homolog

*-Abbreviations of names of most genes, other than the Lamins, are not included in this list, but rather, are noted where appropriate in the text.

CHAPTER 1

INTRODUCTION

The Nuclear Lamins

The nuclear lamins are a Class V family of intermediate filament proteins that form a thin, fibrous scaffold lining the inner nuclear membrane, thereby providing structural rigidity to the nucleus^{1,2}. Two primary types of lamina proteins exist: the A-type and B-type lamins. Three genes encode the 2 primary lamina proteins. The A-type lamins, Lamins A and C, are both encoded by the single Lamin A (LMNA) gene by alternative splicing³⁻⁵. There are 2 Lamin B isoforms, B1 and B2, that are encoded by the LMNB1 and LMNB2 genes, respectively⁶. The B-type lamins are ubiquitously expressed in vertebrate cells from the earliest stages of development throughout differentiation and have been described as “essential^{1,7},” whereas expression of A-type lamins is associated with the advent of some level of cellular differentiation⁸, and are expressed in most, but not all differentiated cells^{9,10}. *Lmnb* ^{-/-} mice die in early developmental stages, demonstrating the null phenotype is lethal. *Lmna* ^{-/-} mice, however, are able to survive at least several weeks after birth, though they demonstrate some phenotypes of disorders experienced by humans with mutations in LMNA or in the genes that code for proteins that process Lamin A (LA)¹¹. Our studies focus on LA, which has been shown to play a role in many cellular functions, the complexities of which are continuously developing. Recent research has revealed important functions in processes ranging broadly from maintenance of structural and mechanical integrity of the nuclear membrane, to modulation of organismal aging and preservation of the fidelity of the genome.

Post-Translational Lamin Processing

LA is initially synthesized as a 74 kDa precursor, Prelamin A (PreA)^{12,13}, which undergoes an unusual maturation sequence in which 2 endoproteolytic cleavages occur to yield a 72 kDa mature LA protein¹⁴ (Figure 1). The first cleavage is initiated by the attachment of a farnesyl group (farnesylation) to the cysteine residue of a C-terminal CaaX-motif (where “C” is a cysteine, “a” is an aliphatic amino acid and “X” is usually serine, glutamine or methionine)¹⁵⁻¹⁷. Farnesylation of mammalian proteins is reported to target the affected proteins to membranes^{18,19}, through inducing specific protein-protein interactions²⁰, and is catalyzed by the enzyme farnesyltransferase (FTase)²¹, which recognizes the C-terminal CaaX motif of its substrate proteins. FTase transfers a farnesyl group from farnesyl pyrophosphate to the CaaX cysteine, forming a thioether linkage. Once farnesylated, these proteins typically undergo 2 further C-terminal modifications. Endoproteolytic removal of 3 C-terminal amino acids, this cleavage (often referred to as “-aaXing”)¹⁶, can be carried out by the endoproteases Zmpste24^{22,23} or Rce1²⁴. The -aaXing cleavage is followed by carboxyl methylation of the newly created C-terminus, carried out by isoprenyl carboxyl methyl transferase (ICMT)²⁵. In a further processing step, LA undergoes a second endoproteolytic cleavage to remove an additional 15 C-terminal amino acid residues (aa 647-661, human sequence), including the farnesylated cysteine^{26,27}. This second cleavage is unique to LA in higher vertebrates, and is specifically carried out by Zmpste24²⁸.

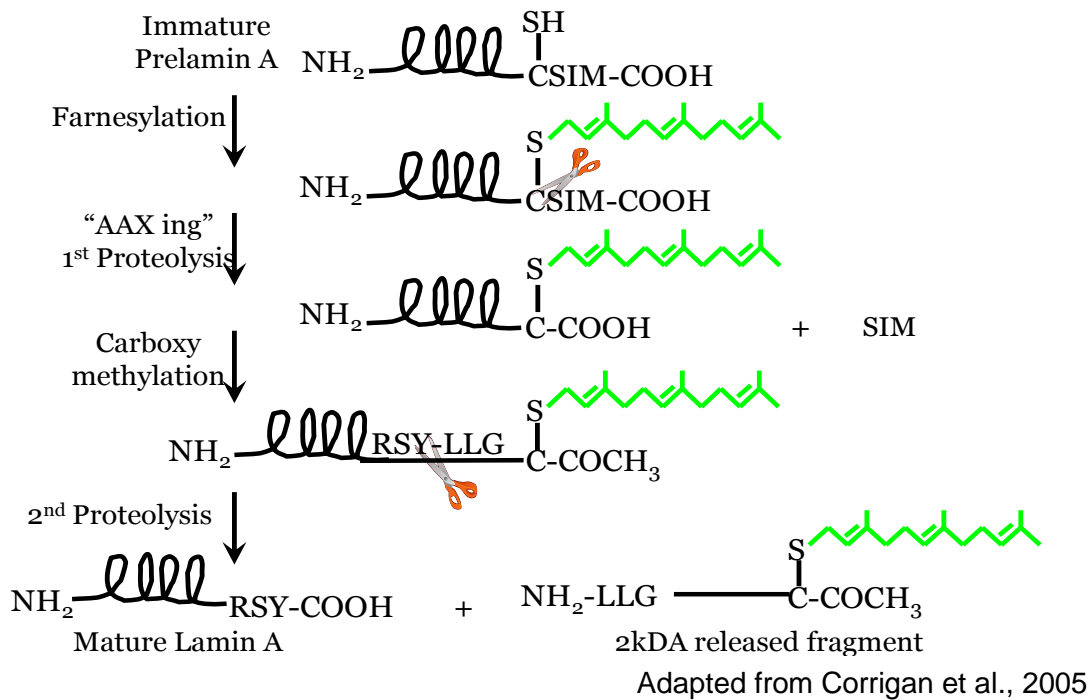


Figure 1. Maturation of Lamin A Protein by Proteolytic Posttranslational Processing. The precursor protein undergoes successive modifications: by the enzyme FTase (which attaches a farnesyl moiety), followed by Zmpste24- or Rce1-mediated cleavage of the –SIM residues (-aaXing), after which ICMT methylates the carboxyl terminus, signalling the 2nd proteolysis, by Zmpste24 (uniquely) between the tyrosine (Y) and leucine (L) residues of the RSYLLG Zmpste24 recognition site, releasing the 2 kDa farnesylated C-terminal fragment to yield mature LA (72 kDa).

The LA precursor isoform is reportedly toxic to the cell, and it accumulates in several laminopathies^{29,30}. Though previous work, including much from our own laboratory [including 21,27,28,31], has provided insight into the processing pathway of PreA, as described above, the functional significance of the pathway remains puzzling. Clearly, the processing introduces differences compared to the other lamins: The B-type lamins also have a CaaX motif, are farnesylated, and undergo the same initial aaX-peptide cleavage processing as Lamin A (in which the 3 c-terminal amino acids are removed), followed by carboxymethylation of the truncated protein. However, because the B

lamins are not subjected to the second cleavage, they maintain the farnesyl modification. By virtue of this permanently farnesylated state, Lamin B remains tightly associated with the membrane even through mitosis, while the A-type lamins dissociate during mitosis and reassemble³²⁻³⁴. Lamin C, which lacks the CaaX motif altogether, and is thus never farnesylated, maintains only a loose association with the nuclear membrane, primarily through polymerization with Lamin B and Lamin A³⁵. Existing in a heteropolymeric tapestry together with each other, the different lamin isoforms demonstrate some structural and functional overlap, yet their different structural characteristics convey different functions from each other, as well.

The Laminopathies

Diseases resulting from mutations in the lamins, or in the genes that encode the proteins responsible for lamin processing, are collectively termed “laminopathies.” At least 12 distinct laminopathies have been described, comprising a surprisingly diverse group of phenotypic disorders^{36,37,38}, and most result from some of the >250 mutations that have been identified within the LMNA gene³⁹. These phenotypes range from inability to properly accumulate and/or process lipids, as in the several different types of lipodystrophies, including Dunnigan’s Partial Lipodystrophy (DPLD) and Familial Partial Lipodystrophy (FPLD2), as well as musculoskeletal phenotypes associated with several types of muscular dystrophies, such as Emery Dreyfus Muscular Dystrophy (EDMD) and Limb-Girdle Muscular Dystrophy (LGMD1B), cardiac defects as found in Dilated Cardiomyopathy (CMD1A), and neurological defects, as in Autosomal Recessive Charcot-Marie-Tooth syndrome (CMT-AR). Additionally, mutations in LMNA, or in genes coding for LA-processing proteins, cause a group of premature aging disorders,

called progerias or progeroid diseases, including Hutchinson Gilford Progeria Syndrome (HGPS), Atypical Werner Syndrome (A-WS), Restrictive Dermopathy (RD), and Mandibuloacral Dysplasia (MAD)^[reviewed in 38,40]. Phenotypic expression in the progerias include several of the aforementioned phenotypes (perturbations of lipid metabolism, cardiac and musculoskeletal defects, etc.), in addition to increased DNA damage accumulation, early cellular senescence, and several other pathogenic phenotypes that are typically associated with progressive aging, such as bone degeneration, alopecia, and atherosclerosis⁴¹⁻⁴⁶. HGPS is perhaps the most studied of these progerias and is usually caused by a heterozygous LMNA point mutation in the third nucleotide of codon 608 that, while not changing the encoded amino acid, introduces a cryptic splice site that removes 150 nucleotides from the mRNA transcript, resulting in a 50 residue-truncation of the protein product⁴⁷⁻⁴⁹. This mutation is frequently referred to as “LAdel50,” and the mutant protein has become known as “progerin.” HGPS patients typically die around a median age of 13 years due to atherosclerotic/cardiac-related pathology^{17,41,47,48,50-55} [and a few of many HGPS/Progeria reviews: 17,22,29,31,40,42-44,46,55-78].

A 2-category classification system for laminopathies has been suggested⁷⁹, grouping them by phenotypic similarity derived through hierarchical cluster analysis. The first class of laminopathies includes those with skeletal muscle, cardiac and neurological involvement, such as EDMD, LGMD1B, CMD1A, and CMT-AR. The second class of laminopathies includes those with partial lipodystrophy, bone dysplasia, and progeric involvements, such as FPLD2, MAD, HGPS, A-WRN, and RD. Interestingly, mutations in the first class of laminopathies are found mainly in the LMNA region upstream of the nuclear localization signal (NLS, located at residues 416–423),

while mutations downstream of the NLS appear to result in diseases in the second class of laminopathies. The structure in Figure 2 schematically represents the domain/exon arrangement of Lamin A⁸⁰.

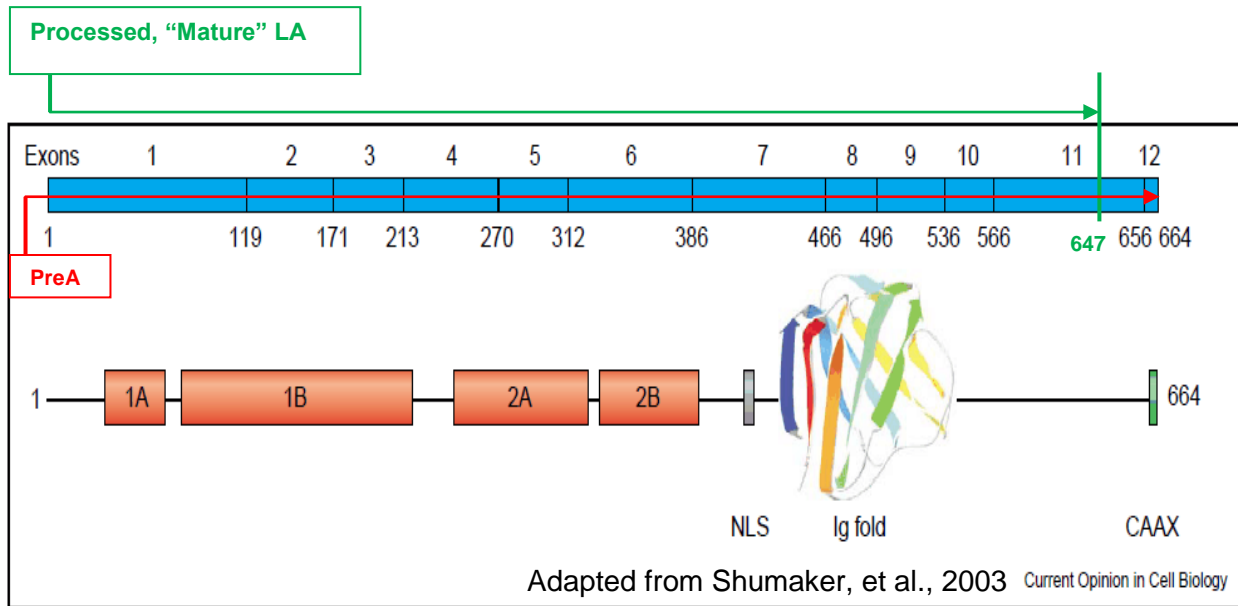


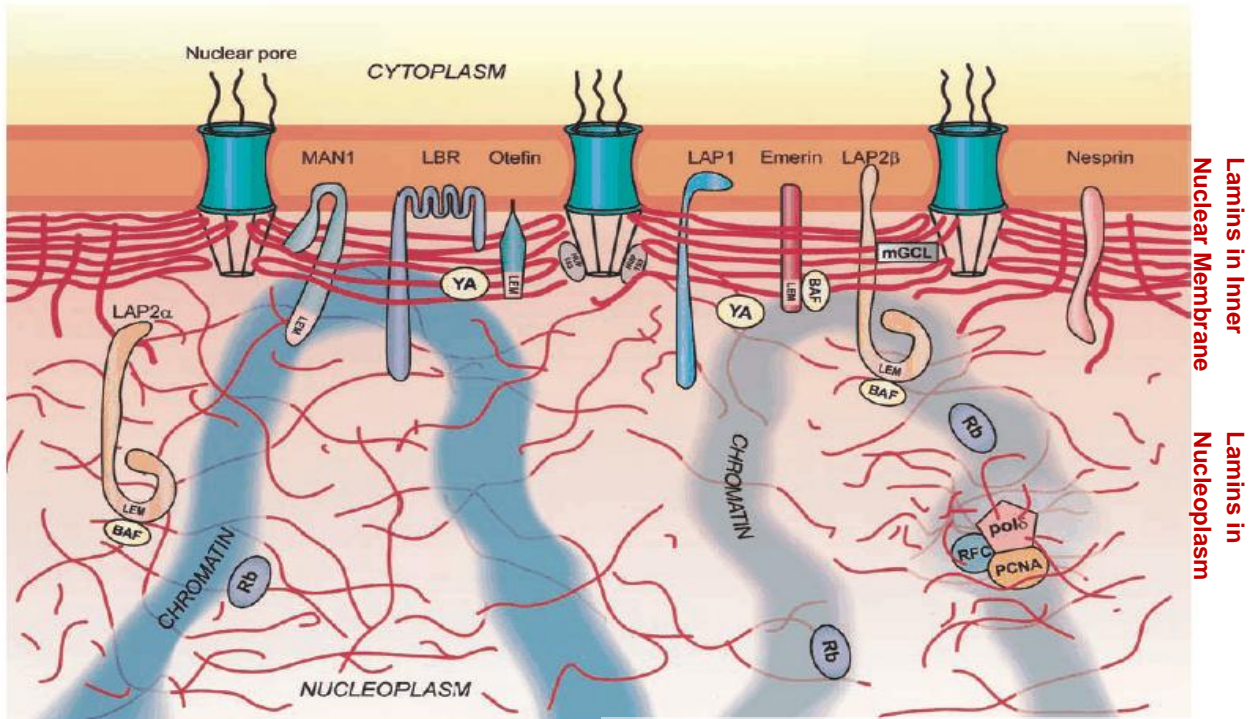
Figure 2. Structure and Domain Arrangement of Lamin A Protein. The Lamin A central rod domain has 4 subdomains 1A, 1B, 2A, 2B (red); the nuclear localization signal (NLS) is indicated by a grey box (residues 417-422); the immunoglobulin (Ig) fold is represented by the molecular ribbon structure (at residues 436-544), and the C-terminal CaaX sequence is represented by a green box (terminal residues 661-664). Exon nucleotide base-pair lengths are demarcated by the blue rectangular bar, top.

The central α -helical rod domain region upstream of the NLS is essential for the intra-molecular interactions in the nuclear lamina that contribute to structural integrity, while the DNA-binding region, located downstream of the NLS, is more likely to be involved in interactions involving chromatin remodeling complexes and transcription factors⁸¹. Such a nonrandom association between the mutation position and organ system involvement suggests a phenotype–genotype relationship⁷⁹, suggestive of different pathogenic mechanisms accounting for the 2 groups of laminopathies, either

involving compromise of the nuclear structure and stability, or aberrance in the chromatin organization that controls transcription^{79,82,83}.

Lamin A Structural Functions

The central rod domain of the A type nuclear lamins, similar to the B-Lamins, is approximately 45 kDa. When these intermediate filaments form polymers by homo- or hetero-dimerizing longitudinally in 50–52-nm long 2-stranded α -helical coiled coils, the coiled coils are flanked at each end by 2 globular heads corresponding to the C-terminal tail domains of each individual filament protein^{2,5}. Once PreA is fully processed to mature LA (mLA), and no longer farnesylated, the obligatory membrane association is apparently relaxed^{20,21}, but multimeric polymerization with Lamin B assists in maintenance of a meshwork of LA proteins on the internal surface of the nuclear membrane. The LA polymers infiltrate the nucleoplasm⁸⁴, thus providing nuclear integrity and shape (Schematic, Figure 3)¹.



Adapted from Goldman et al., Genes Dev 2002

Figure 3. Lamin A at Nuclear Envelope and throughout Nucleoplasm. Peripheral nuclear Lamin A and fibrous structural permeation of the nucleoplasm (red structures). Various binding partners/lamina-associated moieties (ie. chromatin (blue), nuclear pore complexes (crossing the membrane), proteins such as Rb or PCNA).

Nuclei of LA-deficient cells have fragile membranes, subject to mechanical rupture, and microscopically presenting deformations such as blebbing and invaginations^{7,80,85,86}. Nuclear organization, stiffness, and shape-stability are reported to rely primarily on A-type lamins⁸⁷. Some have suggested the mechanisms of pathology related to LA mutation derive simply from a compromised nuclear membrane structure, such as aberrant placement and stability of nuclear pore complexes, alteration of membrane transport of molecules, impaired access to receptors for membrane binding proteins, general nuclear disorganization, and cell death due to rupture of the fragile nucleus^{88,89}.

Lamin A Non-Structural Functions

In addition to providing nuclear integrity and shape, the Lamin A polymer mesh permeating the nucleoplasm provides a scaffolding system upon which numerous proteins rely for spatiotemporal organization of interactions and processes. In this role, Lamin A has been demonstrated as critical to the functional control of many transcriptional regulators and cellular processes that regulate cellular homeostasis. This function is more widely accepted as the source of LA-dysfunction-related pathology mechanisms that result in the most devastating phenotypic outcomes for affected organisms. In addition to spatiotemporal organization of interacting molecules, binding to LA has been shown to affect expression levels of many proteins. Typically, the effects on expression are through stabilization of the bound protein, usually by preventing ubiquitination and subsequent proteosomal degradation. These interactions are defective even in many cases in which LMNA mutations do not alter the nuclear envelope structure and fail to perturb the structural nucleoplasmic mesh. Therefore, LA-related dysfunction in such disorders could not be attributed merely to integrity of the nuclear structure. Instead, control of cellular functions involving these molecules rely on interactions with LA in a role independent of structural maintenance of the nucleus^[Reviews include 85,86,88-91].

Lamin A Functions in Cell Cycle Regulation

Many studies have examined contributions of the A-type lamins to regulation of cell proliferation and tissue homeostasis^[reviewed 92,93]. The LA role in cell cycle regulation incorporates both structural and nonstructural functions. For instance, as cells replicate genetic material and divide in proliferation, the nuclear envelope must depolymerize and

“dissolve” properly when needed, but then must repolymerize and reassemble with precision of arrangement and timing to form viable daughter cells³², providing implications of a structural LA function in the process. At the same time, cell cycle progression involves extremely tight regulation of the spatiotemporal control of the interactions between a large number of different molecules, such as transcriptional regulators and target proteins, thus involving nonstructural LA functions. Cells that are committed to differentiate but still undergoing proliferation contain intra-nuclear populations of A-type lamins that interact with the major lamin-associated protein LAP2 α ⁹². This lamin-LAP2 α complex has been shown to bind to and regulate the localization and activity of a major cell cycle regulatory protein, the tumor suppressor retinoblastoma protein (pRb)⁹⁴. The harmonic expression of these components appears to be the keystone determining cellular decisions at the most fundamental points of regulation of cell proliferation and differentiation^{95,96}.

In cells that express the A/C lamins, LA is one of the most abundantly expressed proteins in the cell, and it has been shown that small amounts of new LA are being incorporated into the lamina on a constant basis¹³. LA proteins exhibit a fairly low rate of turnover (though, even that rate is higher than for B-type lamins), which, coupled with the steady low-level synthesis of new LA, leads to a gradual increase in the actual level of protein expression in the cell. However, as cell size increases with cell growth, mainly through G1 phase, the overall result is a relatively stable proportion of lamin protein to cell size, maintained throughout the entire cell cycle^{35,97}. Phosphorylation induces dramatic depolymerization of the lamins in mitosis, effectively dissolving the nuclear membrane. Studies have shown that much LA protein appears to be conserved

in the process of cell division, as cytokinesis occurs fairly rapidly, and daughter cells are able to regenerate much of their nuclear membranes from the pre-existing, depolymerized, residual LA from the parent cell^{13,32,33,97,98}. It is the reuse of existing LA protein in daughter cells that contributes to the accumulation of progressively higher levels of mutant protein with aging or successive cell culture passaging.

The endoproteolytic cleaving of PreA is such an efficient and rapidly executed process⁸⁴, the progenitor is largely undetectable in cycling cells. However, we and others^{99,100} have noted PreA accumulation in senescent cells. We also detect PreA accumulation under conditions of quiescence, such as with serum starvation or high-density cell culture plating. Cells that express the A/C lamins are typically able to enter quiescence under conditions of contact inhibition or mitogen deprivation, as from serum starvation of cultured cells. Conversely, cells that do not express A/C lamins lack a quiescent state^{7,8}. Frequently, cell cycle-dependent changes in expression of a particular protein, such as those detected for PreA, indicate some role in regulating the cycle. While numerous studies provide demonstration of LA functions in cell cycle control [reviewed in (among others): 63,68,86,88,94,101-103], less is known about the precursor isoform, which is the specific isoform of the LA protein that seems to exhibit a cell cycle-dependent expression pattern.

Our hypothesis: accumulation of the PreA protein isoform is induced as part of program of modulating gene expression and posttranslational modifications to an array of regulators from several different cell cycle pathways, thereby coordinating these into a network of interactions resulting in spatio-temporal regulation of the cell cycle, wherein different isoforms of LA exert different effects on cell cycle control, regulation of mitotic

progression, DNA repair checkpoint controls, chromatin organization, and influences on the processes leading to and maintaining cell cycle exit.

Aims of This Study

This study aims to investigate the role of PreA as a cell cycle regulator, by examining its expression patterns and the effects of its expression on, or interactions with, other known mediators of control over mitotic cell cycle progression. Owing to the aforementioned efficiency of the proteolytic processing of PreA, in order to assist in the study of the effects of expression of the unprocessed, immature protein, we have developed a stable cell line harboring an inducibly-expressed uncleavable mutant form of PreA in which the site of the second cleavage is mutated ("L647R PreA"). Several relationships between PreA and its interacting partners indicate this protein isoform could have a distinct purpose of its own, independent of simply existing as a precursor form of the mature LA (mLA). In all likelihood, PreA serves as an integral scaffolding protein for many interactions, as does mLA, though perhaps each of the 2 isoforms, and other isoforms, as well, are able to interact uniquely with distinct molecules in a mechanism that helps to coordinate cellular operations in a cell cycle specific manner. We ask 3 main questions. First, is accumulation of the PreA isoform is a byproduct of cell cycle arrest or an induction factor for that arrest? Second, does expression of the PreA isoform result in effects on cell cycle regulatory genes and proteins? Finally, do cell cycle regulators have interactions with the C-terminal fragment of the PreA isoform, that constitutes the difference between the LA isoforms, and therefore would imply isoform-specific activity?

Our current study evaluates some PreA-specific effects on cell cycle control by comparing the differential effects on cell cycle related genes when exogenous PreA is expressed versus conditions without exogenous expression of any LA isoform. We examine PreA isoform-expression effects on direct and indirect interaction partners already known to act in cell cycle regulatory roles. Among these are transcription factors and coactivators, such as E2F, p300 and FOXO proteins; cyclins, such as cyclins D and E; cyclin dependent kinase inhibitors (CKIs), such as p27^{Kip1} and p21^{Waf1}; and tumor suppressors retinoblastoma (RB/pRB) and p53. We evaluate the overall profile of altered cell cycle gene expression induced by exogenous PreA expression in the context of the known cellular functions of the affected genes to begin to ascertain potential PreA functional roles in regulation of the cell cycle. Additionally, we consider a motif analysis of the c-terminal region of the full length LA protein, which constitutes the differentiating peptide sequence between PreA and mature LA. We focus the motif analysis on the kinase substrate sites and phosphorylation-mediated protein-binding sites and consider, as well, these phosphorylation-related motifs in the context of sites for many of the known binding proteins for this region. Finally, we examine the potentially LA-relevant expression of Pin1, a peptidyl prolyl cis/trans isomerase, shown to play a key role in control of mitosis and cell cycle progression.

CHAPTER 2

MATERIALS AND METHODS

Materials

General Laboratory Chemicals, Buffers, and Reagents

100bp DNA Ladder, GibcoBRL Life technologies, USA
1Kb DNA Ladder, GibcoBRL Life technologies, USA
Agar, Bacto, BD Diagnostics, Sparks, MD, USA
Agarose, NuSieve, Lonza/Fisher Scientific, USA
Albumin bovine fraction, Sigma, USA
Ampicillin, MP Biomedical/Fisher Scientific
Bacto-peptone, Difco, BD Diagnostics, USA
Bacto-yeast extracts, Difco, BD Diagnostics, USA
Bis-Tris 4-12% Gradient Polyacrylamide Gels, NuPAGE, Invitrogen/Life Technologies, USA
BondBreaker tris(2-carboxyethyl)phosphine (TCEP), Pierce/Thermofisher, USA
BSA (bovine serum albumin) Pierce/Thermofisher, USA
Calcium chloride dehydrate, Fisher Scientific, USA
Coomassie Blue G250, GelCode Blue Safe Protein Stain, Pierce/Thermofisher, USA
DNA Loading Solution, 6X, Sigma-Aldrich, USA
Dithiothreitol (DTT), Pierce/Thermofisher, Rockford, IL, USA
Doxycyclin, MP Biomedicals, USA
Dulbecco's modified eagle medium (DMEM) with and without Phenol Red /with and without Phosphate, Lonza/Fisher Scientific, USA
Dimethyl Sulfoxide (DMSO), Sigma-Aldrich, USA
ECL Hyperfilm GE Healthcare Amersham/Fisher Scientific, USA
Ethylenediaminetetraacetic acid (EDTA), ACROS Organics/Fisher Scientific, USA
Ethanol, Fisher BioReagents/Fisher Scientific, USA
Ethidium Bromide, Sigma-Aldrich, USA
Fetal bovine serum, Lonza/Fisher Scientific, USA /Gibco, USA
Fetal calf serum, Lonza/Fisher Scientific, USA /Gibco, USA
Formaldehyde 16%, Fisher BioReagents, Fisher Scientific, USA
G418 antibiotic, MP Biomedicals, USA
GenoStat, Millipore/Fisher Scientific, USA
Glycerin (Glycerol), Sigma-Aldrich, USA
HCl Fisher BioReagents, Fisher Scientific, USA
HygromycinB, MP Biomedicals, USA
Iodoacetamide, Sigma-Aldrich, USA
Isopropanol, Fisher BioReagents, Fisher Scientific, USA
Juglone, Santa Cruz Biotechnology, USA
Kanamycin, MP Biomedicals, USA
2/β- Mercaptoethanol (2-ME/BME), Sigma-Aldrich, USA
MES 20X Buffer concentrate, NuPAGE, Invitrogen/Life Sciences, USA
Methanol, Sigma-Aldrich, USA

Milk powder, various, USA
MOPS 20X Buffer concentrate, NuPAGE Invitrogen/Life Sciences, USA
NP-40, Sigma, USA
Orthophosphate (³²P-orthophosphate), New England Nuclear
PBS (phosphate-buffered saline), Lonza-Biowhittaker/Fisher Scientific, USA
Penicillin/Streptomycin, MP Biomedicals, USA
Propidium iodide (PI)+ RNase, BD Diagnostics, USA
Protease and Phosphatase Inhibitor Cocktail, Halt, Pierce/ThermoFisher, USA
Protein A Magnetic Protein Separation/Immunoprecipitation Beads, Dynabeads, Invitrogen/Life Sciences, USA
Protein A Agarose Beads, Invitrogen/Life Sciences, USA
Protein Molecular Weight Marker: Sharp Prestained, Invitrogen/Life Sciences, USA
Protein Molecular Weight Marker: Cruz Marker, Santa Cruz Biotechnology, USA
RheoSwitch® Ligand RSL1 (5 mM in DMSO), New England Biolabs (NEB), USA
Skatole/ BNPS Skatole (3-bromo-3-methyl-2-[(2-nitrophenyl)thio]-3H indole), Sigma-Aldrich, USA
SDS (sodium dodecyl sulphate), Sigma, USA
Sodium acetate Sigma-Aldrich, USA
Sodium chloride Fisher BioReagents, Fisher Scientific, USA
[³H]-Thymidine, New England Nuclear, USA
Tris base, Fisher BioReagents, Fisher Scientific, USA
Triton X-100, Sigma-Aldrich, USA
Trypsin, Proteomics Grade, Bioreagent, Dimethylated, Sigma-Aldrich, USA
Trypsin/Versene-EDTA, Lonza-Biowhittaker/Fisher Scientific, USA
Tryptone, Difco, BD Diagnostics, USA
Tween 20, Sigma-Aldrich, USA
Yeast extracts, Difco, BD Diagnostics, USA

Enzymes, Kits

Enzymes for DNA Manipulation:

DNA restriction endonucleases, NEB, USA (NotI, Sall, AclI, MluI)
DNA restriction endonucleases, Promega, USA (NotI, Sall)
DNase I, Qiagen, USA
RNase A Qiagen, USA
Shrimp Alkaline Phosphatase, TSAP, Promega, USA
T4 DNA Ligase Kit, Ligafast Rapid, Promega, USA
TaqGold® DNA Polymerase, PCR Buffer, and dNTPs, Applied Biosystems, USA

Commercial Kits:

BCA protein assay(Reducing Agent Compatible), Pierce/ThermoFisher, USA
BioRad
DC Detergent Compatible Protein Assay, BioRad, USA
Cell Cycle Control Pathway Antibody Array, Full Moon Biosystems, USA

Magnetofect Polymag Transfection System, OzBiosciences, France
NE PER Nuclear/Cytoplasmic Extract Reagent Kit, Pierce/Thermofisher, USA
MicroBCA Protein Assay Reagent Kit, Pierce Chemical, Rockford, IL
SuperSignal West Pico ECL Western Blotting Detection Reagents Kit, Pierce/
Thermofisher, USA
SuperSignal West Dura ECL Western Blotting Detection Reagents Kit, Pierce/
Thermofisher, USA
GeneAmp PCR Reagent Kit, Applied Biosystems, USA
Plasmid Mini Plasmid DNA Extraction Kit, Qiagen, USA
Plasmid Miniprep Kit, Zymo, USA
Plasmid Midi Plasmid DNA Extraction Kit, Qiagen, USA
Plasmid Maxi Endo-free Kit Plasmid DNA Extraction Kit, Qiagen, USA
Qiaquick DNA Gel-Extraction Kit, Qiagen, USA
QuikChange® Lightning Site-Directed Mutagenesis Kit, Stratagene/Agilent
Technologies, USA
Rheoswitch Inducible Gene Expression Vector System, New England Biolabs,
Germany/USA
RNEasy Protect Cell Mini RNA Extraction Kit, Qiagen, USA
SA- β -Galactosidase Staining Assay Kit, Cell Signaling, USA
SABiosciences RNA Extraction Kit, SABiosciences/Qiagen, USA
SABiosciences RT² Profiler Mouse Cell Cycle PCR Arrays, PAMM-020
SABiosciences/Qiagen, USA
RT² First-Stand cDNA Synthesis Kit, SABiosciences/Qiagen, USA
RT² qPCR SYBR Green Master Mixes, SABiosciences/Qiagen, USA

General Laboratory Supplies and Equipment

Microcentrifuge, Eppendorf MiniSpin, Eppendorf, USA
Tabletop Centrifuge, Sorvall, Thermofisher, USA
High Performance Centrifuge, Beckman J-14, Beckman, USA
Flow Cytometer, Accuri C6 Modular, BD, USA / Heidelberg, Germany
Gel Documentation & Imaging System, Alpha Innotech, USA
Hunter Thin Layer Electrophoresis (HTLE) Chromatography System, CBS Scientific,
USA
MiniGel Electrophoresis System, XCell Surelock MiniCell, Invitrogen/Life Sciences, USA
iBlot Dry Gel Blot Transfer System, Invitrogen/Life Technologies, USA
iBlot Transfer Stacks, Regular or Mini, PVDF or Nitrocellulose, Invitrogen/Life
Technologies, USA
Micropipettors, Gilson, Rainin Pipetman,
Needles (22, 26 Gauge)/Syringes, BD-Becton Dickinson, USA
Spectrophotometer, NanoDrop ND 1000, Thermofisher, USA
Sterile filter 0.22 μ m, Millipore/Fisher Scientific, USA
Fluorescent Microscope, Nikon, USA/Germany
pH Meter, Corning, USA

Chemiluminescence Imaging System, Fujifilm LAS4000
Gel Imaging System, Alpha Innotech, USA
Thermocyclers (9700, 9720, 9600), Applied Biosystems
Genetic Analyzers/ "Sequencers" (3100, 3130), Applied Biosystems

Materials Used in Cloning/Subcloning and Bacterial Cell Culture

Bacterial Strains (*E.coli*):

XL1-Blue, Stratagene, USA
XL10-Gold, Stratagene, USA
Zymo Z-competent DH5- α , Zymo, USA

Media:

Normal Growth Medium-
LB (Luria Bertani) Medium (10 g/L tryptone, 5 g/L yeast extract,
5g/L NaCl, pH 7.2)

Antibiotic Selection Media-
LB/Ampicillin Medium (50 μ g/ml Ampicillin)
LB/ Kanamycin (25 μ g/ml Kanamycin)

Plasmids and Oligonucleotides

Cloning vectors:

pCMV6-XL: TruORF Entry Vector, Expressed Zmpste24 protein in mammalian cells, Origene, USA
pCMV6-AN-GFP: TruORF Destination Vector, Expressed Zmpste24 protein in mammalian cells, Origene, USA
pEGFP-C1: Expressed a green fluorescence fusion protein in mammalian cells, Clontech, USA
pEGFP-C3: Expressed a green fluorescence fusion protein in mammalian cells, used as a transfection control plasmid, Clontech, USA
pNEBR-R1 Rheoswitch regulator plasmid: Inducibly expressed regulatory protein in mammalian cells, NEB, USA
pNEBR-X1 Hygro Rheoswitch expression plasmid: Inducibly expressed protein in mammalian cells, under control of pNEBR-R1 Rheoswitch regulator plasmid, NEB, USA

Constructs Used in Experiments:

pCMV6-XL-Zmpste24, Origene, USA
pEGFP-C1-Myc-Lamin A (Gift from Francis Collins⁶⁵ to Michael Sinensky)

pEGFP-C1-Myc-Lamin A-del50 (Gift from Francis Collins⁶⁵ to Michael Sinensky)
pEGFP-C1-Myc-Lamin A-L647R (generated by site-directed mutagenesis from pEGFP-C1-Myc-LaminA)
pEGFP-C1-Myc-Lamin A stably in Tet-On HeLa cells (Gift from Robert D. Goldman⁶³ to Michael Sinensky and Antonio Rusinol)
pEGFP-C1-Myc-Progerin (Lamin A-del50) stably in Tet-On HeLa cells (Gift from Robert D. Goldman⁶³ to Michael Sinensky and Antonio Rusinol)
pNEBR-X1-Hygro-EGFP-Myc-Lamin A (generated by subcloning EGFP-Myc-Lamin A from pEGFP-C1-Myc-Lamin A into pNEBR-X1-Hygro)
pNEBR-X1-Hygro-EGFP-Myc-Lamin A-L647R (generated by subcloning EGFP-Myc-Lamin A-L647R from pEGFP-C1-Myc-Lamin A-L647R into pNEBR-X1-Hygro)
pNEBR-X1-Hygro-EGFP-Myc-Lamin A-del50 (generated by subcloning EGFP-Myc-Lamin A-del50 from pEGFP-C1-Myc-Lamin A-del50 into pNEBR-X1-Hygro)
pNEBR-X1-Hygro-EGFP (generated by subcloning EGFP from pEGFP-C1 into pNEBR-X1-Hygro)
pGST-Pin1 (from Addgene, plasmid #19027, deposited by MB Yaffe¹⁰⁴)

Oligonucleotides Used:

DNA Amplification Primers-

Insert Amplification* from pEGFP-C1-Lamin A/ Lamin A del50

NotI-EGFP-Fwd 5'-ATCAGCGGCCGCATGGTGAGCAAG-3'

LA-Sal1-Rev 5'-GCGCGTCTGACTGCAG AATT CTTAC ATGATG-3'

*also used as sequencing primers in confirmation of DNA isolated from stably transfected cells

DNA Sequencing Primers-

Origene TruORF vector sequencing, for Zmpste24 construct sequencing, provided with kit from manufacturer, sequence not provided:

“VP1.5” Forward Sequencing Primer for Origene TruORF vector sequencing; “XL39” Reverse Sequencing Primer for Origene TruORF vector sequencing

pEGFP-C1-1465-1485 reverse sequencing primer for pEGFP-C1 constructs:

5'-gttcagggggagggtgtgggag-3'

RheoSwitch R-X1 Sequencing Primer for confirming constructs in Rheoswitch pNEBR-X1 vector:

5' (GGGTATATAATGGGGGC) 3'

Mutagenesis Primers-

Mutagenesis of pEGFP-C1-Myc-Lamin A to generate pEGFP-C1-Myc-Lamin A-L647R:

FWD Primer 5'-GACCCCGCTGAGTACAACCTG -3'

REV Primer 5'-AAAGAAAATAACCCTTTGGTTTTTTTC-3'

Transfection Reagents

TransPass D1, NEB, Ipswich, MA, USA/Frankfurt, Germany

Polymag Magnetofection reagent, OzBiosciences, France

Mirus TransIT-3T3, Mirus Bio, USA

Antibodies

Primary Antibodies: The following primary antibodies were used either in immunoblot analysis or as primary antibodies in immunoprecipitation.

Anti-GFP, Rabbit, ab290, Abcam, USA

Anti-PreA (In House, Rabbit IgG Anti-Serum)

Anti-Lamin A (H102), C-Term 563-664, Rabbit, #20680, Santa Cruz, USA

Anti-Lamin A/C (H-110), N-Term, Rabbit #20681, Santa Cruz, USA

Anti-Lamin A 4C11, Mouse, #4777, Cell Signaling, USA

Anti-Pin1 (H-123), Rabbit, sc-15340, Santa Cruz, USA

Anti-FoxO3a, rabbit, #9467, Cell Signaling, USA

Anti-p27 (M-197), Rabbit, #776, Santa Cruz, USA

Anti-Ki67, Rabbit, Cellomics/Thermofisher, USA

Anti-Tubulin, Abcam, USA

Anti- β -actin, Abcam, USA

Secondary Antibodies:

From Santa Cruz, USA-

Goat Anti-Rabbit IgG-HRP sc-# 2030,

Rabbit Anti-Mouse IgG-HRP, sc-#358914

From Cell Signaling Technology, USA-

Goat Anti-Rabbit-AlexaFluor®488 (Green) and -Alexa Fluor®555 (Red)

Rabbit Anti-Mouse-Alexa Fluor®488 (Green) and -Alexa Fluor®555 (Red)

From Molecular Probes, Invitrogen, USA

Rabbit Anti-Mouse-FITC(Green) and -Texas Red (Red)

Goat Anti-Rabbit-FITC and -Texas Red

Mammalian Cell Culture

Mammalian Cell Lines:

WI-38 (Human lung adherent fibroblast cells growing as monolayer, 24 hr doubling time, approx 40-50 psgs competent), CCL-75, ATCC, USA

BJ (Human foreskin fibroblast adherent monolayer cells, telomerase negative, 72 psgs competency), CRL-2522, ATCC, USA

HeLa (Human cervical epithelial adenocarcinoma fibroblast adherent monolayer cells) CCL-2, ATCC, USA

3T3-L1 (Swiss mouse embryo fibroblast pre-adipocyte adherent monolayer cells, capable of chemical induction of differentiation), CL-173, ATCC, USA
Inoculate 3 to 5 X 10³ cells/cm²

NIH 3T3 (Swiss mouse embryo fibroblast adherent monolayer cells), CRL-1658, ATCC, USA
Inoculate 3 to 5 X 10³ cells/cm²

NIH 3T3 (Rheoswitch, containing pNEBR-R1 regulator plasmid), NEB, USA

Mammalian Cell Culture Media, Reagents, Antibiotics:

Doxycyclin, MP Biomedicals, USA

Dulbecco's modified eagle medium (DMEM) with and without Phenol Red /with and without Phosphate, Lonza/Fisher Scientific, USA

Dimethyl Sulfoxide (DMSO) Sigma-Aldrich, USA

Fetal bovine serum, Lonza/Fisher Scientific, USA /Gibco, USA

Fetal calf serum, Lonza/Fisher Scientific, USA /Gibco, USA

G418 antibiotic, MP Biomedicals, USA

HygromycinB, MP Biomedicals, USA

PBS (phosphate-buffered saline), Lonza-Biowhittaker/ Fisher Scientific, USA

Penicillin/Streptomycin, MP Biomedicals, USA

Trypsin/Versene-EDTA, Lonza-Biowhittaker/ Fisher Scientific, USA

Buffers

Cell Lysis:

Standard Cell Lysis Buffer-

10 mM Tris-HCl, pH 7.0, 10 mM NaCl, 3 mM MgCl₂, 0.4% Nonidet P-40 (NP-40)

Immunoprecipitation (IP) Lysis Buffer (Non Denaturing)-

20 mM Tris HCl pH 8; 137 mM NaCl; 10% glycerol; 1% NP-40 or Triton X-100; 2 mM EDTA

RIPA buffer-

1% (v/v) NP40; 0.5%(w/v) Deoxycholate; 0.1%(w/v) SDS; 0.15 M NaCl
5mM EDTA; 50 mM Tris pH 8.0

Other Buffers:

TBE (5X)-

0.45 M Tris-Borate; 0.01 M EDTA pH8.3, autoclaved

TBS (10X)-
0.2 M Tris base; 1.5 M NaCl pH7.4, autoclaved

TE (10X)-
0.1 M Tris-HCl; 0.01 M EDTA pH 7.5, autoclaved

MOPS and MES electrophoresis buffers-
1X solutions were prepared from commercial concentrates, 20X)

Software

SABiosciences Online/Web-Based Array Data Analysis Software

Used to analyze RT-qPCR gene expression array data, and calculate statistics.

BioRad iQData

Used to process raw data from RT-qPCR, to prepare for SABiosciences analysis.

PANDA Online/Web-Based Array Data Analysis Software

Used to analyze data from Full Moon Biosystems Antibody Array, and calculate statistics.

ScreenHunter5.1 from Wisdom-Soft

Was used to capture images from computer desktop and save in convenient digital photo formats.

Adobe photoshop

This image manipulation software was used to change the size and improve the contrast of experimental images.

Primer3

This software was used analyze the secondary structure (hairpin etc.) and annealing temperature of PCR primers.

GeneRunner

This software was used analyze the secondary structure (hairpin etc.) and annealing temperature of PCR primers.

ClustaW Web Based NCBI

Used for comparing the homology between the target DNA and sequenced DNA.

Sequencher Sequence Analysis Software, Gene Codes Software Co.

ModFit LT 3.2 from Verity House Software and FCS Express V3 De Novo Software

Methods I.: Molecular Biology Methods

Preparation and Purification of Plasmid DNA from Bacteria

Plasmid Midi and Mini preparations were carried out with QIAquick commercial kits from Qiagen or the Zymo Plasmid Mini kit. The process followed the manuals

provided with the kits. The Plasmid Midi Kit was used to purify up to 100 µg of plasmid DNA. The Endo-free plasmid Max preparation Kit was used to obtain endotoxin-free plasmid DNA for all transfections into mammalian cells.

Digestion of DNA with Restriction Endonucleases

The restriction digestions were performed by the protocol provided by the supplier companies. For example, 1 µg plasmid DNA was digested with 5 units of a given enzyme and 1x digestion buffer in 20 µl total volume for an incubation of 1 hour at 37°C.

Polymerase Chain Reaction (PCR)

Polymerase chain reaction was used to amplify DNA targets of interest, using Applied Biosystems reagents, ABI thermocycler, and standard ABI protocol. Primers noted in Oligonucleotides Section. PCR products were analyzed by agarose gel-sizing and/or Sequencing.

Automated DNA Cycle Sequencing

Cycle sequencing was performed using the dye dideoxy chain termination method based on the original dideoxy chain termination method developed by Sanger. PCR products or plasmid vectors were sequenced in this work, using commercially pre-prepared solutions from Applied Biosciences: Big Dye Terminator Ready Reaction Mix V1.3, and the manufacturer's protocol. Unincorporated dye was removed from the sequencing reaction using a resin-based clean-up column, the Qiagen Dye-Ex 2.0 spin

prep system. Purified reactions were dried with heat in a Speed-Vac system and resuspended in 15 µl Hi-Di Formamide. The suspension was denatured at 95°C for 5 min prior to loading onto an automated capillary sequencing analyzer, the ABI 3100 or 3130. Sequence results were analyzed using Sequencher Software or web-based tools such as ClustalW.

Site-Directed Mutagenesis of DNA

Primer design for site directed mutagenesis, used the following guidelines: The mutagenic oligonucleotide primers were designed to incorporate the desired point mutations and bind to adjacent sequences of the template plasmids. The length of primer should be between 25 and 45 bases with the melting temperature at least 75°C. The GC percent of the whole primer should be more than 40% and at least 1 C or G at 3' terminal. (Primer sequences are listed under Oligonucleotides Section) Primers were designed using Primer3 web- program (<http://frodo.wi.mit.edu/primer3/>)¹⁰⁵.

Mutagenesis Reactions used the Stratagene QuikChange® Lightning Site-Directed Mutagenesis Kit (Stratagene is now Agilent Technologies, USA) per manufacturer's protocol. Briefly, the following Mutagenesis PCR Reaction Mix was prepared (per each reaction):

- 5 µl 10x rxn buffer
- 1.25 µl (125 ng) of primer L647R Fwd[100ng/µl]
- 1.25 µl (125 ng) of primer L647R Rev[100ng/µl]
- 1 µl of dNTP mix
- 8.5 uL mix each rxn, added to
- 3 µl (30 ng) of dsDNA template plasmid (pEGFP-C1-Myc-Lamin A)
- dH2O to 50 µl TV=11.5 µl
- 1 µl *PfuUltra* HF DNA polymerase (2.5 U/µl)

And thermocycled with the following conditions:

95° C 30 seconds
 18 cycles — { 95°C 30 seconds
 55°C 1 minute
 68°C 5 minutes (1 minute/kb of plasmid length)
 4°C Hold Infinity

After the PCR reaction had cooled to 37°C , 1µl Dpn I (10 units) was added to the PCR reaction, followed by incubation at 37°C for 1 hour to digest the parental (i.e., the nonmutated) supercoiled dsDNA.

Transformation of mutated plasmids into competent cells (Note: this protocol is also used for transformation of other plasmids into bacteria, the specific feature related to SDM, here, is the use of the Ultracompetent cells to enhance transformation, otherwise, “traditional” competent cells are used in routine cloning exercises).

After *Dpn* I treatment, XL10-Gold® ultra competent *E. coli* cells were transformed with the mutagenesis mixture. In this step, 1µl of the treated reaction mixture was transformed into 50 µl of the ultra competent cells, which had been thawed on ice. After gently swirling and incubating on ice 30 minutes, the tubes were heat pulsed at 42°C in a waterbath for 45 seconds, then placed on ice for 2 minutes. Prewarmed (42°C) SOC broth (0.5 ml aliquot) was added to the bacteria/mutagenesis mix in the Falcon tube, and incubated, with 250 rpm shaking, for 1 hour at 37°C. Finally, 250 µl was plated on each of 2 LB agar plates containing 25 µg/ml Kanamycin. The plates were incubated at 37°C overnight (>16 hours) and examined for colony formation.

Colony Selection: Isolated colonies were marked with a permanent marker on the bottom of the agar plate and each (typically 5 colonies per transformation) was picked up with a sterile 10 µl micropipette tip and transferred into prewarmed (37°C) LB broth

medium containing 25 µg/ml Kanamycin. The cultures were incubated at 37°C, shaking at 250 rpm, overnight (approximately 16-22 hours).

DNA Gel Electrophoresis

DNA gel electrophoresis was used to check the results of restriction enzyme digestions, PCR reactions and DNA purification. Fragments of between 400 bp and 12 Kbp were separated by using 0.5% agarose gels. The gels were stained with ethidium bromide (EtBr) at a concentration of 0.5 µg/ml and the DNA was visualized under UV light (365 nm). DNA fragments less than 400 bp were separated on 1% or 1.5% agarose gels.

Purification of DNA Fragments from Agarose

In order to obtain single DNA fragments from digested plasmids, gel electrophoresis was performed, and the QIAquick Gel Extraction kit was used to extract the DNA from the gel. The band of interest was excised from the gel and the weight of the gel slice was determined. Three volumes solubilisation buffer (components proprietary) from the kit were added into the sample tube. The tube was vortexed and incubated at 50°C for 10 minutes or longer until the agarose was completely dissolved. The solution was loaded onto the ion-exchange column by centrifugation at 12,000 x g for 1 minute. 500 µl solubilisation buffer was added to wash the column followed by an additional centrifugation at 12,000 x g for 1 minute. Three volumes high salt ethanol wash buffer were used to wash the column. Elution of the DNA from the column was carried out by adding 50µl of 10 mM Tris-HCl, pH8.5 to the column and centrifuging 1

minute at 12,000 x g. In experiments where it was necessary to increase the DNA concentration in the eluate, the eluate was centrifuged through the column an additional time. This procedure was also used for the purification of PCR products.

Precipitation of DNA

When the DNA fragment was used for sequencing or some enzymatic reaction that was sensitive to residual salt, it was necessary to precipitate the DNA. The precipitation of DNA was achieved by adding 0.1 volume (of the starting DNA) of 3M KAc and 2.5 volumes 100% ethanol, and incubating at -20°C for 10 minutes. After removal of the supernatant the pellet was washed with 70% ethanol and air-dried.

Cloning and Sub-Cloning of DNA

Restriction Enzyme-Based Method. Cloning was performed by restriction endonuclease digest to remove the Zmpste24 cDNA sequence from the pCMV6-XL-Zmpste24 construct (Entry Vector) and transfer to the pCMV6-AN-GFP destination vector. Per manufacturer instruction, restriction enzymes *MluI* and *AsiI* were used. Digests were performed according to manufacturer instructions. Following digests, fragments were separated on an agarose gel and visualized with EtBr on an ultraviolet lightbox. Size discrimination was used to discern insert fragment from vector. The fragment was cut from the agarose and extracted/purified using the QIAquick Gel Extraction protocol, as described.

PCR-Based Method. The EGFP and EGFP-Lamin A/ Lamin A-L647R/ Lamin A-del50 fragments were copied from the pEGFP-C1-Myc-Lamin A/ Lamin A-L647R/ Lamin

A-del50 constructs by PCR amplification, using primers (described in Oligonucleotides section), to copy the EGFP/EGFP-lamin fusion coding region and add on a restriction enzyme cutting site. The Forward primer incorporated a *NotI* recognition site N-terminal to the EGFP sequence, and the Reverse primer attached a *SaII* site to the C-terminus of the coding section. PCR product was gel-purified and analyzed for appropriateness of molecular weight of the amplified insert, with extraction by the QIAquick Gel Extraction protocol, as described.

DNA Ligation. This procedure was performed to construct a new plasmid by ligating the purified target fragment with vector plasmid. First, the target vector was digested with the restriction enzymes compatible to the insert, and after heat inactivation of that enzyme, the vector was then treated with shrimp alkaline phosphatase (SAP) to prepare the ends for ligation. SAP catalyzes the removal of 5' phosphate groups from DNA, thus preventing the recircularization and deletion of linearized (empty) cloning vector DNA during ligation. The DNA ligation reaction was performed following the protocol for Ligafast T4 DNA Ligase (Promega, USA). Briefly, 4 μ l 5X Ligase Reaction Buffer (250 mM Tris-HCl (pH 7.6), 50 mM MgCl₂, 5 mM ATP, 5 mM DTT, 25% PEG8000) from kit, 1 μ l T4 DNA Ligase (1U/ μ l) and 3:1 (molar ratio) insert DNA: vector DNA were mixed together in a microcentrifuge tube. The reaction mix was incubated at room temperature for 2 to 4 hours or for 16 hours at 16°C. Bacterial transformation was then carried out as in the Site Directed Mutagenesis section, but Zymocompetent cells were used as the "ultracompetency" needed in mutagenesis reactions is not required for this routine subcloning.

Transfection of Mammalian Cells

Transient Transfections. Two different methods of introducing plasmid DNA into mammalian cells (magnetic or cationic lipid polymer-mediated transfection) were used in this work. The magnetic method was carried out as described by the manufacturer (OzBiosciences, France) for the Polymag Magnetofection reagent, in which the DNA is adhered to microscopic magnetic particles prior to bathing adhered cells with the DNA/magnet particle suspension, then placing the dish on an ultrastrong magnet, forcing the microscopic/DNA coated particles to pierce the membranes of the cells. The Mirus Transit-3T3 or NEB TransPass D1 reagents are cationic lipid vesicle-based reagents, that carry the complexed DNA through the membrane using those membrane-permeation qualities. The tissue culture plates (0.5×10^6 cells per 100 mm plate) were prepared 1 day before the transfection. The incubation time of plasmid DNA/liposome mixture with the cells was about 24 hours at 37°C with 10% CO₂, after which fresh medium was added to the plates. Two days after transfection, the cells were harvested or processed for selection, depending on the exact experiments. The transfection efficiency was assessed by using fluorescence microscopy for the GFP-fused constructs, or otherwise by indirect immunofluorescence. Transient transfections of WI-38 and NIH 3T3-L1 cells with pCMV6-AN-GFP-ZMPSTE24 were performed using Polymag Magnetofection Transfection Reagent, per manufacturer instructions.

Stable Transfections. To generate the RheoSwitch Inducible Gene Expression Cell line system, RheoSwitch NIH3T3-47 cells (“Rheoswitch 3T3 cells”) were purchased already harboring the optimally selected pNEBR-R1 regulator plasmid encoding the RheoReceptor-1 and RheoActivator protein. The pNEBR-X1-Hygro EGFP

and pNEBR-X1-Hygro EGFP-Myc-Lamin A/ Lamin A-L647R/ Lamin A del50 constructs, as described under Plasmid Constructs section, were transfected with TransPass D1 according to the manufacturer's instructions. The day before transfection, Rheoswitch 3T3 cells were seeded at 1.5×10^5 cells/cm². The cells were then transfected with the inducible pNEBR-X1-Hygro constructs. After 30 hours, 500 nM RSL1 or GenoStat ("induction reagent") was added to medium. The cells were incubated/induced 14 hours and observed for GFP expression by fluorescence microscopy. Following visual confirmation of transfection, medium containing induction reagent was removed, cells were rinsed 2 times with 1X PBS, split, and plated out under sparse conditions in medium containing both G418 and Hygromycin to establish stable cell lines. Single colonies were picked, reseeded, and expanded. From expanded clonal populations, cells were plated, induced 24 hours, then observed for GFP expression. Three clonal lines with the strongest intensity of expression were selected for each construct and further expanded, while other clones were discontinued. Finally, 1 clone was selected as the best expresser and cultivated as the primary cell line for the stable expression of each construct.

Cotransfection. This process involved transient transfection of GST-Pin1 as an additional plasmid vector into the RheoSwitch Cell Lines (which already stably harbored the pNEBR-X1-Hygro-EGFP-Lamin A-L647R construct). The cotransfection was performed using Mirus TransIT-3T3, per manufacturer recommendations, and as noted above. Cells were harvested after 48 hours.

Methods II.: Protein Chemistry and Biochemistry Methods

Preparation of Mammalian Cell Lysates

In order to analyze target protein expression in mammalian cells, cells were typically lysed in RIPA buffer. Transfected cells were washed with PBS 2 times at room temperature, then 0.25% Trypsin/EDTA was added, followed by incubation at 37°C until the adherent cells were detached. DMEM medium with fetal calf serum was added to neutralize the activity of Trypsin. The cells were transferred to a fresh 15 ml tube and centrifuged at 1500 rpm for 3 minutes. Ice-cold PBS was added to wash the cell pellet 2 times. The cell pellet was resuspended in 600 µl of RIPA buffer, containing Halt Protease and Phosphatase Inhibitor Cocktail (1X). The resuspended cells were transferred to a fresh microcentrifuge tube and incubated on ice for 30 minutes. The sample was vortexed for 30 seconds every 10 minutes. Then the solution was centrifuged at 10,000 x g for 10 minutes at 4°C. The supernatant was transferred to a new microcentrifuge tube. The cell pellet was resuspended in an additional 300 µl Lysis Buffer with inhibitors, sonicated on ice (on low setting), 5 times in 3 second pulses with 10 seconds between pulses. After an additional centrifugation at 10,000 x g for 10 minutes at 4°C, the supernatant was transferred to the microcentrifuge tube containing the previous supernatant, and vortexed to mix well, forming the total cell lysate. Lysates were stored briefly at -20°C, or at -80°C for longer term storage, thawed, and kept on ice during experimental set-up. Protein concentration was assayed using Pierce BCA, micro BCA, or detergent-compatible protein assay methods, per kit instructions, with measurements taken spectrophotometrically, comparing to a standard curve generated

by measurement of a dilution series, in the lysis buffer used for the cell lysates being assayed, using BSA protein standard of known concentration.

Cellular Compartment Lysate Fraction Preparation

Cytoplasmic and Nuclear fractions were separated, per manufacturer instructions, using the NE-PER nuclear protein extraction method. Stepwise lysis of cells and centrifugal isolation of nuclear and cytoplasmic protein fractions, involving a short series of progressively more harsh lysis buffers and faster speeds of centrifugation, using a benchtop microcentrifuge. Whole cell fractions were maintained for each lysate that underwent fractioning, as reference.

Electrophoretic Separation of Proteins

Protein samples were solubilized by boiling in the presence of 1X NuPAGE LDS Buffer, with 10% reducing agent (Bond Breaker TCEP or DTT). An aliquot of the sample was loaded onto a precast 1-dimensional denaturing NuPAGE Novex 4-12% Bis-Tris SDS PAGE gel (typically 50 µg total protein for most applications, or other, as noted for each experiment). Electrophoresis was performed at a constant 200 volts, running time approximately 45 minutes to 1 hour, dependent upon the sizes of the expected protein bands. Commercial protein standards enabled the estimation of apparent molecular weights.

Protein Blotting

Protein transfer from gel to PVDF or nitrocellulose membrane was carried out by electroblotting in a dry electroblotter, the iBlot, as described by the manufacturer (Invitrogen/Life Technologies, USA). The protein transfer process lasted approximately 7 minutes. After transfer, gel and membranes were checked to verify the protein standards were clearly visible on the membrane.

Immunodetection (Western Blotting)

The Western Blotting procedure was performed according to the protocols from Santa Cruz Biotechnology, Cell Signaling Technology, and Abcam. Briefly, the membrane was blocked against nonspecific binding by incubating the membrane in freshly prepared 1X TBST/5% Nonfat Milk (or BSA, if instructed by antibody manufacturer) for 1 hour at room temperature or overnight at 4°C. The membrane was washed in 1X TBST 5 times (2 x 1 min, 3 x 5-10 min) and incubated with primary antibody diluted at appropriate concentration for the antibody in 1X TBST/5% Nonfat Milk (or BSA) for 1 hour at room temperature or overnight at 4°C. The membrane was washed in 1X TBST 5 times (2x1 min, 3x 5-10 min), and incubated with the secondary (2°) antibody-HRP (horseradish peroxidase) conjugate at room temperature for 1 hour. After this, the membrane was washed in 1X TBST 5 times (2x1 min, 3x 5-10 min) at room temperature to remove excess 2° antibody conjugate. The specific protein bands were detected using ECL chemiluminescence reagent and developed for 5 minutes at room temperature. Excess chemiluminescence reagent was drained, and membranes with were wrapped in plastic film and imaged on a Fuji Chemiluminescence Imaging

System, with digital photo-documentation using Multi Gauge Software that was also used for digital semi-quantitative densitometry analysis for graphics production in some experiments.

Zmpste 24 Protease Activity Assay

Zmpste24 was assayed in triplicate on crude human diploid fibroblast nuclei from cells essentially as previously described²⁶. A significant modification was that the substrate used was the simple hexapeptide: RSY*LLG, where Y* is a ¹⁴C-labeled tyrosine. The labeled peptide was prepared by conjugation with ¹⁴C-methylamine-glutaraldehyde, also as previously described¹⁰⁶. Briefly, nuclei were prepared from cell pellets by resuspending the cells to a final density of 4×10^8 cells/ml in lysis buffer. Nuclei were isolated after 2 more washes, in the same buffer, and pelleting by centrifugation in a Beckman J-14 rotor for 10 minutes at 365 x g. For assay, the nuclei were resuspended in the same buffer without NP-40. Protein concentration was obtained by means of the Micro BCA Protein Assay Reagent Kit. The endoprotease reaction is initiated by the addition of ¹⁴C-labeled peptide (RSY* LLG, final concentration: 5 μ M) to the nuclear preparation in a final volume of 200 μ l in 10 mM MES, pH: 6.0. The reaction stopped at the end of 20 min by the addition of 5 μ l of glacial acetic acid. The RSY* peptide reaction product was isolated by reverse phase thin layer chromatography (Analtech, Inc. Newark, DE) and visualized by autoradiography. A synthetic, ¹⁴C-RSY* peptide standard was run on each plate to aid in the identification of this expected product. The amount of labeled RSY formed in the

assay was determined by scraping the appropriate spots into tubes and quantitation of radioactivity with a gamma counter.

Peptide Phosphorylation Residue Mapping by Edman Degradation

This assay detects phosphorylation of amino acid residues. HeLa cells containing a Doxycycline-Inducible GFP-LA or GFP-Progerin (A gift from Dr. R. Goldman, Northwestern University) construct were induced for expression for 24 hours prior to labeling, as described in “Cell Culture” section. Labeling of phosphopeptides was achieved by removing growth medium from adhered, induced cells, rinsing with phosphate-free medium containing 10% phosphate-reduced fetal-bovine serum, doxycyclin, and [^{32}P]-orthophosphate (1mCi/ml). Cells were incubated overnight at 37°C in 5% CO_2 ^{107,108}. Lysates were prepared in immunoprecipitation buffer from expression induced, phospho-labeled cells expressing GFP-fused wild type LA or GFP-Progerin that had been incubated overnight with ^{32}P to label phospho-proteins. Immunoprecipitation was performed with anti-GFP antibody bound to Protein A-conjugated sepharose beads overnight at 4°C. Immunoprecipitated protein was digested with 3-bromo-3-methyl-2-l(2-nitrophenyl)thiol-3H indole (BNPS-skatole), as previously described¹⁰⁹. Briefly, cleavages were performed in 70% distilled acetic acid 0.1%/phenol for 48 hours at room temperature by using a 10-fold excess of the reagent. After the addition of β -mercaptoethanol (10-fold excess) and a further incubation for 5 hours at 37°C, the excess BNPS-skatole was extracted with ethyl acetate and the resulting aqueous phase dried by evaporation. The protein was precipitated 1 hour in the presence of BSA and 15-20% ice cold trichloroacetic acid (TCA) then centrifuged at 3000 rpm for 5 minutes at 4°C. Supernatant was removed and pellet was centrifuged

again to remove additional supernatant before washing with ice cold absolute ethanol. Ethanol supernatant was removed in 2 additional centrifugation-supernatant removal steps, and the pellet was air dried then resuspended in 250 μ l 1X LDS Sample Buffer. 25 μ l aliquots of the suspensions were loaded onto SDS gels alongside protein ladders, electrophoresed, and transferred to PVDF by electroblotting. Coomassie staining revealed 5 peptide fragments generated by the BNPS-skatole, and the C-terminal band was identified by Western blot with an antibody directed to C-terminal Lamin A. Using the staining gels as a guide, the portions of the PVDF membranes containing the Western Blot-identified C-termini were excised and incubated with trypsin^{110,111}. To avoid the formation of oxidation-state isomers, the protein was oxidized to completion by resuspension of the TCA pellet in 50 μ l cold performic acid and incubating for 1 hour on ice, before adding 400 μ l deionized water, freezing, and lyophilizing. Manual Edman degradation was initiated by resuspending the lyophilized pellet in 50 μ l 6 M HCl and incubating for 1 hour at 110°C to hydrolyze the protein to liberate the individual phosphoamino acids. After additional lyophilization to remove HCl, Hunter Thin Layer Electrophoresis (HTLE) was performed as directed for phosphoamino acid analysis by the manufacturer (CBS Scientific, USA), and as previously described¹¹².

Preparation of Cell Extracts for Mass Spectrophotometry

Proteins were separated and purified by SDS-PAGE, visualized by Coomassie staining and the appropriate bands excised. The isolated proteins were treated with iodoacetamide and digested with trypsin. MALDI-TOF was performed with a PerSeptive

Voyager DE-RP mass spectrometer in the linear or reflector mode by staff at the Protein Chemistry Core Facility at Columbia University.

Methods III.: Cell Biology Methods

Cell Culture-General Cell Culture Techniques

All mammalian cell lines were cultured in a humidified incubator at 37°C with 5% or 10% CO₂, per cell requirements. Cell culture work was done in a laminar-flow hood for which sterility was promoted by UV light treatment at all times when not in use. All work surfaces within, and materials used inside the hood were surface-cleaned with 70% ethanol before and after work in the hood.

HeLa cells, BJ human diploid fibroblasts, and WI-38 human diploid fibroblasts were plated in standard DMEM growth supplemented with 10% fetal bovine serum (FBS) in 5% CO₂, at 37°C. Tet-On HeLa cells containing pEGFP-C1-Myc-LA/LA-del50 had 2 µg/ml doxycyclin added to the growth medium for 24–50 h when induction of expression was desired only. All 3T3 cells were cultivated in DMEM supplemented with 10% calf serum (CS) and incubated at 37°C with 5% or 10% CO₂. As the DMEM formulation contains 3.7% NHCO₃, 10% CO₂ was used to prevent ammonia buildup in the medium, when required to optimize growth pH for the transfected cell cultures, as recommended by NEB and Invitrogen. DMEM from ATCC was also used, and as it contains 1.5% NHCO₃, 5% CO₂ was used. The fibroblast RheoSwitch Cell Line NIH3T3–47 (“Rheoswitch Cells,” New England Biolabs, Frankfurt, Germany) were derived from mouse NIH 3T3 cells, stably transfected with pNEBR-R1 Vector (“Regulator Plasmid,” see details below describing plasmid constructs), and selected for

optimal RSL1 inducible expression properties. These cells were additionally supplemented with 800 µg/mL G418 antibiotic as selection reagent to maintain the stable transfection with the Regulator Plasmid, as well as 200 µg/ml Hygromycin B to maintain the Expression Plasmid.

Induction of Rheoswitch Expression System

RSL1 ligand (New England Biolabs, Frankfurt, Germany) or GenoStat (Millipore, Billerica, MA, USA) are both synthetic diacylhydrazine [(N-(2-ethyl-3-methoxybenzoyl)-N'-(3,5-dimethylbenzoyl)-N'-tert-butylhydrazine]. Diacylhydrazine is one member of a family of compounds that have been found to act as nonsteroidal ecdysone agonists and can function as gene inducers^{113,114}.

Indirect Immunofluorescence and Protein-Protein Co-Localization in Mammalian Cells

To examine intracellular protein localization, fluorescent microscopic analysis of the green fluorescent protein-fused proteins was used. Growth medium was removed prior to visualization, cells were rinsed with 1X PBS, and medium was replaced using DMEM without additives (including no Phenol Red) for visualization under fluorescence microscopy. The cells were cultured in coverslip chamber cell culture dishes or plated as usual in culture dishes and harvested by trypsinization prior to transferring to coverslip chamber dishes. For microscopic visualization using indirect immunofluorescence, cells were plated on glass coverslips in culture dishes, treated, and incubated as per the requirements of the specific experiment, then rinsed with 1X PBS prior to fixing by incubation in 4% formaldehyde PBS (pH 7.4) for 15 minutes at

room temperature, or 100% methanol for 5 minutes at -20°C. Following 3 washes in PBS, the cells were permeabilized with 0.2% Triton X-100 in PBS for 5 minutes on ice, quickly washed, and blocked with 10% BSA in PBS for 5 minutes on ice. The coverslips were incubated for 1 hour at room temperature with primary antibody at concentrations noted per experiment. Cells were then washed and incubated at room temperature for 1 hour with fluorophore-conjugated 2^o antibody. After 3 final PBS washes, DAPI-perfused antifade mounting edium was used to seal the stained cells between the coverslip and a microscope slide. Images were obtained by on a Nikon Diaphot 200 microscope equipped with a Photometrics Sensys cooled CCD digital camera.

Cell Cycle Manipulation

For serum starvation experiments, medium was removed from actively growing cells, cells were rinsed with PBS, and medium was added containing the minimum amount of serum required for survival (0.5% serum for HeLa, WI-38, or BJ cells; 0.3% serum for the 3T3 cells). The minimal serum is insufficient to supply mitogens for cell proliferation. Cells were collected at stated time points after serum removal. For contact inhibition experiments, the cells were seeded sparsely (2.5×10^3 cells/cm²) or densely (1×10^5 cells/cm²) and cultivated for indicated times.

Cell Cycle Analysis Methods:

Cell Cycle Analysis by Flow Cytometry. Cells were plated at the same density and control and experimental cells treated the same way except that no DMSO was added instead of induction reagent, in a volume to duplicate the DMSO vehicle of the

induction reagent used for the experimental cells. Cells were harvested by trypsinization using 0.25% Trypsin-EDTA, washed 3 times with 5-10 ml 1X PBS, and fixed in ice cold 70% ethanol, added dropwise with gentle trituration, with tubes in ice, to a volume of 3-5 ml ethanol. Tubes were then transferred to -20°C for a minimum of 2 hours, or overnight to allow for complete fixation. To stain DNA for flow cytometric DNA content/cell cycle analysis, cells were centrifuged to form a loose pellet, washed 3 times with 10 ml PBS, then after removal of supernatant PBS, cells were spun again to remove residual PBS. After removal of ethanol, cells were stained with 50 $\mu\text{g}/\text{ml}$ Propidium Iodide/RNase in the dark for 30 minutes at room temperature and analyzed on an Accuri C6 flow cytometer. Collected data were further analyzed by using FCS Express V3 or ModFit LT 3.2 cell cycle analysis software programs. Gates were set over each of the sub-G1, G0/G1, S, and G2/M peaks, and then the percentages of cells in different cell cycle phases were calculated to determine percentages of cells in different cell cycle phases.

Assay of Cellular Proliferation by BrdU Incorporation. 3T3 cells or L647R RheoSwitch cells were seeded in triplicate at 4×10^3 cells/well in a 96-well plate and incubated overnight. Cells were then treated with various concentrations of GenoStat inducer, or DMSO as vehicle control, for 48 hours. Finally, 10 μM BrdU was added to the plate and cells were incubated for 4 hours. BrdU incorporated into DNA was detected by incubation with monoclonal anti-BrdU antibody linked to horseradish peroxidase (HRP). The HRP substrate 3,3', 5,5'-tetramethyl-benzidine (TMB) was used to develop the color. Stop solution was added after 30 minutes of development, and absorbance at 450 nm was measured using a platereader, with quantification of

absorbance representing amount of BrdU incorporated into cells to indicate level of proliferation occurring in the corresponding cells.

Assay of Cellular Proliferation by Incorporation of [³H]-Thymidine. This proliferation assay was performed in conjunction with the Zmpste24 activity assay. DNA synthesis was monitored by pulse labeling for 30 min with (1 uCi/ml) [³H]-thymidine at various times. The plates (1 x 10⁶/100mm plate) were washed 2 times with cold PBS (1X), and the cells harvested by scraping with a rubber policeman into 1 ml of PBS. The suspension was homogenized by sonication, and a 0.2-ml aliquot was mixed with 1 ml of 10% cold trichloroacetic acid (TCA). The insoluble material was collected on a Millipore filter and washed with cold TCA. The filter was dried and the radioactivity incorporated was determined by liquid scintillation counting.

Assay of Cellular Proliferation by Detection of Ki-67. Ki-67 is a nuclear protein commonly used as a negative marker for quiescence, as G₀ is the only cell cycle phase in which it is not found. Detection was carried out by immunostaining with an anti-Ki67 primary antibody and a fluorescence-conjugated secondary antibody, as described in “Indirect Immunofluorescence” on L647R PreA construct Rheoswitch cells that were plated on coverslips and treated with induction reagent or DMSO, as indicated.

Presence of Ki-67 indicates active cell cycling.

Methods IV.: Gene Expression Analysis Methods

Whole Genome Exon Transcript Microarray

Total RNA was isolated and pooled from 3 culture dishes 48-hours posttransfection, for whole genome microarray gene expression profiling, using an

Affymetrix Mouse Exon 1.0ST GeneArray, as directed by the Affymetrix GeneChip Whole Transcript (WT) Assay for Exon Chips Labeling Manual Ver 4 (Affymetrix, Santa Clara, CA). Processing of the GeneChip and initial extraction of raw data was performed at the University of Tennessee-Knoxville, Microarray Corelab Facility. In brief, RNA reduction was performed using a RiboMinus kit from Invitrogen using 1 µg total RNA starting material, which was subjected to first and second strand cDNA synthesis with the GeneChip Sample Cleanup Module for cRNA. The resultant cRNA product was quantified with the Nanodrop ND-1000. A second round of cDNA synthesis was performed with the GeneChip WT cDNA synthesis kit with 10 µg of cRNA. The remaining cRNA strand was hydrolyzed with RNase H and the single-stranded cDNA was isolated with the GeneChip Sample Cleanup Module for cDNA. The single stranded cDNA was quantified by Nanodrop and 5.5 µg of ssDNA was fragmented to 50-200 bp with WT Terminal Labeling kit UDG and APE1 enzymes. The fragmented ssDNA was terminally labeled with the DNA labeling reagent and TdT enzyme from the kit. A hybridization cocktail was prepared with the resultant cDNA and recommended controls then injected into the Mouse Exon 1.0ST arrays prior to hybridization for 16 hours at 45°C in Affymetrix's 640 Hybridization Oven. Hybridized arrays were washed and stained using the Affymetrix 450 Fluidics Station and the GeneChip Hybridization Wash and Stain kit. Arrays were held in the dark at room temperature and immediately scanned with the Affymetrix 7G GeneChip Scanner. Resultant raw signal files were imported into Partek Genomics Suite 6.4 (St. Louis, MO) using the RMA (robust multichip algorithm) for normalization. All data were log₂ transformed during the importation process, and a PCA (Principle Components Analysis) plot was generated

with all probe sets to determine that samples grouped according to treatment. Initial results indicated the chips grouped according to treatment as expected (quality evaluation plots not shown). A gene level summary was created as recommended by the EXON flow path in Partek using the following parameters: Mean, Exclude outliers above and below 3 standard deviations from the mean. Detection of differentially expressed genes was performed by ANOVA with exclusion criteria of $p\text{-value} \leq 0.05$. After receiving the raw data, these were uploaded to Ingenuity Pathways Analysis™ Software (Ingenuity® Systems, www.ingenuity.com) for further evaluation. This software was used to formulate a “Functional Analysis,” a “Canonical Pathways Analysis,” and to generate “Networks” and “Pathways” of the implicated molecules. Molecules from the dataset that met the differential gene expression value cutoff of $p\text{-value} \leq 0.05$, as determined by the ANOVA analysis from the Partek software, were considered for the Ingenuity analyses. The Functional Analysis identified the biological functions and/or diseases that were most significant to the dataset, while the Canonical pathways analysis identified the pathways from the IPA library of canonical pathways that were most significant to the data set. For the Functional Analysis, molecules from the dataset were associated with biological functions and/or diseases in the Ingenuity Knowledge Base, and a Right-tailed Fisher’s exact test was used to calculate a p-value determining the probability that each biological function and/or disease assigned to that data set is due to chance alone. The Canonical Pathway Analysis associated the molecules with a canonical pathway in the Ingenuity Knowledge Base. The significance of the association between the data set and the canonical pathway was measured in 2 ways:

- 1) a ratio of the number of molecules from the data set that map to the pathway divided

by the total number of molecules that map to the canonical pathway is displayed. 2) Fisher's exact test was used to calculate a p-value determining the probability that the association between the genes in the dataset and the canonical pathway is explained by chance alone. For the "Network Generation," the molecules, were overlaid onto a global molecular network developed from information contained in the Ingenuity Knowledge Base. Networks were then algorithmically generated based on their connectivity. The "My Pathways" Path Designer produces graphical representations of the molecular relationships between molecules. Molecules are represented as nodes, and the biological relationship between 2 nodes is represented as an edge (line). All edges are supported by at least one reference from the literature, from a textbook, or from canonical information stored in the Ingenuity Knowledge Base. Human, mouse, and rat orthologs of a gene are stored as separate objects in the Ingenuity Knowledge Base but are represented as a single node in the network. The intensity of the node color indicates the degree of up- (red) or down-(green) regulation. Nodes assayed in the dataset but not revealing a statistically significant change in regulation are in gray, while genes not assayed but contained in the IPA knowledge base as related to the assayed genes are represented as white nodes. Nodes are displayed using various shapes that represent the functional class of the gene product. Edges are displayed with various labels that describe the nature of the relationship between the nodes (e.g., P for phosphorylation, T for transcription).

Cell Cycle Pathway-Focused RT-qPCR Array

Cell cycle gene expression was determined using SABiosciences RT-qPCR Cell Cycle Gene Expression Analysis Assay (RT² Profiler PCR Array Cell Cycle Pathway

Focused Assay), and the My iQ5 system (Bio-Rad) according to the manufacturer's protocol. In preparation for the cells from the Rheoswitch 3T3 inducible construct expression cell lines (as described in "Development of a Model System of Inducible Stable Lamin Isoform Expression Cell Lines" section), cells were plated in standard growth medium for the Rheoswitch Inducible cell lines (as described in Cell Culture section) at 3×10^6 cells/50 cm² tissue culture dish and allowed to adhere in the incubator for at least 4 hours prior to adding induction reagent (Genostat) or DMSO. 500nM Genostat was used for induction, with a corresponding volume of DMSO added to the media of control (uninduced/NI "Not-Induced") plates. The cells were incubated for an additional 24 hours, at which time they were collected by brief trypsinization, which was neutralized by addition of serum-containing medium, prior to gentle (1,300 x g) centrifugation in a 50 ml conical tube for 5 minutes, followed by rinsing 2x in cold 1X PBS. Cells were then flash frozen in liquid nitrogen and stored at -80°C until RNA isolation was performed. For the RNA isolation, the cells were thawed briefly on ice, 3 samples were pooled for each genotype and purified using the Qiagen™ RNeasy Mini kit protocol. RNA quantity and purity were determined using a NanoDrop ND-1000, and aliquots were submitted to the ETSU Molecular Biology Core Facility for assessment of RNA integrity by determining the 28S/18S ratio and RNA integrity number using the Expert Eukaryote Total RNA Nano assay on the Bioanalyzer 2100 (Agilent Technologies, USA). Results indicated excellent RNA quality (RNA Integrity Scores ranged from 9.7/10-10/10), and concentrations varied from 59 ng/μl to 768 ng/μl. A quantity of 2μg of high-quality RNA (260/280 ratios slightly higher than 2.0 and 260/230 ratios higher than 1.7, RIN>8.0) for each pooled sample was used to perform each cell

cycle gene pathway-focused quantitative RT-PCR (RT-qPCR) array plate assay. The assays were performed as directed by the manufacturer, beginning with Genomic DNA Elimination, followed by first strand cDNA synthesis using the RT² First Strand cDNA Kit. All RT-qPCR reactions use the RT² SYBR Green qPCR Master Mix. Each cDNA sample is used to prepare a single reaction mix aliquoted equally into all wells of a single 96-well reaction plate. This plate contains a primer set for 84 separate cell cycle pathway-focused genes, along with a standard set of 5 routinely used “housekeeping genes” for normalization of experimental runs. In addition, each plate has 3 control wells for demonstration of genomic DNA contamination, reverse transcription efficiency, and PCR efficiency. All significant changes in gene expression levels are reported in the article; the complete list of genes assayed on the array are presented in the full assay results in Appendix A. Further information can be found at the manufacturer's website (http://www.sabioscience.com/rt_pcr_product/HTML/PAMM-020A.html).

The BioRad iQcycler Raw data were analyzed on BioRad iQ5 software, with parameters set uniformly for all plates as follows: Data Analysis Window was set at Full cycle scan, Rolling Boxcar Intracycle Digital Filter, PCR Baseline Subtracted Curve Fit Analysis Method, with Base Line Cycles set automatically by the software using the built-in optimization algorithm, and a baseline threshold set at 61 (above background and within lower $\frac{3}{4}$ of logarithmic amplification phase for all samples assayed). For each gene included on the array, the threshold cycle (C_t) data, representing the cycle number at which amplification for a given analyte surpassed the baseline threshold, indicating amplification above background, and, once normalized, represents the amount of a given transcript that is present within the assayed sample. The C_t data

were assembled into an Excel upload file per SABiosciences Data Analysis Instructions and uploaded to the SABiosciences web-based data analysis module. In determining which genes available on the array to use as our reference (“housekeeping”) gene, Heat-Shock Protein 90 (Hsp90) was selected because no significant effect on its expression level had been detected in any of our gene expression analyses involving these lamin constructs or the EGFP-only construct, compared to uninduced cells. Hsp90, along with data for the Reverse Transcription Control and Positive PCR Control, were used to normalize the data for comparison. Initial data from 2 array plate assays of uninduced cells (DMSO-treated/NI, “Not Induced”), per cell line (wtLA, L647R PreA, and del50 cells), were compared to each other to establish consistency of “baseline gene expression” among uninduced cells. The establishment of a consistent baseline of gene expression between uninduced cells is critical for comparative evaluation of gene expression changes, between each cell line, that are due to induction of expression of the lamin constructs. As the cells used in development of the cell lines were each originally taken from the same parent culture, transfected with the different constructs and then clonally selected, we expected to see only the most subtle differences in gene expression between the 3 uninduced cell lines. Upon comparison to each other, we found more gene expression variation among the uninduced cell lines than we had expected. Therefore, subsequent experiments were postponed for wtLA and del50, and a triplicate assay for statistical relevance focused only upon comparing L647R PreA induced cells and the uninduced cells of the same line. After determining cell line-cell line variation of gene expression was exhibited among uninduced cells of each cell line, a third assay of uninduced cells was performed only for the L647R PreA

cell line, followed by a triplicate set of array plates for the induced L647R PreA cell line. The gene expression profile of the induced L647R PreA-expressing cells was compared to the uninduced cells of the same line. Using the SABiosciences data analysis software, Volcano Plot analyses were prepared, representing the statistical significance of gene expression changes. In those graphic analyses, the X-axis plots the log₂ of the fold-differences, while the y-axis plots their p-values based on the student's *t*-test of the uploaded replicate raw C_t data. Symbols outside the gray area indicate fold-differences larger than the user defined threshold, which was set to 2-fold-expression for these analyses. The red symbols identify up-regulated genes, and the green symbols identify down-regulated genes. Symbols in the Volcano Plots above the blue line identify fold-differences at least as statistically significant as the defined threshold, which was set to p<=0.05. The Volcano Plot can be found as Appendix B. Using the Volcano Plot data, Excel graphics were prepared for further visual comparison of the data, and are included within Chapter 3 Results Section text.

RT qPCR Cycling Conditions: Cycles—Duration--Temperature
 1 cycle--10 minutes--95°C

40 cycles-- $\left\{ \begin{array}{l} 15 \text{ seconds } 95^{\circ}\text{C} \\ 1 \text{ minute } 2 \text{ } 60^{\circ}\text{C} \end{array} \right.$

Followed by 2-Step Amp+Melt.tmo Dissociation (Melting) Curve, as recommended by SABiosciences for BioRad: iCycler®, MyiQ cycler, iQ5.

Cell Cycle Control Pathway-Specific Antibody Array (Protein Array)

The Full Moon Biosystems Cell Cycle Control Phospho Antibody Array (PCC238) Assay was performed as per manufacturer instructions. Briefly: L647R PreA cells that had been plated in 2 50 cm² cell culture dishes and induced 72 hours using

500 nM GenoStat, or, for control, treated with DMSO for 72 hours, were rinsed twice in 1X PBS, before adding 500 μ l of ice cold 1X PBS containing 1X Halt Protease and Phosphatase Inhibitors, and using a cell scraper to scrape the cells from the dish culture surface and transfer to a microcentrifuge tube on ice. Culture density at harvest was approximately 60-70%. Cell lysates were prepared as previously described, except using the Protein Extraction Buffer provided in the Full Moon Biosystems Antibody Array Kit, to which Halt Protease and Phosphatase Inhibitors had been added (1X final concentration). The protein concentration was measured by performing a micro BCA assay per manufacturer protocol (Pierce/ThermoFisher), and concentration was adjusted to 10 μ g/ μ l using additional Lysis Buffer with inhibitors. Lysates were packaged in parafilm-secured microcentrifuge tubes and shipped on dry ice overnight to the Full Moon Biosystems Facility in California, USA, to the attention of Dr. Yaping Zong, who graciously performed the next steps of the assay in his laboratory, where conditions and equipment are optimized for the processing.

Proteins were labeled in Labeling Buffer, using the Biotin/Dimethylformamide, both reagents from the Antibody Array kit, with a 2-hour incubation at room temperature. Stop Reagent (from the kit) was added and the mix was incubated an additional 30 minutes at room temperature, with mixing. Full Moon Biosystems Cell Cycle Control Phospho Antibody Array (PCC238) Slides were submerged in Blocking Buffer (from the kit) and shaken 40 minutes at room temperature. After rinsing the slides with Milli-Q grade water, they were incubated in the Coupling Chamber (from the kit) with 85 μ g of labeled protein sample in 6 ml Coupling Solution (from the kit) on an orbital shaker for 2 hours at room temperature. Slides were removed from the coupling chamber and

washed 3 times with fresh Wash Buffer then rinsed extensively with deionized (DI) water. For detection, each slide was submerged in 30 ml of Cy3-Streptavidin solution (5 µg/ml), and incubated on an orbital shaker for 45 minutes at room temperature in the dark. Slides were then washed 3 times with fresh Wash Buffer and rinsed extensively with DI water, then dried with compressed nitrogen before scanning on the Axon GenePix Array Scanner. PANDA software was used for analysis.

Peptidyl Prolyl Isomerase (Pin1) Inhibition with Juglone

Juglone, a chemical derived from the Black Walnut, has been shown to specifically and irreversibly inhibit the prolyl isomerization/rotamase activity of mammalian/human Pin1, Ess1 in yeast, or parvulin in *E. coli*. Cells were treated with 5-15 µM Juglone for 72 hours, as previously described¹¹⁵.

Lamin A Multi-Isoform Motif Analysis

The publicly available online databases Human Protein Reference Database (HPRD, www.HPRD.org), Phospho.ELM Database (<http://elm.eu.org/>)¹¹⁶ and PhosphoSite (www.Phosphosite.org)¹¹⁷⁻¹¹⁹ were used to survey the LA protein sequence (with a focus on the PreA C-Terminal 66-Amino Acid Residue Fragment), for sites known to be substrates of indicated kinases or binding sites of indicated proteins, or sites known to, in similar context, act as substrates or bind the proteins. The sites were queried, cross-referenced among each other and among published scientific literature. HPRD is a compendium of annotated motifs for which curated literature is cross-referenced to support the indicated interactions with the recognized motifs¹²⁰.

The Phosphosite website is also a curated database of protein phosphorylation information that was valuable. While curated data are maintained in the Phospho.ELM Database, this database also generates predictive interaction information¹¹⁶.

CHAPTER 3

RESULTS

PreA Expression is Detected in Cell Cycle Arrest

PreA expression is not readily detected in proliferating cells but can be induced by conditions that stimulate cell cycle exit, as in quiescence induced by serum starvation, contact inhibition, or as in senescence by passaging cultured cells to high population doublings. Ukekawa and associates described a dramatic increase in PreA expression in cells induced to enter senescence and postulated PreA might cause cells to become senescent in response to a disruption of interaction of chromatin, pRb, or other molecules with mature LA¹²¹. The Kennedy group found short-term overexpression of PreA to reduce cellular proliferation, while they associated long-term overexpression with delayed entry to senescence¹⁰³. Additionally, Ragnauth et al. recently suggested PreA expression occurred prior to vascular smooth muscle cells' arrival at senescence, under inducing conditions, and furthermore, this expression accelerated entry to senescence¹²². To investigate whether PreA expression is directly related to quiescence, as well, we first address the question of whether PreA expression appears to be a side effect or cause of quiescence. Initially, we demonstrated PreA expression when cells are induced to enter quiescence by serum starvation. In Figure 4, immunoblotting of lysates collected from HeLa cells at 24 and 48 hours after removal of serum from the culture reveal increasing accumulation of PreA. Detection of this expression in serum starved cells is in contrast to the absence of detectable PreA in lysates from proliferating cells maintained in full serum. The levels of mLA are consistent, with a minimal degree of decreasing expression as the precursor

accumulates rather than contributing to the continuing supply of processed lamin.

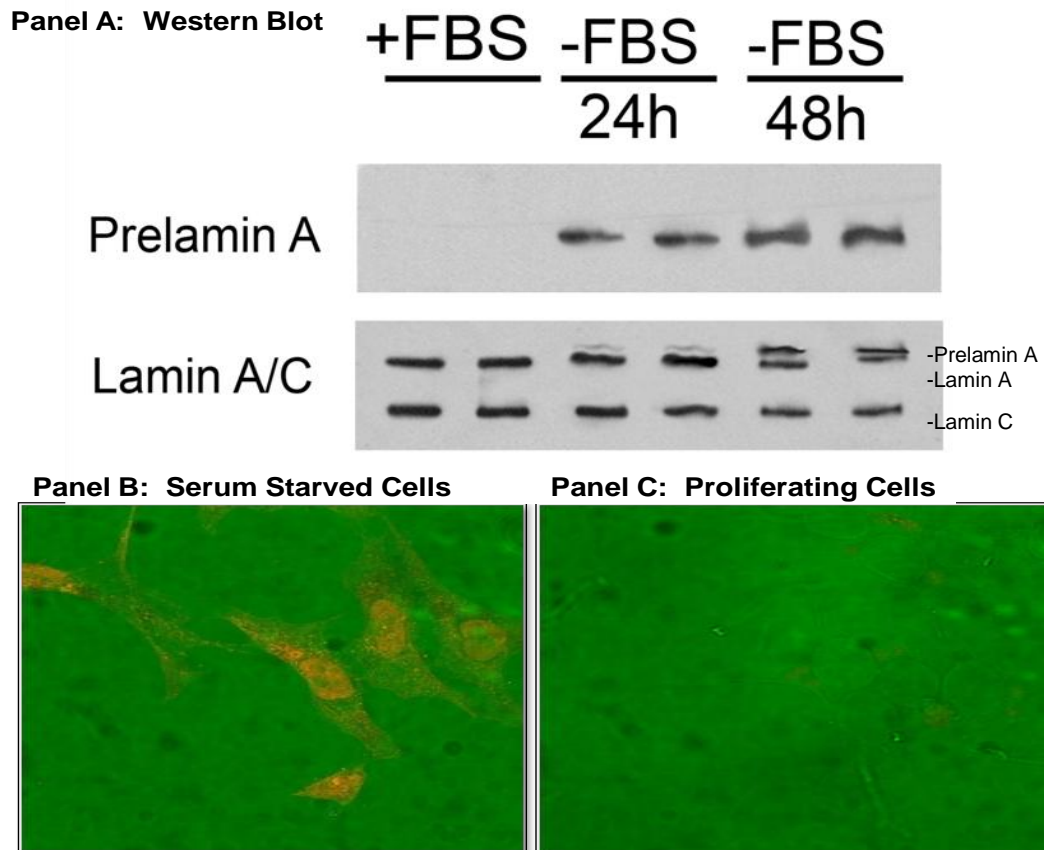


Figure 4. Accumulation of Prelamin A as Cells Enter Quiescence. Panel A: Western Blot of lysates from proliferating HeLa cells in full serum (+FBS), 24 hours and 48 hours after removal of serum (-FBS), using a PreA C-terminus specific antibody (Top blot panel), and an antibody that detects multiple LA isoforms (Lower blot panel). Immunofluorescence using the PreA C-terminus antibody in 48-hour serum starved BJ (human foreskin) fibroblasts (Panel B), and full serum (Panel C).

In Figure 4, the smaller A-type lamin isoform, Lamin C, is demonstrated as a band below the mature LA (mLA) band. PreA presents as an additional band situated above the mLA band, present in the -FBS lanes only, with increased accumulation evident at 48 hours compared to 24 hours of serum starvation. Immunofluorescence using the PreA c-terminus antibody demonstrates PreA accumulation in the nuclei of serum-starved BJ fibroblasts that is completely absent from the proliferating cells in full serum.

Accumulated PreA is Farnesylated and Carboxymethylated

As mitogen deprivation and contact inhibition are able induce quiescence and PreA accumulation, and FTI-treatment of cells also causes quiescence and accumulation of PreA, we asked the question if mitogen deprivation or contact inhibition, then, might interfere with the enzyme-mediated modifications that trigger proteolytic cleavage of PreA? We subjected lysates isolated from serum-starved or contact-inhibited, quiescent cells to analysis by mass spectrometry (Figure 5).

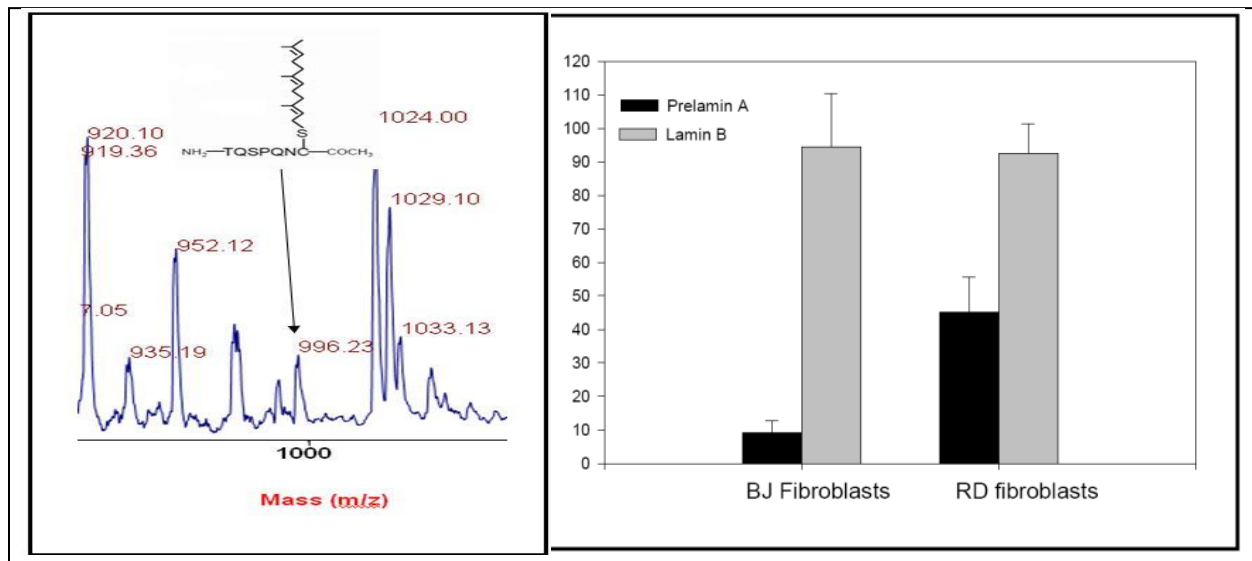


Figure 5. Mass Spectrometry Analysis Reveals Accumulated Prelamin A is Farnesyl-Carboxymethylated (FC'd). A Mass Spectrometry Trace of Serum-starved BJ demonstrates the presence of FC-PreA (arrow), Left Panel. The graphic in the right panel compares the ratio of FC-PreA in proliferating BJ Fibroblasts, to that in RD Fibroblasts (Zmpste24-null or -deficient) which accumulate PreA. Lamin B is permanently FC'd.

As shown in Figure 5, Mass Spectrometry demonstrates accumulated PreA in serum starved or Zmpste24-deficient cells is farnesylated and carboxy-methylated. The farnesylated-carboxymethylated status of PreA in these cells indicates that

accumulating PreA has undergone FC-processing. This means the posttranslational enzymatic processing system that prepares PreA for the Zmpste24-specific cleavage is intact in these cells. Therefore, the accumulation of PreA seen in serum-deprived, quiescent cells is not due to lack of FT or ICMT activity.

Zmpste24 Expression Level Does Not Parallel Activity Level in Quiescent Cells

As we demonstrated, the enzymatic modification pathway that prepares the PreA substrate for proteolytic processing remains intact in quiescent cells, yet Zmpste24 proteolysis fails to occur. We reasoned, therefore, some direct inhibition of the Zmpste24 protease must occur. To investigate if Zmpste24 activity is hindered in conditions that induce quiescence, such as serum starvation, we assayed Zmpste24 activity in proliferating cells and serum starved cells, as they progress toward quiescence. We used a fluorescently-tagged synthetic substrate to measure Zmpste24 activity, and radioactively labeled thymidine to simultaneously measure cell proliferation (Figure 6). Measurement of the fluorescence level produced by cleavage-fluorophore activation serves to indicate the level of Zmpste24 activity in the lysates, while the level of retained radioactivity indicates rate of proliferation of the cells.

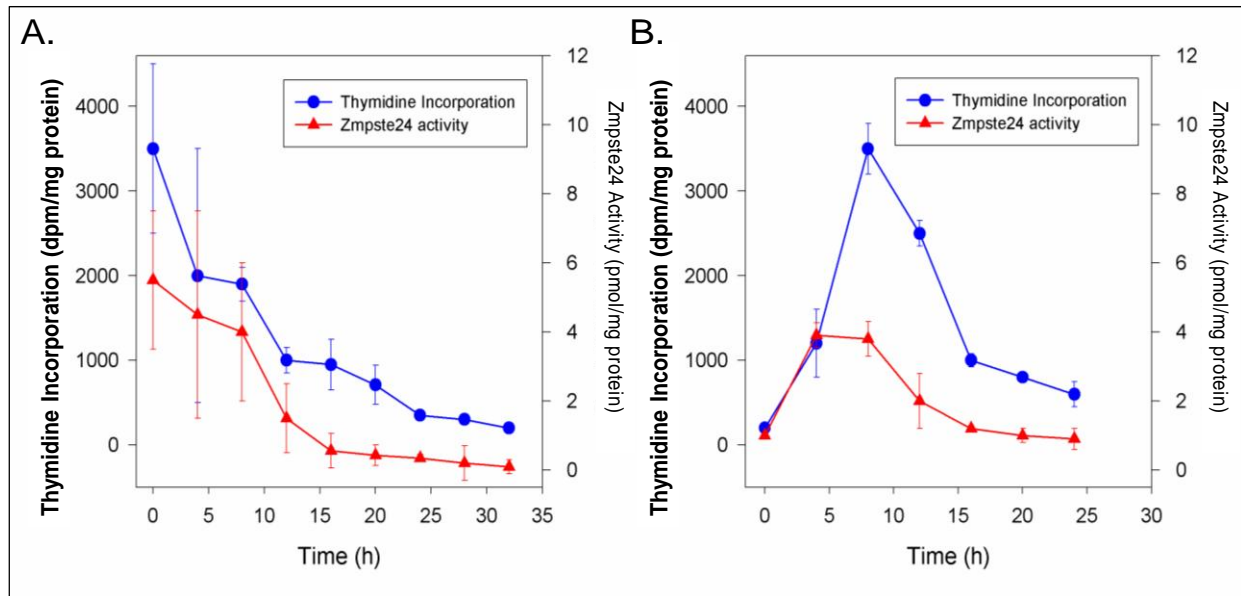


Figure 6. Zmpste24 Activity Decreases Parallel to the Rate of Cellular Proliferation as Serum Starvation Induces Quiescence. Cells were incubated with ^3H -Thymidine for 30 minutes prior to collection of lysates. In Panel A, lysates were collected at the time of serum removal (0 h), and at 4-hour increments over a 32-hour serum deprivation time course. Scintillation counting measured the radioactive nucleotide in the lysate, which indicates the rate of DNA synthesis in the cells assayed, and thus the rate of cellular proliferation (dpm/mg protein, Y1-axis, left). Lysates from the same timepoints were incubated with a fluorophore-conjugated synthetic peptide substrate, homologous to the PreA cleavage site. Zmpste24 cleavage exposes the fluorophore, allowing measurable fluorescence emission. Cleaved substrate was measured in proportion to the input substrate to indicate the level of Zmpste24 activity in the lysates (pmol/mg protein, Y2-axis, right). In Panel B, following quiescence, cellular proliferation and Zmpste24 activity are measured upon return of serum to the cultures. Timepoints are shown on the X-axis.

Clearly, the rate of substrate cleavage declines in parallel to the rate of DNA synthesis, indicating Zmpste24 activity is decreased in quiescent cells and correlates with the accumulating levels of PreA we previously demonstrated. When serum was returned to these cells, proliferation was stimulated, and a concurrent spike in Zmpste24 activity is observed. Proliferation and Zmpste24 activity then gradually decrease as the dividing cells progress toward contact-inhibition-induced quiescence.

Next, we asked whether the mitigation of Zmpste24 activity in quiescence is related to a decreased level of expression of the endoprotease. While it was previously

noted that PreA expression in senescence was accompanied by a decreased expression level of Zmpste24 mRNA¹²¹, it is important to note the transcript was measured after 3 days of senescence induction, and that senescence and quiescence might not, necessarily, follow the same paths. Also, as we found the enzymatic activity level was significantly abolished in less than 10 hours following removal of serum and had reached a state of virtual inactivity within approximately 30 hours, we were interested to measure the expression level of Zmpste24 during the first 2 days after serum removal, as well.

As shown in Figure 7, we measured expression levels of Zmpste24 protein and mRNA transcripts in proliferating cells in full serum culture conditions (10% FBS), and daily during a quiescence-inducing 5-day course of serum starvation (0.5% FBS).

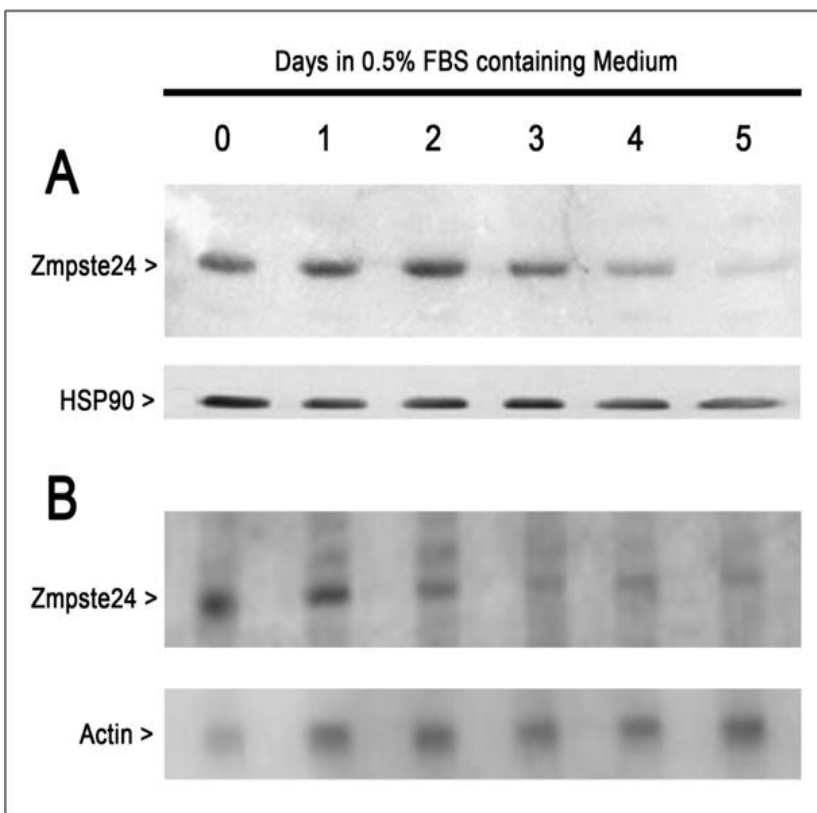


Figure 7. Zmpste24 Expression and Proteolytic Activity Do Not Decrease at the Same Rate with Induction of Quiescence. Western blot (Panel A) using anti-Zmpste24 antibody on lysates collected from proliferating cells in full serum, and at 24-hour timepoints for 5 days after removal of serum from cultures (Anti-Hsp90 loading control). Northern blotting of RNA collected at the same timepoints, was performed with a Zmpste24-directed oligonucleotide probe (Panel B, anti-Actin-probe loading control).

The Western blotting with a Zmpste24 antibody revealed a decrease in the expression of Zmpste24 protein after approximately 3 days of serum starvation (Panel A), while Northern blotting demonstrates the level of Zmpste24 mRNA is diminished after 2 days (Panel B). Both findings are consistent with the previous study¹²¹. Importantly, however, neither the Zmpste24 protein nor transcript levels decrease during the initial 24 hours of serum starvation, in contrast to enzymatic activity that dropped sharply (by at least 60%) within 10 hours. After 48-hours of serum deprivation, the Zmpste24 protein level is unchanged, and although the level of transcript is decreased compared to the full serum- or 24-hour timepoints, a significant quantity of RNA remains, findings that are incongruous with the lack of activity of the enzyme observed within approximately 30 hours of serum removal. In fact, both transcript and protein levels persist at significant, though progressively decreasing, levels for the entire 5 days of serum starvation. Taken together these results demonstrate the expression of Zmpste24 is not significantly decreased in a mode parallel to quiescence-associated accumulation of PreA, suggesting a posttranslational mode of Zmpste24 regulation is likely. Given the tendency of cell cycle regulated proteins to be controlled by phosphorylation, and the presence of several kinase substrate motifs within the amino acid sequence of Zmpste24, indicated by Phosphosite¹¹⁷⁻¹¹⁹, Phospho.ELM¹¹⁶, and HPRD^{120,123-125} databases, phosphorylation seems an obvious likelihood for this regulatory mechanism. This prediction is supported by evidence that at least one residue, Ser-310, undergoes cell-cycle-related phosphorylation, specifically in mitosis¹²⁶. Further studies will reveal if phosphorylation is, indeed, the mechanism controlling Zmpste24 activity, and if so, which residues and kinases are involved.

Overexpression of Zmpste24 Leads to Bypass of Quiescence

Our results indicate PreA accumulation upon stimulation of quiescence corresponds to a decrease in Zmpste24 activity and not directly to a decreased Zmpste24 expression level. However, in diseases in which Zmpste 24 expression is deficient or otherwise inhibited, cells also chronically accumulate PreA. We asked whether, as the reverse, overexpression of Zmpste24 protein may serve to provide sufficient excess of Zmpste24 to overwhelm the activity-limiting mechanism(s) that appear to be initiated upon quiescence-inducing stimuli. If so, we could test whether prevention of PreA accumulation has an effect on cell cycle progression. We used transient transfection of WI-38 human diploid fibroblast cells with a vector expressing the Zmpste24 endoprotease (pCMV6-XL-Zmpste24) to demonstrate effects of Zmpste24 overexpression. Zmpste24 expression was verified by Western Blot (data not shown). Transfected cells and mock-transfected control cells (empty vector) plated at high- or low-density were treated with BrdU to measure cell proliferation. Detection of BrdU foci in treated cells by fluorescence microscopy indicates active proliferation. High density plating normally induces quiescence. Figure 8 reveals WI-38 cells expressing exogenous Zmpste24 continue to proliferate despite high density plating conditions, apparently bypassing cell cycle arrest. These results suggest the cells may be unable to arrest in the absence of accumulated PreA.

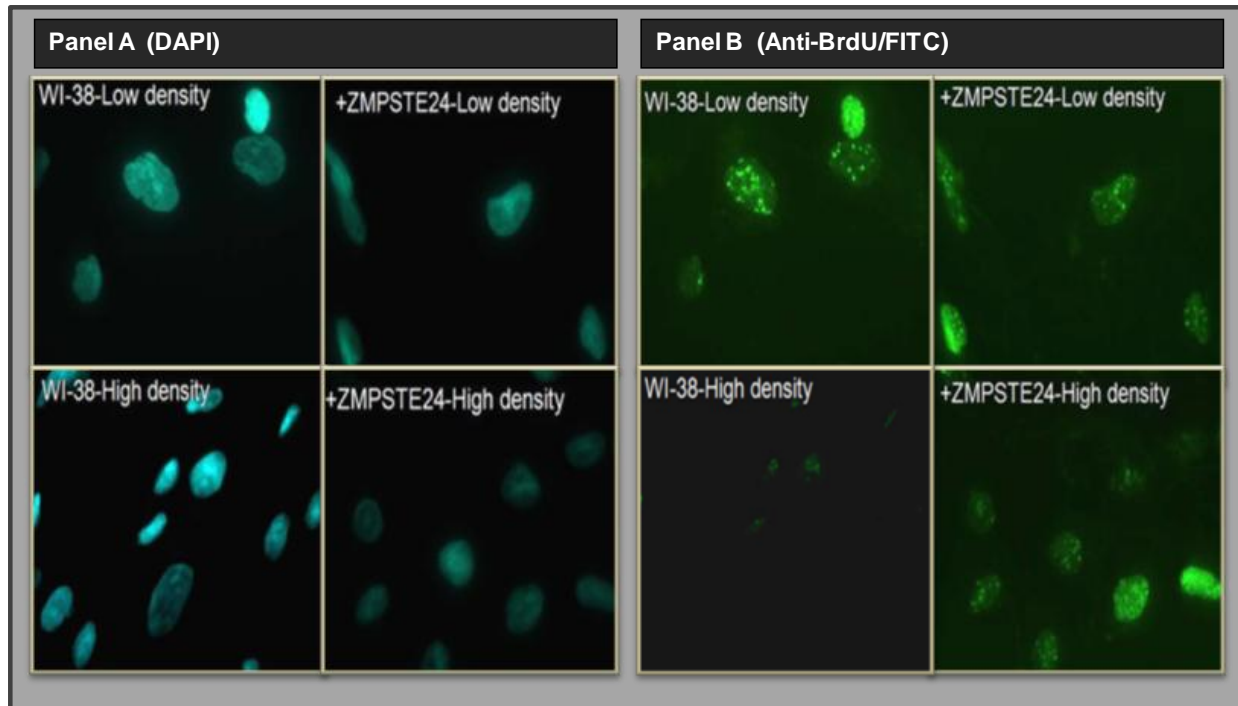


Figure 8. Zmpste24-Overexpressing Cells Bypass Cell Cycle Exit Under Quiescence-Inducing Conditions. WI-38 human diploid fibroblasts were plated on glass coverslips at low density (upper panels), or high density (lower panels), transiently transfected with Zmpste24 expression vector (right panels), or left untransfected (left panels), incubated for different timepoints, BrdU pulse labeled (30 min). Anti-BrdU-FITC left panels), incubated for different timepoints, BrdU pulse labeled (30 min). Anti-BrdU-FITC foci highlight replicating cells, nuclei are DAPI stained. Panels A (DAPI) and B (anti-BrdU-FITC) are from the timepoint at 48-hours posttransfection.

Figure 9 plots time after Zmpste24 transient transfection against the percentage of cells containing BrdU foci. These experiments suggest quiescence-inducing treatments lead to accumulation of PreA protein that is dependent on Zmpste24 activity level, but not on normally-limited Zmpste24 expression levels. Additionally, when Zmpste24 is exogenously overexpressed, we observe cells' failure to arrest as usual, also suggesting that preventing PreA accumulation prevents cell cycle arrest. Taken together, these findings support the suggestion that PreA accumulation is necessary for cell cycle exit, indicating it to be a cause of cell cycle exit rather than a byproduct.

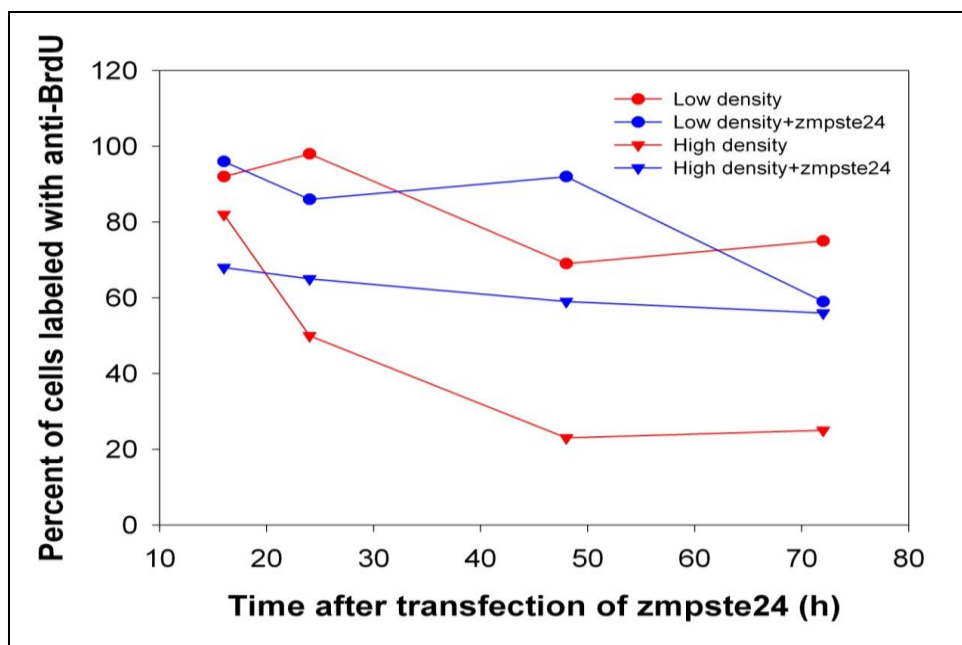


Figure 9. Cells Overexpressing Zmpste24 Bypass Quiescence. Graphic demonstrates failure of Zmpste24-overexpressing cells to properly quiesce when exposed to high density cell plating conditions that otherwise cause a drastic contact-inhibition-mediated decrease in proliferation. Proportions of BrdU-foci-containing cells in untransfected cells at low density (red circles) and high density (red triangles), to Zmpste24-transfected cells at low density (blue circles) and high density (blue triangles).

Development of an Uncleavable PreA Expression Construct

We reasoned if preventing accumulation of endogenous PreA prevents cell cycle exit, then overexpression of PreA might induce cell cycle exit and would offer further evidence that PreA accumulation induces cell cycle exit. Progression through the mitotic cell cycle is governed by a complex program regulating gene expression¹²⁷⁻¹²⁹ and by many posttranslational modifications^{126,130,131}. Therefore, a PreA-mediated role controlling cell cycle arrest would require PreA protein expression to alter the expression pattern of genes involved in cell cycle control. To investigate, we used site-directed mutagenesis to mutate the Zmpste24 cleavage site in the LMNA cDNA

sequence in a green fluorescent protein-tagged recombinant vector-based expression system, thus generating a full-length PreA protein that is unable to undergo the final maturation cleavage to form mature Lamin A. The construct, pEGFP-C3-EGFP-LMNA-L647R, produces an EGFP-tagged protein termed “L647R PreA,” in which the CaaX-box is intact, so the farnesyl modification, -aaX cleavage and carboxyl methylation can occur as for Wild-Type PreA.

Effects of Accumulated PreA on Global Gene Expression by Microarray Analysis

To examine effects of PreA expression on functional gene pathways, we first assayed for effects on global gene expression. We transiently transfected mouse 3T3 cells with either the EGFP-L647R PreA- expressing construct or the pEGFP-C3 empty vector, which expresses EGFP alone, and isolated total RNA from these cells 48 hours after transfection. We elected to use the EGFP-expressing vector as a control for comparison because a model over-expressing “wild-type” (unmutated) LA can quickly become an expression system for PreA, instead, once available Zmpste24 in the cells is exhausted from processing the exogenous protein. From the total RNA, cDNA was prepared and used to interrogate mouse whole genome-scale transcript microarrays (Affymetrix). We note results indicating altered expression levels on the microarray for the cyclin dependent kinase inhibitors (CKIs) p16INK4A, p19ARF, p21Waf1, and p27Kip1, all of which demonstrate upregulated transcript expression levels in L647R PreA-expressing cells (each upregulated approximately 1.5- to 2-fold). Also, Cdc25A, CDK2, and c-Myc, genes associated with promotion of proliferation, each demonstrate decreased transcript expression levels (approximately -2-fold). Rather than making an

attempt to study individual genes that demonstrate altered regulation with L647R PreA expression in the cells, we chose to first evaluate the microarray data in terms of likely functional roles and affected pathways for gene expression changes, then narrow the scope in subsequent investigations.

Ingenuity Pathways™ Analysis: Physiological Function Analysis

Ingenuity Pathways Analysis™¹³² software was used to interpret the impact on gene expression in the context of cellular functions in “Functional Analysis” (Figure 10). In this analysis, changes in gene expression related to particular cellular functions or disease conditions indicate which of these cellular functions experience the most statistically significant impact from L647R PreA expression, compared to EGFP expression.

The functional analysis indicates expression of L647R PreA affects cell cycle, cell growth and differentiation, cell death, and numerous metabolic processes and disease states that would be largely impacted by altered cell cycle regulation. Aside from the distinct cell-cycle regulation pathways, an impact on cell cycle regulation could indirectly impact several of the other functional processes found to be affected by expression of L647R PreA, but the implications may be less obvious. For instance, genes involved in “Organismal Injury” or “Cellular and Tissue Development” would certainly be affected by altered control of the cell cycle, as these are pathways involving cell proliferation, cell death and turnover, and tissue repair or regeneration. Loss of LA has been previously shown to be associated with disease recurrence in colon cancer¹³³, and it is not unlikely that potential roles in apoptosis, cellular proliferation, and growth would implicate PreA

expression in other Gastrointestinal Diseases, Reproductive System Diseases, or Responses to Infection or Inflammation. Modes of Cellular Signaling could affect, and be affected by, any factor that would affect cell cycle regulation, as well as the obvious role the nuclear lamina would play in maintaining nuclear pore complexes and overall nuclear structure and integrity.

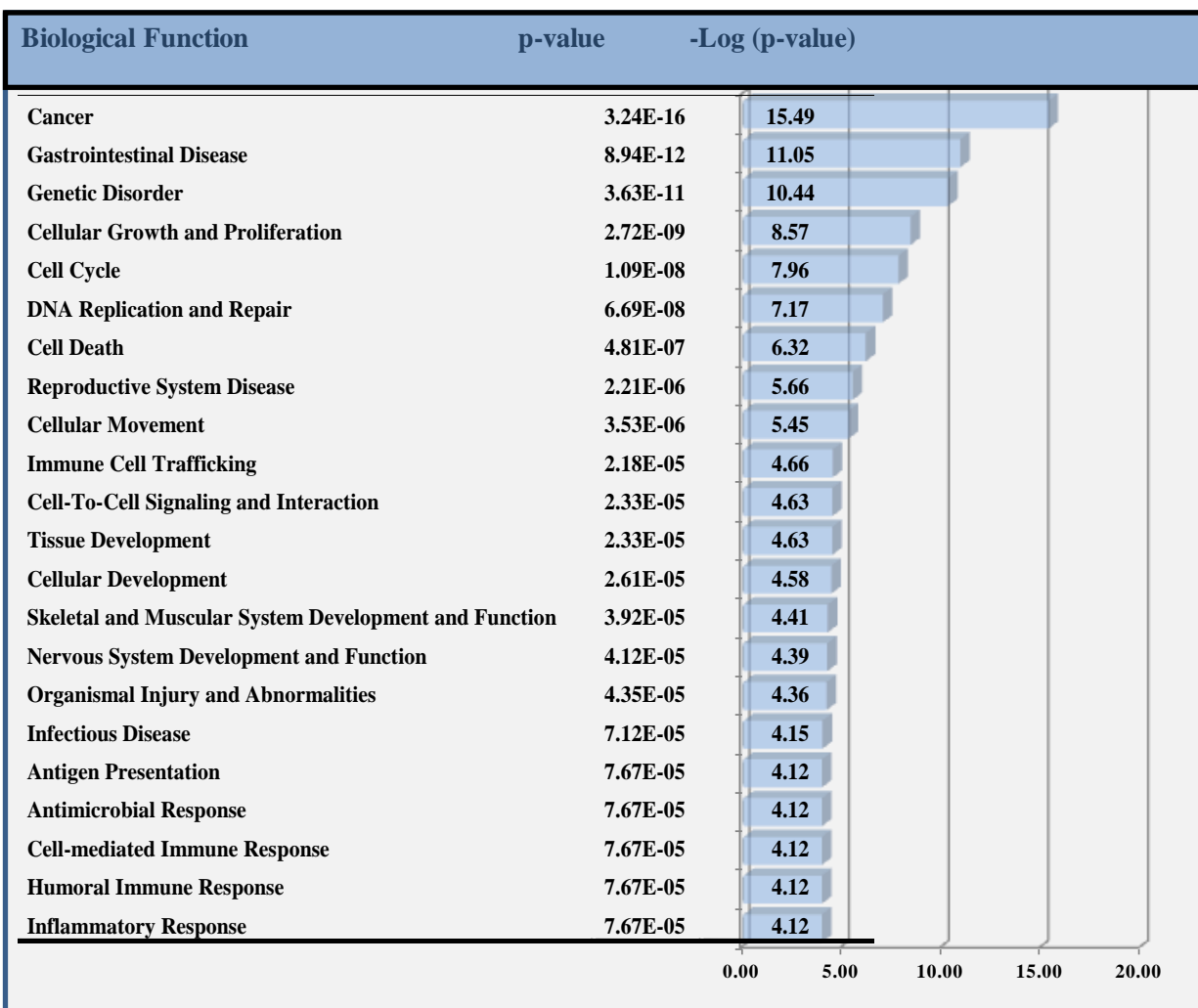


Figure 10. Ingenuity Pathways Analysis™ “Functional Analysis.” Shows the 22 most statistically significant gene expression changes induced by transient L647R PreA expression in 3T3 cells, in the context of cellular functions and diseases, as compared to levels in EGFP-expressing cells. Analysis used data from a mouse whole genome-scale transcript assay (Affymetrix). Genes with altered expression levels were compared and grouped by function according to the Ingenuity Knowledge Base. A Right-tailed Fisher’s exact test was used to calculate a p-value (converted to –Log of the p-value).

Ingenuity Pathways™ Analysis: Canonical Pathways Analysis

Pathways of gene expression influenced by expression of L647R PreA were evaluated for pathway-relevance by the “Canonical Pathways Analysis.” (Table 1, Figures 11-12). This analysis associated the genes in the dataset having altered expression with known canonical pathways in the Ingenuity™ Knowledge Base. The significance of the association between the data set and the canonical pathway was measured in 2 ways: 1) a ratio of the number of genes from the data set that map to the pathway divided by the total number of genes that map to the canonical pathway, and 2) Fisher’s exact test was used to calculate a p-value determining the probability that the association between the genes in the dataset and the canonical pathway is explained by chance alone. Table 1 lists the 21 canonical pathways that demonstrate statistically significant changes in gene expression in L647R PreA-expressing cells, versus those expressing EGFP alone.

Table 1. The Canonical Pathway Analysis™

Ingenuity™ Canonical Gene Pathway	-Log (p-Value)	Overall Fold-Change Pathway Gene Expression	Genes in Pathway
Aryl Hydrocarbon Receptor Signaling	3.72E00	-3.28	CCNE1, CCNE2, CCNA2, CDKN1A, CHEK1, NR2F1, GSTT1, FOS, RARA, TGFB2, DHFR, GSTO2, ALDH3A1, ALDH6A1, MGST1, MCM7, P300, RB, SUMO, AHR, ARNT, AIP, MYC, SP1, ESR, NFKB
Glutathione Metabolism	3.01E00	-3.46	GSTT1, MGST1, TRHDE, IDH3A, GSTO2, GSS, ANPEP, GSTT3, IDH1
Bacteria/Virus Pattern Recognition Receptors	2.82E00	-3.13	PTX3, TLR2, IFIH1, TLR1, IRF7, C3, DDX58, TLR6, CCL5, TLR3
Nicotinate and Nicotinamide Metabolism	2.39E00	-3.69	NNMT, DAPK1, ENPP1, NEK2, SGK1, ENPP5, AOX1, TTK, CDC2, AOX3
BRCA1DNA Damage Response	2.36E00	-2.89	SMARCA2, CDKN1A, SLC19A1, RFC5, STAT1, CHEK1, RFC3
Interferon Signaling	2.27E00	-2.54	STAT2, IRF9, IFNAR2, STAT1, TAP1
Bile Acid Biosynthesis	2.19E00	-4.01	LIPA, ADH7, ALDH1A7, ADH1C, ALDH3A1, ACAA2
Pyrimidine Metabolism	2.11E00	-4.13	TYMS, PRIM1, NME1, POLR2D, APOBEC1, DCK, DPYSL3, RFC5, UMPS, RRM1, NME3, TK1, RFC3
Cell Cycle: G1/S Checkpoint Regulation	2.09E00	-3.07	CCNE2, CCNE1, PA2G4, SUV39H1, CDKN1A, CDKN1B, CDKN2A, TGFB2, HDAC9, MYC, CDK2, CDC25A
JAK/Stat Signaling	1.89E00	-3.20	RRAS, CISH, CDKN1A, SOCS2, SOCS6, STAT2, STAT1
p38 MAPK Signaling	1.83E00	-3.40	IL18, TIFA, DDIT3, DUSP1, TGFB2, MEF2C, STAT1, FAS, PLA2G4C
Valine, Leucine and Isoleucine Degradation	1.82E00	-3.93	ALDH1A7, MCEE, AOX1, ALDH3A1, ACAA2, ALDH6A1, AOX3
Metabolism of Xenobiotics by Cytochrome P450	1.78E00	-4.25	GSTT1, ADH7, MGST1, AKR1C3, ADH1C, CYP2J2, CYP2J9, GSTO2, ALDH3A1, GSTT3, EPHX1
IRF Activation by Cytosolic Pattern Recognition Receptors	1.75E00	-3.38	DHX58, IFIH1, IRF7, DDX58, STAT2, IRF9, STAT1
Factors Promoting Cardiogenesis in Vertebrates	1.72E00	-3.46	CCNE2, CCNE1, FZD4, CDC6, FZD3, TGFB2, MEF2C, FZD7
N-Glycan Degradation	1.67E00	-2.91	FUCA2, MAN2B2, GM2A, HEXB
p53 Signaling	1.56E00	-3.48	PRKDC, TP53INP1, SNAI2, CDKN1A, HDAC9, BIRC5, CHEK1, SERPINE2
Glycerolipid Metabolism	1.56E00	-4.18	NAGA, LIPA, ADH7, ALDH1A7, LPL, ADH1C, LIPG, ALDH3A1
VDR/RXR Activation	1.39E00	-3.51	SPP1, IL1RL1, CDKN1A, TGFB2, HES1, VDR, CCL5
Eicosanoid Signaling	1.37E00	-3.81	PTGIR, AKR1C3, PLA2R1, PTGS2, WISP2, PTGER4
Toll-like Receptor Signaling	1.32E00	-3.43	TLR2, TLR1, FOS, TLR6, TLR3

Similar to the Functional Analysis, results of analyzing the canonical pathways affected by expression of L647R PreA indicate an effect on cell cycle regulation. While other pathways not clearly related to cell cycle regulation are indicated, we have concentrated further analysis of results on those functional pathways with a clear relationship to cell cycle control, as investigation of the cell cycle regulatory role of PreA

is the focus of this study. Some genes show overlap among pathways, such as the cell cycle inhibitory kinase, Chk1, and the cyclin dependent kinase inhibitor CDKN1A (also known as p21^{WAF1}). Figure 11 shows the statistical significance of L647R PreA expression effects on gene expression within cell cycle-related pathways, versus EGFP expression. Those pathways containing the highest proportion of genes demonstrating effects on expression are considered to be the most significant pathways for this analysis. Level of expression changes of the implicated genes is not factored into this part of the analysis.

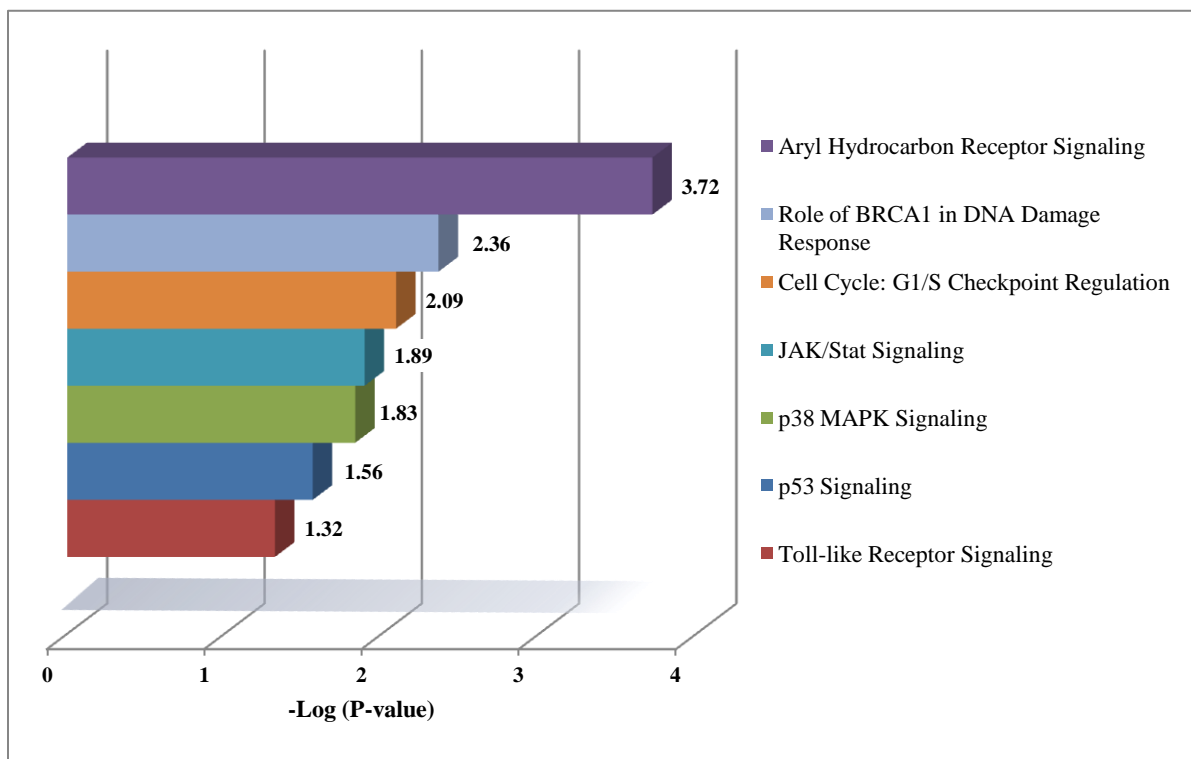


Figure 11. Ingenuity Pathways Analysis™ Pathways Demonstrating Statistically Significant Gene Expression Regulation. Analysis of expression data from Affymetrix microarray indicates Cell Cycle-Related Pathways of Gene Expression that are affected by L647R PreA expression with statistical significance. Significance is determined by dividing the total number of genes in the pathway by the number of genes in the pathway with changed expression in cells expressing L647R PreA versus EGFP, Fisher's exact test was used to calculate p-value (converted to -Log of the p-value).

Surprisingly, the AHR Pathway was determined to be the most statistically significantly regulated gene expression pathway in L647R PreA-expressing cells compared to cells expressing EGFP only. Not a well known factor in cell cycle regulation, the AHR is a transcriptional regulator implicated in development and a variety of physiological processes such as response to hypoxia, hormone receptor function, and toxin metabolism¹³⁴. As a number of compounds, including several toxic chemicals, act as AHR ligands¹³⁵, most literature involving this pathway is focused on studies of toxin metabolism. Other studies, however, have also recently found AHR contributes to the inhibition of cell cycle progression by directly interacting with the RB/E2F complex to block its phosphorylation in G1^{136,137}. This interaction constitutes a major G1 checkpoint in cells exposed to AHR ligands¹³⁸, and according to some researchers, in the absence of ligand, as an elemental, though relatively little known, mechanism of cell cycle control¹³⁷. As for the BRCA1 Role in DNA Damage Response pathway, the statistically significant indication of a role for L647R PreA expression is consistent with previous studies indicating LA roles in DNA damage repair and perturbation of the assembly of DNA damage repair response proteins in cells expressing PreA^{69,139} [reviewed in 101]. Also, BRCA1 overexpression has been shown to have an inhibitory effect on cell cycle progression and affect the expression of various other cell cycle regulatory genes¹⁴⁰. Thus, perhaps PreA-induced effects on gene expression within this pathway may indicate it is a mechanism of PreA-related cell cycle control, or that PreA expression is used as a mechanism to affect expression of other cell cycle genes by the BRCA1-mediated DNA damage repair and cell cycle control pathway.

Significant regulation of the G1/S checkpoint and p53 signaling is an important, and expected, indication from this data, and these pathways comprise an integral part of our further investigation of the cell cycle regulatory roles of PreA. In fact, in another type of evaluation of the L647R PreA effects on cell cycle-related gene pathways in the Ingenuity Pathway Analysis™, we consider the magnitude of impact from L647R PreA expression, compared to EGFP expression, on the expression levels of genes within the indicated pathways, and we find p53 signaling to be most affected (Figure 12).

Whereas the previous measure counted statistical significance as the proportion of genes within the pathways demonstrating *any* level of changed expression, this analysis looks at the actual *level* of gene expression changes within the pathways, regardless of the affected number of genes within that pathway.



Figure 12. Ingenuity Pathways Analysis™ Pathways Demonstrating the Highest Level of Impact from L647R PreA Expression. These pathways experienced the most altered levels of gene expression when L647R PreA was expressed, compared to EGFP. demonstrating statistical significance of effects from expression of L647R PreA.

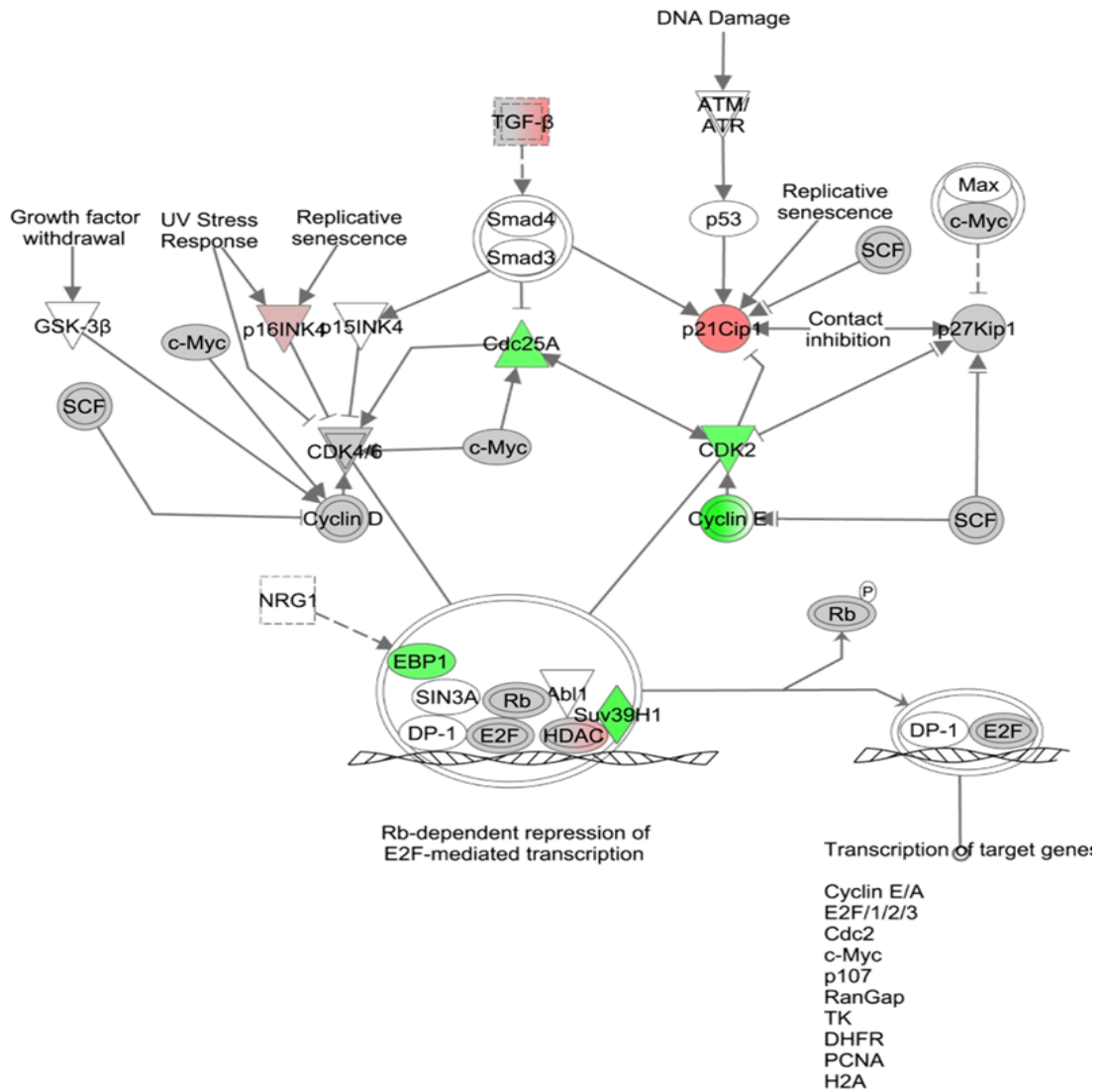
As shown in Figure 12, the genes involved with or affected by p53 signaling experience the most change in expression levels when L647R PreA is expressed compared to levels in the EGFP-expressing cells. A similar level of gene expression downregulation is indicated for genes related to Toll-Like Receptor Signaling, p38MAPK signaling, the Aryl Hydrocarbon Receptor Pathway, JAK/Stat signaling, G1/S checkpoint regulation, and the BRCA1-DNA damage response.

Ingenuity Pathways™ Analysis: Integrated Pathway Network Analysis

As a form of integrated analysis of overlapping gene expression pathways, the patterns of regulated gene expression specifically indicated in our test system were considered by Ingenuity Pathways Analysis™ to generate the “Networks and Pathways” analyses (Figures 13-16). These analyses generated a series of “GeneNetworks” by comparing gene expression in cells expressing L647R PreA compared to cells expressing EGFP (48 hours posttransfection), and overlaying the altered genes onto a global molecular network developed from information contained in the Ingenuity Knowledge Base. Networks were then algorithmically generated based on their connectivity. Graphical representations of relationships between molecules were produced, each relationship indicated is supported by at least one reference from the literature or from canonical information stored in the Ingenuity Knowledge Base. Each gene occupying a position within a Network is called a “node.” The intensity of the node color in the figures indicates the degree of regulation. Also, included in the graphics are assayed gene products not demonstrating a statistically significant expression change, and genes not assayed but related to the assayed genes according to the IPA

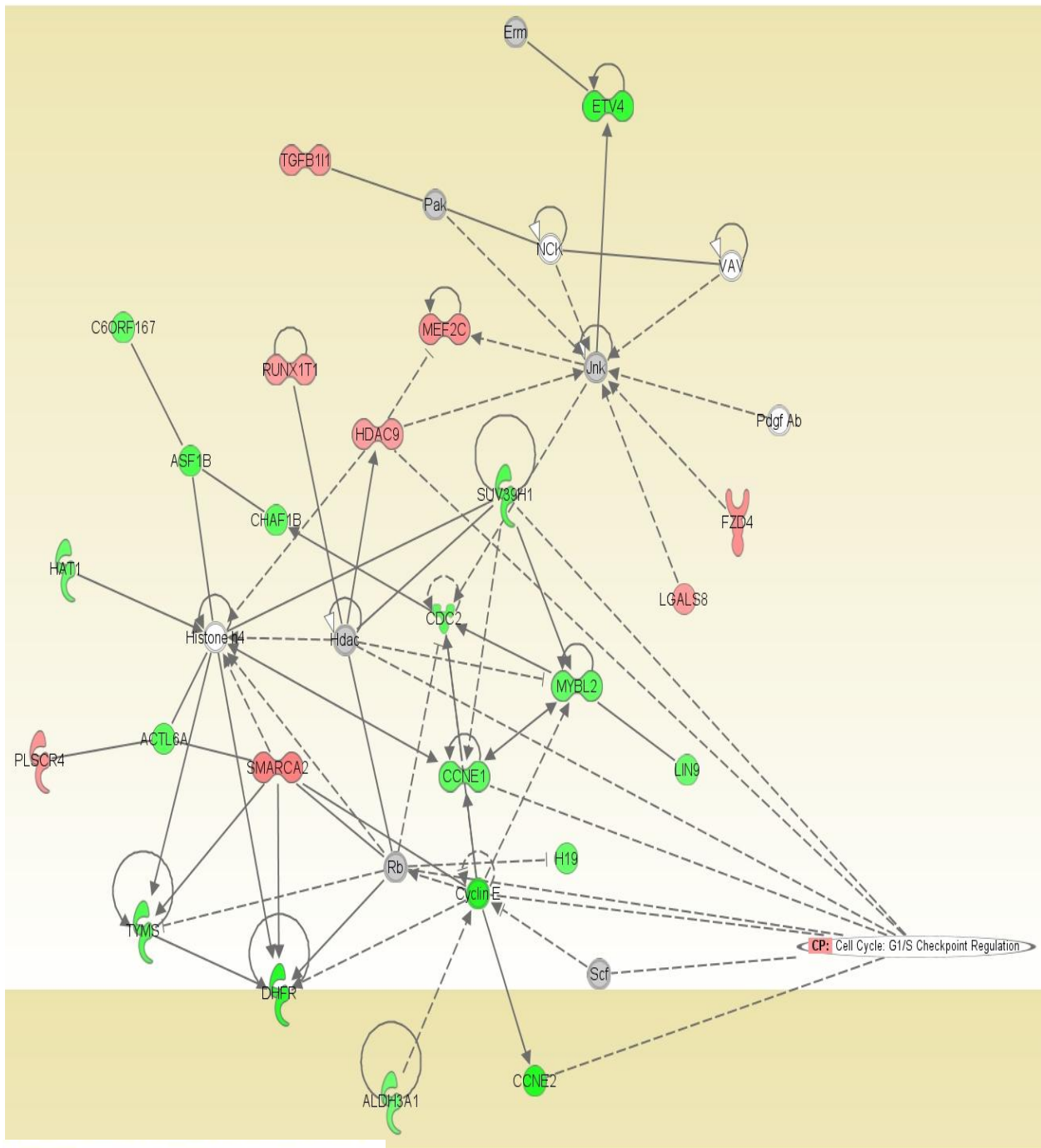
Knowledge Base. Nodes are displayed using various shapes that represent the functional class of the gene product. Edges (connecting lines) are displayed with various labels describing the nature of the node relationships (e.g., P for phosphorylation, T for transcription).

Cell Cycle: G1/S Check point Regulation



© 2000-2009 Ingenuity Systems, Inc. All rights reserved.

Figure 13. Ingenuity Pathways Analysis™ GeneNetwork1(with L647R PreA Expression): G1/S Checkpoint Regulation Part 1. Generated from gene expression change data in L647R PreA expressing cells vs. EGFP-expressing cells. Green=downregulated/ Red=upregulated/ Gray=not regulated/ No color=not assayed, but related to assayed genes.



© 2000-2009 Ingenuity Systems, Inc. All rights reserved.

Figure 14. Ingenuity Pathways Analysis™ GeneNetwork 2(with L647R PreA Expression): G1/S Checkpoint Regulation Part 2. Network generated from gene expression change data in L647R PreA expressing cells vs. EGFP-expressing cells. Green=downregulated gene expression/ Red=upregulated gene expression/ Gray=no change/ No color=not assayed, but related to assayed genes.

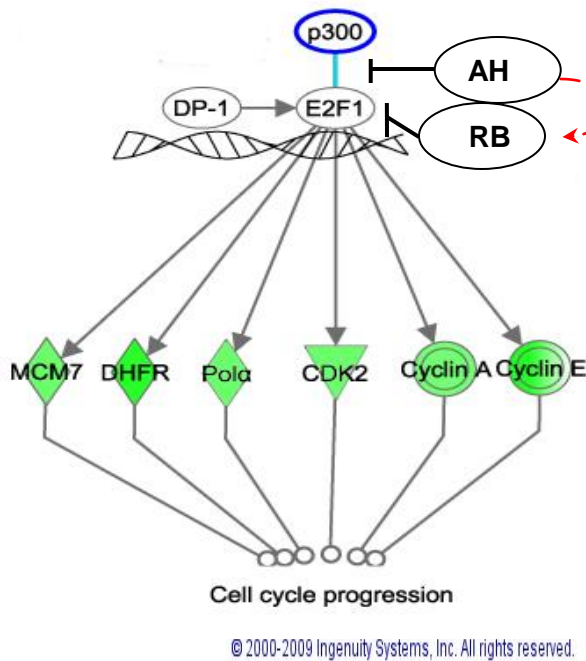


Figure 16. Ingenuity Pathways Analysis™ GeneNetwork 4 (with L647R PreAExpression): AHR-RB-p300 Control of E2F Transcription. Adapted from Gene Network generated by IPA analysis of gene expression changes in L647R PreA expressing 3T3 cells (48 hours post-transfection), compared to those expressing EGFP. Figure enhanced to reflect AHR ability to displace p300 from E2F promoters, thus inhibiting E2F-regulated gene transcription, and AHR role enhancing RB inhibitory effects. Green=downregulated gene expression/Red=upregulated gene expression. No color=not assayed, but related to assayed genes. Red dashed line=enhances activity.

Development of a Model System of Inducible, Stable

Lamin Isoform Expression Cell Lines

While the pathway-focused gene expression analysis of cells transiently transfected to express L647R PreA demonstrated a significant level of impact on gene expression in several cell cycle-related gene expression pathways, including the p53 signaling pathway, the AHR pathway, the G1/S cell cycle checkpoint, BRCA1-mediated DNA damage repair pathway, and signaling within Jak/Stat, p38 MAPK, and Toll-Like Receptor Pathways, an acknowledged limitation of the transient transfection is the likely dilution of effects of subtle changes in gene expression, as transfection efficiency does not approach 100%. To further distill the cell cycle-specific gene expression effects of L647R PreA, generated a stable system of inducible expression cell lines. To do this, we transferred the N-terminally EGFP-fused LMNA-L647R cDNA cassette to the

RheoSwitch Mammalian Inducible Expression System (New England Biolabs, MA), for construction of a stable cell line. This is a dual vector switch system in which the target cells are cotransfected with 2 plasmids, one that requires an induction reagent to express a ligand, this ligand is required to activate target gene expression from the second plasmid¹⁴¹⁻¹⁴⁴.

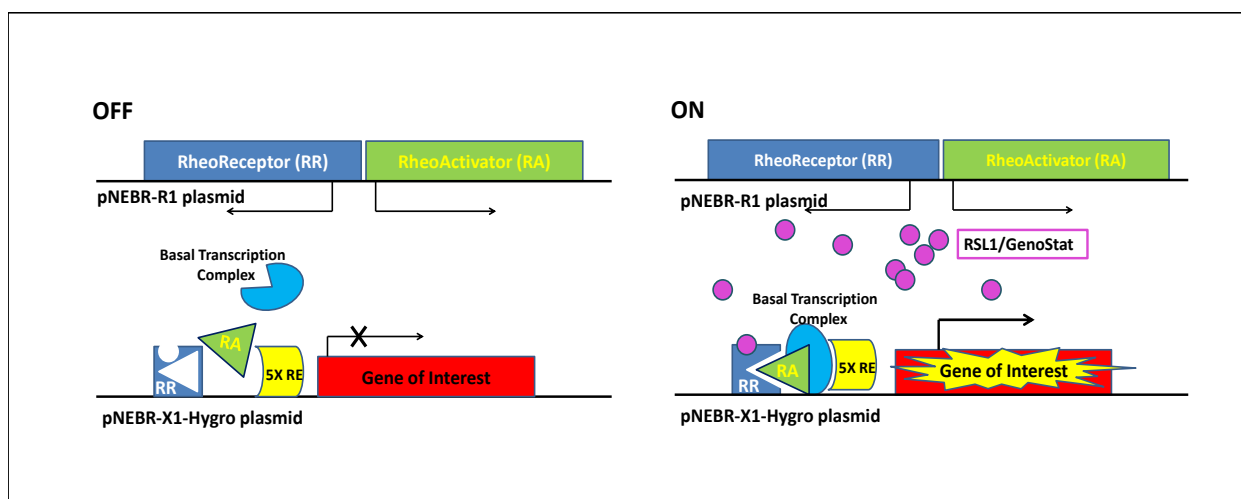


Figure 17. The RheoSwitch® Mammalian Dual Vector Inducible Expression System. Dual vectors are transfected into the target cell, where the ligand is expressed by the pNEBR-R1 plasmid when induction reagent (RSL1 or GenoStat brands of synthetic diacylhydrazine, in these experiments) is added to the culture medium. The expressed ligand is necessary for target gene expression to occur from the pNEBR-X1Hygro plasmid. (Adapted From New England Biolabs, Inc.)

The induction reagent, [N-(2-ethyl-3-methoxybenzoyl)-N'-(3,5-dimethylbenzoyl)-N'-tert-butylhydrazine], is a synthetic diacylhydrazine. Diacylhydrazine is a nonsteroidal analogue of the insect molting hormone, ecdysone^{114,145}. The synthetic reagent (RSL1 from New England Biolabs, Inc., MA; or GenoStat from Millipore Corp., MA) has been shown to be invisible to mammalian nuclear receptors and inert within all cell lines tested¹⁴¹. The result is an expression system not affected by the sometimes “leaky” expression of the target DNA seen in many inducible systems, as well as quick

response of activating or deactivating expression by addition or removal, respectively, of the induction reagent. After using restriction enzyme digestion to remove the EGFP-LMNA-L647R cDNA sequence from the pEGFP-C3 plasmid, it was ligated into the second plasmid in the RheoSwitch® pNEBR-X1Hygro vector, and the resulting expression construct, pNEBR-X1Hygro-EGFP-LMNA-L647R was transfected into the target cells. The cells used were mouse NIH3T3 fibroblast cells already containing the ligand-expressing plasmid vector (pNEBR-R1). Retention of pNEBR-R1, which contains a Neomycin resistance cassette, was maintained by supplementing the culture medium with G418 antibiotic. Following transfection with the pNEBR-X1Hygro-EGFP-LMNA-L647R plasmid vector, which contains a Hygromycin resistance cassette, cells containing the second plasmid in addition to the first were selected by additionally supplementing the G418-containing culture medium with Hygromycin. Twelve separate cell colonies were selected and transferred to new culture vessels for propagation, and after a sufficient number of cells were present, a sampling of these were transferred to coverslip culture chambers in medium containing 500 nM GenoStat induction reagent. After 24 hours of induction, cells were observed under fluorescence microscopy for evaluation of EGFP-fused L647R PreA expression. The 3 colonies with cells expressing the most EGFP-tagged protein were identified, and cultures of the other 9 cell colonies were discarded. The 3 colonies selected for further propagation were evaluated for morphology, growth patterns, in addition to induction of EGFP-L647R PreA. In the absence of induction reagent, the cell lines demonstrated normal morphology resembling that of the cells prior to transfection, all 3 appeared to proliferate at a rate within a range similar to the proliferation rate of the untransfected cells

(empirical observations, not quantitatively measured), and upon induction all 3 expressed EGFP-tagged protein in a pattern consistent with documented PreA expression^{62,146}. Expression of some genes can be detected within 1 hour of induction in the RheoSwitch® system, with maximal levels of expression at 48-72 hours, and some dosage-effect can be obtained with different dose amounts of the induction reagent. We were able to detect faint expression of some GFP-tagged protein after approximately 4-hours, with maximal levels reached around 72 hours. The cell line that consistently expressed a slightly more intense fluorescence of its EGFP-tagged protein was selected for future experiments, and cells from the other 2 cultures were frozen and maintained as back-up cell lines. We also used this system, and the same procedures, to construct stable inducible cell lines expressing the wild type Lamin A sequence (wtLA), a mutant Lamin A sequence (del50), and the EGFP protein alone. The wtLA construct expresses the full length immature PreA protein, modified only by the N-terminal EGFP fusion, and undergoes the full maturation processing to yield LA, and likely, though unconfirmed, alternative splicing to produce Lamin C. The del50 mutant construct, with a deletion of 150 nucleotides near the C-terminus of the Lamin A coding sequence, expresses a 50-amino acid-truncated protein that mimics the HGPS mutant protein progerin. While expression of progerin in HGPS patients typically results from a point mutation introducing a cryptic alternative splice site that leads to deletion of the corresponding nucleotides from the processed RNA transcript, this methodology of engineering the truncated protein by deleting nucleotides from the cDNA sequence is commonly used by researchers and regarded to yield a mutant protein equivalent to progerin^{60,147,148}.

To characterize the expression of the constructs from these cell lines, DNA was extracted from the cells and sequenced with an EGFP primer and LA C-terminal primer to confirm expression of the EGFP/lamin fusion-constructs. Also, the protein expression patterns were evaluated by fluorescence microscopy detection of the GFP fused to the lamins. In Figure 18, fluorescence microscopy images reveal the expected expression pattern of the EGFP-fused L647R PreA protein, demonstrating GFP concentration at the nuclear rim with amorphous-shaped aggregates in the nucleoplasm with an uneven nuclear topography demonstrating ridges, invaginations, and some blebbing. Likewise, expression patterns of GFP-fused LA and del50 were examined and found to match expected patterns: LA presents as a smooth veil over and throughout rounded, oval, or slightly bean shaped nuclei with smooth-appearing surface texture with a subtle concentration of GFP at the nuclear rim. The del50 expression manifests as dramatic intranuclear aggregate clumps and highly irregular nuclear membranes. These nuclei present the same type of blebbing, ridges, and invaginations as the L647R PreA-expressing cells but on a more extreme scale. These patterns are consistent with all known descriptions of these isoforms. Finally, EGFP-only expressing cells, the control line, presents light green fluorescence throughout the cell that is not localized in the nucleus.

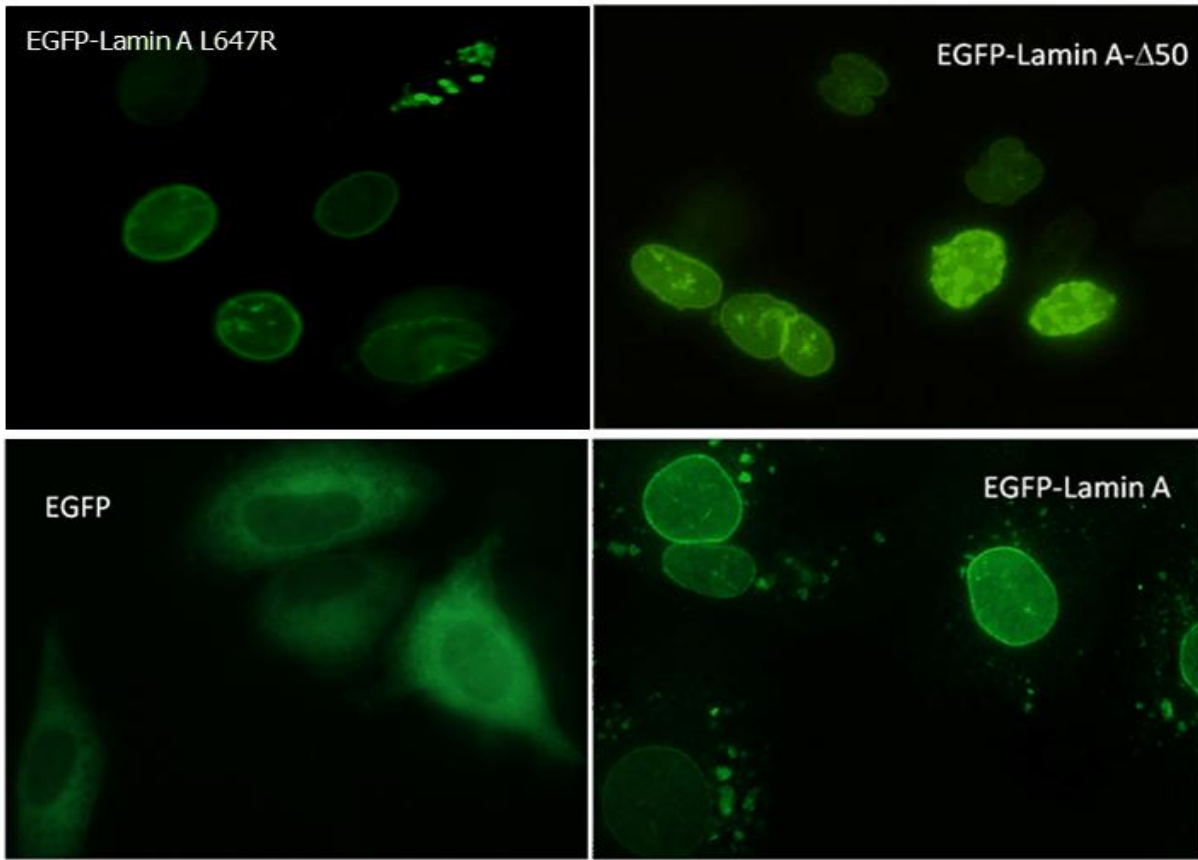


Figure 18. Evaluation of Induced Recombinant Protein Expression in the RheoSwitch® Lamin Isoform-Construct Expression Model System (GFP). Fluorescence microscopy (Top, L-R) demonstrates expression from the GFP-fused L647R-Lamin A (PreA) cell line and GFP-Lamin A (LA), and (Bottom, L-R) demonstrates expression from the GFP control cell line and the GFP-Lamin A-del50 cell line. Expression represented is after 48 hours induction with 500 nM Genostat.

In addition to the direct fluorescence detection of expression of the GFP- lamins, we also further examined the induced expression in the L647R PreA cell line by indirect immunofluorescence with an antibody to GFP, after imaging the direct GFP expression (Figure 19).

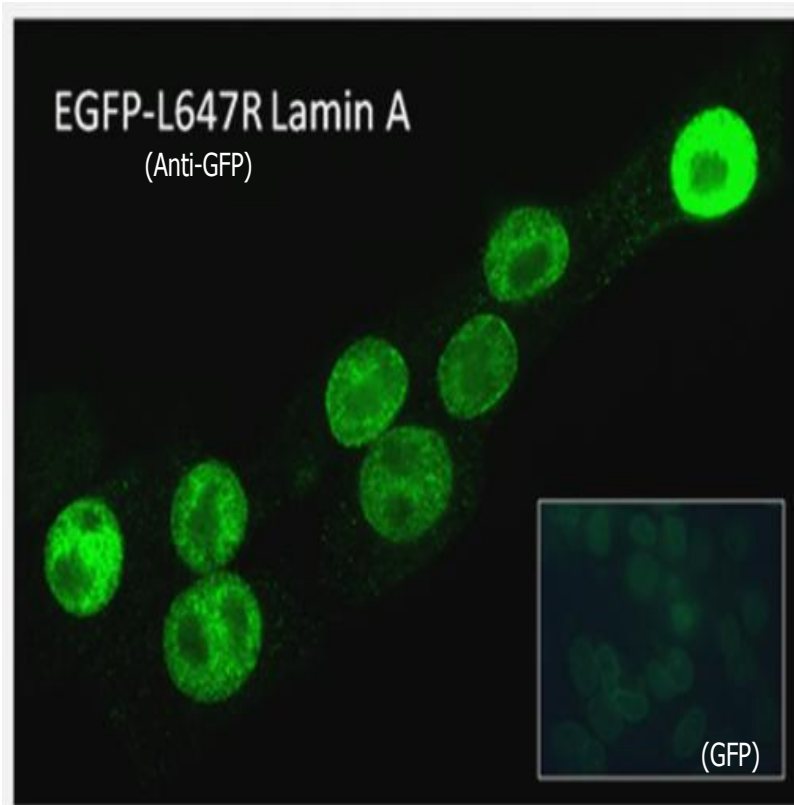


Figure 19. Immunostaining of EGFP-L647R Lamin A (PreA), with Antibody to GFP. This imaging demonstrates indirect immunofluorescence, and enhanced microfluoroscopic visualization of lamin distribution after induction (500 nM Genostat, 48 hours), compared to detection of the direct fluorescence emission from the protein (inset). Cells were plated on coverslips and induced 48 hours to express the protein (500 nM Genostat). After imaging the direct fluorescence of GFP-construct expression, cells were immunostained as described for indirect immunofluorescence detection.

While the recombinant GFP-lamin expressed in the engineered cell lines demonstrates the appropriate subcellular localization, to further evaluate the integrity of the expressed proteins, we performed immunoblotting of lysates prepared from each cell line to confirm the protein is reactive with an antibody specific for Lamin A/C as well as anti-GFP. Reactivity of the same bands with both anti-Lamin A/C and anti-GFP, is indicative of an expressed fusion protein (Figure 20).

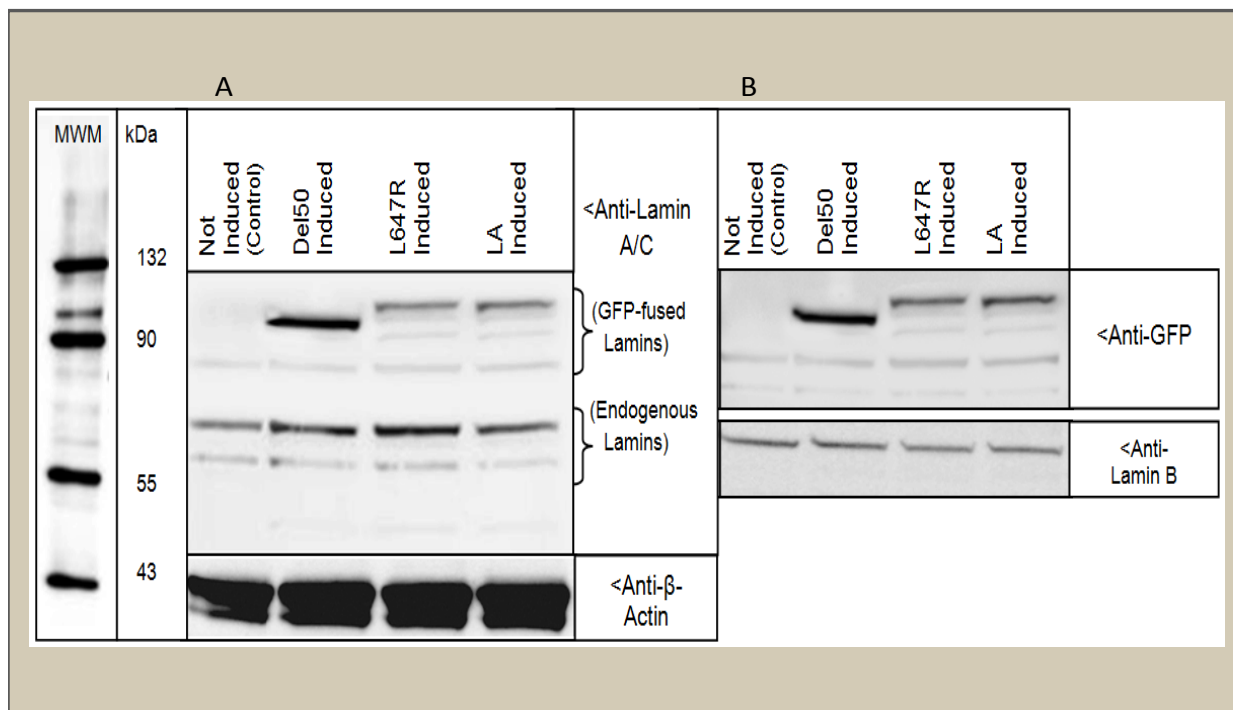


Figure 20. Immunoblotting of Expressed Lamin Isoforms Using the Rheoswitch Inducible Expression System. Rheoswitch cells (Del50, L647R PreA, or wtLA) were induced with 500 nM Genostat for 48 hours. L647R cells treated with equal volume of DMSO were used for the uninduced control. A volume of each cell lysate to equal 50 μ g total protein per lane was separated by SDS PAGE on two 4-12% gradient Bis Tris Gels, in duplicate, and transferred to nitrocellulose membranes. One membrane was immunoblotted with a Lamin A/C antibody (Panel A) and β -actin antibody, and the second membrane was probed with anti-GFP antibody (Panel B), and Lamin B antibody, as a loading control.

As it was critical that the isoform expressed by the L647R PreA cell line was the uncleaved isoform, and that we were certain it is posttranslationally modified in the same manner as endogenous protein (specifically, farnesylation and carboxy-methylation), we also prepared lysates from the L647R PreA cells, induced for 48 hours with 500 nM Genostat, for mass spectrometry analysis (Figure 21). The trace patterns in the analysis indicate that the FC-PreA isoform is abundant in the L647R PreA-expressing cells (barely detectable in cycling cells not exogenously expressing it), while, as we would expect, endogenous mLA is present in the cells, as well.

L647R (average) 800-1800Da

Voyager Spec #1 MC=>MC=>SM19=>MC[BP = 1297.4, 2405]

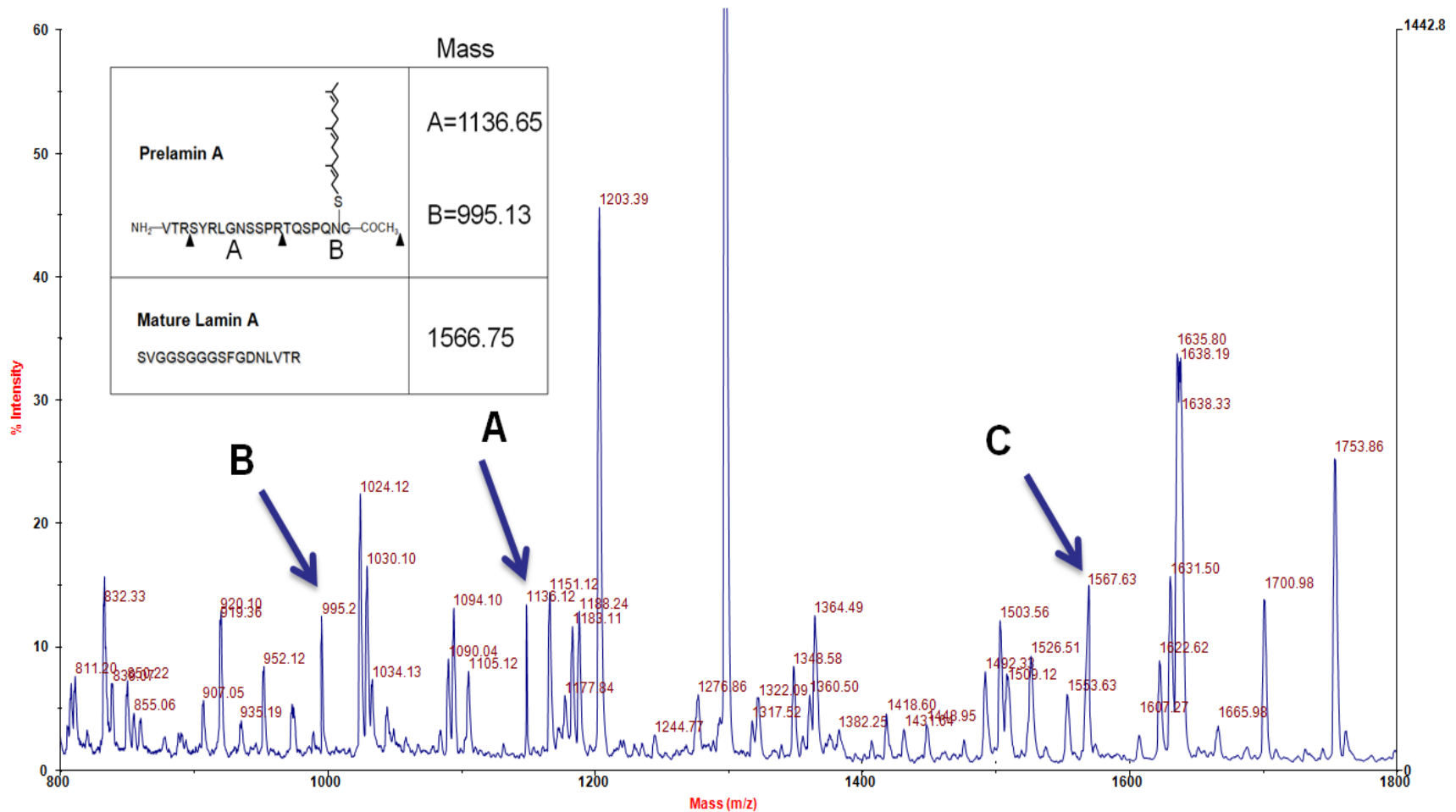


Figure 21. Mass Spectrometry Demonstrates RheoSwitch® Model L647R PreA Recombinant Protein Expressed is FC-PreA. Peak A represents a peptide fragment representative of unprocessed PreA, while Peak B specifically represents Farnesylated, Carboxymethylated (FC) PreA. Peak C represents cleaved, mature LA.

Effects of Uncleavable PreA (L647R PreA) Expression on Cell Cycle Progression

Using these stable cell lines, we further investigated the effects of PreA protein accumulation on cell cycle progression. In support of our earlier suggestion that PreA accumulation is a cause, rather than a byproduct, of cell cycle exit, we show cells induced to express L647R PreA exhibit decreased proliferation. First, a -bromo-2'-deoxyuridine (BrdU, a pyrimidine analogue)-uptake assay demonstrates cellular proliferation by labeling newly synthesized DNA (Figure 22). Using 3T3 cells that do not contain a lamin expression vector as controls, they, as well as cells from the RheoSwitch L647R PreA cell line, were treated with various concentrations of the induction reagent, GenoStat, or DMSO, for 48 hours before addition BrdU to the medium to label cells undergoing active proliferation.

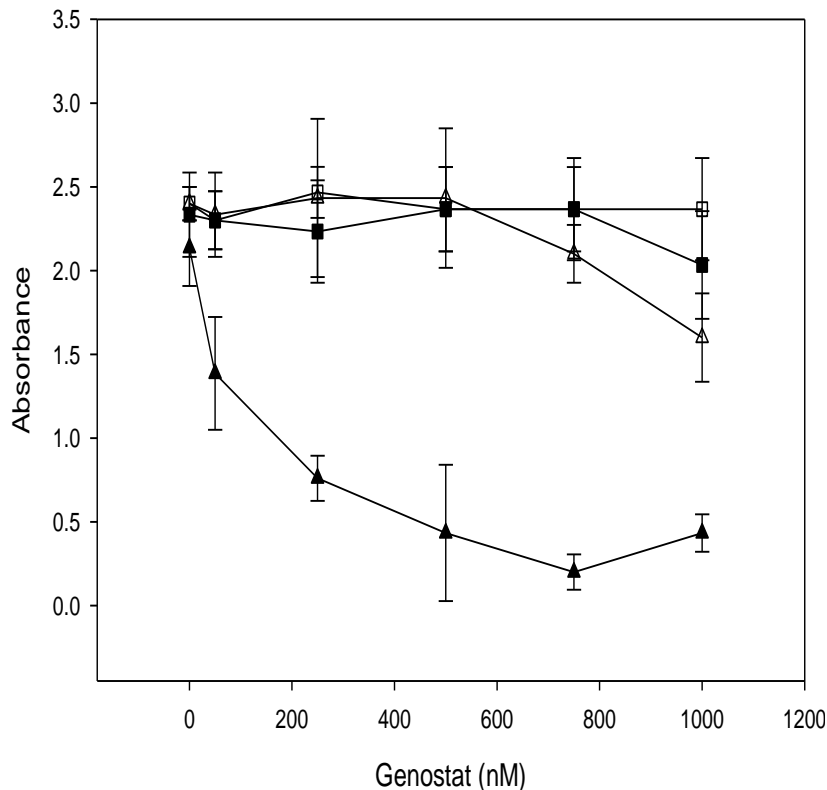


Figure 22. Decreased Rate of Cellular Proliferation in L647R PreA-Expressing Cells (BrdU Incorporation Assay). This assay demonstrates L647R PreA Expression inhibits cell proliferation. 3T3 cells (Squares) or L647R PreA Rheoswitch cells (Triangles) were treated with various concentrations of GenoStat inducer (filled symbols) or DMSO (empty symbols) for 48 hours. BrdU (10 μ M) was added to the plate and cells were incubated for 4 hours. Incorporated BrdU was detected by monoclonal anti-BrdU antibody linked to HRP. HRP substrate TMB was used to develop the color (Absorbance: 450 nm).

Figure 22 also demonstrates repressed proliferation in L647R PreA-expressing cells does not result simply due to toxicity of increasing GenoStat inducer dosage, per the lack of effects on proliferation in the unmodified 3T3 cells (ie, 3T3 cells not adulterated with recombinant DNA construct) treated with the same doses of GenoStat. The lack of effects on proliferation in DMSO-treated cells ensures the effects on GenoStat-treated RheoSwitch cells are due to induction of the expression system.

To further explore the effects of L647R PreA expression on cell cycle progression, we used flow cytometry to assay DNA content as an indicator of cell cycle phase. Cell cycle phase distribution analyses of asynchronously growing cells induced to express L647R PreA were compared to uninduced (passage-matched, L647R PreA construct-containing, DMSO-treated) cells under the same conditions. We also used Ki-67 protein-staining as a final measure of cell proliferation in these cells. Ki-67 is a nuclear protein associated with DNA replication and proliferation, though its exact role is not well understood. Ki-67 protein expression is absent only in the G₀ stage of the cell cycle, and it is a commonly-used and widely available indicator of cellular proliferation. We assayed for presence of the Ki-67 protein using immunofluorescence microscopy and an antibody directed to the Ki-67 protein (Figure 23).

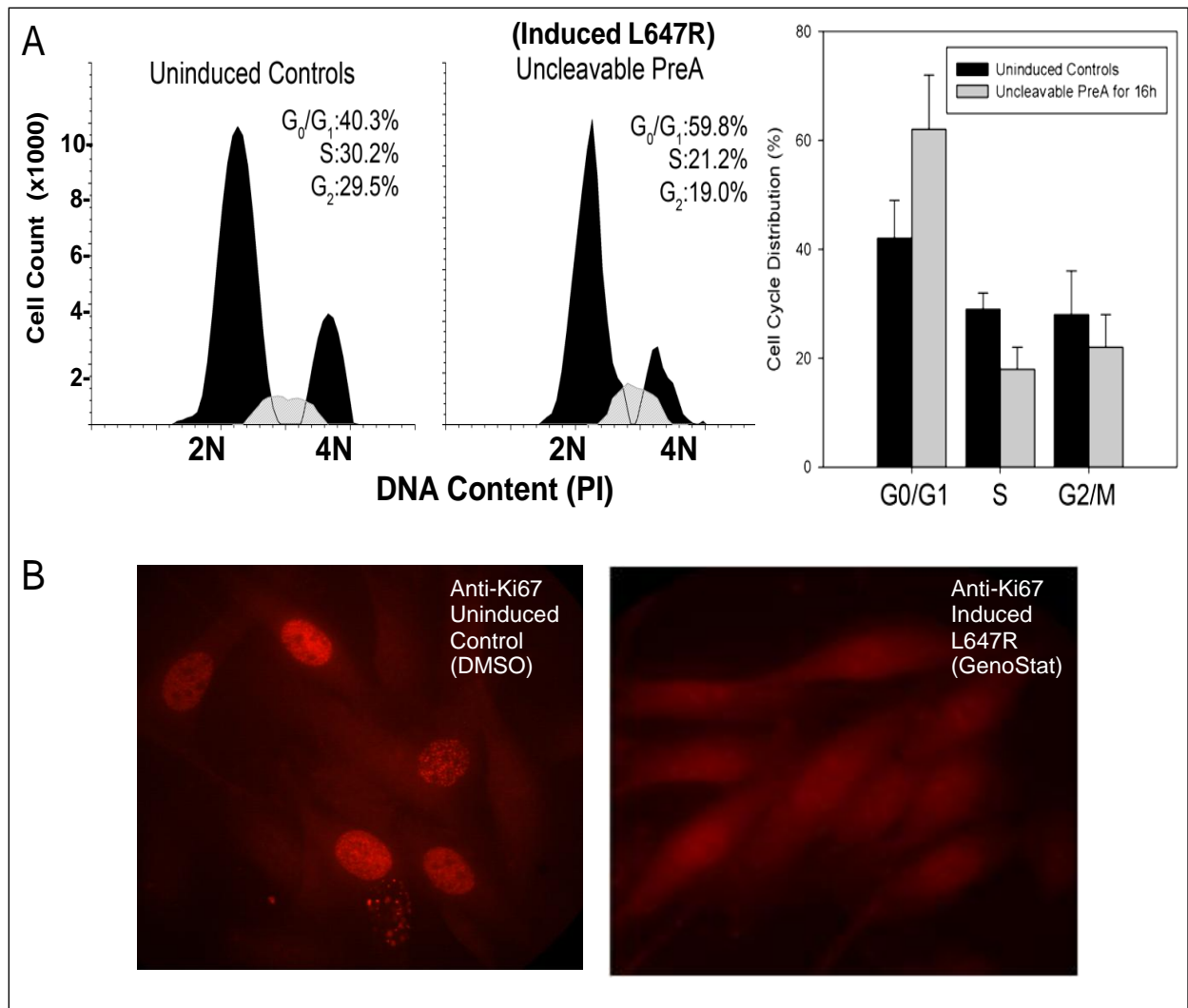


Figure 23. Decreased Rate of Cellular Proliferation in L647R PreA-Expressing Cells (Flow Cytometry and Ki67 Immunofluorescent Stain Assay). Flow cytometry analysis reveals L647R PreA affects cell cycle progress. In Panel A, Flow cytometry was used to measure propidium iodide (PI)-stained cellular DNA content to demonstrate cell cycle phase, where 2N DNA content represents G0/G1 phase cells, 4N represents G2/M phase cells, and S-phase cells are located between the 2N-G0/G1 and 4N-G2/M peaks. Uninduced Cells (DMSO-treated) are shown in Left Panel, Induced L647R PreA Cells in Center Panel, with a bar graph quantitative comparison in Panel A, far right. Panel B shows Ki67 immunostaining of Uninduced Cells (Left), and Induced L647R Cells (Right). Induction method: 500 nM GenoStat, 48 hours.

As expected, flow cytometry analysis reveals uninduced cells cultured in full serum demonstrate normal proliferation, while, in comparison, a G0/G1 peak-shift (representative of progression toward cell cycle arrest, and consistent with a developing

quiescent phenotype) is seen in cells induced to express L647R PreA for 48 hours. Ki67 protein is readily detected in uninduced cells but almost absent in the induced cells, further indicating exit from the cell cycle. Taken together, results of the proliferation assays by measurement of BrdU uptake, flow cytometry approximations of cell cycle progress, and nuclear immunostaining for Ki67, suggest expression of L647R PreA has an inhibitory effect on cell cycle progression.

Effects of Accumulated PreA on Cell Cycle Pathway-Specific Gene Expression (by RT-qPCR Array)

To more specifically evaluate the effects of PreA expression on cell cycle specific genes, we used cDNA derived by reverse transcription of total RNA extracted from cells induced 72 hours to express L647R PreA in a quantitative real-time polymerase chain reaction (RT-qPCR) assay of cell cycle related genes. For comparison, RheoSwitch cells induced to express wtLA and del50 were also assayed. Uninduced cells (passage-matched to their induced counterparts) from each cell line were used to determine baseline expression of the assayed genes for each cell line. When results of the gene expression assays on uninduced cells of each cell line were compared, there were some modest differences in the expression profiles (data not shown). We attribute these “baseline” expression differences in uninduced cells to clonal variation. The cell lines were all created by transfection into cells from the same original host cell line, from the same culture, and from within a few passages of the same culture. However, it is common for subtle differences to arise in cells derived after the repeated passages involved in clonal expansion of populations from single cell isolates of a common

culture. In addition to clonal variation, another possibility we considered to explain the different baselines of gene expression among the uninduced L647R PreA cells and wtLA cells is the difference in passage number, as the passage numbers were not matched between cell lines (after the clonal expansion process and maintenance passaging of working cultures). In future studies, matching of passages of compared cells could provide more uniformity of cell line-to-cell line expression baselines, allowing a more reliable comparison of the L647R PreA and wtLA cell lines. However, we do acknowledge accumulation of endogenous LA occurs as PreA and note the likelihood that the endoproteolytic processing capability of endogenous Zmpste24 could be quickly overwhelmed by increasing accumulation of EGFP-wtLA protein. This would result in the presence of some processed EGFP-wtLA, and some unprocessed EGFP-wtPreA. Therefore, this model would become another model for overexpressing the PreA isoform and would not suffice as a control for comparison to the L647R PreA-expressing model. Future experiments might include a cell line containing a LA construct in which the cDNA is modified to directly encode a truncated protein equivalent to a posttranslationally modified mature LA protein. This model could allow a more accurate comparison of effects of overexpressing a PreA isoform, represented by the L647R PreA construct, to effects of overexpressing mL A isoform. Additionally, with replicates in future experiments, it could be possible to determine if a ratio can be deconvolved for “housekeeping” reference genes to allow meaningful comparison among all of the cell lines. Regardless, for the purposes of the current study, we have chosen *not* to compare the gene expression data from the induced cells to each other, as such comparison could yield false exaggeration of differences in gene expression, or fail to

detect subtle, but true, changes in expression of some genes. Rather, we simply compare the expression profile of cell cycle-related genes in the cells induced to express L647R PreA versus the uninduced (treated with DMSO vehicle only), passage-matched cells split from the same culture, to determine expression level changes related to the expression of the uncleavable lamin mutant.

Table 2 lists all genes demonstrating a fold-change in expression with statistical significance, which we define here as having at least a 2-fold change in expression level with a p-value ≤ 0.05 (-log p-value of ≥ 1.3). A complete listing of all assayed genes is presented as Appendix A, with a corollary Volcano Plot as Appendix B. For ease of reference, this assay is referred to herein simply as “the RT-qPCR assay.” Also, for simplification purposes, all gene references using the short-hand notations of “upregulated,” or “downregulated,” mean the *gene expression levels* have the indicated regulation as indicated by RT-qPCR assay of transcript levels for the gene in induced L647R PreA-expressing cells (24-hours/500nM GenoStat) compared to the expression levels in the passage-matched, DMSO-treated, uninduced control cells.

Table 2. Cell Cycle-Related Genes Demonstrating Statistically Significant Altered Expression in Response to L647R PreA Induction[†]

Gene Symbol	Fold Regulation	p-value	-Log (pvalue)
Actb	14.8	0.001826	2.74
Ak1	7.9	0.007293	2.14
Apbb1	40.9	0.024349	1.61
Atm	4.0	0.000362	3.44
Brca1	19.4	0.001086	2.96
Brca2	14.1	0.000323	3.49
Camk2a	13.8	0.00348	2.46
Camk2b	15.2	0.000098	4.01
Casp3	4.5	0.007064	2.15
Ccna1	6.2	0.043674	1.36
Ccna2	4.5	0.000071	4.15
Ccnb2	-2.1	0.035362	1.45
Ccnc	10.0	0.002486	2.60
Ccnd1	5.8	0.003651	2.44
Ccne1	18.4	0.002771	2.56
Cdk2	2.1	0.000622	3.21
Cdk4	37.3	0.001031	2.99
Cdk5rap1	9.0	0.000637	3.20
Cdkn1a	6.3	0.001935	2.71
Cdkn1b	23.2	0.000095	4.02
Chek1	22.1	0.000703	3.15
Ddit3	4.6	0.000761	3.12
Dst	25.4	0.000002	5.70
E2f1	6.4	0.00158	2.80
E2f3	2.8	0.000833	3.08
E2f4	9.6	0.00157	2.80
Gapdh	3.8	0.003657	2.44
Hus1	17.6	0.000044	4.36
Inha	7.0	0.001369	2.86
Itgb1	9.6	0.000031	4.51

Gene Symbol	Fold Regulation	p-value	-Log (pvalue)
Macf1	9.8	0.001208	2.92
Mad2l1	2.7	0.002314	2.64
Mcm2	17.7	0.003508	2.45
Mdm2	2.1	0.004183	2.38
Mre11a	6.3	0.000679	3.17
Mtbp	17.5	0.001469	2.83
Nek2	15.6	0.000507	3.29
Nfatc1	5.5	0.000785	3.11
Notch2	10.7	0.000094	4.03
Npm2	16.5	0.000513	3.29
Pkd1	4.6	0.000072	4.14
Ppm1d	4.3	0.003941	2.40
Ppp2r3a	20.5	0.001368	2.86
Ppp3ca	2.8	0.020588	1.69
Psmg2	3.0	0.00115	2.94
Rad9	5.4	0.002484	2.60
Rad21	2.4	0.000601	3.22
Rbl1 p107	11.5	0.000749	3.13
Rbl2 p130	2.5	0.011955	1.92
Sesn2	5.5	0.000701	3.15
Sfn	25.3	0.000532	3.27
Shc1	6.0	0.00036	3.44
Skp2	4.0	0.00511	2.29
Smc1a	19.5	0.000743	3.13
Stag1	2.4	0.001397	2.85
Taf10	2.5	0.004552	2.34
Terf1	3.4	0.000185	3.73
Tfdp1	2.8	0.001374	2.86
Trp53	2.8	0.000597	3.22
Wee1	24.9	0.000156	3.81

[†]SABiosciences Cell Cycle Pathway specific RT-qPCR analysis results demonstrating expression fold-change in total RNA isolated from RheoSwitch 3T3 cells induced 24 hours with 500 nM GenoStat to express L647R PreA versus from uninduced control cells (DMSO-treated)

The variety among genes demonstrating altered levels of transcript expression in the L647R PreA expressing cells compared to the uninduced cells complicates interpretation of the specific and direct PreA-interactions that lead to the overall effect of PreA on cell cycle gene expression. Is it possible *all* of these gene products directly bind or associate with PreA? While possible, the more likely explanation of the variety is related to the very nature of cell cycle regulatory signaling, which occurs with cascades of gene activation or repression among individual pathways, as well as crosstalk with other pathways. In an effort to focus on particular gene-types in evaluating the expression data from the qPCR assay, we used literature sources and databases (GeneCards¹⁴⁹ and Entrez Gene¹⁵⁰) to categorize the data as follows: 1- Cyclins, Cyclin Dependent Kinases, Cyclin Dependent Kinase Inhibitors; 2-Kinases and Phosphatases; 3-Transcription Factor-Related Genes; 4-DNA Damage-Related Genes; and 5-Genes Associated with Chromosomal/ Nuclear/Cellular Integrity or Microtubule/ Mitotic Assembly. To begin to unravel the direct effects of PreA expression on cell-cycle related gene expression, we examined the expression profile in the context of the known functions of affected genes.

Cyclins, Cyclin Dependent Kinases (CDKs), Cyclin Dependent Kinase Inhibitors (CKIs)

Cyclins are eukaryotic proteins that play an active role in controlling nuclear cell division cycles¹⁵¹. In brief review: in vertebrates, there are 2 G2-phase cyclins, A and B, and at least 3 G1 cyclins, C, D, and E¹⁵². It has been shown recently that, upon mitogenic signaling, Cyclin C, in complex with CDK3, helps cells to exit the G0 state and enter the G1 phase by stimulation of retinoblastoma protein (pRb) phosphorylation at

S807/811¹⁵³. From the G1 phase, Cyclin D complexes with CDK4/6 to begin the phosphorylation of pRb that is complexed with the transcription factors E2F/DP. Following pRb phosphorylation, cyclin E activates CDK2 to effect further phosphorylation of pRb, thereby enabling the cells to cross the G1-restriction point. The pRb-E2F/DP complex disassociates, providing a positive signal for DNA synthesis in the S phase. Cyclin E is replaced by cyclin A, which binds to CDK2 and leads to phosphorylation of DP-1 subunits (inhibitor of DNA binding), and CDC6 (initiator of DNA replication) to complete DNA replication. On completion of the S phase, Cyclin B-CDK1 complex (mitosis-promoting factor) is activated. Progression from G2 to M phase requires sustained activity of CDK1-Cyclin B complex within the nucleus. Subsequent entry into anaphase relies critically on the sudden destruction of the CDK1-Cyclin B activity that guarantees the global inhibition of protein biosynthesis, DNA replication, and DNA transcription^{154,155}.

It was surprising to find an overall *increase* in cyclin gene expression in L647R-PreA expressing cells compared to uninduced cells, as this seems contrary to our observations of PreA expression leading to decreased cell proliferation and potential cell cycle exit. In the cyclin gene expression profile (Figure 24), upregulation was demonstrated for Cyclin A1/2, C, D, and E. The key regulator of G2–M transition of the cell cycle is M-phase promoting factor (MPF), a complex composed of CDK1/CDC2 and a B-type cyclin. Cyclin B was the only gene we observed to be significantly downregulated, possibly indicating a modest inhibition of entry to mitosis in these cells. Cyclin F interacts with Cyclin B to control Cyclin B nuclear localization, thus controlling activation of MPF through regulation of the amount of Cyclin B available in the nucleus

to form the MPF complex^{150,156}. Notably, there was no change in Cyclin F expression in L647R PreA-expressing cells compared to uninduced cells, thus no increased level of nuclear localization of Cyclin B should be expected, perhaps correlating to an overall downregulation of Cyclin B activity.

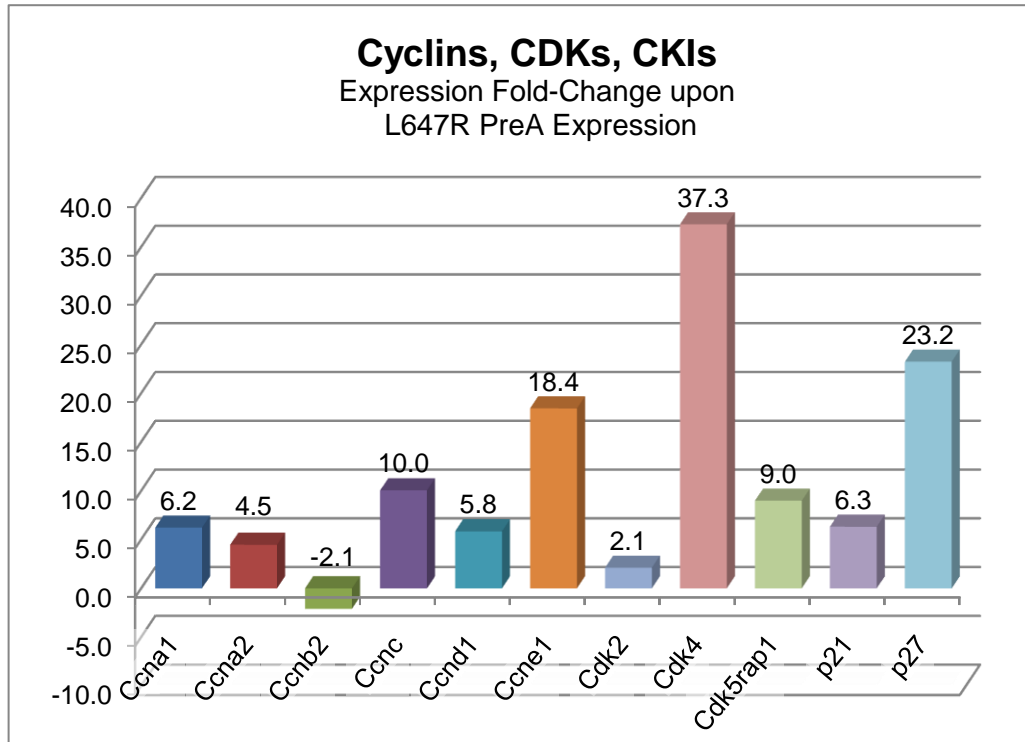


Figure 24. L647R Effects on Gene Expression (RT-qPCR Assay of Transcript Expression): Cyclins, CDKs, CKIs. Results compare cells induced 24 hours (500 nM GenoStat), versus uninduced cells treated with DMSO only. P-values ≤ 0.05 for each fold-change value, see Table 2.

Although cyclin levels vary with cell cycle stage, the kinases regulated by them are described to be constitutively expressed, dependent on the varying cyclin levels to direct control of the complexes in cell cycle regulation. Considering this, altered expression levels of the CDKs between different cells may or may not be of consequence, but we observed a slight expression upregulation of CDK2 (2.1-fold) and

a strong upregulation of CDK4 (37.3-fold) in L647R PreA expressing cells compared to uninduced cells (Figure 24). As described, Cyclin E-CDK2 complexes initiate the G1/S transition of the cell cycle, and Cyclin D-CDK4 complexes phosphorylate Rb protein, leading to liberation of E2F. E2F transcription factors, several of which (E2F1, 3, and 4) were observed to be upregulated by L647R PreA, control expression of key genes in controlling the transition from G1 to S phase. Increases in CDK2 and CDK4 expression, as well as in their respective cyclin counterparts, Cyclin E and Cyclin D, within the same cells, accompanied by E2F-upregulation, surely indicates pressure to progress forward in the cell cycle.

An important consideration, however, in cyclin-CDK control of cell cycle progression, is the fact CKIs bind these complexes and potently inhibit their activity. We observed the CKI Cdkn1a/p21Cip1/Waf (herein p21^{Waf1}) demonstrates a 6.3-fold upregulation of expression, while Cdkn1b/p27/Kip1 (herein p27^{Kip1}) is upregulated 23.2-fold (Figure 22). These inhibitors, along with p19^{Arf} (for which no statistically significant change in expression was observed between cells expressing L647R PreA and uninduced cells), are known to be the primary mediators of cell cycle arrest and are associated with quiescence, senescence, and/or apoptosis^[as reviewed in 157]. The transcript upregulation of these inhibitors could imply early stage initiation of cell cycle arrest despite the increased expression levels of the cyclins and CDKs. Several researchers have demonstrated p21^{Waf1} has a “threshold level” of activation, whereby modest induction stimulates proliferation, which is quickly staunched upon reaching the p21^{Waf1} expression level threshold^[as reviewed in 158]. Additionally, Cdk5rap1 (expression upregulated 9-fold, Figure 24) is a specific inhibitor of CDK5, a CDK shown to

phosphorylate and activate the p53 transcription factor, promoting apoptosis^{150,159}, so upregulation of Cdk5rap1 would favor cell survival over apoptosis. Overall, the Cyclin, CDK, CKI profile in 24-hours-induced L647R PreA-expressing cells suggests a forward pressure to cycle and avoid apoptosis with strong indications of early-stage cell cycle arrest initiation in progress.

Kinases (Non-Cyclin-Dependent) and Phosphatases

Other kinases, besides those dependent on cyclins, are active in regulation of the cell cycle, as well. Whereas phosphorylation activates the functions of some proteins, others are deactivated or tagged for degradation by the modification, thus phosphatases are also important in regulation of expression and activity of kinase substrate proteins. Several kinases and phosphatases demonstrate altered expression levels in response to induction of L647R PreA expression (Figure 25). Among these, Adenylate kinase 1 (AK1) is associated with metabolic sensing of body energy and facilitating phosphotransfer in the adenosine triphosphate (ATP) synthesizing pathway in which a phosphate is transferred from one adenosine diphosphate to another, leaving an adenosine monophosphate (AMP) as an ATP is formed ($ADP+ADP \rightarrow AMP+ATP$ energy producing exchange)¹⁶⁰. In addition, an AK1 isoform that is associated with the nuclear membrane and is a transcriptional target of the transcription factor p53 (p53 transcript expression is elevated 2.8-fold in cells induced to express L647R PreA versus control, Figure 26-Transcription Factors and Related Genes).

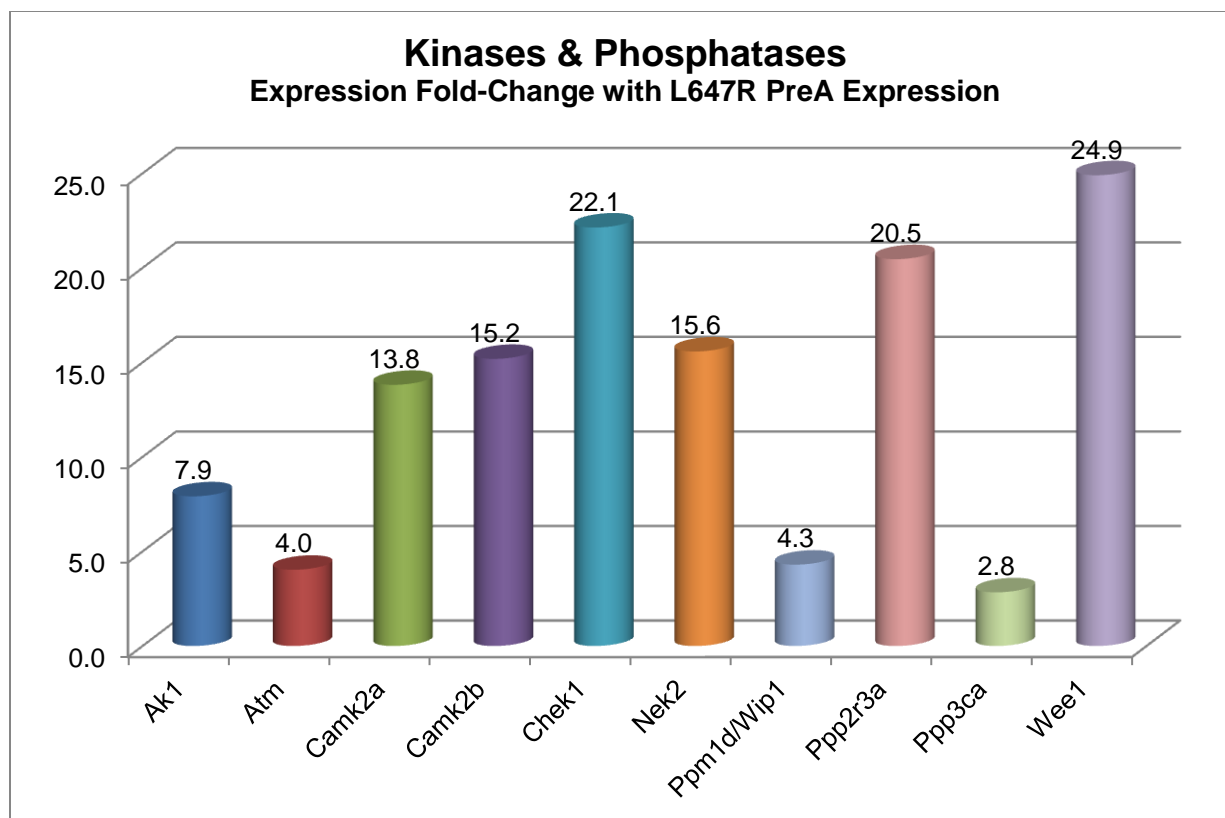


Figure 25. L647R Effects on Gene Expression (RT-qPCR Assay of Transcript Expression): Kinases & Phosphatases. Expression of Kinase and Phosphatase Genes in L647R PreA-expressing cells was altered. Changes shown are between cells induced (24 hours, 500 nM GenoStat) to express L647R PreA, compared to uninduced cells (DMSO-treated control), as assayed by RT-qPCR. P-values ≤ 0.05 for each fold-change value, see Table 2.

The p53-activated AK1 was shown to be a critical part of p53-mediated cell cycle arrest in response to cellular stresses such as hypoxia or DNA damage from irradiation. AK1 overexpression is sufficient to induce a reversible p53-mediated cell cycle arrest without apoptosis induction for extended periods of time¹⁶¹. Also, in this metabolic stress pathway, the Ca⁺/Calmodulin dependent kinase II isoforms (Camk2a/b) were upregulated. Camk2a/b inhibit activity of the cAMP response element binding protein (CREB) transcription factor, which lists c-Fos, Cyclin A1, and Cyclin D2 among its nearly 5000 transcriptional targets¹⁶². Camk2b also activates AMP-activated protein

kinase (AMPK), a critical regulator of cellular energy homeostasis. AMPK is activated following periods of cellular stress during which the ATP to AMP ratio decreases (such as during mitogen deprivation/starvation), which correlates to an increase in intracellular calcium, thus activating the Ca⁺/calmodulin dependent kinases¹⁶³. The activation of AMPK serves to stimulate several metabolic processes to conserve energy or use energy stores, activate cell cycle checkpoints, and halt cell cycle progression. AMPK inhibits protein synthesis by downregulating growth factor and nutrient sensing mTOR-mediated S6 ribosomal translation. AMPK partners with p53 in these processes, as its expression and activity are shown to be upregulated by p53, and p53 transcriptional targets Sestrin1 (Sesn1, expression level not measured in RT-qPCR assay) and Sestrin 2 (Sesn 2, transcript expression upregulated 5.5-fold in L647R PreA-expressing cells, Figure 26-Transcription Factors and Related Genes) have also been shown to activate AMPK. The Ataxia telangiectasia-mutated (ATM) kinase also phosphorylates AMPK in response to depleted cellular energy and metabolic stress¹⁶⁴. Transcript expression, according to the RT-qPCR assay, of the ATM serine/threonine kinase, a phosphatidylinositol-3 kinase-like kinase (PIKK) family member, is upregulated 4-fold in L647R PreA-induced cells compared to control. Though the AMPK transcript expression level is not directly measured in the RT-qPCR assay, increased expression of ATM and Camk2b, as well as p53 and Sesn2, creates a favorable set of conditions for activation of AMPK. Control of cell cycling, cellular homeostasis and aging, cell fate decisions between apoptosis, quiescence, and senescence by p53 and mTOR is significant, and we discuss this in more detail in other sections of this work.

ATM and Checkpoint kinase 1 (Chk1/Chk1) are most commonly associated with response to DNA damage but also have important functions in mediating cell cycle progression and control of traversing cell cycle checkpoints. ATM is activated by auto-phosphorylation or *trans*-phosphorylation in response to double strand DNA breaks (DSBs), whether these are caused by a genotoxic insult or as a normal phenomenon in the course of DNA replication, transcription, or V(D)J and class-switch recombination. ATM phosphorylates a number of effector proteins, primarily Chk2 (expression not assayed in the qPCR) but also Chk1. Chk1 (expression upregulated 22.1-fold) is most often part of the single strand DNA break (SSB) response and is thus typically activated by the Ataxia telangiectasia-related kinase (ATR, not included in the qPCR assay), the close PIKK relative of ATM that is most frequently associated with response to SSBs^{165,166}. As both DSBs and SSBs can occur during DNA replication, ATM and ATR are both often recruited to the DNA breaks that occur in DNA replication¹⁶⁷. In fact, ATR activity is activated by ATM, and possibly vice-versa¹⁶⁸.

Increased expression and activation of Chk1 can negatively regulate cell cycle progression even when checkpoints are unperturbed. This occurs in part by inhibitory phosphorylation of CDKs and by phosphorylation of Cdc25 proteins, which leads to their degradation thus, decreases the rate of dephosphorylation of CDK. Chk1 has been shown to repress gene transcription (of, for example, cyclin genes) through participating in histone modifications. In addition to being required for the intra-S-phase checkpoint response to stalled replication forks, Chk1 plays a role in proper formation of the mitotic spindle and in activation of the spindle checkpoint to prevent entry to mitosis with spindle aberrances. Chk1 phosphorylates Rb to enhance its binding to E2F, thus

antagonizing E2F-related transcription¹⁶⁹, although, as an apparent negative-feedback loop, Chk1 is an apparent E2F transcriptional target¹⁵³. To further introduce fine-tuned control to this regulatory loop, E2F1 is one of the transcription factors phosphorylated by ATM (E2F1 demonstrates a 6.4-fold expression upregulation with L647R PreA expression, in the qPCR assay, Figure 26).

Another transcription factor substrate for ATM phosphorylation is p53 (slightly upregulated, Figure 26), which is also phosphorylated by Chk1 and Chk2. Chk1/2-dependent phosphorylation of the tumor suppressor protein p53 leads to its stabilization and activation of both the G1 and G2 checkpoint pathways^{166,170-173}. Chk1 also interacts with, and recruits the activity of, the nucleolar protein nucleophosmin, which stabilizes p53 and p21 by preventing their degradation^{174,175}. Nucleophosmin (Npm2), which demonstrates a 16.5-fold upregulation in L647R-expressing cells (Figure 23-Transcription Factors and Related Genes), functions as a threshold modulator for p53, acting to repress its tumor suppressive and apoptosis-induction activities when p53 expression is below a threshold level. Once p53 expression level reaches a high level, Npm2 switches to its strong role as a p53- and p21-stabilization factor¹⁷⁶.

Ppp2r3a (upregulated 20.5-fold) is a subunit of a protein phosphatase holoenzyme (formerly known as “Pp2A”) that is 1 of 4 major serine/threonine kinases implicated in negative regulation of cell growth and division, as it actively reverses the phosphorylations carried out by kinases, especially the cyclin dependent kinases^{150,177}. For example, the cell division control protein 6 (Cdc6) is required for DNA replication by its action in forming the pre-replication complexes necessary for “licensing” of replication origins to control the timing of replication. Cyclin dependent kinases

phosphorylate Cdc6 to protect it from ubiquitination and degradation, thus promoting S- and M-phase entry, replication of genetic material and cell division. Protein phosphatase 2 reverses Cdc6 phosphorylation, leading to its degradation and consequently prevents DNA replication and arrests the cell cycle¹⁷⁸. Additionally, this phosphatase is reported to dephosphorylate pRb to mediate the hypophosphorylated status required for pRb to remain in its inhibitory complex with the E2F transcription factor.

Wee1 is tyrosine kinase responsible for inhibitory phosphorylation of Cdc2/Cdk1 in complex with CyclinB. This modification disables the Cyclin B/Cdk1-mediated entry of cells to mitosis, and thus results in cell cycle arrest at the G2/M transition¹⁷⁹. In the RT-qPCR assay, we find a 24.9-fold upregulation of Wee1, implying the possibility of its actions in negative regulation of cell proliferation and division.

The phosphatases Ppmd1/Wip1 and Ppp3a were upregulated in L647R PreA-expressing cells. Ppmd1/Wip1 (herein Wip1) dephosphorylates and thus inhibits p53 (Ser 15) and Chk1 (Ser 345), thereby abrogating cell cycle checkpoints. While this is an antiapoptotic action, and necessary for cells to re-enter the cell cycle following a completed checkpoint, it can also serve to promote potential tumorigenesis and Wip1 is often deregulated in cancers¹⁸⁰. Ppp3a is a subunit of another protein phosphatase holoenzyme, protein phosphatase 3 (formerly called 2B), and functions in calcium-dependent dephosphorylation of proteins¹⁴⁹. Taken together, the kinase/phosphatase profile of L647R PreA-expressing cells is difficult to interpret in terms of elucidating specific mechanisms of direct PreA effects on cell cycle gene-regulation; however, it

does strongly suggest activation of several moieties that participate in cell cycle arrest processes.

Transcription Factors and Associated Genes

In addition to the transcription factors and related genes already mentioned (p53, E2Fs, Npm2, Sesn2) several others demonstrate expression level effects from L647R PreA expression (Figure 26). As the 2 primary systems of cell cycle-related transcriptional control, expression of genes related to Rb-E2F association or p53 function are critical in evaluating regulation of the cycle. These pathways are controlled by a multitude of posttranscriptional and posttranslational mechanisms. Therefore, measurement of transcript expression levels, alone, for Rb-family suppressors, and E2F-family transcription factors, might not ultimately be informative regarding actual function.

While pRb expression was not directly measured in the qPCR assay, the other pocket proteins, Rbl1 (p107) and Rbl2 (p130), were assayed and shown to have transcript expression upregulation, while E2Fs 1, 3, and 4 also demonstrate upregulation. Also slightly upregulated in this gene category is Tfdp1 (DP-1), a transcription cofactor protein that complexes with E2F transcription factors to enhance inhibitory binding of hypophosphorylated pRB to the E2F/DP complex, or, when pRB becomes phosphorylated and dissociates from the complex, DP-1 actually stimulates E2F-mediated transcription of its target genes.

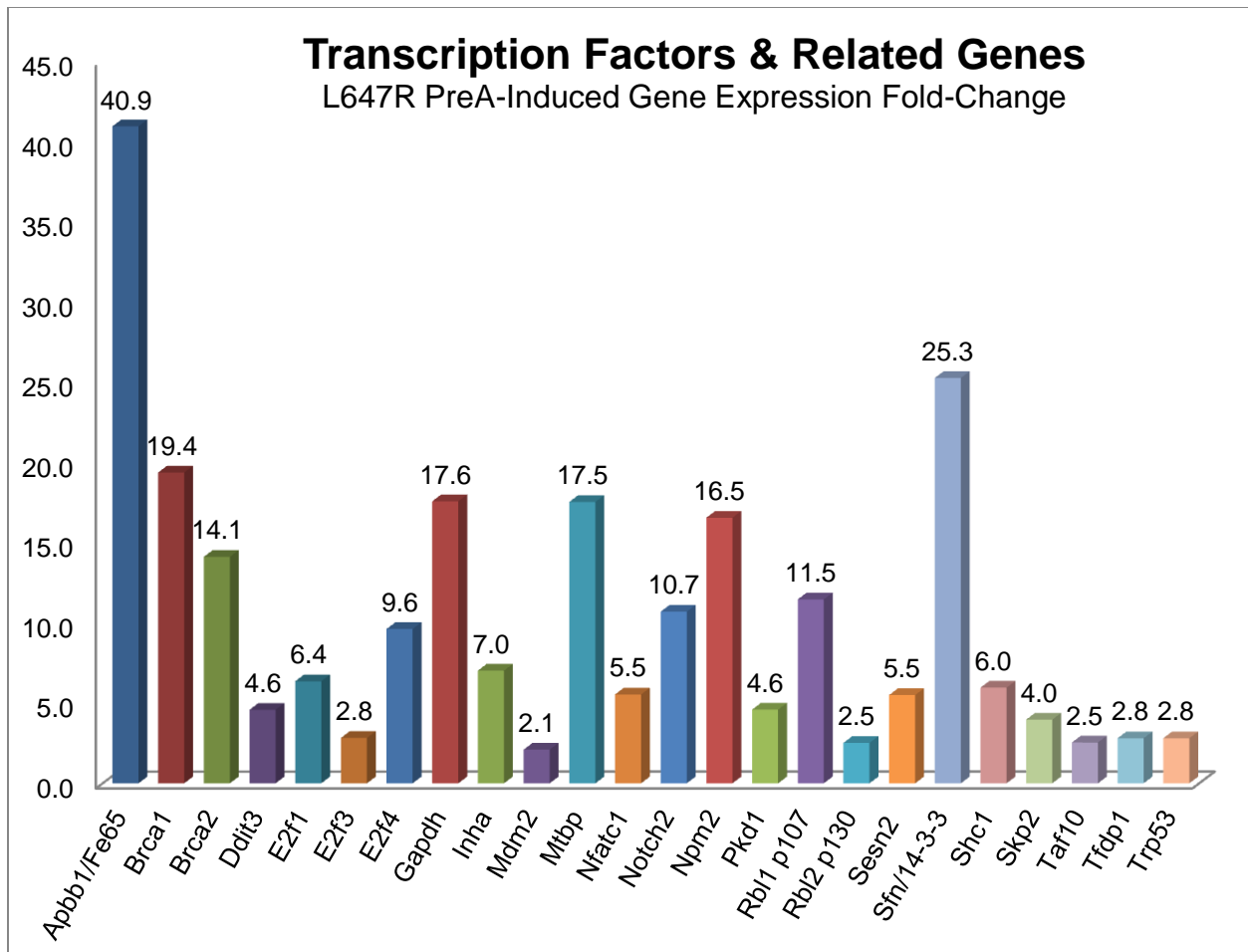


Figure 26. L647R Effects on Gene Expression (RT-qPCR Assay of Transcript Expression): Transcription Factors & Related Genes. Changes were found in expression of transcription factors and related genes in L647R PreA-expressing cells. Transcript levels in cells induced (24 hours, 500 nM GenoStat) to express L647R PreA were compared to uninduced cells (DMSO-treated control) by RT-qPCR assay. P-values ≤ 0.05 for each fold-change value, see Table 2.

In terms of regulating the actual expression level of p53, few other genes are more important than “mouse double minute 2” (Mdm2). Mdm2 (upregulated 2.1-fold with L647R PreA expression) is an E3 ubiquitin ligase that negatively regulates p53 function by promoting its proteasomal degradation¹⁸¹ [and reviewed in 182]. Interestingly, Mdm2 is a p53 transcriptional target apparently expressed as part of a negative feedback regulator of p53 expression¹⁸³. In another layer of control, Mdm2 can also

undergo autoubiquitination in which it directs its own targeting for proteasomal degradation. As a result, Mdm2 inhibitory effects on p53 are relieved, resulting in stabilization and increased activity of p53 in its cell cycle arrest and apoptotic functions. In addition to a role in negative regulation of the expression level of p53, Mdm2 also negatively regulates the expression levels of p21^{Waf1 184} and pRb¹⁸⁵, as well as the Mdm2-binding protein (Mtbp). Mtbp, which is upregulated with L647R PreA expression, has an apparent “switch” mechanism in which it can either function to stabilize or destabilize Mdm2 expression and function, depending on the ratio of expression between the 2 proteins. When Mdm2 expression levels are higher, Mtbp levels are lower, and Mdm2-autoubiquitination is blocked, thus directing Mdm2 ubiquitin ligase activity toward p53. Mtbp also enhances Mdm2 binding to p53, facilitating p53 degradation and promoting cell survival. Conversely, when expressed at higher levels, Mtbp can effectively reverse its stabilizing effects on Mdm2, facilitating Mdm2 autoubiquitination and degradation, thereby promoting p53 stabilization and increased p53 activity¹⁸⁶. Rb can be ubiquitinated and downregulated by Mdm2. In another negative regulatory role toward Mdm2, Mtbp interacts with pRb to elicit a p53-independent cell cycle arrest¹⁸⁷. Possibly, this set of opposing activities exists as a means to arrest the cell cycle when necessary without activating apoptosis.

The stratifin gene (Sfn), more commonly known as 14-3-3 σ , is significantly upregulated (25.3-fold), at the transcript level in cells expressing L647R PreA versus control. Members of the 14-3-3 family of proteins are directly involved in many of the cellular processes crucial for normal growth and development, including cytokinesis, cell-contact inhibition, anchorage-independent growth, and cell adhesion--the same

pathways often dysregulated in disease states such as cancer. Most 14-3-3 family members enhance the activity of survival and/or proliferation-associated proteins (such as the Raf kinase), or they antagonize the activity of proteins that promote cell death and senescence (such as Bad, Bim, and Bax). In contrast, however, 14-3-3 σ acts as a tumor suppressor and its expression is typically upregulated coordinately with p53 and BRCA1. This isoform serves to sequester Cdk1-Cyclin B complexes in the cytoplasm, thus delaying cell cycle progression, and is also a crucial regulator of translation during mitosis. Additional 14-3-3 σ tumor suppressor activity comes from its dual roles in stabilization of p53. First, it binds and negatively regulates Mdm2 by promoting its ubiquitination and degradation, thus stabilizing p53 by protecting it from Mdm2-mediated ubiquitination. Second, 14-3-3 σ enhances p53 stability and activity by scaffolding it to assist formation of p53 tetramer structures¹⁸⁸.

Glyceraldehyde-3-phosphate dehydrogenase (GAPDH) is an essential glycolytic enzyme that is expressed in all prokaryotic and eukaryotic organisms and found to be upregulated 17.6-fold in cells expressing L647R PreA in our RT-qPCR assay. Studies suggest that GAPDH is a multifunctional protein with a number of functions independent of its role in glycolysis. These activities include phosphorylating transverse-tubule proteins¹⁸⁹, stimulating RNA transcription¹⁹⁰, interacting with microtubules¹⁹¹, influencing RNA catalysis¹⁹², and acting as a diadenosine tetraphosphate binding protein to influence DNA replication and DNA repair¹⁹³. GAPDH is also upregulated by p53 after exposure to apoptotic insult¹⁹⁴.

The transcription factors BRCA1 and BRCA2 (upregulated 19.4-fold and 14.1-fold, respectively) are activated by ATM, ATR, and Chk1 in response to DNA damage

upon genotoxic exposure, as well as in the DNA breakage that occurs in DNA replication. They mediate intra-S phase and cell cycle checkpoints and function to ensure error-proof DNA repair. It has previously been demonstrated that BRCA1 can transcriptionally activate expression of p27^{Kip1} [195], upregulate p21^{Waf1} and GADD45^{196,197}, as well as coactivate the transcription of other p53-regulated genes¹⁹⁶. BRCA2 has also been shown to be phosphorylated in a cell cycle dependent manner by cyclin dependent kinases, to potentially mediate cytokinesis, and functions nonredundantly with BRCA1, especially in the G2/M cell cycle checkpoint¹⁹⁸.

Expression of the gene mutated in Polycystic Kidney Disease, Pkd1, is upregulated 4.6-fold in the L647R PreA-induced cells compared to the uninduced cells. The gene product of Pkd1, the Polycystin protein, inhibits mTOR by complexing with Tuberous Sclerosis 1 and 2 (TSC1/2) to stabilize the complex by inhibiting ERK-mediated phosphorylation of TSC1/2. The Polycystin-stabilized TSC1/2 complex inhibits the mTORC1 activating GTPase activity of Rheb, thereby inactivating the mTOR promotion of S6 ribosomal translation of a multitude of proteins¹⁹⁹. Polycystin-1 also activates the JAK/STAT pathway, thereby upregulating p21^{Waf1}, and inducing cell cycle arrest in G0/G1²⁰⁰. Suppressing DNA synthesis as well as protein synthesis, and also serving to upregulate p21^{Waf1} expression, is the Notch signaling pathway receptor protein Notch2. Notch2 demonstrates a 10.7-fold transcript upregulation with L647R PreA expression over uninduced cells. In contrast to the Notch1-mediated inhibition of transcription of the phosphatase and tensin homologue (PTEN) protein, Notch2 has been shown upregulate PTEN expression and lead to Akt dephosphorylation, thus inhibiting the Akt-mediated mTOR pathway of protein synthesis²⁰¹.

Amyloid β -precursor binding protein B (Apbb1/Fe65), herein Fe65, is an adapter protein that binds the β -amyloid precursor protein, which has a central role in the pathology of Alzheimers Disease. Recent studies have also shown overexpression of Fe65 is sufficient to effectively block cell cycle progression in G1 phase by completely abolishing the activation of a key S phase gene, the thymidylate synthase (TS) gene, which is driven by the transcription factor LSF/CP2/LBP1 (LSF)²⁰². Additionally, Fe65 has been shown to stabilize p53²⁰³. The significant upregulation of expression of Fe65 (40.9-fold) in cells induced to express L647R PreA, compared to uninduced cells, certainly warrants further investigation as a potential PreA mechanism of inducing cell cycle arrest. A PreA-mediated increase in Fe65 at such a dramatic level could lead to cell cycle arrest^{202,203}, although posttranslational factors would likely play a critical role in determining if that phenomenon occurs.

The DNA damage inducible transcript 3(Ddit3) transcription factor, also known as Chop10/Gadd153 (herein Chop10), is modestly upregulated in L647R PreA expressing cells. Chop10 is a Forkhead box O1 (FoxO1) transcriptional target expressed in response to cell stresses, especially those directly affecting the endoplasmic reticulum, such as increased reactive oxygen species and presence of unfolded proteins²⁰⁴. Chop10 dimerizes with the C/EBP transcription factor to inhibit transcription and induces growth arrest or apoptosis²⁰⁵. Interestingly, the amyloid β -precursor protein (APP, which regulates and is regulated by Fe65²⁰⁶) potentiates Chop10 induction and cell death in response to ER Ca²⁺ depletion²⁰⁷. The RT-qPCR assay revealed that the spectrum of transcription factors and transcription factor-related genes demonstrating altered transcript levels is quite broad upon L647R PreA

expression. Therefore, the data offer little clarification of specific mechanisms of PreA in regulating the cell cycle. However, the response to L647R PreA-expression by such a multitude of these factors strongly suggests the activation and involvement of multiple pathways in arrest of the cell cycle.

DNA Damage-Related Genes

As mentioned, although ATM phosphorylation has roles in unperturbed cell cycle progression, its primary functions are in relation to DNA damage response. In addition to the previously noted substrates involved in unperturbed cell cycling in addition to the response to DNA damage (BRCA1/2, p21/p27, Chk1, Ddit3, p53), ATM also phosphorylates the mediator and adaptor proteins MDC1, 53BP1, H2AX, and Mre11, all which assist in the assembly of multiprotein complexes at the sites of DSBs and in the subsequent DNA repair activities^{149,150,167,168}. Of those 4 target proteins, only the Mre11 (meiotic recombination 11) transcript level is assayed in our RT-qPCR panel and is upregulated 6.3-fold (Figure 27). The nuclease activity of ATM-activated Mre11 is required for the processing of DNA double-strand breaks (DSBs) to generate the replication protein A (RPA)-coated ssDNA needed for ATR recruitment and the subsequent phosphorylation and activation of Chk1¹⁶⁷.

Structural maintenance of chromosomes 1a (Smc1a), as the central component of the Cohesin complex required for proper cohesion of sister chromatids after DNA replication, is most aptly fit into the category for mitotic structure proteins; however, it is activated by ATM and does participate with ATM- or ATR-activated BRCA1 in mediating S-phase checkpoint control and DNA repair and thus bears mention in this category.

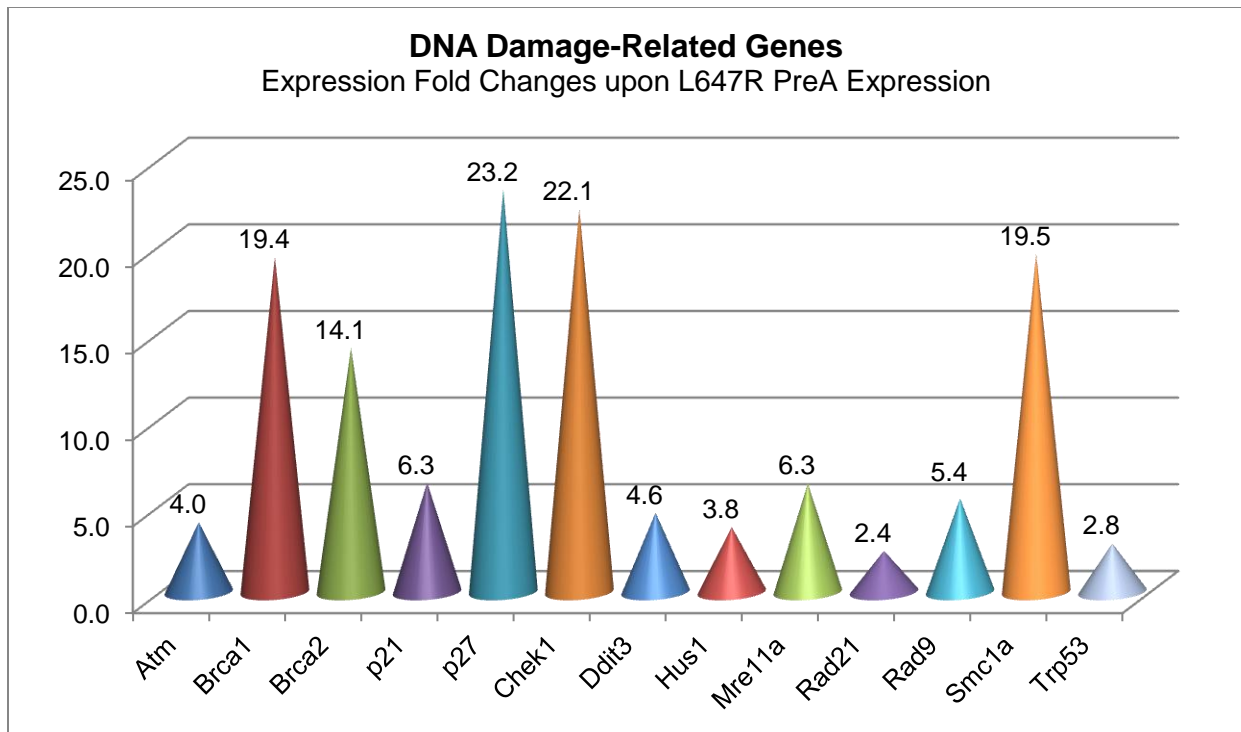


Figure 27. L647R Effects on Gene Expression (RT-qPCR Assay of Transcript Expression): DNA Damage-Related Genes. Expression changes were seen in several DNA damage-related genes in L647R PreA-expressing cells. Cells induced (24 hours, 500 nM GenoStat) to express L647R PreA were compared to uninduced cells (DMSO-treated control), using the RT-qPCR assay. P-values ≤ 0.05 for each fold-change value, see Table 2.

As seen in Figure 27, the Smc1a transcript expression level in L647R PreA-induced cells is upregulated a substantial 19.5-fold over the level found in uninduced cells. As demonstrated by altered expression of several kinases, transcription factors and transcription factor-associated genes, and DNA damage response and repair effectors, some role for PreA accumulation in affecting the gene expression program in DNA damage response appears evident. Although previous studies have suggested a potential inhibitory role for PreA in modulating DNA repair²⁰⁸, considering the complexity of the response and the potentially PreA-regulated participants, future studies should consider PreA-mediated roles of these genes.

Genes Associated with Cell Structure and Integrity/Chromatin/Chromosome Organization and Maintenance/Mitotic Assembly

Actin is one of the most highly-conserved proteins known and is ubiquitously expressed in all eukaryotic cells. Actin polymers form polar intracellular 'tracks' for kinesin motor proteins, allowing the transport of vesicles, organelles, and other cargo. These polymers also give mechanical support to cells and attach them to each other and the extracellular matrix at adherens junctions. In combination with myosin, actin forms the myofibrils that polymerize and depolymerize to function in cell motility. As manipulation of the cell cycle involves rearrangement and trafficking of many cellular components, as well as morphological changes to the cell (and even cytokinesis), it comes as no surprise to find β -Actin upregulated (14.8-fold) in cells overexpressing a protein (the L647R PreA) that has apparent functions in alteration of the progress of the cell cycle.

Expression of other filamentous cytoskeletal components are upregulated in the L647R PreA-expressing cells, as well, such as the Microtubule-actin crosslinking factors 1 and 2 (Macf1/2). These proteins link intermediate filaments, actin, and microtubules to play a role in organizing the cytoskeletal and nuclear envelope structure of the cell. Macf1 is upregulated 9.8-fold, while Macf2, also known as Dystonin (Dst), and noted as important in adhesion junctions as well as anchoring keratin-containing intermediate filaments to hemidesmosomes²⁰⁹, is upregulated 25.4-fold. Integrin β 1 (Itgb1), for which cells expressing L647R PreA demonstrate a 9.6-fold upregulation, also functions in cell adhesion and cell signaling.

Several genes with products responsible for regulating formation of the mitotic spindle demonstrate an increased expression in cells induced to express L647R PreA,

such as the NIMA (never in mitosis gene A)-related expressed kinase 2 (Nek2). The Nek2 protein kinase (upregulated 15.6-fold) is involved in regulating the G2/M transition by controlling the mitotic spindle-assembly checkpoint that is necessary for proper chromosome segregation during metaphase-anaphase transition. Nek2 activity is required for association of another protein, mitotic arrest deficient 2-like 1 (Mad211), to the kinetochore. Mad211 (upregulated 2.7-fold) is also required for the execution of the mitotic checkpoint and monitors the process of kinetochore-spindle attachment, functioning to inhibit the activity of the anaphase promoting complex (APC), thus preventing onset of anaphase, by sequestering Cdc20 until all chromosomes are properly aligned at the metaphase plate.

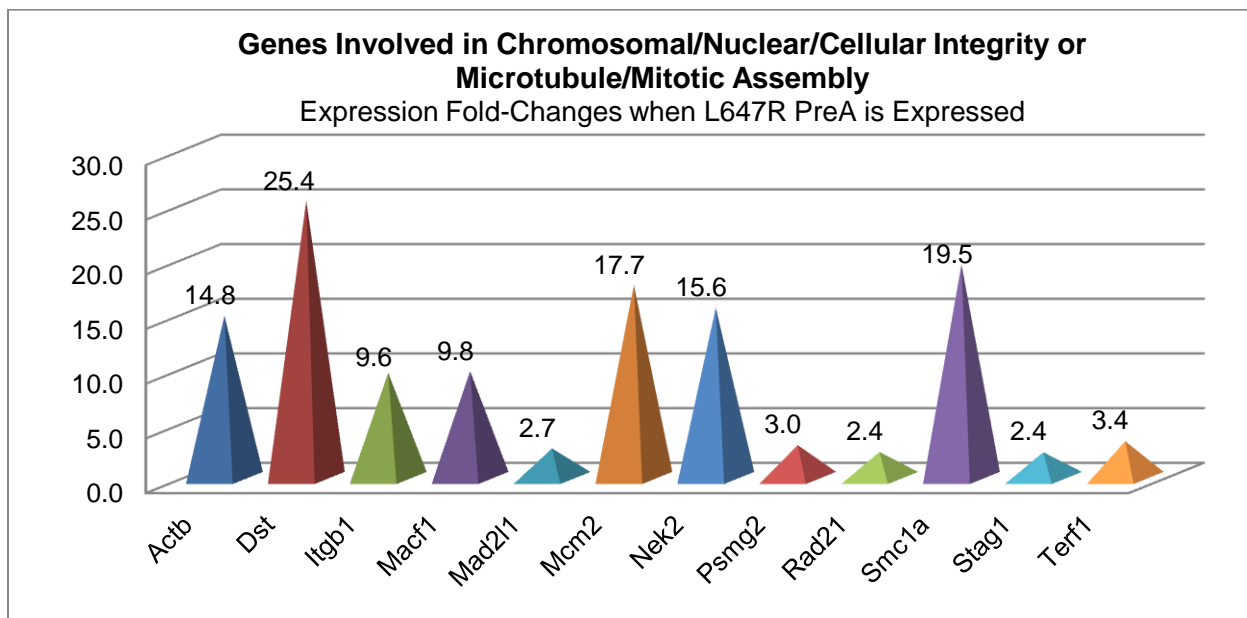


Figure 28. L647R Effects on Gene Expression (RT-qPCR Assay of Transcript Expression): Genes Involved in Chromosomal/Nuclear/Cellular Integrity or Microtubule/Mitotic Assembly. L647R PreA-expressing cells had altered expression of genes involved with chromosomal organization, structural integrity, assembly of microtubules, and the mitotic spindle. Expression levels in cells induced (24 hours, 500 nM GenoStat) to express L647R PreA were compared to levels in uninduced cells (DMSO-treated control), by the RT-qPCR assay. P-values ≤ 0.05 for each fold-change value, see Table 2.

Mcm2, a phosphorylation substrate of Cdc2/Cdk1 and Cdc7, is one of the highly conserved mini-chromosome maintenance proteins (MCM) that are involved in the initiation of eukaryotic genome replication and is upregulated 17.7-fold in the L647R PreA-induced cells. The hexameric protein complex formed by MCM proteins (Mcm2, along with Mcm4, 6, and 7) is the putative replicative helicase essential for 'once per cell cycle' DNA replication initiation and elongation in eukaryotic cells. Mcm2 is reported to be the regulator of the helicase activity of the Mcm-complex, and as such, it is a key component of the prereplication complex (pre-RC) and may be involved in the formation of replication forks and in the recruitment of other DNA replication related proteins^{149,150}.

Finally, the expression level of the TRF1/Terf1 gene, the transcript of which is translated to yield a component of the Shelterin telomere-capping protein complex, is upregulated 3.4-fold upon expression of L647R PreA. While this is not a spectacular increase, it is potentially significant given the critical nature of maintenance of telomeric structure in the preservation of genomic integrity, activation of senescence, apoptosis, and cellular aging²¹⁰⁻²¹³.

Effects of Accumulated PreA on Cell Cycle Control-Specific Protein Expression and Phosphorylation Assay by Antibody Array

While the data from the RT-qPCR assay of transcript levels of cell cycle related genes present compelling evidence of some role for the PreA isoform of LA in the regulation of the genes that control the cell cycle, we acknowledge significant regulation of many of these factors occurs primarily at the level of the protein and through posttranslational modifications. To expand the profiling of PreA-mediated effects on cell cycle, we assayed the expression level of a number of proteins involved in cell cycle

control. We used a commercially available protein/antibody microarray comprising biotinylated antibodies specific to proteins that control the cell cycle (Fullmoon Biosystems). Additionally, as the bulk of cell cycle-related posttranslational modification occurs in the form of protein phosphorylation, this array system also features phospho-specific antibodies to measure the comparative levels of phosphorylation of many cell cycle control proteins. Analysis of the array results revealed changes in expression levels and phosphorylation status of several key cell cycle proteins when we induced expression of L647R PreA.

From cells of the Rheoswitch 3T3 L647R PreA cell line, whole cell lysates were prepared as per the antibody array manufacturer instructions in a lysis buffer containing both protease and phosphatase inhibitors. Two lysate samples were prepared from replicate cultures, one from cells induced with 500 nM GenoStat for 72 hours to express the L647R PreA mutant protein and the other, an uninduced control sample (treated only with DMSO for the 72-hour period). A 72-hour timepoint was selected to encourage an optimal level of L647R PreA expression induction in asynchronously growing cells (as we have tried to avoid “artificial interruption” of the cell cycle by commonly used synchronization methods). The antibody array slides were hybridized and scanned at the Fullmoon Biosystems facility to ensure correctness of the processing steps without the expense of conducting trials necessary to optimize the processing in house. Each antibody was spotted in replicates of 6 on each slide, statistical evaluation of the 6 antibody fields per protein and hybridization and fluorescence controls were conducted on an “interslide basis,” in comparison between the L647R PreA-induced cell lysate slide and the noninduced slide, as well as on an

“intraslide” basis to determine outliers resulting from any inefficient or uneven labeling or hybridization within the replicates on the same slide. After subtracting fluorescence background of negative controls, outliers were excluded and relative expression levels of proteins compared. In addition, we analyzed the levels of phosphorylation of the proteins using PANDA, (Phosphor Antibody Array Data Analysis), which is a web-based software program developed at Emory University for analyzing phosphorylation antibody arrays²¹⁴. It identifies phosphorylated antibodies in the microarray and statistically quantifies the extent of phosphorylation for targets of these antibodies, enabling the quantitative evaluation of the phosphorylation changes, at each phosphorylation site, with a 95% confidence interval. Results of the antibody array assay are shown in Table 3. In the text, references to a particular protein’s “upregulation” or “downregulation” are intended, for simplicity to refer to the *expression level* or the phosphorylation *level* of the protein, in L647R PreA-expressing cells (after 72 hours of expression, induced by 500 nM GenoStat), compared to uninduced control cells.

Table 3. Results of Antibody Array: Changes in Protein Expression Levels and Phosphorylation

Protein List	Total Protein Expression Ratio		log2 of Ratio (Fold Change)		CV of 6 Replicates on a Slide		Phospho-Protein	Phospho Protein Ratio†		log2 of Ratio (Fold Change)		CV of 6 Replicates on a Slide	
	L647R/NI	L647R/NI	(Fold Change)	(Fold Change)	NI	L647R		P/NP-L647R/P/NP-NI	P/NP-L647R/P/NP-NI	(Fold Change)	(Fold Change)	NI	L647R
14-3-3 theta/tau (Ab-232)	0.84	-0.26	0.03	0.02			14-3-3 theta/tau (Phospho-Ser232)	0.69	-0.53	0.08	0.06		
14-3-3 zeta (Ab-58)	1.38	0.47	0.03	0.02			14-3-3 zeta (Phospho-Ser58)	0.27	-1.90	0.13	0.20		
14-3-3 zeta/delta (Ab-232)	0.76	-0.40	0.17	0.19			14-3-3 zeta/delta (Phospho-Thr232)	0.63	-0.66	0.18	0.05		
ABL1 (Ab-204)	0.98	-0.03	0.33	0.38**			Abl1 (Phospho-Tyr204)	2.00	1.00	0.09	0.07		
ABL1 (Ab-754/735)	0.88	-0.19	0.03	0.02			ABL1 (Phospho-Thr754/735)	0.59	-0.75	0.12	0.06		
c-Abl (Ab-412)	0.88	-0.18	0.13	0.07			Abl1 (Phospho-Tyr412)	0.88	-0.18	0.05	0.06		
Average for ABL1/c-Abl	0.88	-0.19					c-Abl (Phospho-Tyr412)	0.87	-0.21	0.24	0.13		
							c-Abl (Phospho-Tyr245)	0.41	-1.27	0.18	0.10		
AKT(Ab-473)	0.61	-0.70	0.14	0.16			AKT (Phospho-Ser473)	0.78	-0.36	0.05	0.02		
AKT1 (Ab-246)	0.86	-0.21	0.03	0.03			AKT1 (Phospho-Ser246)	0.65	-0.62	0.33**	0.05		
AKT (Ab-308)	0.72	-0.46	0.07	0.06			AKT (Phospho-Thr308)	0.80	-0.31	0.09	0.19		
AKT (Ab-326)	0.82	-0.29	0.02	0.03			AKT (Phospho-Tyr326)	0.27	-1.90	0.20	0.01		
AKT1 (Ab-124)	0.90	-0.15	0.10	0.14			AKT1 (Phospho-Ser124)	0.15	-2.70	0.04	0.02		
AKT1 (Ab-450)	0.66	-0.61	0.07	0.09			AKT1 (Phospho-Thr450)	0.95	-0.07	0.14	0.09		
AKT1 (Ab-72)	0.77	-0.38	0.06	0.09			AKT1 (Phospho-Thr72)	0.98	-0.03	0.03	0.03		
AKT1 (Ab-474)	1.01	0.14	0.03	0.03			AKT1 (Phospho-Tyr474)	0.59	-0.76	0.05	0.03		
Average for AKT1	0.79	-0.35											
AKT2 (Ab-474)	0.72	-0.48	0.05	0.02			AKT2 (Phospho-Ser474)	0.82	-0.29	0.16	0.05		
ATM (Ab-1981)	0.98	-0.03	0.03	0.09									
ATRIP (Ab-68/72)	1.02	0.03	0.07	0.09			ATRIP (Phospho-Ser68/72)	0.54	-0.89	0.10	0.09		
Beta actin	1.91	0.93	0.02	0.06									
BRCA1 (Ab-1423)	1.04	0.06	0.09	0.09			BRCA1 (Phospho-Ser1423)	0.88	-0.19	0.10	0.06		
BRCA1 (Ab-1457)	0.66	-0.60	0.16	0.05			BRCA1 (Phospho-Ser1457)	1.02	0.03	0.11	0.06		
BRCA1 (Ab-1524)	0.85	-0.23	0.03	0.05			BRCA1 (Phospho-Ser1524)	1.64	0.72	0.11	0.02		
Average for BRCA1	0.82	-0.29											
CDC25A (Ab-124)	0.63	-0.66	0.02	0.02			CDC25A (Phospho-Ser124)	1.04	0.06	0.16	0.17		
CDC25A (Ab-75)	0.85	-0.24	0.05	0.05			CDC25A (Phospho-Ser75)	1.16	0.21	0.35**	0.11		
Average for CDC25A	0.75	-0.42											
CDC25B (Ab-323)	0.79	-0.34	0.04	0.03			CDC25B (Phospho-Ser323)	0.85	-0.24	0.03	0.09		
CDC25B (Ab-353)	0.50	-0.99	0.04	0.01			CDC25B (Phospho-Ser353)	1.10	0.14	0.07	0.04		
Average for CDC25B	0.65	-0.62											
CDC25C (Ab-216)	1.44	0.53	0.16	0.13			CDC25C (Phospho-Ser216)	0.57	-0.82	0.08	0.09		
							CDC25C (Phospho-Thr48)	0.47	-1.09	0.14	0.01		
CDC2 (Ab-15)	0.84	-0.25	0.07	0.06			CDC2 (Phospho-Tyr15)	0.44	-1.17	0.14	0.28**		
CDK1/CDC2 (Ab-14)	0.80	-0.32	0.08	0.06			CDK1/CDC2 (Phospho-Thr14)	0.60	-0.73	0.16	0.02		
Average for CDK1/CDC2	0.82	-0.29											
CDK2 (Ab-160)	0.82	-0.28	0.06	0.14			CDK2 (Phospho-Thr160)	0.81	-0.30	0.07	0.11		
CDK7 (Ab-170)	0.67	-0.57	0.02	0.08			CDK7 (Phospho-Thr170)	0.97	-0.04	0.05	0.06		
Chk1 (Ab-280)	0.75	-0.42	0.10	0.04			Chk1 (Phospho-Ser280)	1.06	0.08	0.10	0.06		
Chk1 (Ab-286)	0.70	-0.51	0.05	0.01			Chk1 (Phospho-Ser286)	1.26	0.33	0.20	0.02		
Chk1 (Ab-317)	0.79	-0.34	0.07	0.02			Chk1 (Phospho-Ser317)	1.14	0.19	0.15	0.08		
Chk1 (Ab-345)	0.80	-0.31	0.02	0.04			Chk1 (Phospho-Ser345)	0.75	-0.42	0.17	0.09		
Average for Chk1	0.76	-0.39					Chk1 (Phospho-Ser296)	0.00	0.00	0.11	0.07		
							Chk1 (Phospho-Ser301)	1.02	0.03	0.10	0.12		
Chk2 (Ab-383)	0.78	-0.37	0.09	0.05			Chk2 (Phospho-Thr383)	0.91	-0.13	0.08	0.09		
Chk2 (Ab-387)	0.82	-0.29	0.11	0.12			Chk2 (Phospho-Thr387)	0.55	-0.87	0.14	0.05		
Chk2 (Ab-516)	0.57	-0.81	0.09	0.06			Chk2 (Phospho-Ser516)	1.49	0.58	0.04	0.09		
Chk2 (Ab-68)	0.94	-0.09	0.08	0.08			Chk2 (Phospho-Thr68)	0.57	-0.80	0.15	0.07		
Average for Chk2	0.78	-0.36											
Cyclin A(A1/A2) (inter)	0.63	-0.68	0.05	0.05									
Cyclin A1 (C-term)	0.66	-0.59	0.11	0.10									
Average for CyclinA1/2	0.65	-0.62											

****Table continues, next page****

Green Text=Expression Significantly Downregulated (≥ 0.31 -fold down = a ratio of 0.80 or less); Red Text=Expression Significantly Upregulated (≥ 0.26 -fold up= a ratio of 1.20 or more)

*L647R="L647R PreA": Lysates extracted from 3T3 RheoSwitch cells induced 72 hours (500nM GenoStat) to express L647R PreA; NI="Not Induced": Lysates extracted from cells treated with DMSO only (no induction reagent)

**Not Statistically Significant: A data-point contained within the set demonstrated a high CV (>0.20)

Text Highlighted in Blue=An Average of the Expression Data Values from Multiple Antibodies to the Same Protein, or for Phospho-protein, the Total Protein Expression Average was used in calculating the Phosphorylation Ratio for some phospho-sites in proteins for which a matched "non-phospho specific" antibody was unavailable or had a high CV

†P/NP-L647R/P/NP-NI= Phosphorylation Ratio (Phosphospecific protein detected in assay/Total protein detected in assay) of L647R PreA Expressing "L647R" (Test) Cell Lysate/Phosphorylation Ratio of "NI" (Not Induced) Control Cell Lysate

Table 3 (continued)

Total Protein	Total Protein Expression Ratio L647R/NI	log2 of Ratio (Fold Change)	CV of 6 Replicates on a Slide		Phospho-Protein	Phospho Protein Ratio† P/NP-L647R/P/NP-NI	log2 of Ratio (Fold Change)	CV of 6 Replicates on a Slide	
			NI	L647R				NI	L647R
Cyclin B1 (Ab-126)	0.76	-0.40	0.03	0.03	Cyclin B1 (phospho-Ser126)	0.89	-0.17	0.01	0.09
Cyclin B1 (Ab-147)	0.74	-0.42	0.07	0.04	Cyclin B1 (phospho-Ser147)	0.89	-0.16	0.10	0.11
Average for CyclinB1	0.75	-0.41							
Cyclin D1 (ab-286)	0.75	-0.41	0.13	0.12	Cyclin D1 (Phospho-Thr286)	0.83	-0.27	0.20	0.07
Cyclin D2 (Ab-280)	0.74	-0.43	0.09	0.05					
Cyclin D3 (Ab-283)	0.67	-0.58	0.07	0.05	Cyclin D3 (Phospho-Thr283)	0.82	-0.29	0.09	0.02
Cyclin E1 (Ab-395)	0.77	-0.37	0.02	0.03	Cyclin E1 (Phospho-Thr395)	0.79	-0.34	0.07	0.08
Cyclin E1 (Ab-77)	0.62	-0.68	0.17	0.11	Cyclin E1 (Phospho-Thr77)	1.26	0.33	0.13	0.04
Average for CyclinE1	0.71	-0.49							
Cyclin E2 (Ab-392)	0.94	-0.09	0.02	0.04					
DNA-PK (Ab-2638)	0.81	-0.30	0.05	0.02	DNA-PK (Phospho-Thr2638)	0.76	-0.40	0.11	0.03
DNA-PK (Ab-2647)	1.80	0.84	0.06	0.08	DNA-PK (Phospho-Thr2647)	0.35	-1.52	0.13	0.16
Average for DNAPK	1.31	0.39							
E2F1 (Ab-433)	0.84	-0.26	0.13	0.09	E2F1 (Phospho-Thr433)	0.73	-0.45	0.12	0.04
E2F2 (inter)	0.76	-0.39	0.09	0.06					
E2F4 (N-term)	0.56	-0.84	0.05	0.04					
E2F6 (inter)	0.31	-1.69	0.10	0.06					
FKHR (Ab-256)	1.79	0.84	0.06	0.05	FKHR (Phospho-Ser256)	0.41	-1.28	0.18	0.19
FKHR (Ab-319)	0.79	-0.33	0.07	0.09	FKHR (Phospho-Ser319)	0.61	-0.71	0.08	0.06
FKHRL1/FOXO3 (Ab-253)	0.88	-0.18	0.06	0.04	FKHRL1 (Phospho-Ser253)	0.97	-0.05	0.11	0.11
FOXO1/3/4-PAN (Ab-24/32)	0.73	-0.46	0.07	0.07	FOXO1/3/4-PAN (Phospho-Thr24/32)	0.19	-2.42	0.03	0.03
FOXO1A (Ab-329)	0.59	-0.77	0.05	0.04	FOXO1A (Phospho-Ser329)	1.06	0.08	0.05	0.05
Average for FoxO1/3/4	0.99	-0.02			FOXO1A/3A (Phospho-Ser322/325)	0.68	-0.56	0.04	0.04
Average for FoxO1/FKHR	1.06	0.08							
GAPDH	1.39	0.48	0.05	0.07					
GSK3 beta (Ab-9)	0.20	-2.36	0.02	0.03	GSK3 beta (Phospho-Ser9)	2.79	1.48	0.06	0.02
GSK3a-b (Ab-216/279)	0.68	-0.55	0.02	0.02	GSK3a-b (Phospho-Tyr216/279)	0.62	-0.68	0.07	0.38**
HDAC1 (Ab-421)	0.90	-0.16	0.12	0.26**	HDAC1 (Phospho-Ser421)	0.73	-0.45	0.17	0.06
HDAC2 (Ab-394)	0.91	-0.13	0.02	0.19	HDAC2 (Phospho-Ser394)	0.96	-0.05	0.09	0.08
HDAC3 (Ab-424)	0.73	-0.46	0.10	0.04	HDAC3 (Phospho-Ser424)	0.93	-0.11	0.09	0.03
HDAC4 (Ab-632)	0.82	-0.28	0.09	0.08	HDAC4 (Phospho-Ser632)	0.98	-0.03	0.08	0.04
HDAC5 (Ab-259)	0.74	-0.43	0.04	0.08	HDAC5 (Phospho-Ser259)	0.94	-0.08	0.04	0.06
HDAC5 (Ab-498)	0.79	-0.33	0.10	0.05	HDAC5 (Phospho-Ser498)	0.94	-0.09	0.10	0.08
Average for HDAC5	0.76	-0.39							
HDAC6 (Ab-22)	0.69	-0.54	0.02	0.06	HDAC6 (Phospho-Ser22)	0.40	-1.33	0.30	0.04
HDAC7 (C-term)	0.60	-0.73	0.05	0.03					
HDAC8 (Ab-39)	0.81	-0.30	0.05	0.02	HDAC8 (Phospho-Ser39)	0.85	-0.23	0.09	0.05
HDAC9 (C-term)	0.57	-0.81	0.07	0.07					
HDAC10 (inter)	0.55	-0.85	0.04	0.03					
Histone H2A.X (Ab-139)	1.12	0.16	0.07	0.07	Histone H2A.X (Phospho-Ser139)	0.67	-0.58	0.11	0.13
MDM2 (Ab-166)	0.97	-0.04	0.12	0.06	MDM2 (Phospho-Ser166)	0.66	-0.59	0.08	0.09
MDM4 (Phospho-Ser367)*	0.75	-0.42	0.10	0.08					
Myc (Ab-358)	0.72	-0.48	0.21	0.08	Myc (Phospho-Thr358)	0.42	-1.25	0.10	0.05
Myc (Ab-373)	0.83	-0.27	0.16	0.05	Myc (Phospho-Ser373)	0.84	-0.25	0.03	0.04
Myc (Ab-58)	0.82	-0.29	0.13	0.04	Myc (Phospho-Thr58)	0.64	-0.64	0.10	0.06
Myc (Ab-62)	0.68	-0.56	0.03	0.08	Myc (Phospho-Ser62)	1.39	0.48	0.08	0.12
Average for Myc	0.75	-0.42							
MYT1 (Ab-83)	0.68	-0.55	0.09	0.06					
P15INK (C-term)	0.75	-0.41	0.07	0.06					
p18INK (inter)	0	0	0.08	0.08					
p21Cip1 (Ab-145)	0.75	-0.42	0.03	0.04	p21Cip1 (Phospho-Thr145)	0.82	-0.28	0.07	0.03
p27Kip1 (Ab-10)	0.79	-0.33	0.03	0.02	p27Kip1 (Phospho-Ser10)	1.57	0.65	0.09	0.08
p27Kip1 (Ab-187)	0.65	-0.62	0.04	0.04	p27Kip1 (Phospho-Thr187)	1.29	0.37	0.11	0.04
Average for p27Kip1	0.67	-0.57							

****Table continues, next page****

Green Text=Expression Significantly Downregulated (>= 0.31-fold down = a ratio of 0.80 or less); Red Text=Expression Significantly Upregulated

*L647R="L647R PreA": Lysates extracted from 3T3 RheoSwitch cells induced 72 hours (500nM GenoStat) to express L647R PreA; NI="Not Induced": Lysates extracted from cells treated with DMSO only (no induction reagent)

**Not Statistically Significant: A data-point contained within the set demonstrated a high CV (>0.20)

***Total Protein Not Measured, Expression is in terms of Phospho-specific Protein only; Ratio of phos/total protein not available

Text Highlighted in Blue=An Average of the Expression Data Values from Multiple Antibodies toward the Same Protein, or for Phospho-protein, the †P/NP-L647R/P/NP-NI= Phosphorylation Ratio (Phosphospecific protein detected in assay/Total protein detected in assay) of L647R PreA Expressing "L647R" (Test) Cell Lysate/Phosphorylation Ratio of "NI" (Not Induced) Control Cell Lysate

Table 3 (continued)

Total Protein Protein List	Total Protein Expression Ratio L647R/NI	log2 of Ratio (Fold Change)	CV of 6 Replicates on a Slide		Phospho-Residue-Specific Protein	Phospho Protein Ratio† P/NP-L647R/ P/NP-NI	log2 of Ratio (Fold Change)	CV of 6 Replicates on a Slide	
			NI	L647R				NI	L647R
p300 (N-term)	0.22	-2.20	0.05	0.06					
p300/CBP (C-term)	0.38	-1.39	0.01	0.03					
Average for p300	0.30	-1.74							
p53 (Ab-15)	0.63	-0.67	0.06	0.05	p53 (Phospho-Ser15)	0.86	-0.22	0.14	0.08
p53 (Ab-18)	0.76	-0.39	0.01	0.03	p53 (Phospho-Thr18)	0.92	-0.11	0.06	0.04
p53 (Ab-20)	0.93	-0.10	0.10	0.07	p53 (Phospho-Ser20)	0.70	-0.52	0.04	0.03
p53 (Ab-315)	0.55	-0.86	0.15	0.04	p53 (Phospho-Ser315)	1.42	0.51	0.05	0.04
p53 (Ab-33)	0.94	-0.08	0.17	0.06	p53 (Phospho-Ser33)	0.52	-0.94	0.17	0.05
p53 (Ab-37)	0.74	-0.43	0.22	0.15	p53 (Phospho-Ser37)	0.80	-0.31	0.09	0.02
p53 (Ab-376)	0.61	-0.70	0.05	0.03					
p53 (Ab-378)	1.63	0.70	0.04	0.13	p53 (Phospho-Ser378)	0.49	-1.03	0.04	0.04
p53 (Ab-387)	0.59	-0.77	0.04	0.13					
p53 (Ab-392)	0.85	-0.24	0.09	0.09	p53 (Phospho-Ser392)	0.70	-0.52	0.11	0.04
p53 (Ab-46)	0.93	-0.10	0.08	0.06	p53 (Phospho-Ser46)	0.82	-0.29	0.08	0.04
p53 (Ab-6)	0.59	-0.77	0.04	0.04	p53 (Phospho-Ser6)	0.94	-0.08	0.07	0.04
p53 (Ab-9)	0.83	-0.28	0.11	0.02	p53 (Phospho-Ser9)	0.25	-2.00	0.30**	0.03
Average for p53	0.80	-0.30			p53 (Phospho-Ser366)	0.93	-0.11	0.12	0.07
					p53 (Phospho-Thr81)	0.89	-0.18	0.15	0.15
P90RSK (Ab-359/363)	1.11	0.15	0.08	0.09	P90RSK (Phospho-Thr359/Ser363)	0.67	-0.59	0.08	0.08
P90RSK (Ab-380)	0.78	-0.36	0.05	0.08	P90RSK (Phospho-Ser380)	0.97	-0.05	0.10	0.13
P90RSK (Ab-573)	0.77	-0.38	0.06	0.09	P90RSK (Phospho-Thr573)	0.91	-0.14	0.05	0.03
Average for p90RSK	0.89	-0.17							
p95/NBS1 (Ab-343)	0.80	-0.32	0.16	0.05	p95/NBS1 (Phospho-Ser343)	0.78	-0.35	0.12	0.16
PLK1 (Ab-210)	0.79	-0.35	0.20	0.20					
PP2A-a (Ab-307)	0.93	-0.11	0.17	0.27	PP2A-a (Phospho-Tyr307)	0.80	-0.31	0.12	0.09
RAD51 (Ab-309)	0.64	-0.64	0.05	0.05	RAD51 (Phospho-Tyr315)	1.15	0.20	0.05	0.03
RAD52 (Ab-104)	0.82	-0.28	0.13	0.08	RAD52 (Phospho-Tyr104)	0.99	-0.02	0.09	0.05
Rb (Ab-608)	0.78	-0.35	0.07	0.15	Rb (Phospho-Ser608)	1.00	0.00	0.11	0.06
Rb (Ab-780)	0.98	-0.02	0.08	0.09	Rb (Phospho-Ser780)	0.78	-0.36	0.03	0.08
Rb (Ab-795)	1.01	0.02	0.11	0.11	Rb (Phospho-Ser795)	0.61	-0.70	0.10	0.08
Rb (Ab-807)	0.94	-0.09	0.11	0.07	Rb (Phospho-Ser807)	0.63	-0.67	0.04	0.04
Rb (Ab-811)	0.79	-0.34	0.06	0.03	Rb (Phospho-Ser811)	1.05	0.07	0.04	0.10
Average for pRb	0.90	-0.10			Rb (Phospho-Thr821)	0.56	-0.84	0.08	0.04
Smad2/3 (Ab-8)	0.75	-0.42	0.03	0.01	Smad2/3 (Phospho-Thr8)	0.89	-0.16	0.20	0.09
Smad3 (Ab-179)	0.70	-0.51	0.02	0.05	Smad3 (Phospho-Thr179)	0.73	-0.46	0.01	0.06
Smad3 (Ab-204)	0.44	-1.20	0.06	0.14	Smad3 (Phospho-Ser204)	0.79	-0.35	0.09	0.02
					Smad3 (Phospho-Ser208)	0.89	-0.17	0.02	0.03
Smad3 (Ab-213)	0.88	-0.18	0.03	0.06	Smad3 (Phospho-Ser213)	0.68	-0.55	0.09	0.07
Smad3 (Ab-425)	0.63	-0.67	0.06	0.07	Smad3 (Phospho-Ser425)	1.12	0.17	0.14	0.04
Average for Smad3	0.66	-0.60							
Smad4 (inter)	0.77	-0.37	0.03	0.03					
SMC1 (Ab-957)	1.09	0.13	0.20	0.04	SMC1 (Phospho-Ser957)	0.69	-0.54	0.04	0.03
TGFBR1 (Ab-165)	0.17	-2.54	0.04	0.14					
TGF beta receptor II (inter)	0.64	-0.65	0.15	0.06					
TGFBR2 (Ab-250)	0.52	-0.93	0.05	0.15					
Average for TGFBR2	0.57	-0.82							
TGF beta1 (inter)	0.74	-0.43	0.06	0.03					
TGF beta2 (inter)	0.81	-0.30	0.06	0.03					
TGF beta3 (inter)	0.78	-0.36	0.06	0.03					
TOP2A/DNA topoisomerase II (Ab-1106)	0.57	-0.81	0.06	0.08	TOP2A/DNA topoisomerase II (Phospho-Ser1106)	1.16	0.22	0.02	0.03
Topoisomerase II beta (inter)	0.65	-0.63	0.04	0.04					
Average for TOPO2	0.61	-0.71							
WEE1 (Ab-53)	0.65	-0.61	0.07	0.04	WEE1 (Phospho-Ser642)	1.01	0.01	0.09	0.03

Green Text=Expression Significantly Downregulated (>= 0.31-fold down = a ratio of 0.80 or less); Red Text=Expression Significantly Upregulated (>= 0.26-fold up= a ratio of 1.20 or more)

*L647R="L647R PreA": Lysates extracted from 3T3 RheoSwitch cells induced 72 hours (500nM GenoStat) to express L647R PreA; NI="Not Induced": Lysates extracted from cells treated with DMSO only (no induction reagent)

**Not Statistically Significant: A data-point contained within the set demonstrated a high CV (>0.20)

Text Highlighted in Blue=An Average of the Expression Data Values from Multiple Antibodies toward the Same Protein, or for Phospho-protein, the †P/NP-L647R/P/NP-NI= Phosphorylation Ratio (Phosphospecific protein detected in assay/Total protein detected in assay) of L647R PreA Expressing "L647R" (Test) Cell Lysate/Phosphorylation Ratio of "NI" (Not Induced) Control Cell Lysate

Cross-Referencing Transcript Expression and Protein Expression

In terms of proteins included in the antibody array for which the qPCR array had indicated transcription was upregulated at 24 hours after L647R PreA expression induction, several indicate a decreased protein level at 72 hours after induction. Among these are Cyclins A, D, and E, cyclin dependent kinase inhibitors p21 and p27, Chk1, E2F4, p53, and Wee1. Cyclin B, for which downregulation of the mRNA transcript was indicated at 24 hours of L647R PreA expression induction, maintained downregulation at the protein level. Differential phosphorylation analysis reveals some additional information about the protein products of those transcripts. The remaining Cyclin E present in the L647R PreA expressing cells has downregulated phosphorylation at one site (Ser 395) on which phosphorylation blocks ubiquitination. At the same time, it has upregulated phosphorylation on a different site (Thr77) where phosphorylation is associated with targeting the protein for ubiquitin-mediated degradation. With the downregulation and upregulation of phosphorylation occurring at -0.34-fold, and +33-fold, respectively. It would seem further Cyclin E degradation is likely to occur in these cells.

Despite an overall downregulation of protein expression, the remaining p27 exhibits a pattern consistent with stabilization of the protein, as phosphorylation of Ser10 phosphorylation is associated with stabilization and upregulated 0.65-fold in L647R PreA- expressing cells. Notably, however, Ser 187 is thought to be a site on which phosphorylation signals ubiquitination, and it demonstrates 0.37-fold upregulation of phosphorylation with L647R expression. However, the stabilizing Ser10 phosphorylation is reported to be more potent²¹⁵. Similarly, though p53 total protein is

downregulated, the remaining p53 should be protected from the degradation-promoting ubiquitin ligase effects of Mdm2, as the demonstrated dephosphorylation of Mdm2 (Ser166) indicates inactivation²¹⁶. The p53 phosphorylation profile (with upregulated phosphorylation of Ser315 along with downregulated phosphorylation of Ser20, 33, and 37, and no change in phosphorylation of Ser 6, 15, 46 or Thr 18 or 81) is most consistent with replicative senescence²¹⁷.

The tumor suppressor gene BRCA1 indicated upregulation of transcript production at 24 hours on the RT-qPCR array, but at 72 hours, the protein level of BRCA1 is either at normal levels or is slightly downregulated with a modest -0.29-fold change from the protein level detected in uninduced cells. The phosphorylation level, however, of Ser1524 is upregulated 0.72-fold. Phosphorylation of this site aids BRCA1 facilitation of ATM-mediated phosphorylation of p53 in response to DNA damage (ATM-mediated but not ATR-mediated response), as part of induction of the G1/S cell cycle arrest program of DNA damage response²¹⁸.

Other DNA damage related proteins downregulated at 72 hours after induction of L647R PreA expression, for which transcript levels had been upregulated at 24 hours, include the DNA DSB-induced S-phase checkpoint-activating protein Smc1a and the phosphatase PP2A/Pppr2r3a. These demonstrate a decreased level of phosphorylation on sites that are known to functionally activate these proteins, thus indicating downregulation of activity of these proteins in L647R PreA-expressing cells^{219,220}.

Significantly Altered Expression of Key Cell Cycle Proteins

The antibody array assayed a number of proteins whose transcripts were not included in the RT-qPCR assay, several of which were significantly affected, either at

the level of expression or phosphorylation, in L647R PreA-expressing cells. Among these, the Rb protein did not demonstrate any significant changes in the expression level but was found to be significantly hypophosphorylated and was thus indicated to be actively repressing E2F-related transcription. Coordinately, in addition to the previously mentioned E2F4, the E2F2 and E2F6 transcriptional regulator proteins are downregulated with 72 hours of L647R PreA expression. Whereas the RT-qPCR measured the transcript levels of the genes encoding p107 and p130, but not pRb, the antibody array measures pRb expression/ phosphorylation, but not that of p107 or p130.

Among other proteins included on the antibody array that were not measured at the transcript level by the RT-qPCR array is the Cdc25 phosphatase family, members A, B, and C. Cdc25A acts during the G1/S phase of the cell cycle in concert with the CDK2/cyclin E complex, which it dephosphorylates to enhance cell cycle progression, and this activity is specifically required for the progression from G1 to S phase. Cdc25A expression is appreciably downregulated (by as much as -0.66-fold) by L647R PreA on the antibody array. CDK2 is not significantly hypophosphorylated, which supports the indication of the relative lack of Cdc25A activity in L647R cells. Also downregulated, by as much as half the normal expression level is Cdc25B, which is required for the G2/M phase transition. Cdc25B is phosphorylated and activated by aurora kinase A at the start of mitosis, and as mitosis progresses is then further phosphorylated in an auto-amplification loop, along with Cdc25C, by the CDK1/Cyclin B complex. Both Cdc25A and Cdc25B can be inactivated by the DNA damage checkpoint kinase, Chk1, thereby inhibiting progression to mitosis.¹⁴⁹ In contrast to members A and B of the Cdc25 phosphatase family, Cdc25C is significantly upregulated with L647R PreA expression,

at 0.53-fold over normal. Cdc25C phosphorylation, whether mediated by the CDK1/Cyclin B complex-autophosphorylating feedback route or by polo-like kinase 1 (Plk1, which also phosphorylates Cdc25C during mitosis), leads to greater activity of the CDK1/Cyclin B complex. CDK1, the M-Phase Promoting Factor serine/threonine kinase required for both G1/S and G2/M phase transitions is tightly controlled in regulation of the cell cycle, and inhibition of its activity is maintained by constitutive phosphorylation of Thr14 and Tyr15. These 2 sites are the targets of dephosphorylating activity of Cdc25C, resulting in activation of CDK1, cell cycle progression at G1/S or G2/M phase transition, and the ability to block p53-induced growth arrest¹⁴⁹. Notably, in addition to an M-phase promoting upregulation of Cdc25C protein level, the Cdc25C hypophosphorylation at Ser216 is also indicative of activated Cdc25C. The inhibitory phosphorylation of Cdc25C at Ser216 facilitates its complexing with 14-3-3, which occurs throughout interphase but not in mitosis, and results in Cdc25C localization and sequestration in the cytoplasm²²¹. On the contrary, the hypophosphorylation of Cdc25C Thr48 indicates inactivation, though it is noted that transitional variants exist between full inactivation and full activation of the phosphatase, featuring combinations of hyper- and hypophosphorylated inhibitory and/or activating regulatory phosphor-sites²²². Meanwhile, although its total protein level is downregulated, CDK1 is hypophosphorylated at Thr14 (Tyr15 demonstrates hypophosphorylation as well, but the CV is too high for this data point to be reliably informative). This implies an activated status for CDK1 (which, in order to be functional, would have to be in complex with either Cyclin A or B, a variable not measured in this study). As previously mentioned,

the expression levels of both Cyclin A and Cyclin B are decreased in this expression profile.

Glycogen synthase kinase 3 (Gsk3) is a kinase involved in glycogen processing and energy metabolism, Wnt signaling, and cellular proliferation via modulation of Cyclin D levels. Gsk3 β is constitutively active, promoting nuclear export and degradation of Cyclin D, but is inactivated by mitogenic stimuli and growth factors that induce phosphorylation on Gsk3 β Ser9 (mediated by Akt, p90Rsk/MAPKAPK1, others)^{223,224}. While we note inactivating Ser9 hyperphosphorylation of the detected Gsk3 β in the antibody array, it is concurrent with a total protein expression level downregulation of almost 2.4-fold compared to cells not induced for L647R expression, indicating a substantial overall downregulation of Gsk3 β . However, as the Cyclin D levels are also significantly downregulated in the L647R PreA expressing cells, the decrease in Gsk3 β likely has more implication for energy metabolism than for proliferation.

The cytokine known as transforming growth factor β (TGF β) has effects on cell proliferation that are context-dependent. In some situations, it can cause “transforming” cellular proliferation, as in the experiments involving its overexpression in normal rat kidney in which it was first described, and from which it derives its name²²⁵. Alternatively it can, apparently more commonly, act as an instigator of cell cycle arrest and apoptosis²²⁶. In the L647R PreA expressing cells, TGF β , its signal transducing proteins, the Smads, and its receptors, TGF β R1 and TGF β R2, each demonstrate downregulated expression on the antibody array. This multi-component downregulation within the pathway seems to clearly demonstrate that, at least by 72 hours of L647R PreA expression, the TGF β pathway is thoroughly inactivated in these cells.

The global transcriptional coactivator p300 demonstrates a significantly decreased expression level in cells induced 72 hours to express L647R PreA. p300 demonstrates 2 modes of activity in transcriptional regulation: as a histone acetyltransferase (HAT)²²⁷ or as a critical bridging coactivator linking the activation domains of numerous transcription factors to the DNA transcriptional machinery, and the RNA pol II, in particular²²⁸. p300 shares a very high level of homology with another such transcriptional coactivator, Creb Binding Protein (CBP), and the 2 are frequently referred to as a single entity, p300/CBP¹⁴⁹. (*Herein, I will simply refer to p300, with the implication CBP could serve many of the same functions.*) p300 acetylates nucleosomal histones to activate transcription^{[reviewed in 229]230,231}, while deacetylation of histone tails by histone deacetylases (HDACs) generally results in transcriptional repression²³². It is required for cell and tissue function during embryonic development, cell differentiation *in vitro*^{233,234,235}, indicating a lack of redundant functions from other coactivators. According to the protein expression levels detected by two different antibodies on the antibody array, one directed toward the N-terminus and the other to the C-terminus of the protein, the L647R PreA-expressing cells demonstrated between -1.39-fold and -2.20-fold change in p300 expression, respectively. Considering p300 cell cycle functions, which include direct regulation of CyclinE expression levels and activity and, consequently, activity of the Cyclin E-Cdk1 complex and E2F transcription factors in promoting cell cycle progression, a decreased p300 protein level could mediate PreA-related cell cycle arrest.

The kinase Akt (also known as protein kinase B, PKB), is a downstream target of the phosphatidylinositol 3-kinase, is stimulated by growth factors and has many

functions in metabolism, differentiation, proliferation, and apoptosis^{149,236}. One important Akt function is to positively regulate the mTOR pathway, controlling protein synthesis and cell growth. Its activity is frequently upregulated in cancers, as it suppresses the cell cycle-inhibiting and apoptosis-promoting expression of the FoxO genes. Akt phosphorylation of FoxO proteins induces binding of 14-3-3 or interaction with the nuclear export protein exportin (Crm1), and subsequent nuclear exclusion, by exporting out of the nucleus and/or sequestering FoxO in the cytoplasm, where it is not functional and tends to be degraded^{149,237-239}. Results of the antibody array indicate a downregulation of Akt in the L647R PreA expressing cells, but the FoxO1 and FoxO3 do not appear to be significantly up- or down-regulated by measuring total protein level. Three different FoxO1 antibodies indicate downregulation at -0.33-, or -0.79-fold, or upregulated at 0.84-fold, respectively, while the FoxO3 antibody indicates a very slight downregulation at -0.18-fold. Antibodies directed toward peptides common to FoxO isoforms 1, 3, and 4, demonstrate -0.46-fold regulation of total protein expression. However, the subcellular localization of FoxO is the primary means by which it is regulated, and this cannot be determined with the antibody array assay. Phosphorylation, which leads to FoxO inactivation and export from the nucleus, is significantly downregulated, indicating likely nuclear localization and activated FoxOs. Likewise, as previously mentioned, expression of transcriptional targets of FoxO, the cell cycle inhibitory p27 and p21, is slightly downregulated. The subcellular localization of those is also critical to functionality and not measured by this assay.

Taken together, the results of the antibody array demonstrate changes in expression levels of a variety of proteins that participate in regulation of the cell cycle,

as well as altered phosphorylation of a number of activating or inhibitory sites on cell cycle control proteins. These proteins represent several different pathways of cell cycle control, and implicate PreA as a potential modulator of a network connecting these pathways in cell cycle regulation.

Motif Analysis of LA Isoforms

An analysis of the peptide motifs of LA isoforms reveals insights to interaction partners and suggests cell cycle regulatory activity related to those interactions. While the array studies provide evidence of L647R PreA mediated changes in the expression levels and apparent functions of many cell cycle proteins, the mechanisms by which PreA interacts with some or all of these regulators, or with factors upstream of the measured proteins, are not clear. Thus, we found it necessary to consider factors that can interact directly with PreA, as potential initiator(s) in cascades of interactions between other molecules to accomplish the expression level changes we have detected among cell cycle regulating factors. It is well documented that LA is phosphorylated in a cell cycle dependent manner and that modification by phosphorylation precedes the dissociation of LA proteins from the nuclear membrane during mitosis^{240,241}. Several different phosphorylation sites have been reported in mature LA²⁴². As phosphorylation modification of proteins is a key regulatory mechanism for directing the cell cycle, we started our motif analysis by focusing on kinase substrate motifs, then we examined binding site motifs that require phosphorylation to activate or inactivate binding potential, and, finally, we briefly review other binding sites or interaction partners described in the current scientific literature.

Kinase Substrate Motifs in PreA

To survey kinase substrate motifs to determine possible PreA binding and interaction partners, we performed an initial motif analysis on the amino acid sequence of full length PreA, using the PhosphoMotif Finder application²⁴³ on the Human Protein Repository Database (HPRD, <http://www.hprd.org/>), which is a compendium of annotated motifs for which curated literature is cross-referenced to support the indicated interactions with the recognized motifs¹²⁰. The Phosphosite website is also a curated database of protein phosphorylation information that was useful (www.Phosphosite.org)¹¹⁷⁻¹¹⁹. We also queried the Phospho.ELM Database (<http://elm.eu.org/>)¹¹⁶, which performs analyses similar to HPRD PhosphoMotif Finder but uses homology to intuitively *predict* interactions (which HPRD claims, specifically, *not* to do), comparing the target sequence to “incidents” (sequence matches against previously encountered motifs) in its database. ELM does cross-reference against annotations from literature sources by pattern hit initiated (PHI) basic local alignment search tool (BLAST) methodology, which focuses a BLAST search on patterns that belong to a known interaction motif^[reviewed in 244]. This database introduces to the analysis a number of filters for “SMART” exclusion of homology-based predictions based upon the domain context of the peptide sequence, such as excluding predicted interactions that would not be known to occur within a globular domain when the motif in question occurs within a sequence indicating the presence of that particular structural domain¹¹⁶. However, this database could also possibly return predicted motif matches that do not have support in literature, and such computational predictions must be interpreted more succinctly as predictions only. In the PhosphoMotif Finder analysis²⁴³,

we found 363 motifs in Prelamin A that would be susceptible to phosphorylation by a variety of Serine/Threonine kinases and 13 Tyrosine kinase substrate sites. As we have particularly focused this study on deciphering functions of the Prelamin A isoform, we narrowed the results of the motif analysis to concentrate on the section of the protein that differs among the isoforms, the C-terminus (PreAct). The posttranslational modifications result in the cleavage processing of the 664 amino acid residue length protein to terminate at the site of Zmpste24 cleavage. The tyrosine residue at amino acid position 646 becomes the C-terminus postcleavage. As the peptide sequence actually differentiating PreA from wtLA consists of residues 647-664, we decided to include a longer c-terminal section in our analysis, beginning with residue 598 (Figure 29). Extending the analysis to include residues 598-646 allows interrogation of any binding sites that might overlap into the sequence 5'-to the Zmpste24 truncation site. Also, as residue 608 is the site introducing the causative cryptic splicing-variant that encodes Progerin, including the additional sequence allows for some comparison of functionality to Progerin. Thus, we reasoned, interrogating residues within the 598-664 residue C-terminal fragment could help differentiate PreA isoform function from Progerin function. We refer to this fragment herein as “the C-terminal 66 fragment.” Table 4 contains results of the Serine/Threonine kinase substrate analysis for the C-terminal 66 fragment, while a full length survey is included as Appendix C.

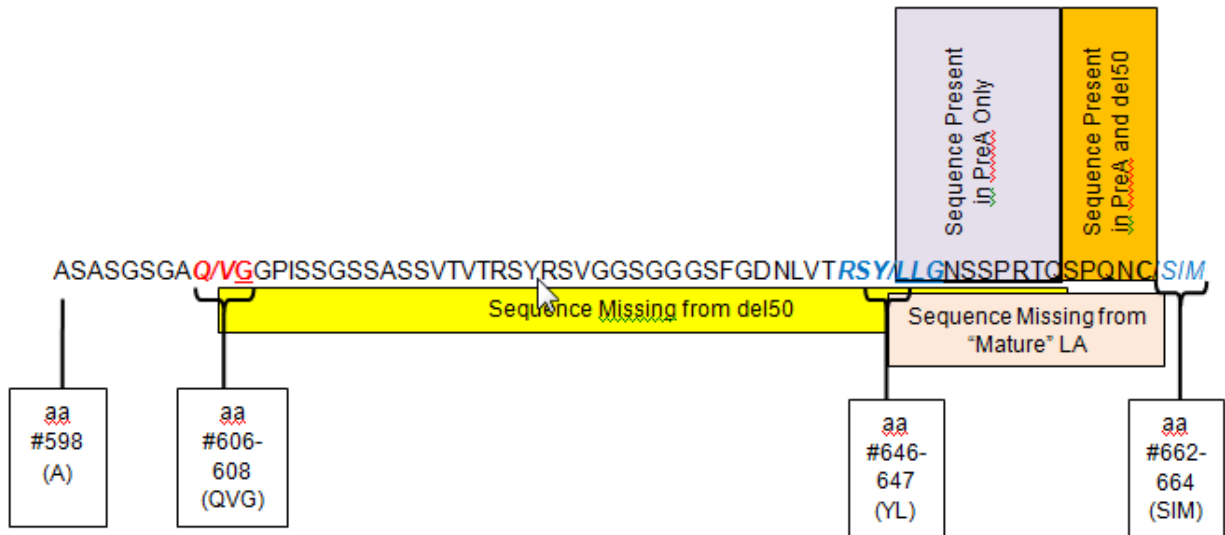


Figure 29. Lamin A C-terminal 66 Amino Acid Fragment Considered In Motif Analysis. Red text (Q/VG) indicates the G608G HGPS mutation site resulting in removal of amino acids 607-656 from the resulting protein (Progerin); the RSY/LLG sequence is recognized by Zmpste24 in normal Lamin A posttranslational maturation, which cleaves the protein between the Y/L residues at amino acid positions 646-647, to yield "mature" Lamin A; the C/SIM residues form the CaaX-box, which undergoes the initial cleavage (-aaXing), to remove the SIM residues 662-664 in the normal maturation process, following farnesylation of the C residue.

Table 4. Prelamin A C-terminus Serine/Threonine Kinase Substrate Motif Analysis

Amino Acid Residue #	AMINO ACID SEQUENCE	SUBSTRATE MOTIF	KINASE FOR THE INDICATED SUBSTRATE MOTIF	Motif # (of 363) ¹
598 - 603	ASASGS	X[pS/pT]XXX[A/P/S/T]	G protein-coupled receptor kinase 1	313
599 - 601	SAS	pSX[E/pS*/pT*]	Casein Kinase II	314
599 - 603	SASGS	pSXXX[pS/pT]	MAPKAPK2 kinase	315
599 - 603	SASGS	pSXXXpS*	GSK3 kinase	316
611 - 616	ISSGSS	X[pS/pT]XXX[A/P/S/T]	G protein-coupled receptor kinase 1	317
612 - 615	SSGS	[pS/pT]XX[S/T]	Casein Kinase I	318
612 - 615	SSGS	pSXX[E/pS*/pT*] ²	Casein Kinase II	319
612 - 615	SSGS	[pS/pT]XX[E/D/pS*/pY*]	Casein Kinase II	320
612 - 616	SSGSS	pSXXX[pS/pT]	MAPKAPK2 kinase	321
612 - 616	SSGSS	pSXXXpS*	GSK3 kinase	322
613 - 615	SGS	pSX[E/pS*/pT*]	Casein Kinase II	323
615 - 620	SSASSV	[pS/pT]XXX[S/T][M/L/V/I/F]	Casein Kinase I	324
616 - 618	SAS	pSX[E/pS*/pT*]	Casein Kinase II	325
616 - 619	SASS	[pS/pT]XX[S/T]	Casein Kinase I	326
616 - 619	SASS	pSXX[E/pS*/pT*]	Casein Kinase II	327
616 - 619	SASS	[pS/pT]XX[E/D/pS*/pY*]	Casein Kinase II	328
618 - 623	SSVTVT	X[pS/pT]XXX[A/P/S/T]	G protein-coupled receptor kinase 1	329
619 - 621	SVT	pSX[E/pS*/pT*]	Casein Kinase II	330
627 - 632	RSVGGS	X[pS/pT]XXX[A/P/S/T]	G protein-coupled receptor kinase 1	337
628 - 632	SVGGS	pSXXX[pS/pT]	MAPKAPK2 kinase	338
628 - 632	SVGGS	pSXXXpS*	GSK3 kinase	339
632 - 637	SGGGSF	[pS/pT]XXX[S/T][M/L/V/I/F]	Casein Kinase I	340
635 - 641	GSFGDNL	XpSXXDXX	Pyruvate dehydrogenase kinase	341
636 - 639	SFGD	pSXX[E/D]	Casein kinase II	342
636 - 639	SFGD	[pS/pT]XX[E/D]	Casein Kinase II	343
636 - 639	SFGD	[pS/pT]XX[E/D/pS*/pY*]	Casein Kinase II	344
636 - 639	SFGD	[pS/pT]XX[E/D]	Casein Kinase II	345
643 - 646	TRSY	[pS/pT]XX[E/D/pS*/pY*]	Casein Kinase II	346

Table continues on next page...

¹ Consecutive order of the indicated motif among the 363 Serine/Threonine Kinase Substrate sites identified within the full-length Prelamin A protein sequence.

² *=This phosphorylation modification “primes” the site, and must occur prior to the substrate recognition and subsequent phosphorylation of other residues within the motif.

Table 4 (continued)

Amino Acid Residue #	AMINO ACID SEQUENCE	SUBSTRATE MOTIF	KINASE FOR THE INDICATED SUBSTRATE MOTIF	Motif # (of 363)
650 - 653	NSSP	XXpSP	GSK-3, ERK1, ERK2, CDK5 *	347
650 - 655	NSSPRT	X[pS/pT]XXX[A/P/S/T]	G protein-coupled receptor kinase 1	348
651 - 653	SSP	X[pS/pT]P	GSK-3, ERK1, ERK2, CDK5	349
651 - 655	SSPRT	pSXXX[pS/pT]	MAPKAPK2 kinase	350
652 - 653	SP	pSP	ERK1, ERK2 Kinase	351
652 - 654	SPR	[pS/pT]P[R/K]	Growth associated histone H1 kinase	352
652 - 654	SPR	[pS/pT]X[R/K]	PKA kinase	353
652 - 654	SPR	[pS/pT]X[R/K]	PKC kinase	354
652 - 655	SPRT	[pS/pT]XX[S/T]	Casein Kinase I	355
652 - 655	SPRT	pSXX[E/pS*/pT*]	Casein Kinase II	356
654 - 657	RTQS	RXXpS	Calmodulin-dependent protein kinase II	357
654 - 657	RTQS	RXXpS	PKA kinase	358
654 - 657	RTQS	RXX[pS/pT]	Calmodulin-dependent protein kinase II	359
654 - 657	RTQS	[R/K]XX[pS/pT]	PKC kinase	360
655 - 658	TQSP	XXpSP	GSK-3, ERK1, ERK2, CDK5 *	361
656 - 658	QSP	X[pS/pT]P	GSK-3, ERK1, ERK2, CDK5	362
657 - 658	SP	pSP	ERK1, ERK2 Kinase	363

* Site also *predicted* by ELM as ProDK (proline directed kinase) substrate

Phosphorylation of the PreA C-Terminus

Using the PhosphoSite database¹¹⁷⁻¹¹⁹, we located curated data documenting *functional effects* of phosphorylation of the indicated LA residues (Figure 27). In addition, a large scale phosphoproteomics study found most of the same sites as HPRD and Phospho.ELM, plus 2 additional sites (Thr623 and Ser625), that were found to be phosphorylated, as well. Interestingly, this study reports LA to be 1 of 27 proteins in the

global proteomic analysis that demonstrate a “high level of phosphorylation site occupancy” during mitosis²⁴². Sites indicated to have a high level of phosphorylation during mitosis are highlighted on the Figure 27 graphic.

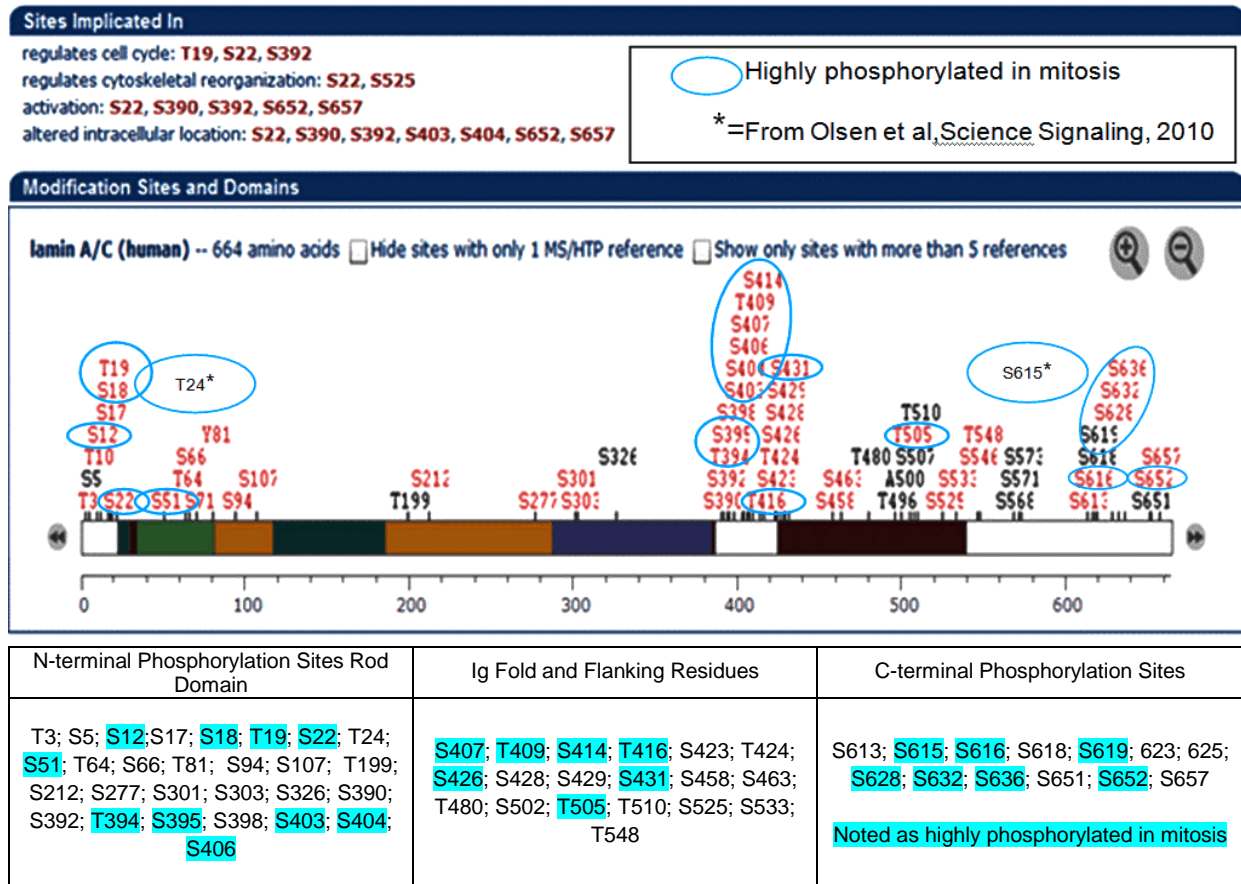


Figure 30. Phosphorylation Sites on Lamin A Protein (Compilation Graphic) with Functional Indications. Phosphorylation Sites on Lamin A protein, indicated by the curated Phosphosite database. Some cellular functions documented to be affected by the phosphorylation modifications are indicated. Also, one of the studies referenced by Phosphosite indicates LA is extensively hyperphosphorylated during mitosis, these sites are circled/highlighted in blue. This figure is adapted from a Phosphosite graphic, using additional data from Olsen, et al., Science Signaling, 2010.

Our own experiments to investigate PreA-tail phosphorylation involved Edman Degradation-based radioisotope-labeled (³²P) amino acid residue sequencing of the C-terminal fragment of PreA. In the Edman Degradation method of peptide mapping, peptides are incubated with the radiolabeled phosphorus, then the N-terminal residues

are “released” from the peptide one-by-one by as the free amino group reacts with phenylisothiocyanate, and can be identified using mass spectrometry on their phenylthiohydantoin derivatives²⁴⁵. As for our purposes, when the sequence and length of a peptide are known, the assay can be used to detect which residues have the radioactively-labeled phosphorus attached to them, indicating that residue was phosphorylated.

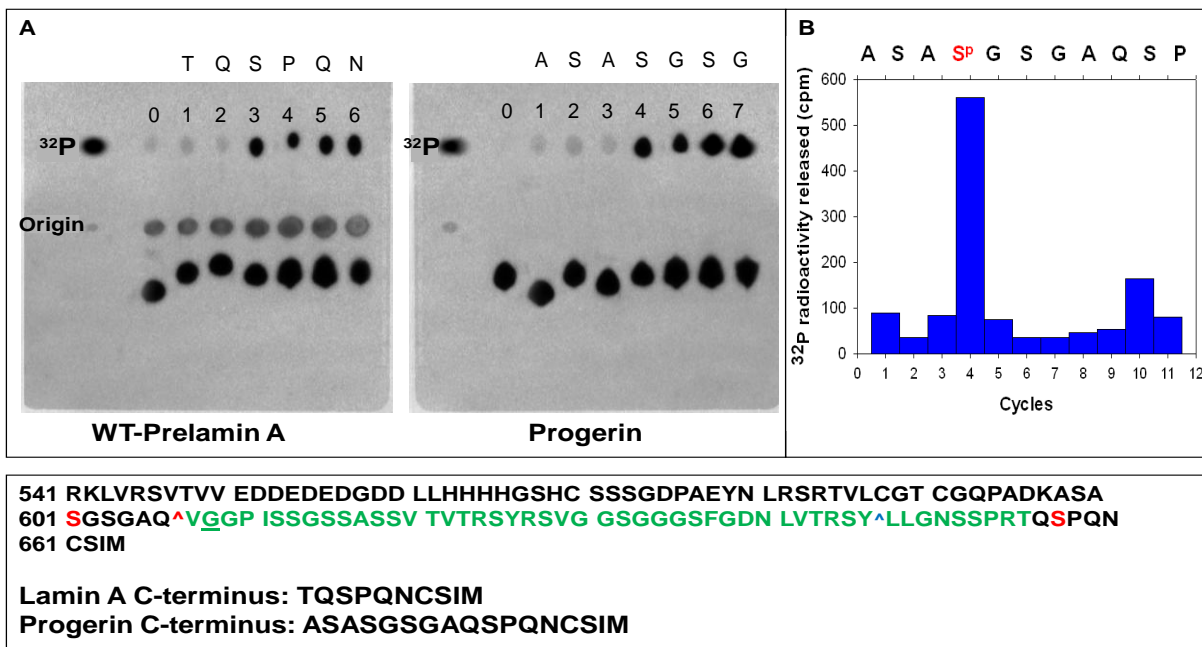


Figure 31. Radiolabeled Phosphorylation Peptide Mapping of the Lamin A C-Terminus. Phospho-mapping of the C-terminal LA peptide fragments by Edman Degradation of [³²P]-labeled wild type Lamin A (PreA, Panel A, left) and Progerin (Panel A, Right) C-terminal peptides involve separation of residues by HTLE and detection by phosphorimaging. The cyclical release of individual N-terminal amino acids of the peptide reveals a radioactive signal with the first [³²P]-labeled residue (phosphorylated) to be released from the peptide. Signal is cumulative when additional phosphorylated residues “cycle off” (release, with each cycle) in subsequent reaction cycles. Panel B graphic combines the Panel A Progerin Degradation, with an additional reaction using a shorter terminal peptide, as the reaction in Panel A was exhausted with the 4 terminal residues unmapped.

The peptide mapping in Figure 31 demonstrates the induced GFP -wtLA (which accumulates primarily as FC-PreA) is phosphorylated on Ser-657. The GFP-Progerin

C-terminus demonstrates substantial phosphorylation of Ser-601 but only a minimal level of Ser-657 phosphorylation. The phosphorylation of LA Ser-657 is described in only one report, a study by Lee et al.²⁴⁶, investigating mechanisms of Epstein Barr Virus (EBV) nuclear egress. During viral nuclear egress, the lamina is depolymerized, apparently through an ability of viral kinases to mimic host endogenous kinases and hijack of phosphosites of proteins, such as LA. The study reports EBV- and herpes virus-mediated depolymerization of LA during nuclear egress of the virion particles, and detection of phosphorylation on Ser-19, Ser-22, Ser-390, Ser-392, Ser-652, and Ser-657 of the depolymerized LA²⁴⁶. HPRD reports the 657 residue to be part of a kinase substrate site for GSK3, ERK1/2, Protein Kinase A or C (PKA/C), and/or CamK2 kinases. While we have been unable to find a study in the current scientific literature demonstrating detection of Ser-601 phosphorylation, HPRD reports the site to be a substrate domain for CK2. Future studies might evaluate for functional effect of this modification and determine if it also exists in wtLA/PreA, as well, or whether the altered sequence context of Progerin differently affects this site.

Phosphorylation-Dependent Protein Binding Motifs in PreA C-Terminus

We continued the database analysis to evaluate protein binding sites that contain phospho-sites and demonstrate phosphorylation-mediated control of the binding. Although 13 Tyrosine kinase substrate motifs were identified, only one of these occur within the C-terminal 66 fragment: a JAK2 kinase substrate motif (pYXX[L/I/V] involving residues 626-629 (YSRV). There were no Tyrosine phospho-dependent protein binding domain sites reported within the fragment, but the sequence does contain 11 binding

sites that require Ser/Thr- kinase phosphorylation, as shown in Table 5 (there are 39, total, indicated in the full PreA sequence, shown in Appendix D).

Table 5. Serine/Threonine Kinase-Dependent Protein Domain Binding Motifs within the Prelamin A C-Terminal Fragment

Amino Acid Residue #	AMINO ACID SEQUENCE	DOMAIN BINDING MOTIF	BINDING MOTIF DESCRIPTION	Motif # (of 39)¹
612 - 614	SSG	S[pS/pT]X	MDC1 BRCT domain binding motif	29
612 - 614	SSG	S[pS/pT]X	Plk1 PBD domain binding motif	30
615 - 617	SSA	S[pS/pT]X	MDC1 BRCT domain binding motif	31
615 - 617	SSA	S[pS/pT]X	Plk1 PBD domain binding motif	32
618 - 620	SSV	S[pS/pT]X	MDC1 BRCT domain binding motif	33
618 - 620	SSV	S[pS/pT]X	Plk1 PBD domain binding motif	34
651 - 653	SSP	S[pS/pT]X	MDC1 BRCT domain binding motif	35
651 - 653	SSP	S[pS/pT]X	Plk1 PBD domain binding motif	36
652 - 653	SP	[pS/pT]P	WW domain binding motif	37
654 - 657	RTQS	RXXpS	14-3-3 domain binding motif	38
657 - 658	SP	[pS/pT]P	WW domain binding motif	39

¹ Consecutive order of the indicated motif among the 39 Serine/Threonine Kinase-Dependent protein domain binding motif sites identified within the full-length Prelamin A protein sequence.

Three different phosphorylation-dependent binding motifs were identified by PhosphoMotif Finder, within the C-terminal 66 fragment. First, there is a series of 4 Mediator of DNA Damage Checkpoints 1 protein (Mdc1)/Polo-like Kinase 1 (Plk1) shared binding sites, of which the first 3 are retained following Zmpste24 proteolysis of the PreA protein to form LA in the normal maturation processing. The second motif is the 14-3-3 binding motif, which occurs only once in the fragment, and is lost with

Zmpste24 cleavage. The third motif is the WW domain-binding site, found in 2 positions that are removed in the normal maturation processing of LA. Notably, all of these binding sites are deleted from del50/Progerin except the most 3' WW domain-binding site at amino acid sequence position 657-658 (graphic representation in Figure 32).

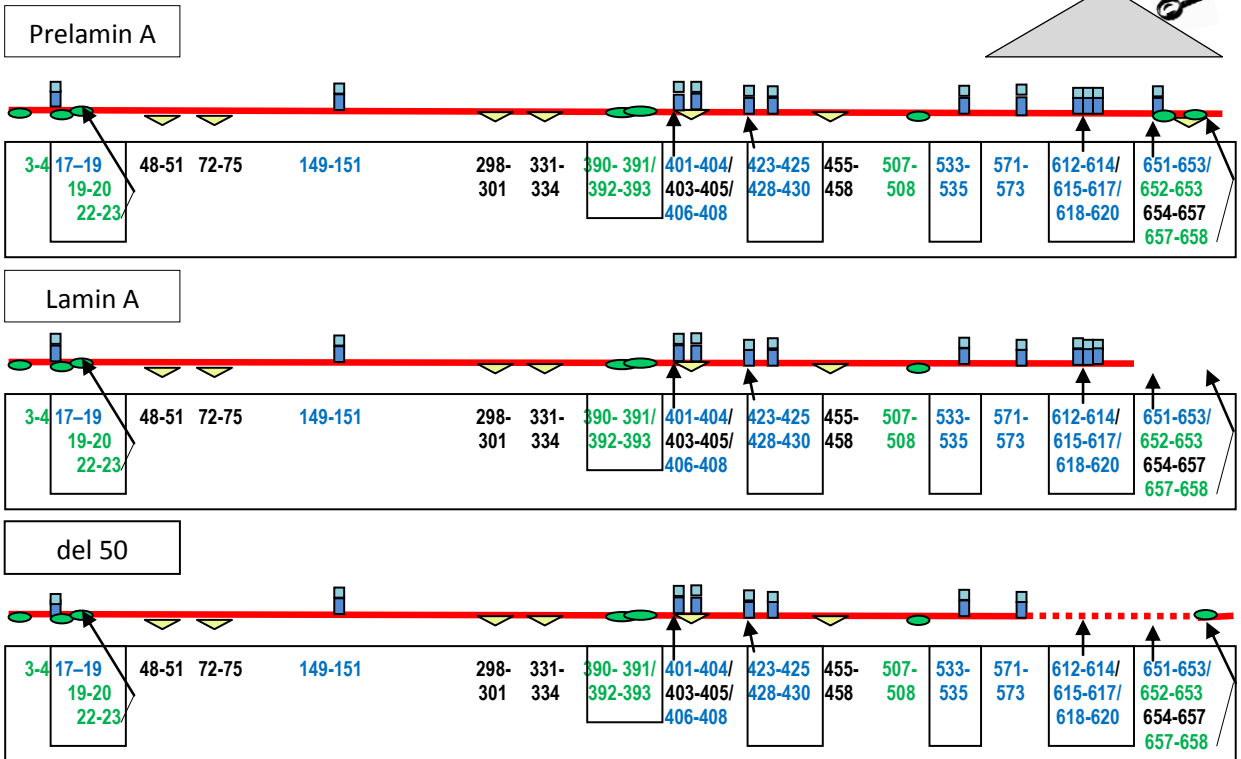
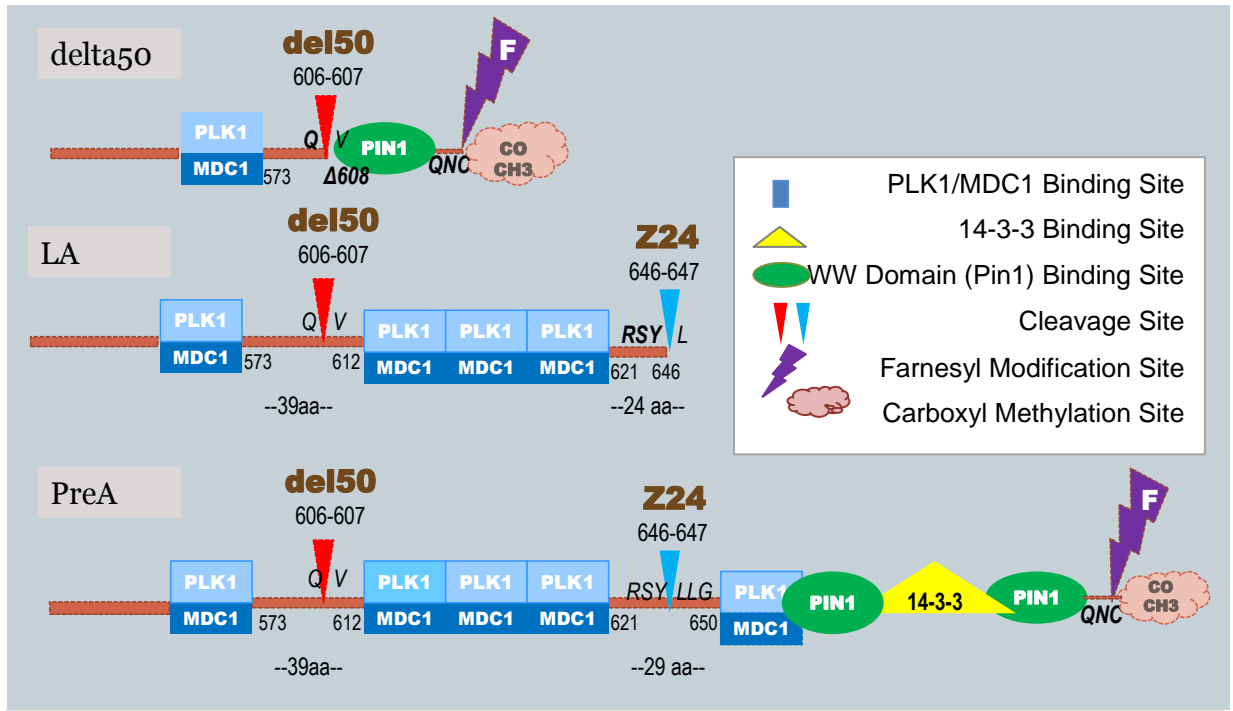


Figure 32. Arrangement of Phosphorylation-Dependent Protein Motif Binding Sites in the PreA C-Terminal 66 Residue Fragment.

Cross-Reference of Kinase Substrate Sites and Kinase-Dependent Protein Motif Binding Sites

The cell cycle-related periodicity of the kinases controlling the phosphorylation-dependent binding for the sites is an important consideration to indicate possible clues as to cell cycle progression-related timing of activation of these binding sites. For instance, determining conditions during which the kinases GSK3, ERK1/2, CDK4/5, and possibly CK1/2, act on LA could provide potential information regarding the sites in LA that are substrate-candidates for those particular kinases (Ser19-20 and Ser22-23), in addition to the CDK1-phosphorylation activity toward Ser22 described previously.²⁴⁷ Similarly, Ser390-391 and 392-393 are possible substrates for ERK1/2, CK1/2, MAPKAPK2 (Rsk90), or DNAPK (DNA dependent Protein Kinase), and Ser652-53 and Ser657-58 are potential substrates for ERK1/2, MAPKAPK2, Growth assoc H1 Kinase, PKA/C, CK1/2; CamK2, or GSK3. Figure 33 provides a graphic representation of the PreA C-terminal 66 amino acid fragment kinase substrate motifs as well as the phosphorylation-dependent binding sites.

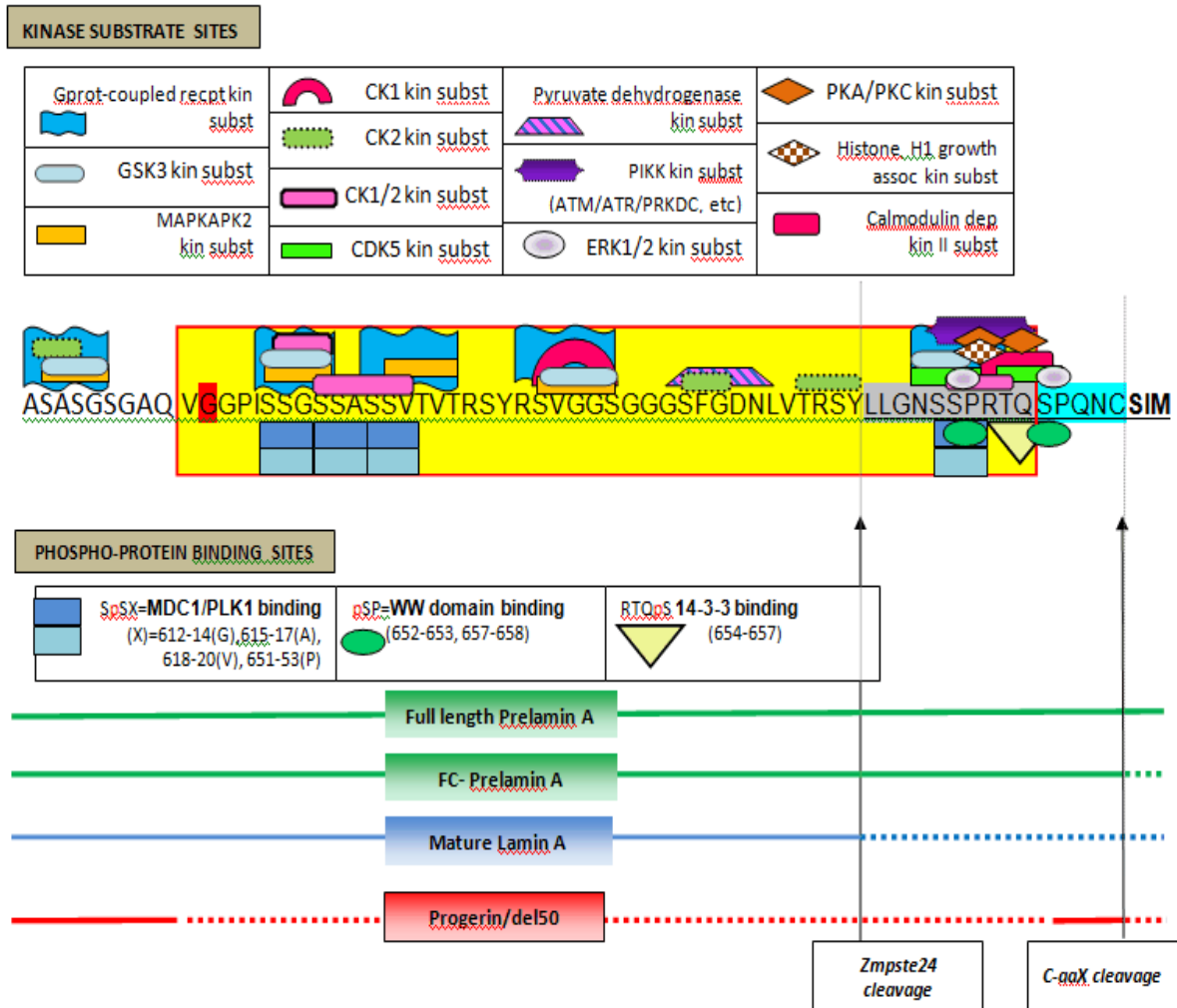


Figure 33. Combined Graphic of Kinase Substrate Motifs/Protein Motif Binding Sites in PreA C-Terminus. Graphic Representation of Kinase Substrate Sites & Phosphorylation-Dependent Binding Sites in PreA C-terminal 66-Amino Acid Fragment.

Cross-Reference of Genes/Proteins with Altered Expression vs. Motif Analysis Findings

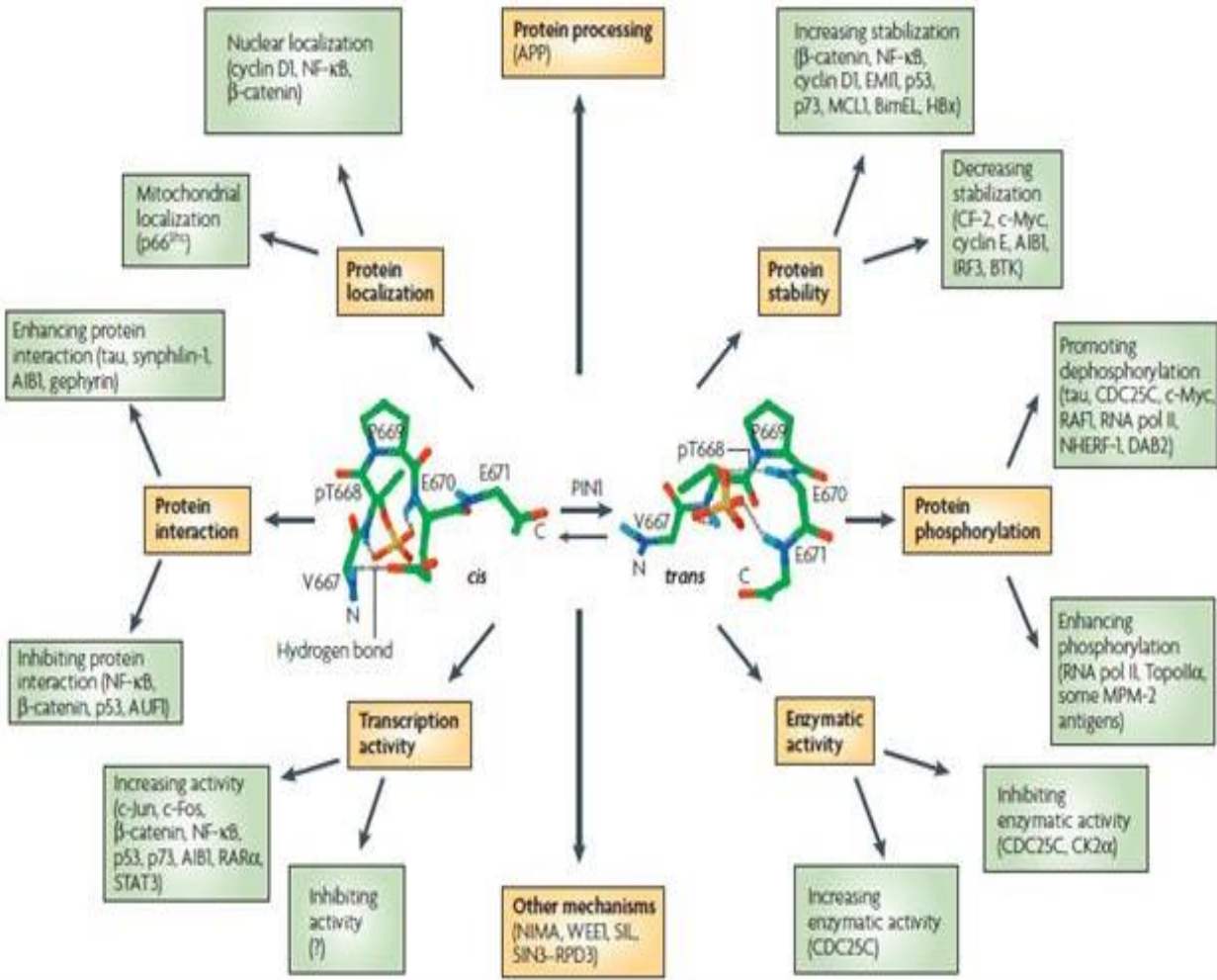
The 14-3-3 “adapter protein” has already been discussed as an important regulator of cell cycle, as it has demonstrated altered expression with L647R PreA expression, on the qPCR and antibody arrays and has been previously annotated as a Lamin A-interacting protein¹⁷². The Polo-like Kinase 1 was included in the antibody array and demonstrates a 0.35-fold downregulation of protein expression in cells induced to express L647R PreA. This kinase shares a phosphorylation-dependent

binding site motif with Mdc1. In addition to ATM, ATR, and Chk1/2, 2 of the most critical DNA damage response proteins are Plk1 and Mdc1. Mdc1 is a key regulator involved in several cellular pathways including apoptosis induction, G2/M, and intra-S-phase cell cycle arrest^{248,249}. Mdc1 acts not only as a mediator of DNA damage checkpoints but also as a mediator of DNA damage repair²⁵⁰. Studies suggest ATM is actually a downstream target of Mdc1^{251,252}, wherein Mdc1-mediated activation of ATM induces phosphorylation/ activation of Chk2, which in turn interacts with Mdc1 and relocalizes to the DNA damage sites, suggesting a critical role for Mdc1 in the Chk2-mediated DNA damage response^{248,253}. Active Chk2 is responsible for the inhibitory phosphorylation of Cdc25C at Ser216, leading to a Cdk2-mediated G2/M arrest (we report Cdc25C Ser216 phosphorylation downregulation, with L647R PreA expression), and Chk2 also promotes apoptosis by phosphorylation of p53 on Ser20 (also downregulated with L647R PreA). Mdc1-ATM-activated Chk2 also negatively regulates Plk1, blocking its ability to promote entry to mitosis, and upregulation of Mdc1 leads to downregulated expression and activity of Plk1, along with accumulation of cells in S-phase or arrested at the G2/M transition^{254,255}. Mdc1 is required for assembly of the Mre11-Rad9-Nbs1 (MRN) DNA damage repair complex with γ H2AX²⁵⁶ and is required for retaining p53-binding protein 1 (53BP1) at sites of DNA damage^{256,257}. Thus, the major factors of DNA damage response and repair are unable to complex and execute repair without Mdc1.

WW Domain Proteins (Pin1)

The 2 WW domain binding motifs residing in the C-terminal 66 fragment are separated by the single 14-3-3 protein binding motif (Figure 32, Table 5). In fact, the 2 WW domain binding sites each overlap one of the other binding motifs, one with a slight

overlap of the last Mdc1/Plk1 binding site in the sequence, and the other WW domain-binding site slightly overlaps the most c-terminal 14-3-3 site. WW domains consist of approximately 35-40 amino acids and contain 2 Tryptophan residues (hence the moniker “WW” domain), with β -sheets formed around the aromatic Tryptophans. Binding motifs for WW domains require proline residues. As for binding partners targeted to the WW domain binding motifs, HPRD identified 53 mammalian proteins with WW domains, 17 of which are nuclear¹²⁰. ProSite, a bioinformatics tool curated by the UniProt Consortium: European Bioinformatics Institute (EMBL-EBI), Swiss Institute of Bioinformatics (SIB) and the US’s Protein Information Resource (PIR), produced a list of 24 human nuclear compartment proteins containing WW domains^{258,259} (Appendix E). Included among these nuclear WW domain-containing proteins are several transcriptional regulators and accessory proteins, others that participate in scaffolding of receptor signaling complexes, ubiquitin ligase proteins (including 2 that are specific to regulation of SMADs), an oxidoreductase involved in apoptosis, Dystrophin (the protein mutated in Duchenne and Becker Muscular Dystrophy), Utrophin (involved in cytoskeletal anchoring), Mlh3 (a mismatch DNA-repair protein), and the peptidyl prolyl *cis-/trans-* isomerase (PPIase) Pin1. While several of these are relevant in terms of specific cell cycle and homeostasis functions, Pin 1 has demonstrated many essential functions in cell cycle control²⁶⁰ and interacts with number of cell cycle regulatory proteins (including Akt^{261,262}, p27^{263,264}, FoxOs^{264,265}, p53^{266,267}, Plk1²⁶⁸, Cdc25^{269,270}, RNA Polymerase II²⁷¹, and Smads²⁷²), see Figure 34.



Reprinted by permission from Macmillan Publishers Ltd: Nature Reviews Molecular Cell Biology, Lu and Zhou (2007)

Figure 34. Pin1 Targets and Molecular Mechanisms. This graphic depicts the variety among Pin1 targets, as well as among the several mechanistic activities of Pin1²⁷³.

Importantly, there are 4 different classes of WW domains, differentiated by ligand specificity. The binding motif repeated in the PreA sequence consists of a phospho-Serine-Proline pairing that fits the Type IV WW Domain classification, for which Pin1 appears to be unique among human nuclear proteins²⁷⁴. Therefore, considering the complexity of pathways regulated by Pin1, and the equally complex effects of L647R PreA expression upon cells (as indicated by the number of gene products demonstrating altered expression), as well as the unique motif specifications and

nuclear compartment localization, Pin1 was the most attractive of the candidate proteins for further investigation. Furthermore, during the course of our study, Milbradt et al. published a study in which they present a fascinating and elegant analysis of a Human Cytomegalovirus (HCMV) mechanism of nuclear egress. HCMV directs viral kinase activity toward Lamin A to induce binding of Pin1 and subsequent localized depolarization of the nuclear lamina, similar to the depolarization involved in cytokinesis, which appears to be dependent upon Pin1 isomerization of the Lamin A proteins. This group used a similar bioinformatics analysis (using the ELM database, only, however) to determine Pin1 as a candidate for binding Lamin A²⁷⁵. They cite a previous report regarding HCMV viral kinase mimicry of Cdk1 in Ser22 phosphorylation of Lamin A and subsequent nuclear membrane disruption²⁴⁷, which directed their attentions toward the N-terminus of the Lamin A protein. Interestingly, Milbradt et al. arrived at the same conclusions as have we regarding a likely fit with Pin1 for the Type IV classification of the WW domain-binding motif in Lamin A, and the results of their work confirm Pin1 binding to Lamin A²⁷⁵. Therefore, we focused our attention regarding the WW-domain-binding motifs in the PreA C-terminus upon Pin1 and refer to the relevant motifs as “Pin1binding motifs.” We find 2 individual sites and 3 sets of 2 adjacent WW/Pin1-binding sites in the sequence of LA, and interestingly, the 3 2-site sets are Ser-19/20, Ser-390/392, and Ser-652/657—the same sites identified in the Lee group study of EBV-mediated depolymerization of LA, which supports the Milbradt work in further implicating Pin1-mediated depolymerization of LA as a mechanism for viral nuclear egress.

Coimmunoprecipitation of Pin1 with L647R PreA

Binding of Pin1 by accumulated PreA could represent an extremely important layer of cell cycle control. Pin1 is sometimes described as a “mitotic rotamase,” as most of its regulatory action promotes mitotic progression²⁷⁶. In the investigation of a Pin1-PreA-mediated role in cell cycle regulation, we first asked the question whether Pin1 can bind to accumulated PreA protein *in vitro*, as the Milbradt group had shown for mature LA²⁷⁵. Immunoblotting, in Figure 35, depicts the increasing level of co-immunoprecipitated Pin1 protein detected in relation to increasing levels of accumulated uncleavable PreA.

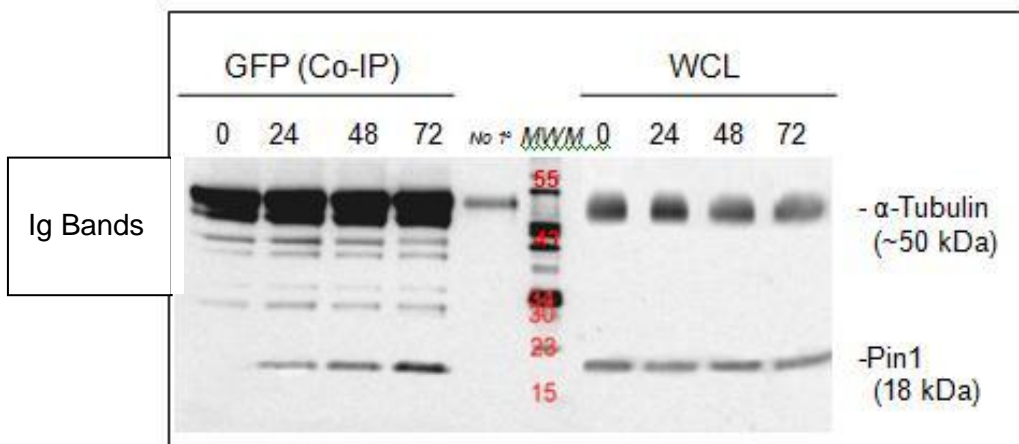


Figure 35. Co-Immunoprecipitation of Pin1 Protein with EGFP-L647R PreA. Lysates were prepared from RheoSwitch L647R-PreA cells prior to induction (0 hours), and after 24, 48, 72 hour timepoints following induction with 500 nM GenoStat. Whole cell lysates were quantitated and 200 µg total protein used for each immunoprecipitation, 50 µg was reserved for whole cell lysate (WCL) loading. Anti-GFP antibody was used to precipitate expressed EGFP-L647R protein. Equal volumes of denatured precipitated protein solution and corresponding WCLs were separated by SDS-PAGE, then blotted using anti-Pin1 antibody. “No 1°” lane sample= Co-IP control (pooled lysate processed as Co-IP without addition of anti-GFP antibody; Anti-tubulin loading control); MWM = molecular weight marker. Immunoglobulins from the IP are evident on the Co-IP blot.

These co-immunoprecipitation studies demonstrate Pin1 complexing with full-length, uncleavable EGFP-fused PreA (in the form of the accumulated EGFP-fused L647R PreA), from induced cells of our RheoSwitch L647R PreA cell line. Pin1 is reported to have some increased expression stimulated by increased growth factors but a relatively steady expression level in proliferative cells. Pin1 does show increased nuclear localization upon increasing levels of activation dependent on the availability of phosphorylated substrates. Pin1 expression is hardly detectable in cells that are not proliferating and is upregulated in many cancers^[as reviewed in 273]. In Figure 35, the WCLs for uninduced cells and for L647R PreA-accumulating cells over the 72-hour time course demonstrate approximately even levels of Pin1 total protein in the cells. As L647R PreA accumulated over the 72 hours, though, an increasing amount of Pin1 is evident in the protein complex precipitated by the GFP antibody. Although specific binding to PreA cannot be concluded from this experiment, association of Pin1 and EGFP-PreA in complexes is indicated. Given that the overall cellular level of Pin1 expression demonstrated very little to no change over the 72-hour course of L647R PreA accumulation, we next asked if the increased concentration of Pin1 in complex with the accumulating EGFP-L647R PreA was representative of an increase in nuclear compartment subcellular localization of Pin1. To investigate, we performed immunofluorescent imaging, using an antibody to Pin1 protein, on L647R PreA-expressing cells and uninduced L674R cells. This analysis reveals the subcellular distribution of Pin1 in these cells, Figure 36.

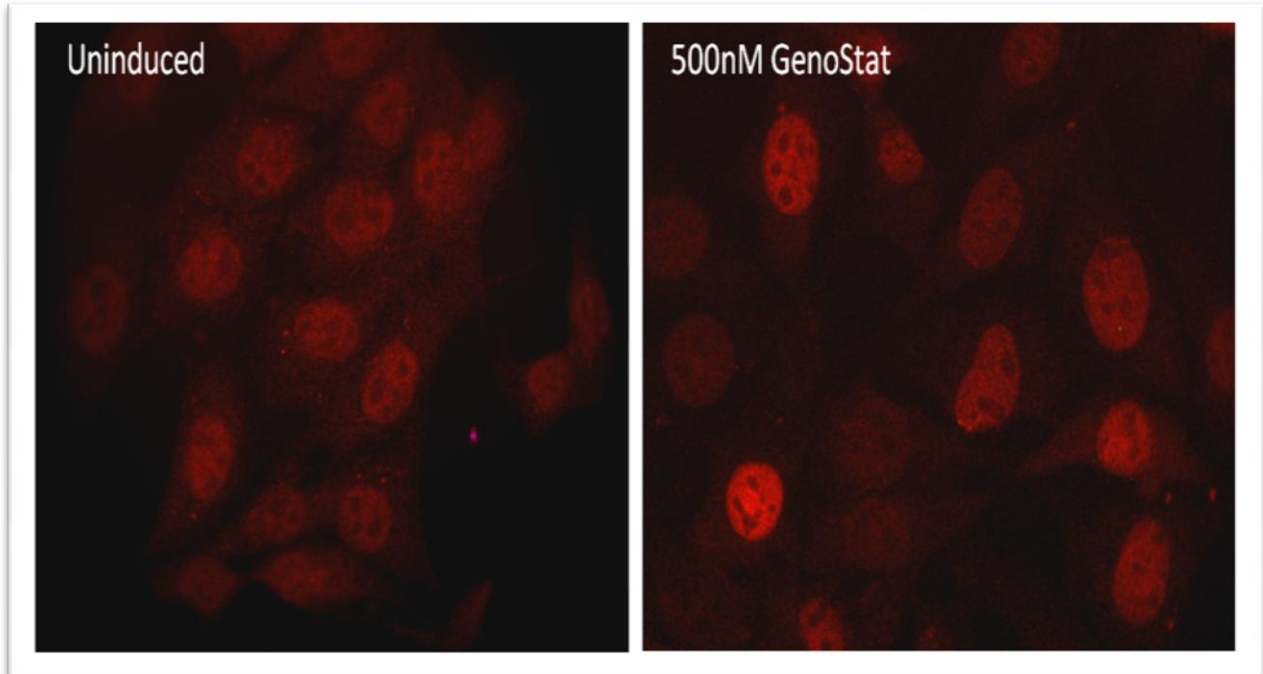


Figure 36. Immunostaining of Pin1 Protein in L647R PreA-Expressing Cells. Pin1 subcellular localization was detected by indirect immunofluorescence, using an antibody to Pin1. Fluorescence pattern is demonstrated for Uninduced (DMSO-treated) cells of the L647R PreA Rheoswitch model in the left panel. The cells shown in the right panel were L647R PreA-expressing Rheoswitch 3T3 Cells, Induced 48 hours (500 nM GenoStat).

The distribution of Pin1 in uninduced cells appears to be primarily nuclear, but with staining evident throughout the cytoplasm. After 48 hours of L647R expression, many cells exhibit a strongly increased pattern of Pin1 nuclear localization.

Taken together, these results indicate induction of L647R PreA-expression has little effect on the cellular expression level of Pin1. However, the nuclear localization is significantly enhanced, and the increased nuclear localization correlates with the increased level of Pin1 detected in complex with GFP-L647R PreA. We suspect Pin1 complex formation with L647R PreA could represent a functional scaffolding of Pin1 upon the lamina for stabilizing and organizing its interactions, or alternatively, that PreA sequesters Pin1 protein. PreA-mediated Pin1 sequestration could have substantial

effects on cell cycle regulation. Future work will investigate for differential effects on Pin1 expression and localization related to expression of different LA isoforms, whether the Pin1-binding is influenced by mutations in the WW/Pin1-binding sites on Lamin A, and whether the PreA C-terminal tail region has specific importance in that binding schema. Although it is shown LA binds Pin1²⁷⁵, because increased expression and accumulation of LA protein occurs in the form of PreA, “increased sequestration” related to increased LA expression would be, in actuality, most likely associated with the accumulated PreA protein isoform. Inhibition or deletion of PIN1 leads to mitotic entry, chromatin condensation and mitotic catastrophe^{277,278} [and reviewed in 273]. Considered along with the facts (1) progerin and PreA both accumulate with cellular passaging as well as in HGPS, and (2) highly passaged cells and HGPS cells demonstrate aberrant mitosis, the ability of different LA isoforms to associate with Pin1, and the potential effects of such associations, could be an important topic to follow up.

Pin1 Target Expression in L647R PreA Expressing Cells: (FoxOs/p27^{Kip1})

In response to low energy or lack of growth factors, as from mitogen deprivation or treatment with cAMP, inhibition of cell proliferation partially depends on a decrease in cyclin D1 or an increase in p27^{Kip1}²⁷⁹⁻²⁸². Cyclin D1 in complex with CDK4 or CDK6 promotes proliferation by phosphorylating pRb, releasing its repressive binding to E2F transcription factors and thus inducing genes involved in DNA replication²⁸³. The PI3K/PKB/Akt pathway regulates cyclin D1 levels posttranscriptionally by targeting it for degradation²⁸⁴, at the translational level involving p70S6 kinase^{285,286} as well as transcriptionally via regulation of forkhead box O (FoxO) transcription factors^{287,288}. The

FoxO family of transcription factors, include FoxO1, FoxO3, and FoxO4, which demonstrate some differences of expression in various tissue types but seem to exhibit significant overlap in function, and FoxO6, whose expression appears to be restricted to the brain²⁸⁹. The different FoxO family members share a common DNA-binding site, regulate overlapping sets of target genes²⁹⁰, and participate in diverse processes including cell proliferation, apoptosis, stress resistance, differentiation, and metabolism²⁹¹. Consistent with their participation in a broad spectrum of processes, the FoxO proteins are regulated by a variety of mechanisms, including phosphorylation, acetylation, ubiquitination, and methylation^{291,292}. These modifications alter FoxO intracellular localization, turnover, transactivation activity, and transcriptional specificity²⁹³. The capacity to undergo such a variety of modifications under context-specific situations, in addition to their ability to associate with many different cofactor complexes to regulate context-dependent programs of gene expression²⁹⁴, make the FoxOs highly versatile in gene regulation. Depending on their status of modification and selection of binding partners, they can act as direct or indirect transcriptional activators or repressors²⁹⁵. E2F1 induces FoxO1 and FoxO3 transcription²⁹⁶, and FoxO3 expression induces a feedback transcriptional upregulation of itself, as well as FoxO1²⁹⁷.

In the absence of growth factors, active FoxOs reside in the nucleus and up-regulate genes that inhibit the cell cycle (p27^{Kip1} and p21^{WAF1}), promote apoptosis (Fas ligand, Bim, and TRAIL), and decrease oxidative stress (superoxide dismutase and catalase). A number of genes are also repressed by activated FoxOs, including Cyclin D isoforms²⁹⁸. Our antibody array data suggest L647R PreA may act to stabilize

FoxOs, for example, we see a significant downregulation of D-type cyclin proteins, and a slight upregulation of FoxO1 protein expression (Table 5). While FoxO3a expression levels were not significantly impacted by L647R PreA expression, this assay does not take into account subcellular localization of the proteins and, therefore, cannot be taken as a direct indication of FoxO3a activity. The antibody array did detect upregulation of FoxO1, transcription of which is mediated by FoxO3, and we consider the observed FoxO1 upregulation to be one likely indicator of FoxO3a activation and stabilization even though detected expression level of FoxO3a is not upregulated. In addition, we consider posttranslational FoxO modifications and examine known FoxO targets for indication of FoxO activation. We note levels of expression of FoxO4 and FoxO6 proteins were not measured. FoxO targets, p27^{KIP1} and p21^{WAF1} offer a confusing picture in our expression studies, as their expression at the transcript level after 24 hours of L647R PreA induction, detected by the qPCR array, indicate upregulation (approximately 26.7-fold upregulation of p27^{KIP1} and more than 2.6-fold upregulation of p21^{WAF1}), whereas the antibody array did not detect an altered regulation of either CKI at the protein level after 72 hours of induction. As phenotypic evidence, from observing signs of induced cell cycle arrest, seems to argue favorably for the likelihood of increased p27^{KIP1} and/or p21^{WAF1} activity, we chose to continue investigating these, in part by continuing our focus on FoxO regulation.

Activity of FoxOs in transcriptional regulation is first dependent on localization to the nucleus. A number of mechanisms exist to exclude from the nucleus and thus inactivate FoxOs, such as phosphorylation by several kinases—including the phosphatidylinositol-3-OH kinase (PI3K) pathway activated kinase PKB/Akt^{299,300}, the

serum- and glucocorticoid-inducible kinase (SGK)³⁰¹, casein kinase I (CK1)³⁰², IKK β ³⁰³, and the mitogen-activated protein kinases ERK and p38^{298,304,305}. Phosphorylation by these kinases induces FoxO interaction with 14-3-3, which reportedly masks the FoxO nuclear localization signal (NLS)^{238,306,307} or enhances binding affinity for nuclear export molecules³⁰², which shuttles FoxO to the cytoplasm. On the other hand, FoxO phosphorylation at some sites can lead to its activation. Two examples are: phosphorylation by c-Jun N-terminal kinase (JNK) kinases upon cell stress activates FoxOs³⁰⁸ and Cdk1 phosphorylation activates FoxO transcription by preventing Akt phosphorylation and consequent 14-3-3 binding-induced nuclear exclusion³⁰⁹. Phosphorylation can also induce the proteosomal degradation of FoxO factors. Erk-mediated FoxO phosphorylation results in FoxO polyubiquitination, carried out by MDM2, the same E3 ligase as is implicated in p53 regulation. As it does for p53, this polyubiquitination results in proteosomal degradation of the FoxO protein³⁰⁴. Another affect of phosphorylation could be positive or negative regulation of FoxO ability to bind to DNA²⁹⁰. The 4 FoxO phosphorylation sites assayed by the antibody array are Akt sites, and the profile of these indicate a significant decrease in phosphorylation status when L647R PreA is expressed. The hypophosphorylated status of FoxO transcription factors in L647R PreA-expressing cells indicates a substantial stabilization of nuclear FoxO proteins. The phosphorylation sites assayed and found to have decreased Akt phosphorylation include sites common to FoxO1, FoxO3, and FoxO4, these are Ser-256, Ser-319, Thr-24/32, and Ser-322/325 (Table 5). Also, on our antibody array, expression of Akt, itself, is downregulated by expression of L647R PreA and demonstrates significant hypophosphorylation on the sites most commonly associated

with Akt activation (Table 5)^{239,310}. FoxO transcriptional activity is further regulated by acetylation in the nucleus²⁹⁰. Interaction with the transcriptional coactivator p300 has been demonstrated to negatively regulate FoxO transcriptional activity³¹¹ in part by enhancing Akt-mediated phosphorylation and subsequent translocation to the cytoplasm³¹² as well as by decreasing its ability to bind and act on target DNA³¹³. Our antibody array demonstrates a marked decrease of p300 expression as an effect of L647R PreA expression (-1.34-fold, Table 5), logically making it less available to act on FoxO proteins, with effects possibly demonstrated by the obvious lack of enhanced Akt phosphorylation of the FoxOs as well as indications of FoxO regulation of several targets.

Another mode of FoxO regulation, ubiquitination, can have different effects on FoxO stability: monoubiquitination can occur in response to oxidative stress and result in increased nuclear localization and stabilization of FoxOs, while polyubiquitination leads to proteasomal degradation^{264,314-316}. Pin1 inhibits ubiquitination of FoxOs, and while this can lead to decreased degradation, it also inhibits the nuclear translocation, and has been demonstrated to inhibit p27^{Kip1} transcription mediated by FoxOs²⁶⁴. As we have demonstrated an increased accumulation of Pin1 in complex with L647R PreA in induced cells, we sought to determine if this accumulation had an effect on FoxO localization and FoxO-mediated p27^{Kip1} expression in L647R PreA expressing cells.

Nuclear Localization of FoxO3a and p27^{Kip1} with L647R PreA Expression

Immunofluorescence imaging (Figure 37) reveals an increased level of FoxO3a localization in the L647R PreA expressing nuclei as compared to the uninduced control.

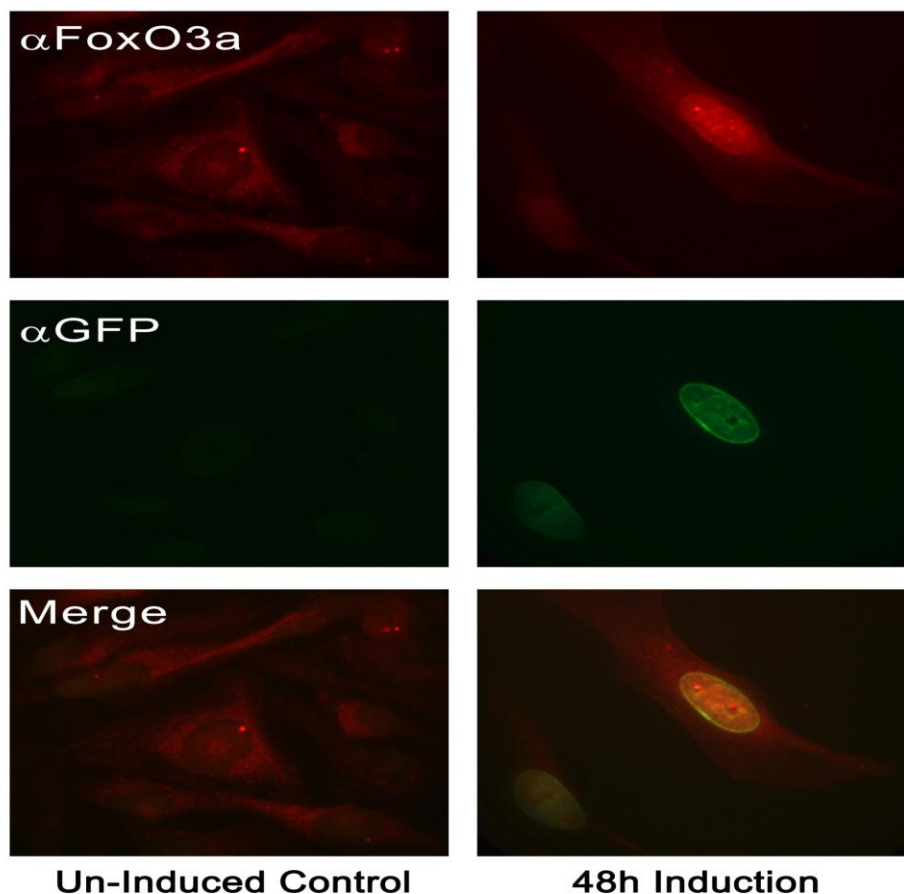


Figure 37. Immunostaining of FoxO3a Protein in EGFP-L647R PreA-Expressing Cells and Colocalization with GFP. Immunofluorescence microscopy detected FoxO3a antibody (top panels, red), and Anti-GFP antibody (middle panels, green), in uninduced (DMSO-treated) Rheoswitch L647R PreA cells (left panels) and the L647R-expressing cells (right panels). Induced cells were incubated 48 hours with 500 nM GenoStat.

The staining with anti-FoxO3a antibody, in Figure 37, demonstrates diffuse expression throughout the uninduced cells, while the cells induced to express L647R PreA for 48 hours demonstrate a marked increase in expression of nuclear FoxO3a. Anti-GFP demonstrates GFP-tagged L647R PreA in the nuclei of the induced cells, which is absent from uninduced cells. Colocalization of L647R PreA and FoxO3a proteins is seen in the nuclei of induced cells. Correspondingly, the L647R PreA-induced cells demonstrated increased p27^{Kip1} expression and nuclear translocation

compared to the uninduced cells. Immunoblotting of equal concentrations of whole cell lysate and corresponding separated cellular compartment fractions (Figure 38) demonstrates the altered expression of FoxO3a and p27^{Kip1} in induced L647R PreA-expressing cells versus uninduced control cells.

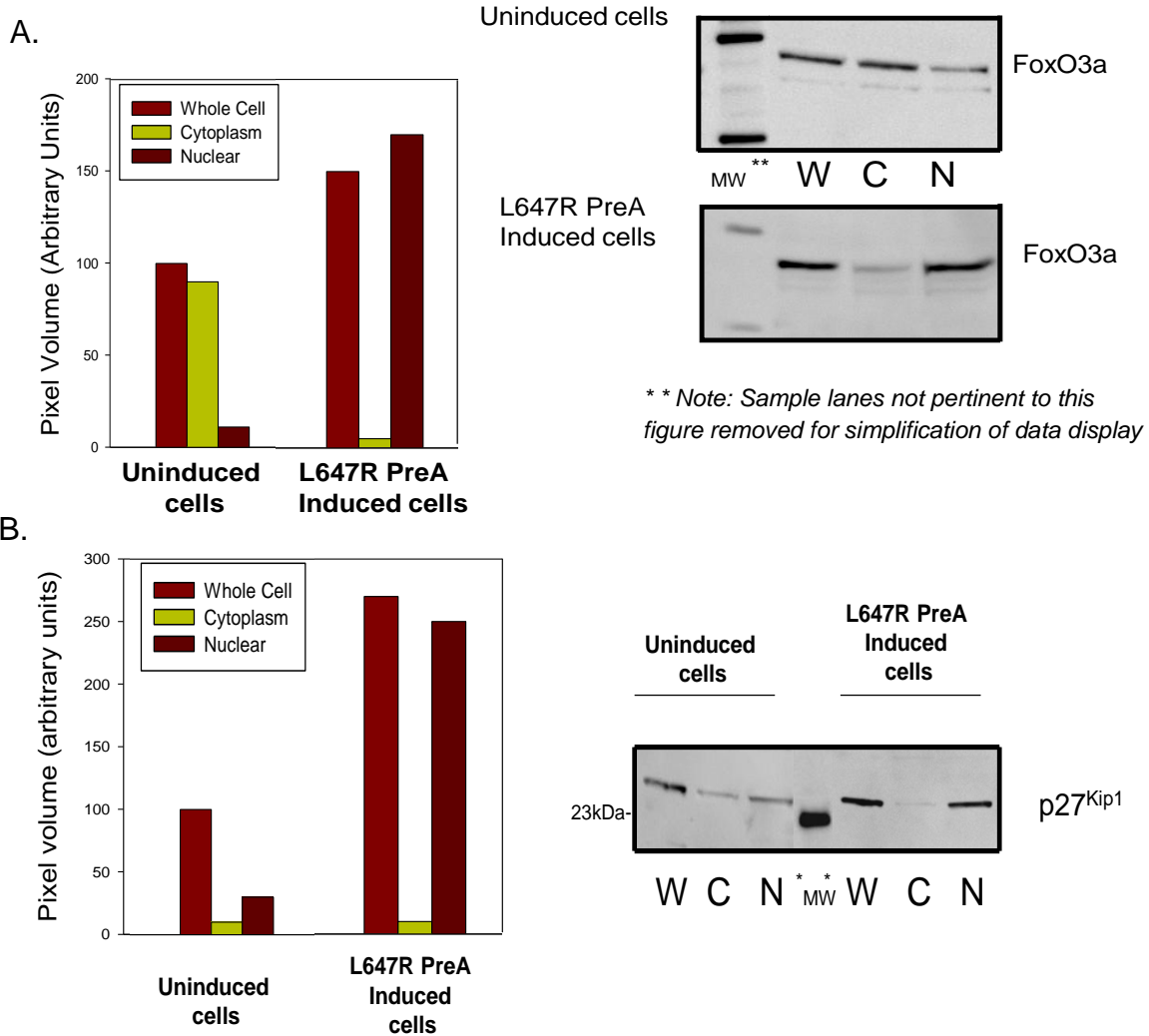


Figure 38. Increased Expression and Nuclear Translocation of FoxO3a and p27^{Kip1} with L647R PreA Expression. Immunoblotting of equal concentrations of total protein [50 µg] from whole cell lysates (W) cytoplasmic (C) and nuclear (N) fractions with anti-FoxO3a (Panel A, right) and anti-p27^{Kip1} (Panel B, right) in Uninduced and Induced cells. Densitometry of pixilation of blots, left panels, provides semiquantitative comparison using arbitrary units. MW= Molecular Weight marker.

The immunoblotting of the whole cell lysates of cells induced 48 hours to express L647R PreA, in Figure 38, demonstrates a small increase in total FoxO3a expression in the induced cells, while comparison of the cytoplasmic and nuclear fractions reveal a significant increase in nuclear translocation of expressed FoxO3a in induced cells, compared to the uninduced cells. The whole cell lysates demonstrate a marked increase in p27^{Kip1} expression in the induced cells expressing L647R PreA compared to the uninduced cells, while the proportion of p27^{Kip1} in the cytoplasm of L647R PreA-expressing was not significantly different from uninduced cells. The nuclear fractions, however, demonstrate the dramatic increase in expression seen in the L647R-expressing induced cells is almost exclusively confined to the nuclei of those cells.

These data demonstrate that L647R PreA expression enhances FoxO3a expression and increases the nuclear translocation of the protein, thus indicating a higher level of FoxO3a activation^[as reviewed in 295]. The accompanying enhanced expression level and nuclear translocation of the CKI, p27^{Kip1}, a FoxO target for transcriptional activation, offers support for an L647R PreA-induced effect on FoxO activation and suggests a potential mechanism of PreA-mediated cell cycle arrest.

Pin1 Inhibition Mimics L647R PreA Effect on FoxOs and p27^{Kip1} in Uninduced Cells

Given that Pin1 functions to suppress FoxO proteins, one might expect the increased presence of PreA-complexed-Pin1 protein in these nuclei to correlate to decreased FoxO activity. On the contrary, taken together, these data suggest Pin1-mediated suppression of FoxO nuclear translocation is inhibited in L647R PreA cells. To test this, we examined the effects of treatment with Juglone, a Pin1 inhibitor, on

FoxO nuclear translocation (Figure 39), and on p27^{Kip1} expression and localization (Figure 40), in these cells.

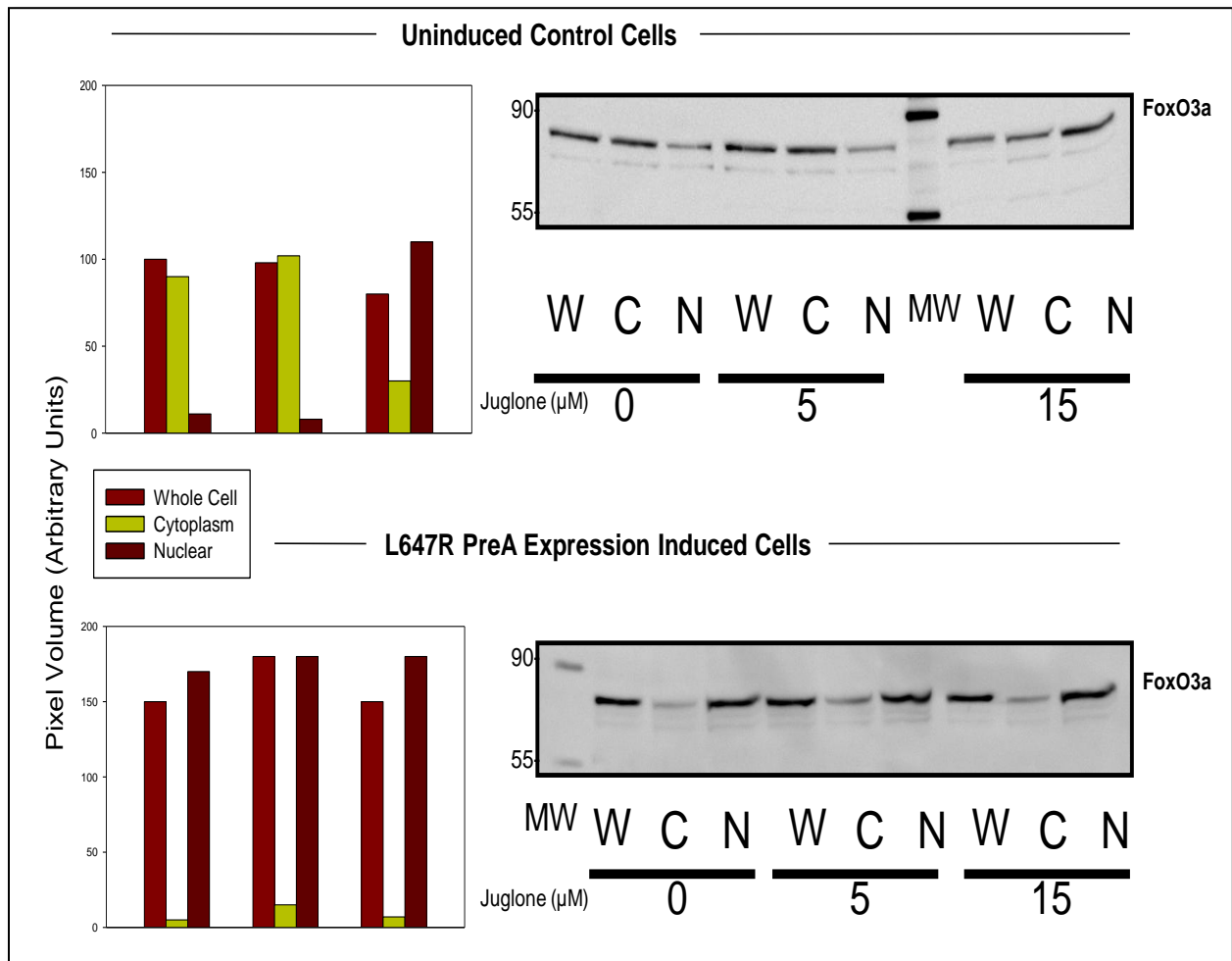


Figure 39. Pin1 Inhibition by Juglone Treatment Mimics L647R PreA Effects in Uninduced Cells, Leads to FoxO3a Nuclear Localization. Juglone treatment leads to Pin1 inhibition and FoxO3a nuclear localization in uninduced cells, while prominent nuclear localization of FoxO3a in L647R PreA cells remains unaltered. Immunoblotting of equal concentrations of total protein [50 μg] from whole cell lysates (W), cytoplasmic (C) and nuclear (N) fractions, with anti-FoxO3a antibody after 72 hour Juglone treatment (at concentrations of [5 μM] and [15 μM], with “0” μM representing no Juglone treatment) of uninduced cells (upper blot), and L647R PreA-expressing induced cells. Densitometry of pixelation of blots, left panels, provides semiquantitative comparison using arbitrary units. MW=Molecular Weight marker.

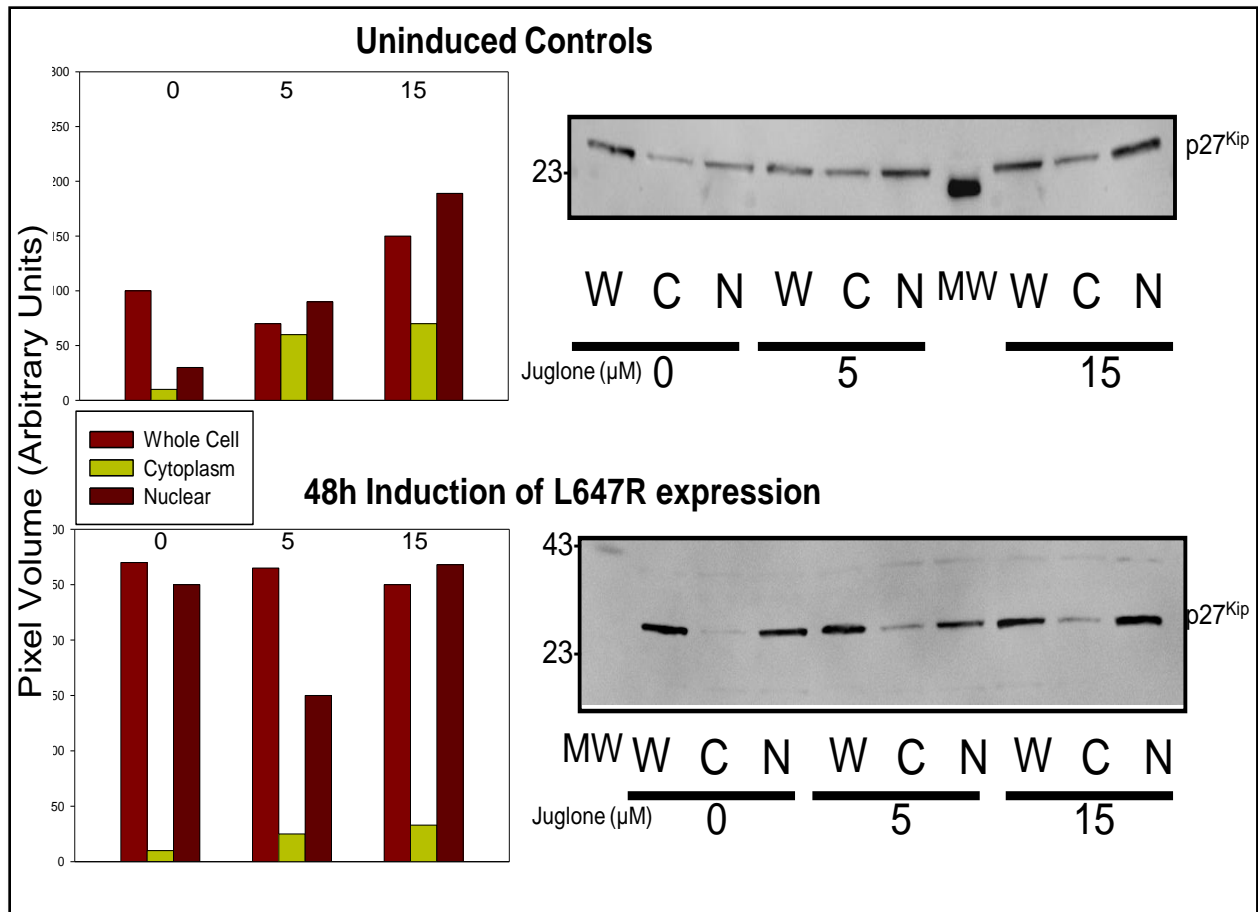


Figure 40. Pin1 Inhibition By Juglone Treatment Mimics L647R PreA Effects in Uninduced Cells, Results in Increased P27^{Kip1} Expression and Nuclear Localization. Pin1 inhibition by Juglone treatment results in an increased expression level of p27^{Kip1} in uninduced cells, with the majority of the protein demonstrating nuclear localization. Meanwhile, the upregulated p27^{Kip1} in L647R PreA-expressing induced cells is not significantly altered. Immunoblotting of equal concentrations of total protein [50 μg] from whole cell lysates (W), cytoplasmic (C) and nuclear (N) fractions, with anti-FoxO3a antibody after 72 hour Juglone treatment (at concentrations of [5 μM] and [15 μM], with “0” μM representing no Juglone treatment) of uninduced cells (upper blot), and L647R PreA-expressing induced cells. Densitometry of pixilation of blots, panels left, provides semiquantitative comparison using arbitrary units. MW=Molecular Weight marker.

Pin1 inhibition by Juglone treatment leads to an increase of p27^{Kip1} expression in uninduced cells, with the majority of the protein demonstrating nuclear localization. As the Juglone-untreated L647R PreA-expressing cells already demonstrate a large increase in p27^{Kip1} expression compared to uninduced cells without Juglone treatment,

little significant change is induced by Pin1 inhibition in these cells. A small p27^{Kip1} expression increase is detected in the cytoplasmic fraction, with an unexplainable downshift in the intensity of the band representing the p27^{Kip1} expression in the nuclear fraction of cells treated with 5 μ M Juglone. This fluctuation is not present in the cells treated with the 15 μ M Juglone, rather, a level consistent with that in induced cells in the absence of Juglone treatment is seen, representing an almost total nuclear localization of p27^{Kip1} expression in these cells.

Taken together, the data from analyses of FoxO3a and p27^{Kip1} expression and subcellular localization in uninduced cells and induced cells expressing L647R PreA indicate a positive effect of PreA on FoxO3a and p27^{Kip1} expression and activity in arresting the cell cycle progression. Furthermore, the data also suggest a similar effect on FoxO3a and p27^{Kip1} expression and activity can be achieved in uninduced cells by inhibiting Pin1. In the context of the demonstrated increase in Pin1 complexing with accumulating L647R PreA without a change in the Pin1 expression levels or subcellular localization, these findings appear to indicate accumulating levels of PreA likely function to sequester, and thus inhibit, Pin1 in the nucleus.

Pin1 Overexpression Reverses L647R PreA Effect on FoxOs & p27^{Kip1}

If Pin1 inhibition is occurring with L647R PreA expression, with the consequent increased nuclear expression of FoxO3a and p27^{Kip1}, we reasoned that overexpressing Pin1 protein in those same L647R PreA-expressing cells should reverse the observed effect. To test this, we cotransfected cells from the Rheoswitch L647R PreA cell line with a GST-Pin1 fusion protein-expressing plasmid.

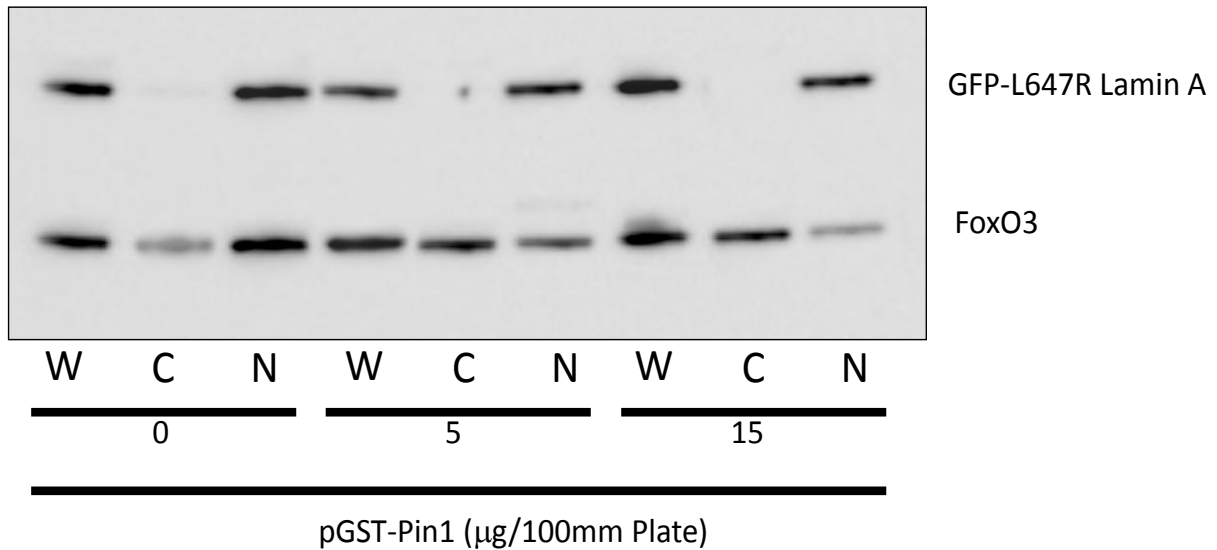


Figure 41. Overexpression of GST-Pin1 in Induced L647R PreA-Expressing Cells Reverses L647R PreA-Mediated Nuclear Localization of FoxO3. Cells were transfected with 0, 5, and 15 μg of GST-Pin1 plasmid DNA. Cells were then induced with 1 μM GenoStat and incubated 48 h, prior to collection and preparation of cell fractions. Cell fractions (C=Cytoplasmic, N=Nuclear, W=Whole Cell Lysate) and WCLs were immunoblotted with GFP and FoxO3 antibodies. Presence or absence of the GFP-PreA band indicate integrity of Nuclear, or Cytoplasmic fractions, respectively.

In Figure 41, a significant reversal of FoxO3a nuclear expression is demonstrated, in the induced L647R PreA-expressing cells, in a GST-Pin1-dosage-dependent manner. The higher level of Pin1 expression results in a more dramatic export of FoxO3a protein from the nucleus. The level of protein exported is indicated by the enrichment of the cytoplasmic fraction, with a proportionate depletion of the protein from the nucleus. The functional consequences of FoxO3a inhibition are indicated by effects on p27^{Kip1} expression (Figure 42).

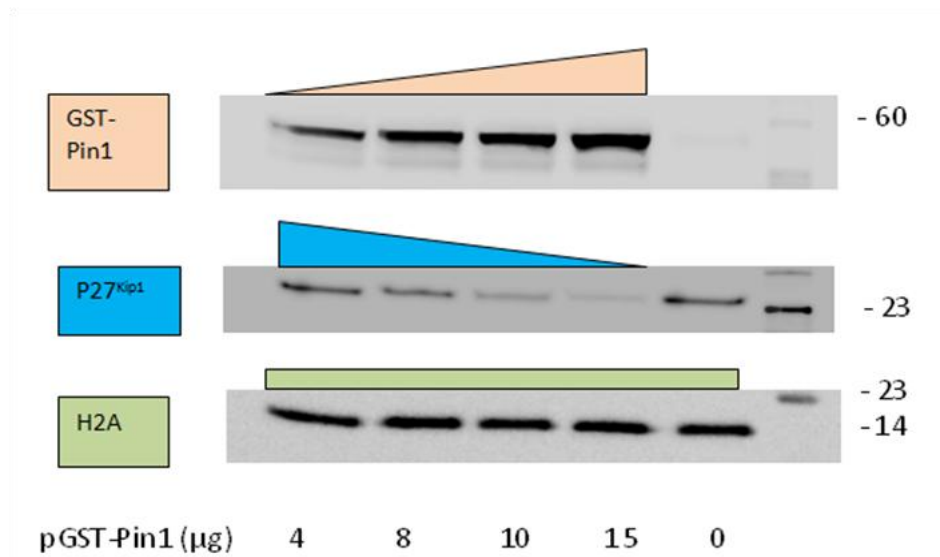


Figure 42. Diminished p27^{Kip1} Expression is Evident upon Overexpression of GST-Pin1. Cells from the Rheoswitch L647R PreA-expressing 3T3 cell line were transfected with varying concentrations of GST-Pin1 expression plasmid (in μg , X-axis). Cells were then induced with 1 μM GenoStat and incubated 48 hours, prior to collection and preparation of cell fractions. Nuclear fractions were subjected to immunoblot using an antibody to Pin1, to detect GST-Pin1, an Anti-p27^{Kip1} antibody detected p27^{Kip1} protein present in the nuclei, and Anti-Histone protein (H2A, nuclear) serves as a loading control.

Senescence Develops in L647R PreA-Expressing Cells

Taken together, the results of the array studies indicate L647R PreA expression alters gene expression to induce conditions of cell cycle arrest. Supporting this regulatory effect, proliferation and cell cycle distribution analyses reflect decreased levels of proliferation in these cells. Furthermore, increased nuclear localization of FoxO and the cell cycle arrest-inducing p27^{Kip1} in L647R PreA-expressing cells is consistent with induction of a program of cellular quiescence. However, as PreA expression is related to both quiescence and senescence conditions, and several of the gene expression patterns are implicated in either condition, we sought to evaluate if the arresting conditions are indicative of quiescence or senescence. In order to assay the

cells for senescence activity, we performed a β -galactosidase staining assay (Figure 43).

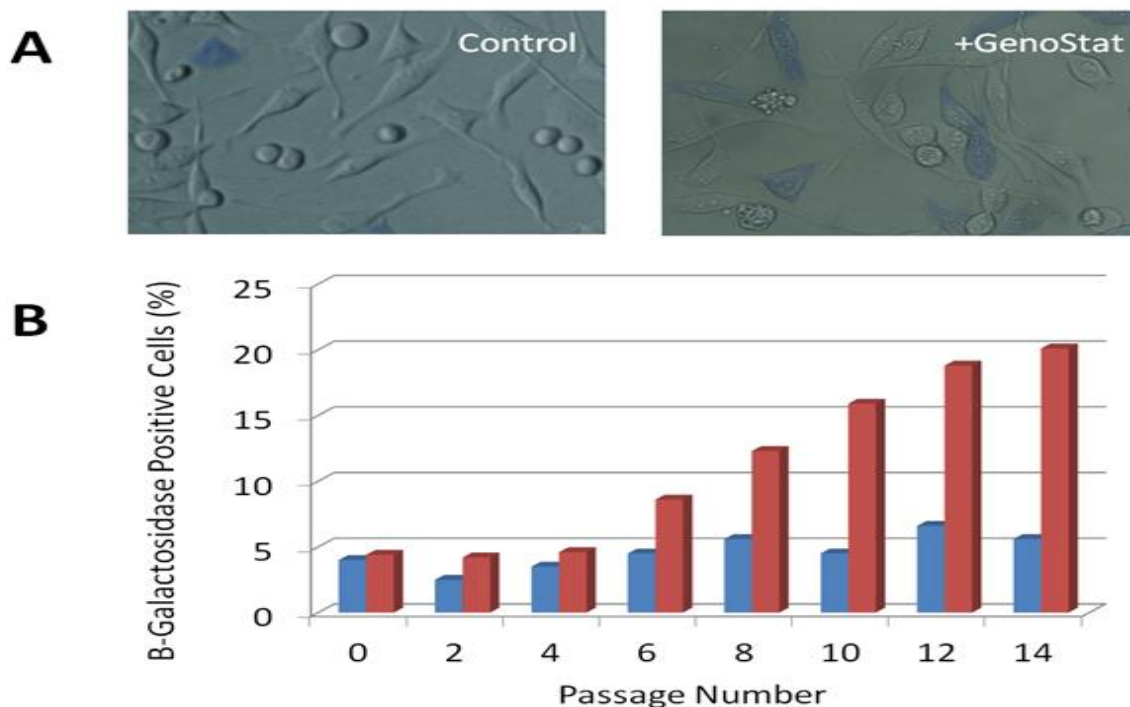


Figure 43. Senescence Assay of L647R PreA-Expressing Cells (β -galactosidase Assay). Senescence develops in L647R PreA-expressing cells with successive cell divisions, as indicated by this β -galactosidase staining assay. L647R PreA Rheoswitch cells, induced for expression (500nM GenoStat, red bars) or Uninduced (DMSO-Vehicle, blue bars) were split every other day in 1:3 ratio. At the indicated passage number, 10^4 cells were plated onto 1.8 cm^2 chambered cover glass and incubated for 16h. Senescence was then measured with a β -galactosidase staining kit. A) Overlay of DIC and bright field images of a representative 40x field at passage 14. B) Percentage of cells positive for β -galactosidase by manual count under microscope.

The β -galactosidase assay detects hydrolase enzyme activity at a pH of 6, which is found only in senescent cells, not in quiescent, presenescent, or immortal cells³¹⁷.

The results of this assay indicate accumulation of PreA protein induces senescence, although only after several successive passages have occurred.

Results Summary

Through multiple assays of cell cycle related gene expression in cells expressing L647R PreA, we have demonstrated a significant impact on the cell cycle gene expression profile in those cells as compared to control cells not expressing the PreA. At the protein level, as well, significant changes were demonstrated in the expression levels and/or the phosphorylation modifications of components of cell cycle regulation in cells induced to express the L647R PreA. The overall expression pattern is indicative of a negative regulation of cell cycle progression by accumulated PreA. Analysis of the peptide sequence differentiating PreA from LA, the C-terminal fragment, reveals potential interacting partners that could mediate cell cycle effects related to expression of PreA. Our studies of such a potential interaction partner, Pin1, demonstrate compelling evidence for a PreA-mediated sequestration of Pin1 to have a major impact on cell cycle regulation.

CHAPTER 4

DISCUSSION

Cell Cycle-Related Expression of PreA

PreA Expression is Cell Cycle Stage-Specific, Related to Arrest

A reason for the existence of a precursor protein for Lamin A does not have been readily apparent. Lamin B remains associated with the nuclear membrane even through mitosis and offers a redundancy in much of the structural function of A type lamins, and it does not have an immature isoform. Also, existence of the Lamin C splicing variant provides an additional level of redundancy in structural function in a protein form that is not obligatorily bound tightly to the nuclear membrane. Thus, even without expression of PreA or LA proteins, lamin filaments are available at the nuclear envelope as well as throughout the nucleoplasm in the form of B-type lamins and Lamin C, respectively. The maturation processing of PreA to form Lamin A is executed in a quick and efficient manner, and as cells progress through mitosis, mature LA is phosphorylated, disassembled, and then reassembled in daughter cells, in an apparently conservative process^{13,32,33,97,98}. Consequently, with a continuous production rate and no obvious harmful effects from an “excess” of mature, normal LA, it seems unlikely that there is such a great need for holding a reserve of this intermediate filament protein in an “inactive” progenitor state, yet the energy-expending processing pathway is highly conserved in vertebrates^[as reviewed in 88]. The cell cycle dependent pattern of PreA accumulation must surely offer insight to the purpose for the precursor protein. It seems likely that a threshold level of expression of PreA is integral to a

program of initiation of exit from the cell cycle. Whether the accumulation of the PreA has a direct effect on the cells' exit from the cell cycle has yet to be determined.

Accumulated PreA is Related to Decreased Zmpste24 Activity

While FTI treated cells demonstrate marked PreA accumulation and are rendered quiescent, other normally prenylated proteins are also affected by the inhibition of farnesyl transferase. However, it is clear in untreated cells, that the accumulation of PreA prior to or during periods of cell cycle arrest occurs despite an intact program of normal posttranslational modifiers, up to the point in the processing pathway at which the protein would normally undergo proteolytic cleavage by Zmpste24. The logical conclusions would be that PreA accumulation must depend upon some direct modification that hinders access of Zmpste24 to the cleavage site or a modification to Zmpste24 resulting in the inhibition of proteolytic activity. Observance of a sharp decrease in Zmpste24 activity level much earlier than a demonstrable decrease in the level of expression of mRNA transcript or protein would seem to suggest Zmpste24 is regulated posttranslationally, likely by phosphorylation. Furthermore, when observing culture behavior of cells transiently transfected with a Zmpste24 expression construct, we found the overexpressing cells appear to proliferate at a rapid rate compared to cultured cells not expressing the recombinant protease, and we have demonstrated the overexpression of Zmpste24 leads to an apparent bypass of entry to quiescence when exposed to conditions that would normally cause cells to enter "resting phase." While ongoing studies are exploring the specifics of Zmpste24 expression and cell cycle, as they relate to effects of preventing PreA accumulation, our

current studies have focused in the other direction, with overexpression of PreA to investigate cell cycle related effects.

Overexpression Of PreA Inhibits Cell Cycle Progression

We have demonstrated that, despite availability of growth factors and prevention of cell-cell contact, L647R PreA-expressing cells demonstrate a decreased S-phase population compared to passage-matched cells not induced to express the mutant lamin, with a tendency to accumulate in G0/G1-phase. Induced cells containing the EGFP-only expression construct do not exhibit the impaired proliferation effects of L647R PreA. Furthermore, when these cells are arrested by serum-deprivation or contact-inhibition, those induced to express L647R PreA demonstrate an impaired ability to re-enter the cell cycle once the arresting agent is removed (serum-return, or trypsinization and replating at lowered density), compared to uninduced cells or those induced to express EGFP only. We conclude, therefore, PreA expression is a cause, rather than an effect, of cell cycle arrest, and its cell cycle-related expression (by accumulation due to lack of maturation processing) is a likely mechanism used by proliferating cells to coordinate the processes of exiting from the cell cycle.

Motif Analysis Suggests Potential Modes of PreA Interaction with Cell Cycle Regulators

As we considered PreA as a protein isoform with activities that might differ from other isoforms, we determined a critical step in the investigation would be analysis of the sequence of the portion of the isoform that differentiates it from the other isoforms, the C-terminus. As our study was focused, specifically, upon a cell cycle-related role—a process so heavily controlled by differential phosphorylation of proteins, and a

process that has already been demonstrated to modify LA in a cell cycle-dependent manner—we elected to investigate the C-terminus in terms of relationships that might be influenced by phosphorylation. We considered, in the analysis, the c-terminal 66 amino acid residues in the sequence in order to encompass motifs that also differentiate the delta50/Progerin isoform from normal, mature LA. The substantial number of phosphorylation motifs within the C-terminal sequence of PreA present a large project for further research: considering the different kinases involved, the implications of the cellular contexts during which those particular kinases are active and under which conditions these act upon the C-terminus as a substrate (or even *if* they can actually be demonstrated to do so), and if effects upon the lamin protein can be detected as a result of these potential modifications. Such an investigation is far beyond the scope of this study, however, although it is noteworthy that the C-terminus, as the differentiating sequence between the LA isoforms is rich with sites for potential activity.

We also examined the C-terminus for phosphorylation-dependent binding motifs, as this more directly addresses the pertinent question that led us to analyze the sequence: What molecules might directly interact with the PreA C-terminus, in a cell cycle-dependent fashion, that could regulate gene expression changes to affect cell cycle regulation? Our analysis produced 3 primary motifs in the C-terminus for consideration, a binding site for the cell cycle regulatory adapter protein, 14-3-3, four binding sites that could be occupied either by the kinase Plk1 (which, interestingly, was not identified among the kinases for which this site could be a *substrate*) or the by the DNA damage repair complex-assembly-required and checkpoint-mediating protein, MDC1, and finally, 2 WW-domain-binding motifs. We have described our evaluation of

WW domain-containing proteins, and our arrival at Pin1 as the likely candidate as a Type IV WW domain-containing protein with nuclear activity.

Pin1 as a Lamin-Binding Protein. The serendipitous timing of the publication by Milbradt and associates of their study on mechanisms of viral egress in CMV-infection, and their work revealing Pin1-mediated isomerization of Lamin A in this capacity, of their study on mechanisms of viral egress in CMV-infection, and their work revealing Pin1-mediated isomerization of Lamin A in this capacity²⁷⁵, reinforced our hypothesis that Pin1 binds LA in a phosphorylation-dependent manner. In fact, as the early stages of the work of this group, in characterizing Pin1 as a Lamin A-binding protein, closely paralleled the work we had done on the characterization. Their progress then surpassed ours when they analyzed crystal structures and demonstrated the binding. Therefore, we determined this work to preclude any need, on our behalf, to investigate further in considering WW-domain-containing proteins that might interact with LA. We therefore refer to the WW domain-binding motifs in LA as “Pin1-binding motifs.”

The Pin1 protein has 2 domains connected by a flexible linker, with the WW domain located N-terminal to the catalytic PPIase domain. Interestingly, both domains recognize the phosphorylated Serine-Proline residue of the Type IV WW domain binding motif.^{318,319} While some proteins have demonstrated PPIase-independent effects from binding of the WW domain alone, the binding of both is required for high affinity Pin1 binding and execution of the rotamase/PPIase cis/trans isomerization effect, which essentially “twists” the substrate protein to introduce conformational changes that result in altered protein function, localization, or stability^{320,321}. In order to bind both domains simultaneously, 2 (or more) WW domain binding motifs, situated

closely within the binding peptide sequence, are required^{322,323}[Reviewed in^{273,324}]. The grouping of the WW domain binding sites at 3 sites within Lamin A appear to have fit the pattern required for dual WW domain-binding and isomerization by Pin1, at the N-terminus: sites 19-20/22-23. This site was determined by the Milbradt group to bind Pin1 HCMV viral kinase mediated-Pin1 isomerization of Lamin A in nuclear egress of the virus²⁷⁵. Binding sites in the approximate center of the protein sequence are sites 390-391/392-393, and in the C-terminus of the full length PreA sequence: at sites 652-653/657-658. As noted, each of the 3 sets of 2 adjacent binding sites were referenced as phosphorylated during viral manipulation of LA polymerization for viral nuclear egress²⁴⁶, the mechanism of which Milbradt et al. attribute to Pin1-mediated binding and action on LA. The del50/Progerin truncated mutant protein does retain the final WW domain-binding site (residues 657-658). However, functionality would be questionable for that site in the mutant protein, considering the apparent requirement for two closely situated binding sites to accommodate Pin1 binding and isomerization activity, if that phenomenon, indeed, is shown to be an operative mechanism in PreA metabolism or function. The other 2 WW domain/Pin1 binding sites found within the LA sequence (at amino acid residues 3-4, and 507-508) occur singly and thus would not meet the criterion of likely sites at which Pin1 isomerization could occur, although the ability to bind Pin1 is not precluded at those sites by the lack of another, closely situated, Pin1 site. While binding sites for MDC1/Plk1, 14-3-3, and WW domains occur scattered periodically throughout the full Prelamin A length, the clustering and overlap of these sites within the C-terminus presents a pattern not found elsewhere in the sequence, and this unique arrangement could have significant impact on protein interactions. Possibly,

Pin1 isomerization of sites overlapping an Mdc1 and 14-3-3 binding motif could affect some regulation of these sites as well as polymerization or other characteristics of the actual lamin filaments themselves. Therefore, we suggest the potential functional implications of the particular arrangement of the phosphorylation-dependent binding motifs in the PreA C-terminus warrants further investigation. Importantly, sequestration of transcription factors by components of the nuclear envelope has been demonstrated as a mechanism of controlling gene expression³²⁵. PreA, specifically, has been shown participate in such a regulatory role by sequestering SREBP1³²⁶. Likewise, a PreA-related sequestration of Pin1 could have a substantial effect on gene expression levels affecting cell cycle progression, potentially such as the effects demonstrated in the gene expression analyses in L647R PreA expressing cells.

One caveat to the correlation of our work with that of Milbradt and coworkers, is that the other group focused their attentions on Pin1 binding to LA that was phosphorylated on Ser22, yet they found Lamin C to interact with Pin 1 with a very low affinity compared to Lamin A²⁷⁵. As LA and Lamin C both contain Ser22, we suggest the discrepancy in the binding affinities between Lamins A and C could suggest a potential importance of the C-terminus in the high-affinity binding demonstrated by Lamin A. However, while they used recombinant proteins Lamin A and Lamin C to clearly demonstrate Pin1 binding differences between those 2 isoforms²⁷⁵, the Lamin A/C antibody used is directed to an epitope common to Lamin C, LA, and PreA isoforms, and thus, PreA might have been indistinguishable from mature LA as the moiety they describe to possess high Pin1 binding affinity. We suggest this is a possibility worth consideration and further evaluation. Nonetheless, we suggest Pin1 as

a primary mediator in PreA regulation of the cell cycle, as Pin1 has been described to directly bind LA in a phosphorylation dependent manner, it has binding sites in the PreA C-terminus, and it has been implicated in the control of a multitude of cell cycle regulators.

PreA Expression Alters the Cellular Gene Expression Profile

Investigation of Gene Expression Effects Using Uncleavable PreA Expression Construct

To determine effects of accumulation of PreA protein, we transiently transfected NIH 3T3 cells with a pEGFP-C3 expression vector containing the Lamin A cDNA, which had been subjected to site-directed mutagenesis of the Lysine 647 residue, converting it to Arginine. This mutation disrupts the recognition/cleavage site for the Zmpste24-mediated second proteolytic maturation processing step. The resulting EGFP-tagged uncleavable PreA protein, L647R-PreA, undergoes irreversible farnesylation and carboxymethylation modifications. A GeneChip Whole Transcript Mouse Exon Gene Array (Affymetrix, Santa Clara, CA) was performed on RNA from NIH3T3 cells transiently transfected (48 hours) with the construct, along with RNA from a parallel control of NIH 3T3 cells transfected with the empty pEGFP-C3 expression vector. Subsequently, we created a set of stable lines harboring inducible constructs for expression of L647R PreA, del50 LA, and wtLA, each tagged N-terminally with EGFP. An additional control line expressing EGFP only was also created. We then began gene expression array analysis on these cell lines using cell cycle gene pathway-specific RT-qPCR analysis. Due, however, to unresolved normalization of gene

expression levels between the uninduced cell lines, most likely owing to the discordant number of culture passages to which each cell line had been subjected at the time of analysis, we elected to focus on the L647R PreA-expressing cell line only for these studies. Future studies should involve careful passage-matching of the cell lines used for comparison of gene expression profiles. Additionally, to eliminate the variable of slight clonal differences in gene expression, systematic comparisons should be performed on a number of reference genes to generate a reliable algorithm to more succinctly normalize comparative analysis of genes of interest between the cell lines.

Gene expression analyses of the cells induced to express L647R PreA, compared to uninduced cells, were conducted by comparing the levels of transcript expression of cell cycle-specific genes, using RT-qPCR array methodology. Additionally, using an array comprising a panel of 82 different antibodies specific to cell cycle regulatory proteins, expression at the protein level (including status of phosphorylation modifications) was measured and compared between L647R PreA-expressing induced cells and uninduced cells. These analyses revealed altered expression of various genes when L647R PreA is expressed. The whole genome microarray indicates L647R PreA affects a range of cellular functions but especially cell cycle control and several pathways with functions that overlap cell cycle control. The cell cycle pathway specific analyses of transcript and protein levels confirm altered expression of numerous cell cycle regulators upon L647R PreA accumulation. These regulators are members of several different regulatory pathways and point to a role for PreA in the coordination of the pathways that control the cell cycle.

Among the key pathways affected by L647R PreA are the AHR pathway, the RB-E2F pathway, and the p53 pathway. Overlapping with these, L647R PreA effects were noted for p300-CyclinE and FoxO-p27^{Kip1} regulation. Acting as a potential common thread in modulating some, if not all, of the observed effects of PreA expression on the cell cycle, is the Pin1 prolyl isomerase. A Pin1-PreA interaction could ultimately prove to be a keystone relationship in control of cell cycle.

Cell Cycle-Control-Related Pathways Demonstrating Effects from L647R PreA Expression

Aryl Hydrocarbon Receptor (AHR) Pathway Regulation

Of the several pathways indicated by microarray analysis and Ingenuity Pathways™ Analysis, the AHR pathway is, surprisingly, indicated to be the most significantly regulated, when L647R PreA is expressed in 3T3 cells. The AHR is a member of the bHLH (basic Helix–Loop–Helix)- PAS (Per-ARNT-Sim) family of transcriptional regulators that control a variety of developmental and physiological events, including neurogenesis, formation of secretory ducts, circadian rhythms, response to hypoxia, hormone receptor function, and toxin metabolism, the latter being, perhaps, the best known role for AHR¹³⁴. Known as the Dioxin receptor, AHR is the mediator for most toxic responses to Polycyclic Aromatic Hydrocarbons (PAH), Dioxins (such as TCDD (2,3,7,8-tetrachlorodibenzo-p-dioxin)), and Polychlorinated Biphenyls. In addition to the toxic chemicals known to be AHR ligands, other ligands include dietary compounds, natural and synthetic flavonoids, and pharmaceuticals¹³⁵. Upon activation by ligand binding, the AHR translocates to the nucleus, and dimerizes with another basic helix-loop-helix protein, ARNT, also known as Hypoxia Inducible Factor β (HIF1- β), which, in complex with HIF1- α , has its own transcriptional activity independent of

AHR in response to hypoxia and, perhaps, some normoxic conditions³²⁷. The activated AHR/ARNT heterodimer complex interacts with AH-responsive elements and activates the expression of AHR target genes³²⁸. AHR binding results in recruiting of CBP/p300, a Histone Acetyltransferase (HAT) Complex coactivator and facilitates binding of the transcription factor SP1, resulting in enhanced expression from the target gene³²⁹, as in case of the Cytochrome P450 xenobiotic metabolism genes³³⁰. AHR can affect cellular signaling through interactions with various other regulatory and signaling proteins, including chaperone and immunophilin-like proteins (such as heat shock proteins), the Aryl Hydrocarbon Receptor-Interacting Protein (AIP), as well as protein kinases and phosphatases (including tyrosine kinases, Casein Kinase-2 (CK2), Protein Kinase-C (PKC)). In addition, AHR is also known to interact with cell cycle-relevant signaling pathways that are mediated by hormone receptors (including Estrogen Receptor), Hypoxia, NF-KappaB (Nuclear Factor-Kappa-B) and Rb (Retinoblastoma) protein^{134,135} and SUMO1-modification^{331,332}. AHR association with coactivators can lead to histone acetylation, Pol II (RNA Polymerase-II) recruitment and subsequent gene transcription, or, in contrast, activation of the AHR results in transcriptional inhibition of some target genes, such as those encoding the Immunoglobulin heavy-chain and Estrogen-inducible p27^{Kip1}. Inhibitors of PKC and Tyrosine Kinase block the induction of AHR target genes, indicating a likelihood they are also involved in AHR signal transduction^{333,334}. AHR also interacts with NF-KappaB signaling pathways. Direct interactions between AHR and RelA (a NF-KappaB subunit) induce transactivation of c-Myc protein^{135,335,336}. Functional cross talk between AHR and NF-KappaB occurs through interactions with common coactivators SRC1 and p300/CBP. AHR and NF-KappaB RelA form an

inactive complex, thereby causing mutual repression. The association between the AHR and RelA provides a physical basis for the functional antagonism³³⁷. AHR may also be involved in cell-cycle regulation through growth factor signaling, cell-cycle arrest, and apoptosis^{134,337,338}. In fact, Puga and coworkers presented a comprehensive review of AHR roles in cell cycle³³⁹ in which they discuss a wide range of AHR-ligand activation induced cell cycle perturbations, including G0/G1 and G2/M arrest, diminished capacity for DNA replication, and inhibition of cell proliferation. AHR-mediated functions are often accomplished in the absence of an exogenous ligand, but the underlying molecular mechanisms governing these processes are poorly understood, partly because no endogenous ligands have been definitively identified. More than a decade of research points to a role for the AHR in cell cycle control, yet the precise mechanism remains ill-defined. Reports suggest that in the absence of an exogenous ligand, the AHR promotes progression through the cell cycle^[reviewed in 340]. In contrast, evidence spanning more than 20 years has shown that TCDD, the prototypical AHR ligand, can inhibit cell proliferation³³⁹. Marlowe and associates show that the repressor activity of the AHR is fully independent of its transcriptional activity, not requiring its transactivation or DNA binding domains or interaction with ARNT, delineating a dual activity of AHR in mediating promotion or inhibition of cell proliferation, dependent upon the cellular environment or ligand exposure³⁴¹. AHR is shown to contribute to p300-mediated induction of DNA synthesis during S-phase³⁴², and in fact was shown to competitively displace p300 from E2F-dependent promoters^{341,343}. Studies also found AHR contributes to the inhibition of cell cycle progression by directly interacting with the RB/E2F complex to block its phosphorylation

in G1^{136,137}. This interaction constitutes a major G1 checkpoint in cells exposed to AHR ligands¹³⁸. AHR and RB have demonstrated a synergistic relationship to reinforce the repression of E2F-dependent gene expression, thus slowing down the progression of cells from G1 into S-phase¹³⁷. In addition, AHR is recruited to RB-regulated promoters, where it functions as a corepressor for RB. Through the formation of specific protein-protein interactions and the exclusion of coactivator proteins from RB-regulated promoters, the interaction with AHR results in repression of transcription of RB target genes such as CDK2 and cyclin A to cause cell cycle arrest^{341,344,345}. It is suggested the AHR tandem effects of RB-corepression and blocking of recruitment of p300 to E2F-regulated genes are interrelated and that inhibition of p300 binding is one of the molecular events responsible for the persistence of active gene repression by AHR-RB complexes³⁴¹. Pin1 is reported to bind, and potentially stabilize p300 expression, as well as increase its affinity for binding its targets³⁴⁶. In this way, sequestration of Pin1, rendering it unavailable to act on p300, presents a potential mechanism by which L647R PreA could contribute to AHR-RB-mediated gene repression. As RB regulation by Lamin A is well-documented^{102,347}, the indication of highly significant regulation of this pathway in our microarray analysis of cells exogenously expressing L647R PreA could represent an important mechanism, heretofore apparently unexplored, by which PreA protein accumulation drives cells toward cell cycle arrest.

RB-E2F Pathway Regulation

Three pRB family members, termed pocket proteins, are expressed in mammalian cells: pRB/p105 (herein, “pRB” will refer to the protein, “RB” to the gene),

pRb1/p107, and pRb2/p130 (proteins referred to herein as “p107” and “p130,” respectively, and “p107 gene,” or “p130 gene,” respectively, for reference to the genes). In their hypophosphorylated state, these proteins bind to members of the E2F-family of transcriptional regulators and inhibit transcription. This inhibition is relieved when the pocket proteins are released from E2F complexes following their phosphorylation by cyclin/CDK activity³⁴⁸, freeing the E2F proteins to influence the transcription of genes whose protein products are necessary for cell cycle progression. The phosphorylation status of each of the RB- family members varies throughout the cell cycle. Several cyclin dependent kinases are implicated in this process³⁴⁹. As their functions and structures differ, members of the E2F- and RB-families exhibit differential interactions with each other in a temporally regulated manner through the cell cycle. E2Fs 1-3 are transcriptional activators and interact only with pRB³⁵⁰. E2F4 and -5 are transcriptional repressors and preferentially bind p130 and p107³⁵¹. The p130/E2F4 complex is thought to possess the primary function of helping maintain a state of transcriptional silence^{352,353} and is the complex most abundant in quiescent cells, although p107/ E2F4 and pRB/E2F4 complexes also accumulate in G1 phase³⁵³. As the cells start to re-enter the cell cycle, in early G1, E2F4 is still found primarily in association with p130, but p130 is replaced in mid to late G1 by p107, and then by pRB in late G1 and S phases³⁵³⁻³⁵⁶. p130 also regulates the expression of the RB and p107 genes, which contain E2F sites in their promoters^{357,358}. In addition, while both p130 and p107 are bound to a number of promoters in asynchronously growing cells, only p130 is recruited to promoters in quiescent or serum-restimulated human cells. Repression of promoters in quiescent cells has been shown to be specifically associated with recruitment of E2F4 and p130

as well as with histone hypoacetylation³⁵⁹. While 9 members of the E2F family have been identified (including 2 isoforms of E2F-3), only E2Fs1-5 interact with the pocket proteins^[reviewed in 360]. E2Fs 6-8, the functions of which are somewhat less well characterized than the other 6 family members, lack the N-terminal sequences of E2Fs1–3 as well as the C-terminal domain common to all the other E2F proteins³⁶¹⁻³⁶⁵. They do not have activation domains or pocket protein interaction domains and, thus, exhibit RB-independent transcriptional-repression activity³⁶⁴⁻³⁶⁷. E2F6, specifically, has been shown to interact with Polycomb proteins to repress transcription³⁶³. E2F1 has well documented target genes that are proapoptotic, such as Caspase 3, 7, 9 and Apaf1³⁶⁸. Furthermore, E2F1 directly induces expression of p19^{ARF} (for which expression of the transcript was upregulated after 48 hours of L647R PreA expression, according to our initial microarray data but is not assayed at the protein level after 72 hours of L647R expression). p19^{ARF}, in turn, activates p53 by binding and inhibiting MDM2 function³⁶⁹. Implications of that relationship are further explored in the p53 pathway discussion section.

In additional paradox to the well-known growth-promoting function of E2F1, its expression is suggested to be counterbalanced by multiple self-imposed safeguard mechanisms, one of which is activation of the promoter of the cyclin dependent kinase inhibitor (CKI) p27^{Kip1} gene, for which E2F1 expression has actually been shown to be necessary for maintaining basal level p27 expression³⁷⁰. In this negative feedback mechanism, expression of p27^{Kip1} cooperates with pRb to suppress E2F1 activity, and this association of p27^{Kip1} with pRb has demonstrated ability to activate cellular senescence³⁷¹. Interestingly, E2F1 protein levels are reduced in a dosage-dependent

manner with expression of p130, which, as mentioned, is a transcriptional target of E2F1. The resulting E2F1 reduction leads to inhibition of cyclin A expression and subsequent reduction in cyclin A-associated kinase activity. Furthermore, induction of p130 expression has also been shown to lead to a substantial induction in the protein levels of p27^{Kip1},³⁷²⁻³⁷⁴. To further complicate this E2F1-negative feedback process, because p27^{Kip1} levels are mainly regulated by ubiquitin-mediated proteasomal degradation that is targeted by cyclin E-Cdk2 phosphorylation of p27^{Kip1} on Thr-187^{375,376}, p130-mediated inhibition of cyclin E-associated kinase activity may induce p27^{Kip1} levels by decreasing or inhibiting targeted proteolysis of p27, extending the feedback loop by stabilizing p27^{Kip1} at expression levels that can propagate further inhibition of CDK activity. In that loop, p130 and other RB-family members are protected from the inactivation-inducing phosphorylation of CDKs³⁷⁷. p27^{Kip1} is discussed again in the FoxO discussion section, involving its FOXO-mediated transcription.

While our data from the RT-qPCR array indicate significant mRNA expression level upregulation of the pRB-interacting, transcription-activating E2Fs1-3, as well as the repressor E2F4, after 24 hours of L647R PreA expression, E2Fs 5-8 were not included in the RT-qPCR assay. Consistent with the increased E2F-1-3 transcript expression, several targets do exhibit increased expression, such as cell cycle regulating genes cyclin A, CDK2, the RB and p107 genes, as well as E2F2 and E2F3 (which are E2F targets, themselves), the DNA replication associated Mcm2 gene, and the DNA repair and checkpoint control regulating genes, PCNA, Rad51, Msh2, Chk1, and MAD2L¹⁵³.

E2Fs are regulated not only at the level of transcription, but also significantly by posttranslational modifications, subcellular localization, association of cofactors, and degradation^{378,379}. Our protein microarray results do not indicate significant changes in the levels of expressed E2Fs after 72 hours of induced L647R PreA expression, except in the case of E2F-6, which demonstrates downregulated levels with L647R PreA expression. Interestingly, though E2F-6 is a transcriptional repressor, repressing the E2F-mediated transcription of genes responsible for the G1/S transition, it is expressed *only during S-phase*, and exogenous expression of E2F-6 has been shown to result in accumulation of cells in S-phase³⁶⁷. Repression of the G1/S transition-inducing genes by E2F-6 could, therefore, potentially have a role in maintaining a unidirectional progression forward of the cell cycle. Nonetheless, the decreased level of expression represented by our antibody array could be a reflection of the proportional decrease in the number of cells in S-phase among the cells expressing L647R PreA as compared to control cells that were not induced to express the mutant lamin protein. Likewise, the measured levels of pRB expression do not indicate differences between cells expressing L647R PreA compared to uninduced cells on the antibody array. However, phosphorylation of pRB Ser-795 is indicated to be significantly downregulated with L647R PreA expression. Phosphorylation of the Ser-795 residue is mediated by CDK4 and requires the activity of MEK-ERK pathway. Moreover, this phosphorylation is functionally significant in that it occurs rapidly and directly correlates with dissociation of E2F-1 from pRB and initiation of E2F-mediated transcription³⁸⁰. Therefore, hypophosphorylation of this site is consistent with RB-mediated transcriptional repression in the L647R PreA-expressing cells. It has been suggested that Pin1 binds

pRB to stabilize its hyperphosphorylated, inactive conformation, thus inhibiting RB-mediated transcriptional repression and cell cycle arrest³⁸¹. In addition to the potential role of Pin1 inhibition in promoting AHR-RB-mediated transcriptional repression, preventing a direct Pin1 conformational inhibitory regulation of pRB presents another mechanism in which PreA sequestration of Pin1 could contribute to cell cycle arrest. Unfortunately, the antibody array does not feature p107 or p130 to confirm results of the qPCR array, which indicated increased mRNA transcript levels for those 2 RB family members, and the qPCR array did not assay for the RB transcript. Considering our data in the context of RB-E2F-related transcriptional control of the cell cycle, the results suggest L647R PreA protein expression has significant effects on this pathway, which is not completely surprising, given several studies have previously revealed a role for A-type lamins in stabilization and regulation of the pRB protein^{102,347}. Taken together, data from the qPCR array and the antibody array strongly suggest the PreA isoform has a role of its own, which appears to be separate from that of mature LA, in regulating expression and interactions of members of the RB-family of pocket proteins with E2F transcriptional regulators in a program regulating cell cycle control.

p300 and Cyclin E Pathway

Pin1 has been shown to facilitate p300 binding to its targets³⁴⁶. Given the Pin1 propensity to stabilize many of its binding partners, it could raise the question of whether PreA sequestration of Pin1 could contribute to destabilization and our observed decrease in the expression level of p300 protein in PreA-expressing cells (decreased nearly 2-fold, according to antibody-detection in our protein microarray). p300,

described as both a transcription cofactor and a HAT, is considered to be a master regulatory protein and molecular switch, integrating transcriptional control of cell cycle progression, DNA repair³⁸², and tumorigenesis^[reviewed in 228,234,383-385] and may be required to maintain tissue homeostasis³⁸⁶. It is required for cell and tissue function during embryonic development, cell differentiation *in vitro*²³³, and in fact, even a 25% decrease in p300/CBP proteins is detrimental for normal development^{234,235}, while p300 nullizygous (p300^{-/-}) embryos die between days 9 and 11.5^[reviewed in 385]. p300 is targeted by viral oncoproteins, mutated in certain forms of cancer, and phosphorylated in a cell cycle-dependent manner^[reviewed in 228]. In addition, p300 interacts with numerous transcription factors including p53, E2F, microphthalmia transcription factor (MITF), and RB³⁸⁷. p300 can stimulate either transactivation or repressor functions of several different transcription factors, suggesting that the interacting proteins, promoter, and cellular context are critical determinants of p300 function^[reviewed in 385,388]. A reduction in p300 levels results in an apparently directly proportionate level of transcriptional repression, from competition between transcription factors for limited amounts p300 in the nucleus³⁸⁵, and has *direct* negative effects on cellular proliferation, as it does for development^{234,235}. The involvement of p300 in maintaining the proliferative state of cells is supported by studies using p300-deficient fibroblasts, including fibroblasts from p300-nullizygous animals, which show slow proliferation and rapid replicative senescence in culture^{235,389}.

Importantly, p300 binds integrally to the cyclin E-CDK2 complex³⁹⁰, of which it controls the activity, and has been determined to be required for the G1-S transition, with a decrease in cyclin E-CDK2 activity directly resulting in inhibition of the G1- to S-

phase transition³⁸⁹. Cyclin E, in its complex with CDK2, controls 3 major S-phase events: DNA replication, centrosome duplication, and histone gene expression^[reviewed in 391]. Overexpression of cyclin E promotes S-phase entry increases the frequency of centrosome duplication and genetic instability³⁹¹ and induces escape from Ras-induced senescence in mouse embryonic fibroblasts³⁹². p300 is a critical regulator of cyclin E transcription *in vivo*, and p300 depletion directly results in cyclin E down-regulation, causing growth arrest and expression of a senescent-like phenotype³⁹³. Access to DNA by transcriptional regulatory proteins is determined by chromatin organization, which regulates activation or repression of transcription. Chromatin structure is primarily controlled by ATP-dependent reorganization of nucleosomal positioning and posttranslational modifications to the histone tails by acetylases or deacetylases, which introduce localized perturbations to the chromatin, either allowing or preventing the binding of transcriptional machinery³⁹⁴. Loss of acetylation may shift the balance toward repressive heterochromatin, causing silencing of genes associated with cell cycle progression. Errors in the maintenance of repressive heterochromatin domains have been proposed to accumulate during the proliferative life span of normal human cells, ultimately triggering a senescence checkpoint and leading to irreversible cell cycle exit.³⁹⁵ It has been suggested, a progressive decline in HAT levels (such as with decreased levels of p300), with further cell divisions, leads to increased HDAC activity and chromatin modifications that cause altered gene regulation and permanent relocation of genes into the heterochromatin compartment, thereby triggering a senescence checkpoint that ultimately results in activation of cellular senescence³⁹³.

Our antibody array study indicates expression of L647R PreA results in significantly decreased protein levels of both p300 and Cyclin E protein levels compared to the uninduced control. These findings strongly suggest a role for PreA in induction of cell cycle arrest and inhibition of cellular proliferation. The association of Cyclin E down-regulation by reduced p300 levels with senescence, and the fact cells expressing L647R PreA demonstrate that particular expression pattern is a potential indicator that PreA protein accumulation has a role in senescence induction. Recruitment of p300 and HDACs to promoters may be a cyclic event in proliferating cells, while a decrease in p300 levels favors recruitment of other repressor proteins³⁹⁶⁻³⁹⁹ to cyclin E and other cell cycle-regulatory gene promoters³⁹³. We reason, therefore, that a transiently cyclic pattern of p300-cyclin E repression might be related to the equally transient accumulation of PreA protein in cycling cells, resulting in quiescence, while it is conceivable that sustained accumulation of the protein could result in senescence, potentially implicating PreA in regulation of cell fate.

FoxO Pathway

A decreased expression level of p300 represents another potential means of PreA-mediated positive regulation of FoxOs. As p300 acetylation of FoxO inhibits its ability to bind DNA, FoxO transcriptional activity is ablated by p300 expression³¹³. Therefore, the observed significant decrease in p300 expression in L647R PreA-expressing cells is consistent with FoxO activation. Likewise, as modulation of the subcellular localization is the primary means by which FoxOs are regulated, Akt downregulation is a highly positive indicator of FoxO activity. Because Akt is the major inducing kinase of FoxO phosphorylation-dependent, 14-3-3-mediated export from the

nucleus, the downregulation of expression and activity-inducing phosphorylation of Akt that we observe in our protein microarray is consistent with nuclear localization and an active status of FoxO transcriptional regulation. Importantly, Pin1 has been shown to be a primary mediator of Akt stability. Inhibition of Pin1 results in destabilization and proteasomal degradation of Akt. Our proposed mechanism of accumulated PreA binding, and thus sequestering, Pin1, should be able to induce the observed downregulation in Akt. A downstream effect would be stable FoxO nuclear localization and active transcription of targets such as p27, such as we see in the immunoblots and immunofluorescence imaging of the L647R PreA expressing cells. Interestingly, while we show that Juglone treatment increased nuclear translocation of FoxO3a and p27^{KIP} in uninduced cells, the already increased nuclear pool of FoxO3a and p27^{KIP} proteins were not significantly altered in L647R PreA expressing cells. This suggests expression of PreA inhibits Pin1 negative effects upon FoxO3a nuclear translocation and consequent p27^{KIP} expression, with at least as much effectiveness as treatment with a chemical Pin1 inhibitor. Also, Pin1 inhibition does not decrease the nuclear translocation of FoxO3a, nor p27^{KIP} expression in L647R PreA cells, thus confirming the increased Pin1 in complex with PreA does not have a negative regulatory effect on FoxO3a or p27^{KIP} expression. These data, taken together, suggest a heretofore undescribed mechanism of PreA cell cycle regulation through sequestration of Pin1, thus limiting its nuclear availability and preventing its binding to targets. This mechanism could have many consequences for cell cycle regulation, considering the plethora of cell cycle targets of Pin1 activity.

In line with their ability to block cell growth and to induce senescence or apoptosis, FoxO genes act as tumor suppressors. Deletion of all FoxO1, FoxO3, and FoxO4 alleles in adult mice induces a cancer prone condition characterized by hemangiomas and thymic lymphomas⁴⁰⁰. In human cancers, several chromosomal translocations disrupt FoxO genes, producing hybrid proteins in which the forkhead DNA-binding domain and the Akt phosphorylation sites are lost⁴⁰¹, and in fact, much of the oncogenic activity of the Ras-Erk pathway depends on inactivation of FoxO transcription factors⁴⁰⁰. It has been suggested that nuclear FoxO and Myc might compete for the promoter site of the p27^{Kip1} gene, where, in character with its oncogenesis-promoting functions, Myc acts in direct opposition to the function of FoxO transcriptional activation of p27^{Kip1}, acting rather to repress transcription of p27^{Kip1}⁴⁰². In addition, Oncogene-Induced Senescence (OIS), as from BRAF, for example, is mediated by JNK phosphorylation of FoxOs but does not activate p27^{Kip1} or p16^{ARF1}. Rather, JNK-mediated FoxO phosphorylation specifically induces p21^{WAF1} expression to induce senescence. PKB/Akt phosphorylation FoxO sites are not affected by JNK-mediated OIS FoxO activation, and ERK phosphorylation does not play a role in this FoxO activation⁴⁰³. Importantly, although a mechanism of tumor suppression, it is argued that induction of cellular senescence is also causative to organismal aging^{404,405}. FoxO response to OIS may therefore represent a trade-off between tumor suppression and lifespan.

Cellular signaling induced by growth factors is propagated, at least in part, by Reactive Oxygen Species (ROS), which are thereby necessary to regulate a variety of cellular processes including proliferation^{406,407}. However, accumulation of ROS above a

certain threshold level causes damage to the cellular interior, referred to as oxidative stress. Toxic levels of ROS can induce cellular senescence⁴⁰⁸, so they are also considered to accelerate aging and age-related pathologies^{409,410}. In response to accumulation of ROS, a poorly understood induction of senescence occurs. FoxOs are known to be mediators of oxidative stress repression³⁰⁸, increasing resistance to oxidative stress through transcription of such enzymes as MnSOD³¹⁰ and Catalase⁴¹¹, through a negative feedback loop, which appears to ultimately result in senescence whenever high levels of ROS are encountered, likely as a measure to avoid cell death, or ensuing tumorigenesis caused by ROS-induced DNA damage. Paradoxically, increased FoxO activity is associated with longevity in model organisms⁴¹² and humans⁴¹³, but at the same time, in managing response to ROS accumulation, FoxOs are responsible for inducing senescence, lending credit to the hypothesis that excessive ROS accelerate aging. It is interesting that both lack of growth factor signaling and increased OIS/ROS result in FoxO activation. However, there is a cost differential to the organism between the 2 programs in which the absence of growth factor signaling can impose a reversible FoxO-p27^{kip1}-mediated G1 cell cycle arrest and/or quiescence, which may, perhaps, be used for cellular maintenance and to repair cellular damage³¹⁰, wherein FoxO proteins may positively affect lifespan with little cost to the organism. In contrast, FoxOs' response to OIS and ROS, while protecting against immediate cell death or tumorigenesis, does so at a significant cost to the organism, as this service is accomplished through induction of senescence—thus defining a limited lifespan. These concepts underline the pivotal role that FoxOs play in minimizing the damage of ROS from normal cellular signaling and in neutralizing intercepted oncogenic signaling, as

well mediating the aging that results from overexposure to ROS or OIS. Thus, while our current study does not assay the sites of JNK-mediated phosphorylation on FoxOs and does not test effects of oxidative stress or OIS upon cells expressing L647R PreA compared to controls, as FoxOs are regulated by ROS and oncogenic signaling, in addition to signals related to growth factors and cell metabolism, and play a role in both tumor suppression and aging, regulation of these effects provide an important paradigm to understanding the relationships between aging and disease such as cancer. Our study does, however, demonstrate a capacity for FoxO regulation by PreA, with the strong indication of a PreA-mediated role for regulation of Pin1 in that mechanism. As PreA has been demonstrated to accumulate with progressive aging and in senescence^{35,43,66,74,146}, and A-type lamins have been associated with cell cycle regulation^{102,103,347}, while both FoxO and Pin1 dysregulation have been implicated in cell cycle dysfunction and numerous cancers (FoxOs and cancer review⁴¹⁴, Pin1 and cancer review⁴¹⁵), we suggest this PreA-Pin1-FoxO regulatory relationship warrants further investigation in the roles of tumor suppression and senescence induction, and thus, on the role of these relationships in cancer and in aging.

p53 Pathway

The pocket proteins can induce expression of both p21^{Waf1} and p27^{Kip1} and are essential for both quiescence and senescence⁴¹⁶. p53, on the other hand, has been thought to play a key role primarily in senescence, mainly by inducing p21^{Waf1}, which permanently blocks cell cycle progression⁴¹⁷. The p53 pathway was indicated by our genomic expression microarray pathway analysis to be highly affected by PreA L647R expression. This pathway controls the expression of hundreds of genes in response to

signaling stimuli from sources of genotoxic insult, as well as from sources of nongenotoxic metabolic stresses and is the subject of many reviews^[217,418-424 and a multitude of others]. The activity of p53 has been shown to be essential to arrest the cell cycle in response to irradiation or DNA-damaging chemical agents (examples of genotoxic stressors)^{170,425}, as well as in response to virus infection-related interferon production, and cytokine signaling in metabolic stresses such as hypoxia (nongenotoxic stressors)⁴²⁶. As a consequence of its large number of downstream effectors, activated p53 can elicit a number of responses, including activation of several kinase-mediated signaling pathways or transcriptional induction or repression of several hundred genes. Results of this signaling are either arrest of cell cycle progression in late G1-, S-, or G2-phases or the induction of apoptosis. Many p53-downstream effectors function in a feedback mechanism with p53, signaling in cooperation to promote cell and tissue homeostasis by directing many repair processes, including transient inhibition of nucleic acid synthesis, DNA repair, control of the cell division cycle, elimination of damaged proteins, autophagy, ATP generation via oxidative phosphorylation, affecting function of the mitochondria, and directing programmed cell death⁴²⁶.

The binding to DNA for transcriptional regulation by p53 involves alteration of the protein conformation and occurs in a DNA sequence-specific manner. Mutations in p53, or in the target genes, that alter the binding specificity or the ability to achieve proper conformation result in suppression of p53 function and are associated with the loss of genomic stability found in a wide range of human cancers^{418,427,428}. In fact, studies have shown that more than 50% of human cancers involve mutations that dysregulate p53^{420,429}. Regulation of p53 is accomplished by posttranslational modifications,

including phosphorylation, acetylation, methylation, and ubiquitination, as well as by interactions with other factor molecules that enhance or diminish activity by altering p53 binding to partner molecules, determining its cellular localization, or affecting its rate of degradation^[426,430,431, and as reviewed in 217,418-420]. Stabilization of p53 is primarily controlled by Mdm2⁴³²⁻⁴³⁵. These proteins act as E3-ubiquitin ligases, binding to and targeting p53 for degradation by the 26S proteasome. Mdm2, a ring-finger protein, is generally considered to be the major regulator of p53 in response to genotoxic stress⁴³⁶ and is amplified in several types of cancers⁴³⁷. Mdm2-binding simultaneously conceals the p53 transcription activation domain and facilitates p53 export out of the nucleus into the cytoplasm, in addition to its targeting the p53 protein for degradation⁴³⁸. Interestingly, expression of Mdm2 is transcriptionally activated by p53 in a negative feedback loop that controls the level, extent, and duration of p53 protein activation⁴³⁹. Upon stress signaling, p53 phosphorylation promotes the dissociation of MDM2 from the MDM2/p53 complex, allowing activation of a stable p53^{424,425,427,440}. Our data show the transcript expression of Mdm2 is upregulated after 24 hours of induced expression of L647R PreA, but the cells demonstrate no significant changes in the protein expression level of Mdm2 after 72 hours of expressing L647R PreA. Importantly, though, the Ser-166 residue of Mdm2 protein in the L647R PreA-expressing cells is hypo-phosphorylated. Phosphorylation of Mdm2 at Ser-166 is accomplished by Akt following growth factor stimulation, and results in increased half-life of Mdm2 protein, enhanced Mdm2-mediated p53 degradation, and nuclear translocation that allows it to inhibit p-53-mediated transcription. Additionally, the p53-inducible phosphatase Wip1/Ppm1d is able to dephosphorylate Mdm2, thereby inactivating its repressive and degradation-

targeting effects on p53. The transcript level of Wip1 in the L647R PreA expressing cells, by RT-qPCR assay, was found to be upregulated, but Wip1 is not assayed by the antibody array. In contrast, Akt is not assayed on the RT-qPCR array. The antibody array, however, demonstrates a significant downregulation of Akt protein expression in L647R PreA-expressing cells. Additionally, the phosphorylation profile of Akt in L647R PreA-expressing cells indicates it is considerably hypoactive. As for p53, itself, the transcript shows a very modest upregulation after 24 hours of L647R PreA expression, and actually a slight downregulation at the protein level, after 72 hours of induced L647R PreA expression, with a phosphorylation profile consistent with response to oxidative damage, microtubule disruption, or replicative senescence.

p53 and mTOR Pathway

The paradigm for the p53 pathway has recently shifted. For many years, p53 was considered, primarily, as the driver of a program of apoptosis, and after several years of work it has been proven to have an equally significant role in cell cycle arrest, most recently, extraordinary revelations have been made about p53 roles in the decision between the pathways quiescence⁴⁴¹ or senescence^[as reviewed in 418,421,424,427]. Notably, p27^{Kip1} is the primary CKI involved in inducing quiescence and is not a target of p53⁴⁴², and thus p53 is considered dispensable in quiescence induction, although, it has also been shown that p53-activation of p21^{Waf1} can trigger pRB-mediated quiescence, possibly by triggering p27^{Kip1} expression⁴⁴³. The recent work of Leontieva, Demidenko, Blagosklonny, and colleagues, have challenged the long-held notion that p53 is primarily an inducer of senescence but propose, rather, that p53 is actually a

suppressor of the senescent phenotype⁴⁴⁴. Additionally, several groups have contributed to the realization that the mammalian Target of Rapamycin (mTOR) signaling pathway and the p53 pathway converge to determine cellular quiescence versus senescence⁴⁴⁵⁻⁴⁴⁹. In fact, p53 has been demonstrated to inhibit mTOR^{445,447,450}. mTOR is a PI3Kinase-like-kinase (PIKK) family kinase, and the mTOR pathway mediates protein synthesis as part of cellular growth when adequate nutrients, energy, and mitogens are supplied in the cell^[as reviewed in 445]. PI3K-activated Akt activates mTOR, when cellular conditions are favorable, while PTEN, AMPK, and TSC1/2 inhibit the pathway when conditions are not favorable, as in serum-starvation or high-density contact, in cell culture. The p53-inhibition of mTOR occurs via p53 activation of AMPK⁴⁴⁵. In the crosstalk between these pathways, activated p53 activates AMPK, which inhibits Akt, and thus mTOR, and p53 is able to induce quiescence. In conditions where the mTOR pathway is active, p53 activates a senescence response to stress signaling. Furthermore, weak induction of p53 is unable to inhibit the mTOR pathway, and thus weakly increased p53 expression is associated with irreversible induction of senescence. Paradoxically, high levels of p53 expression/activation, such as would occur acutely in response to a DNA-damaging event, potentially inhibit mTOR signaling, initiating quiescence, conceivably to allow the cell to execute repair processes⁴⁵¹⁻⁴⁵⁵. If cellular stressors such as hypoxia or DNA damage occur during the conditions in which mTOR is inhibited, p53 would not induce senescence but, rather, would continue to participate in mediating the mTOR inhibition and maintenance of quiescence. If p53 signaling is resolved prior to restimulation of mTOR, then the cells re-enter the cell cycle. However, if serum is returned while p53 signaling is still increased, and high

levels of mitogen-signaling overrides the p53-AMPK inhibition of mTOR, senescence will be induced.

If one considers the cell cycle related expression pattern we have described for PreA, it is seen in conditions of serum starvation or high-density plating, where quiescence is induced (wherein, mTOR would be inhibited), but it is also expressed in replicative senescence (wherein, plating conditions could be spacious and plenty of serum provided in the medium, and mTOR would not be inhibited), according to this work and that of others^{35, 121,122}. This phenomenon is inconsistent with our theory that PreA-mediated inhibition of Akt and the mTOR pathway could play a role in the recently described function of the p53-mTOR pathway in selecting for quiescence in conditions inhibiting the mTOR pathway^{444,451,452,455}. In that model, senescence activation occurs only in conditions of p53 activation without mTOR inhibition. Therefore, in the normal physiological circumstances of its accumulation, PreA would likely participate in the mTOR-inhibited induction of quiescence, where p53 induction would be related to the cellular stressors of the conditions of starvation or crowding. The cells are able to re-enter the cell cycle upon mitogen restimulation or replating, as this simultaneously relieves the p53-inducing stress and releases inhibition of mTOR. As we are expressing PreA exogenously in the cells of our current study, in conditions of plentiful mitogens and low- to medium-plating densities, it seems that mTOR inhibition should not be in effect, and yet, we see the downregulated Akt that must indicate mTOR repression, as would the increased transcription of the Camk2s and Sestrin 2 that we see in these cells. We also see the nuclear localization of FoxOs and p27^{Kip1} that would

indicate quiescence, and the p300 and Cyclin E downregulation that signify either quiescence or senescence.

In the absence of serum starvation or contact-inhibition induced stress, we also do not see strong activation of p53. Our observed low p53 expression level in the cells expressing L647R PreA, seems congruent with a the noted senescence induction by continued low-level p53 expression, or with a p53-independent mode of quiescence initiation, and is consistent with previous findings related to a relative lack of p53 induction by PreA¹⁰³. We presume the low p53 levels observed are because the cells are not being serum starved, crowded, or treated with stressing agents in order to induce the PreA accumulation. However, the phosphorylation signature (indicative of hypoxic stress, microtubule dysfunction, or replicative senescence), and the fact that PreA is found in senescent cells as well, leads us to the question of how cells are able to enter senescence despite accumulation of PreA, when PreA accumulation apparently downregulates Akt and would presumably lead to mTOR inhibition?

A possible answer for this question comes in the form of Pin1. Pin1 phosphorylation-dependent binding to p53 is required for the DNA damage-induced response of p53. The specific sites reportedly requiring phosphorylation to bind Pin1 are Ser-33, Thr-81, and Ser-315 (notably, Ser-33 and Thr-81 are somewhat hypophosphorylated, with L647R PreA expression, while Ser-315 phosphorylation is upregulated)^{267,456}. We hypothesize PreA accumulation, in the absence of mitogen deprivation or cell crowding, would not typically be present at the initiation of DNA damage signaling related to substantial genotoxic insult to the cell, or at the induction of telomere-uncapping-mediated DNA damage signaling as cells reach the replicative limit.

Therefore, our proposed PreA-Pin1 sequestration-related inhibition of Akt and the mTOR pathway would not be in effect at the initiation of that mode of p53-activation. Also, Pin1 sequestration by PreA would not be a factor, and thus Pin1 could freely interact with p53 to promote its DNA damage response cell cycle arrest activities. On the other hand, it has been recently demonstrated that Pin1 must be inhibited to allow induction of replicative senescence⁴⁵⁷. It is possible, then, that PreA-mediated Pin1 inhibition could be the key to directing cells with p53 activated by shortened telomeres to senescence. Future studies will demonstrate if PreA accumulation occurs *subsequent* to p53-mediated cell cycle arrest in cells that enter senescence due to DNA damage signaling, including that which occurs from uncapped telomeres as the replicative limit is reached. Successive passaging of cells expressing L647R PreA results in progressive PreA accumulation to levels that have been shown to demonstrate perturbations of cell cycle function, defective mitosis, altered chromatin organization, and telomere stability. For this reason, we suggest use of this exogenous PreA-expressing model could make it difficult to determine if normal pathways leading to senescence involve PreA accumulation *after* p53-activation has already occurred. Activation of p53 by telomere-uncapping-induced DNA damage signaling could induce senescence directly, before the effects of PreA-mediated mTOR-inhibition-related quiescence induction could occur. However, the effects of DNA damage signaling upon the proposed PreA-Pin1 sequestration must be evaluated. Given the overlap of putative Pin1- and MDC1-binding sites in the PreA c-terminal tail, the possibility exists for DNA damage signaling to alter the ability of accumulated PreA to bind Pin1. Such interference could neutralize the proposed sequestration effect and consequences such

as Akt-mTOR inhibition. This latter phenomenon could reconcile the contradictions of PreA-mediated inhibition of Akt/mTOR (and implied p53-mediated direction to a quiescent state), and the known expression of PreA in replicatively senescent cells. The ability of L647R PreA-expressing cells to enter senescence after successive passaging, as demonstrated in the β -galactosidase assay for the L647R PreA-expressing cells, could be attributed to the ability of “prolonged” cell cycle arrest/quiescence to convert to senescence. Some researchers have demonstrated depletion of mTOR pathway inhibitors, such as TSC2, can allow reactivation of the mTOR pathway despite continued stress conditions. This reactivation initiates conversion of prolonged quiescence into senescence.⁴⁵⁵ Perhaps a conversion to replicative senescence is allowed after p53-mediated quiescence is induced in response to telomere-uncapping DNA damage signaling, once PreA accumulation occurs to a level at which it is able to adequately sequester and inhibit Pin1. Future work should examine this relationship in the absence of exogenously expressed PreA, in the context of DNA damage induction in young, proliferating cells, in highly passaged cells, and in disease cells such as RD, HGPS, and WS (typical/ atypical). The diagram in Figure 44 represents the mTOR signaling pathway and proposed regulatory effects of PreA expression and sequestration of Pin1.

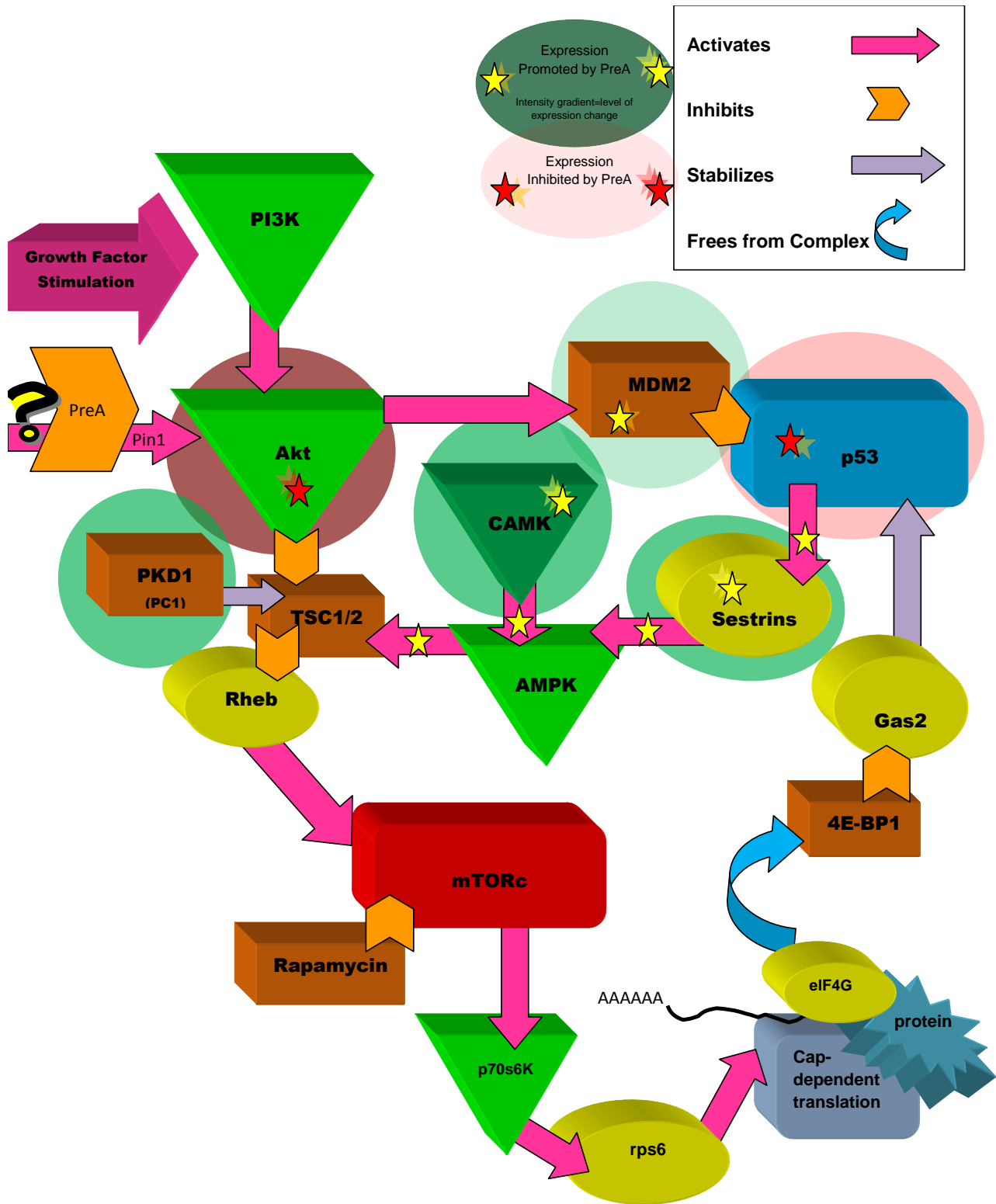


Figure 44. Discussion Graphic: mTOR Pathway and Proposed Pathway Inhibitory Effects of PreA Expression and Putative Pin1 Sequestration.

Conclusions

Cellular senescence is considered to be a tumor-suppressive mechanism and to contribute to cellular aging. Senescent cells exhibit multiple changes in gene expression of cell cycle-regulatory and stress response genes as well as matrix-remodeling proteins⁴⁵⁸, involving some combination of up-regulation of one or more of the CKIs p16INK4a, p21^{Waf-1} and p27^{Kip1}, down-regulation of cyclin E, down-regulation of CDK4 and CDK2 activities, and hypophosphorylation of the RB protein^[reviewed in459]. Our data suggest that PreA complexes with Pin1 in a manner such that Pin1 is rendered largely inactive. We hypothesize PreA-mediated Pin1 inhibition could have dramatic effects on a broad range of cell cycle regulators, and thus, it could be a central mechanism in determining lifespan and healthspan of organisms ranging from fruit flies, to mice, to humans. High order changes in chromatin structure may be involved in the generation of the senescence, considering the complexity of the phenotype. The senescence induced prematurely in HGPS cells⁵⁸ and the altered chromatin organization⁴⁶⁰ could be related, at least in part, to the phenomenon of PreA accumulation reported in HGPS cells. In fact, Pin1 has been reported to control the ability of cells to condense and organize chromatin^{461 462}, to control major channels of transcription^{271,463,464}, and to mediate protein translation, most likely due at least in part to its control of the mTOR pathway²⁶¹. Key factors in support of suggesting the PreA-mediated Pin1 sequestration/inhibition would have major cell cycle and cell fate-decision impact include the Akt regulatory function of Pin1 and our observed downregulation of Akt expression and activity levels. Modulation of FoxO-p27^{Kip1} expression and the mTOR pathway are among Akt-related mechanisms of cell cycle

and cell fate determination, and together with the direct effects of Pin1 on critical regulators including pRB, p53, p300, Cyclin D, and Cyclin E, it is clear that control of Pin1 function is a fundamental cell cycle and cell fate-controlling mechanism. Successive passaging of cells expressing PreA result in its progressive accumulation to levels that demonstrate cell cycle perturbation, and senescence ensues. Researchers have previously demonstrated overexpression of PreA results in rapid progression to senescence with telomeres that are shortened to critical levels that induce DNA damage signaling^{43,66,69,71,99,121}. A primary pathology of HGPS is early, or premature, senescence (some researchers refer to “early” senescence as entry to senescence with long telomeres that would appear capable of many further divisions, while “premature” senescence refers to an accelerated progression toward the normal replicative limit of cells). Examples of stimuli to enter early senescence would be OIS, ROS, or other signaling factors that communicate high levels of stress or risk to the cell. On the other hand, the normal process of aging and repeated cellular replication is the most common example of entering senescence due to shortened telomeres. It has been demonstrated that the rate of alternative splicing increases with aging, and potentially as a result, progerin accumulation increases with age-related cell passaging^{75,92}. Furthermore, progerin has been shown to elicit recruitment of PreA expression^{65,71,208}, and it is interesting to consider the potential role of exponential effects of Pin1-related alternative splicing, progerin accumulation and further PreA accumulation, possibly leading to acceleration of telomere erosion via effects of Pin1-sequestration on TRF1, ultimately controlling the rate of the cell’s progression to its fate of replicative senescence.

The findings of this project suggest many interesting, and potentially highly impactful, avenues of research that could be followed. Among the most interesting are those involving the tantalizing clues to help us understand our own mortality. Modulation of quiescence and senescence is critical to maintain genomic integrity, to allow cells to grow, repair, and organize between cell cycles, or to navigate checkpoints to assure fidelity of genomic replication, and to avoid the need for cells to undergo apoptosis with each insult to its systems, or decide to initiate apoptosis when sacrifice of the cell is beneficial to the organism. A PreA-specific role in organizing the interactions between several important cell cycle regulatory pathways, including those we have described, place a potentially tremendous importance on the PreA isoform in the functions of LA as a master regulator of cellular proliferation, genomic integrity, lifespan, disease, and aging.

REFERENCES

1. Goldman RD, Gruenbaum Y, Moir RD, Shumaker DK, Spann TP. Nuclear lamins: building blocks of nuclear architecture. *Genes & Development* 2002;16(5):533-547.
2. Aebi U, Cohn J, Buhle L, Gerace L. The nuclear lamina is a meshwork of intermediate-type filaments. *Nature* 1986;323:560-564.
3. Fisher DZ, Chaudhary N, Blobel G. cDNA sequencing of nuclear lamins A and C reveals primary and secondary structural homology to intermediate filament proteins. *Proc Natl Acad Sci USA* 1986;83:6450-6454.
4. Fuchs E, Weber K. Intermediate filaments: structure, dynamics, function, and disease. *Annu Rev Biochem* 1994;63:345-382.
5. Stuurman N, Heins S, Aebi U. Nuclear lamins: their structure, assembly, and interactions. *J Struct Biol* 1999;122:42-66.
6. Schutz W, Benavente R, Alsheimer M. Dynamic properties of germ line-specific lamin B3: The role of the shortened rod domain. *European Journal of Cell Biology* 2005;84(7):649-662.
7. Broers JLV, Machiels BM, Kuijpers HJH, Smedts F, van den Kieboom R, Raymond Y, Ramaekers FCS. A- and B-type lamins are differentially expressed in normal human tissues. *Histochemistry and Cell Biology* 1997;107(6):505-517.
8. Stewart C, Burke B. Teratocarcinoma stem cells and early mouse embryos contain only a single major lamin polypeptide closely resembling lamin B. *Cell* 1987;51(3):383-392.
9. Schirmer EC, Gerace L. The Stability of the Nuclear Lamina Polymer Changes with the Composition of Lamin Subtypes According to Their Individual Binding Strengths. *Journal of Biological Chemistry* 2004;279(41):42811-42817.
10. Lehner CF, Stick R, Eppenberger HM, Nigg EA. Differential expression of nuclear lamin proteins during chicken development. *J Cell Biol* 1987;105:577-587.

11. Sullivan T, Escalante-Alcalde D, Bhatt H, Anver M, Bhat N, Nagashima K, Stewart CL, Burke B. Loss of A-type lamin expression compromises nuclear envelope integrity leading to muscular dystrophy. *J Cell Biol* 1999;147(5):913-20.
12. Beck LA, Hosick TJ, Sinensky M. Incorporation of a product of mevalonic acid metabolism into proteins of Chinese hamster ovary cell nuclei. *J Cell Biol* 1988;107(4):1307-16.
13. Gerace L, Comeau C, Benson M. Organization and modulation of nuclear lamina structure. *J Cell Sci Suppl* 1984;1:137-160.
14. Beck LA, Hosick TJ, Sinensky M. Isoprenylation is required for the processing of the lamin A precursor. *The Journal of Cell Biology* 1990;110(5):1489-1499.
15. Clarke S. Protein isoprenylation and methylation at carboxyl-terminal cysteine residues. *Annu Rev Biochem* 1992;61:355-86.
16. Zhang FL, Casey PJ. Protein Prenylation: Molecular Mechanisms and Functional Consequences. *Annual Review of Biochemistry* 1996;65(1):241-269.
17. Young S, Fong L, Michaelis S. Prelamin A, Zmpste24, misshapen cell nuclei, and progeria - new evidence suggesting that protein farnesylation could be important for disease pathogenesis. *J Lipid Res* 2005;46:2531 - 2558.
18. Holtz D, Tanaka RA, Hartwig J, McKeon F. The CaaX motif of lamin A functions in conjunction with the nuclear localization signal to target assembly to the nuclear envelope. *Cell* 1989;59(6):969-977.
19. Hennekes H, Nigg EA. The role of isoprenylation in membrane attachment of nuclear lamins. A single point mutation prevents proteolytic cleavage of the lamin A precursor and confers membrane binding properties. *J Cell Sci* 1994;107 (Pt 4):1019-29.
20. Marshall CJ. Protein prenylation: a mediator of protein-protein interactions. *Science* 1993;259:1865-6.
21. Sinensky M, Fantle K, Trujillo M, McLain T, Kupfer A, Dalton M. The processing pathway of prelamin A *J Cell Sci* 1994;107:61-67.

22. Bergo MO, Gavino B, Ross J, Schmidt WK, Hong C, Kendall LV, Mohr A, Meta M, Genant H, Jiang Y and others. Zmpste24 deficiency in mice causes spontaneous bone fractures, muscle weakness, and a prelamin A processing defect. *Proc Natl Acad Sci U S A* 2002;99(20):13049-54.
23. Gruber J, Lampe T, Osborn M, Weber K. RNAi of FACE1 protease results in growth inhibition of human cells expressing lamin A: implications for Hutchinson-Gilford progeria syndrome. *J Cell Sci* 2005;118(4):689-696.
24. Otto JC, Kim E, Young SG, Casey PJ. Cloning and Characterization of a Mammalian Prenyl Protein-specific Protease. *Journal of Biological Chemistry* 1999;274(13):8379-8382.
25. Maske CP, Hollinshead MS, Higbee NC, Bergo MO, Young SG, Vaux DJ. A carboxyl-terminal interaction of lamin B1 is dependent on the CAAX endoprotease Rce1 and carboxymethylation. *The Journal of Cell Biology* 2003;162(7):1223-1232.
26. Kilic F, Dalton MB, Burrell SK, Mayer JP, Patterson SD, Sinensky M. In vitro assay and characterization of the farnesylation-dependent prelamin A endoprotease. *J Biol Chem* 1997;272:5298-5304.
27. Kilic F, Johnson D, Sinensky M. Subcellular localization and partial purification of prelamin A endoprotease: an enzyme which catalyzes the conversion of farnesylated prelamin A to mature lamin A. *FEBS Letters* 1999;450:61 - 65.
28. Corrigan DP, Kuszczak D, Rusinol AE, Thewke DP, Hrycyna CA, Michaelis S, Sinensky MS. Prelamin A endoproteolytic processing in vitro by recombinant Zmpste24. *Biochem J* 2005;387:129-138.
29. Glynn M, Glover T. Incomplete processing of mutant lamin A in Hutchinson-Gilford progeria leads to nuclear abnormalities, which are reversed by farnesyltransferase inhibition. *Hum Mol Gen* 2005;14:2959 - 2969.
30. Navarro CL, De Sandre-Giovannoli A, Bernard R, Boccaccio I, Boyer A, Genevieve D. Lamin A and ZMPSTE24 (FACE-1) defects cause nuclear disorganization and identify restrictive dermopathy as a lethal neonatal laminopathy. *Hum Mol Genet* 2004;13:2493-2503.

31. Rusinol AE, Sinensky MS. Farnesylated lamins, progeroid syndromes and farnesyl transferase inhibitors. *J Cell Sci* 2006;119(16):3265-3272.
32. Gerace L, Blobel G. The nuclear envelope lamina is reversibly depolymerized during mitosis. *Cell* 1980;19:277-287.
33. Gerace L, Blobel G. Nuclear lamina and the structural organization of the nuclear envelope. *Cold Spring Harbor Symp Quant Biol* 1982;46:967-978.
34. Moir RD, Yoon M, Khuon S, Goldman RD. Nuclear Lamins A and B1: Different Pathways of Assembly during Nuclear Envelope Formation in Living Cells. *The Journal of Cell Biology* 2000;151(6):1155-1168.
35. Pugh GE, Coates PJ, Lane EB, Raymond Y, Quinlan RA. Distinct nuclear assembly pathways for lamins A and C lead to their increase during quiescence in Swiss 3T3 cells. *Journal of Cell Science* 1997;110: 2483-2493.
36. Capell B, Collins F. Human laminopathies: nuclei gone genetically awry. *Nature Rev Gen* 2006;7:940 - 952.
37. Gruenbaum Y, Margalit A, Goldman RD, Shumaker DK, Wilson KL. The nuclear lamina comes of age. *Nat Rev Mol Cell Biol* 2005;6(1):21-31.
38. Worman HJ, Åstlund C, Wang Y. Diseases of the Nuclear Envelope. *Cold Spring Harbor Perspectives in Biology* 2010;2(2):-.
39. Worman HJ, Fong LG, Muchir A, Young SG. Laminopathies and the long strange trip from basic cell biology to therapy. *J Clin Invest* 2009;119:1825-1836.
40. Chi Y-H, Chen Z- J, Jeang K-T. Review: The nuclear envelopathies and human diseases. *Journal of Biomedical Science* 2009;16(96).
41. Hutchinson J. Case of congenital absence of hair, with atrophic condition of the skin and its appendages, in a boy whose mother had been almost wholly bald from alopecia areata from the age of six. *Lancet* 1886;1:923.

42. Merideth M, Gordon L, Clauss S, Sachdev V, Smith A, Perry M, Brewer C, Zalewski C, Kim H, Solomon B and others. Phenotype and course of Hutchinson-Gilford Progeria Syndrome. *N Eng J Med* 2008;358:592 - 604.
43. Candelario J, Sudhakar S, Navarro S, Reddy S, Comai L. Perturbation of wild-type lamin A metabolism results in a progeroid phenotype. *Aging Cell* 2008;7(3):355-367.
44. Hegele R. Drawing the line in progeria syndrome. *Lancet* 2003;362:416 - 417.
45. Sarkar P, Shinton R. Hutchinson-Guilford Progeria syndrome. *Postgrad Med J* 2001;77:312 - 317.
46. Neveling K, Bechtold A, Hoehn H. Genetic instability syndromes with progeroid features. *Z Gerontol Geriatr* 2007;40:339 - 348.
47. Eriksson M, Brown W, Gordon L, Glynn M, Singer J, Scott L, Erdos M, Robbins C, Moses T, Berglund P and others. Recurrent de novo point mutations in lamin A cause Hutchinson-Gilford progeria syndrome. *Nature* 2003;423:293 - 298.
48. De Sandre-Giovannoli A, Bernard R, Cau P, Navarro C, Amiel J, Boccaccio I, Lyonnet S, Stewart C, Munnich A, Merrer M and others. Lamin A Truncation in Hutchinson-Gilford Progeria. *Science* 2003;300:2055.
49. Cao H, Hegele RA. LMNA is mutated in Hutchinson-Gilford progeria (MIM 176670) but not in Wiedemann-Rautenstrauch progeroid syndrome (MIM 264090). *J Hum Genet* 2003;48:271-274.
50. Gilford H. Ateleiosis and progeria: Continuous youth and premature old age. *Brit Med J* 1904;2:914-918.
51. McKusick VA. The clinical observations of Jonathan Hutchinson. *Am J Syph Gonorrhoea Vener Dis* 1952;36:101-126.
52. DeBusk FL. The Hutchinson-Gilford progeria syndrome. *J Pediat* 1972;80:697-724.

53. Fernandez-Palazzi F, McLaren AT, Slowie DF. Report on a case of Hutchinson-Gilford progeria, with special reference to orthopedic problems. *Eur J Pediatr Surg* 1992;2(6):378-82.
54. Glynn MW, Glover TW. Incomplete processing of mutant lamin A in Hutchinson-Gilford progeria leads to nuclear abnormalities, which are reversed by farnesyltransferase inhibition. *Hum Mol Genet* 2005;14(20):2959-69.
55. Young S, Meta M, Yang S, Fong L. Prelamin A Farnesylation and progeroid syndromes. *J Biol Chem* 2006;281:39741 - 39745.
56. Arboleda G, Ramirez N, Arboleda H. The neonatal progeroid syndrome (Wiedemann-Rautenstrauch): a model for the study of human aging? *Exp Gerontol* 2007;42:939 - 943.
57. Benson EK, Lee SW, Aaronson SA. Role of progerin-induced telomere dysfunction in HGPS premature cellular senescence. *J Cell Sci* 2010;jcs.067306.
58. Cao K, Blair CD, Faddah DA, Kieckhaefer JE, Olive M, Erdos MR, Nabel EG, Collins FS. Progerin and telomere dysfunction collaborate to trigger cellular senescence in normal human fibroblasts. *The Journal of Clinical Investigation* 2011;121(7):2833-2844.
59. Capell B, Olive M, Erdos M, Cao K, Faddah D, Tavarez U, Conneely K, Qu X, San H, ganesh S and others. A farnesyltransferase inhibitor prevents both the onset and late progression of cardiovascular disease in a progeria mouse model. *Proc Nat Acad Sci USA* 2008;105:15902 - 15907.
60. Capell BC, Erdos MR, Madigan JP, Fiordalisi JJ, Varga R, Conneely KN, Gordon LB, Der CJ, Cox AD, Collins FS. Inhibiting farnesylation of progerin prevents the characteristic nuclear blebbing of Hutchinson-Gilford progeria syndrome. *Proc Natl Acad Sci U S A* 2005;102(36):12879-84.
61. Coutinho H, Falcao-Silva V, Goncalves G, da Nobrega R. Molecular ageing in progeroid syndromes: Hutchinson-Gilford progeria syndrome as a model. *Immunity & Ageing* 2009;6(1):4.
62. Davies BS, Barnes RH, 2nd, Tu Y, Ren S, Andres DA, Spielmann HP, Lammerding J, Wang Y, Young SG, Fong LG. An accumulation of non-

- farnesylated prelamin A causes cardiomyopathy but not progeria. *Hum Mol Genet* 2010;19(13):2682-94.
63. Dechat T, Shimi T, Adam SA, Rusinol AE, Andres DA, Spielmann HP, Sinensky MS, Goldman RD. Alterations in mitosis and cell cycle progression caused by a mutant lamin A known to accelerate human aging. *Proceedings of the National Academy of Sciences* 2007;104(12):4955-4960.
 64. Fong LG, Frost D, Meta M, Qiao X, Yang SH, Coffinier C, Young SG. A protein farnesyltransferase inhibitor ameliorates disease in a mouse model of progeria. *Science* 2006;311(5767):1621-3.
 65. Goldman RD, Shumaker DK, Erdos MR, Eriksson M, Goldman AE, Gordon LB, Gruenbaum Y, Khuon S, Mendez M, Varga R and others. Accumulation of mutant lamin A causes progressive changes in nuclear architecture in Hutchinson-Gilford progeria syndrome. *Proc Natl Acad Sci U S A* 2004;101(24):8963-8.
 66. Huang S, Risques RA, Martin GM, Rabinovitch PS, Oshima J. Accelerated telomere shortening and replicative senescence in human fibroblasts overexpressing mutant and wild-type lamin A. *Experimental Cell Research* 2008;314(1):82-91.
 67. Kieran MW, Gordon L, Kleinman M. New approaches to progeria. *Pediatrics* 2007;120(4):834-41.
 68. Kudlow B, Kennedy B, Monnat R. Werner and Hutchinson-Gilford progeria syndromes: mechanistic basis of human progeroid diseases. *Nat Rev Mol Cell Biol* 2007;8:394 - 404.
 69. Liu B, Wang J, Chan KM, Tjia WM, Deng W, Guan X, Huang J-d, Li KM, Chau PY, Chen DJ and others. Genomic instability in laminopathy-based premature aging. *Nat Med* 2005;11(7):780-785.
 70. Mazereeuw-Hautier J, Wilson L, Mohammed S, Smallwood D, Shackleton S, Atherton D, Harper J. Hutchinson-Gilford progeria syndrome: clinical findings in three patients carrying the G608G mutation in LMNA and review of the literature. *Br J Dermatol* 2007;156:1308 - 1314.

71. Liu Y, Rusinol A, Sinensky M, Wang Y, Zou Y. DNA damage responses in progeroid syndromes arise from defective maturation of prelamin A. *J Cell Sci* 2006;119(22):4644-4649.
72. Meta M, Yang S, Bergo M, Fong L, Young S. Protein farnesyltransferase inhibitors and progeria. *Trends Mol Med* 2006;12:480 - 487.
73. Pardo R, Castillo S. Progeria. *Rev Chil Pediatr* 2002;73:5 - 8.
74. Reddy S, Comai L. Lamin A, farnesylation and aging. *Experimental Cell Research* 2011;In Press, Corrected Proof.
75. Rodriguez S, Coppede F, Sagelius H, Eriksson M. Increased expression of the Hutchinson-Gilford progeria syndrome truncated lamin A transcript during cell aging. *Eur J Hum Genet* 2009;17(7):928-937.
76. Scaffidi P, Misteli T. Lamin A dependent nuclear defects in human aging. *Science* 2006;312:1059 - 1063.
77. Yang S, Bergo M, Toth J, Qiao X, Hu Y, Sandoval S, Meta M, Bendale P, Gelb M, Young S and others. Blocking protein farnesyltransferase improves nuclear blebbing in mouse fibroblasts with a targeted Hutchinson-Gilford progeria syndrome mutation. *Proc Natl Acad Sci USA* 2005;102:10291 - 10296.
78. Yang SH, Andres DA, Spielmann HP, Young SG, Fong LG. Progerin elicits disease phenotypes of progeria in mice whether or not it is farnesylated. *J Clin Invest* 2008;118(10):3291-300.
79. Hegele RA. LMNA mutation position predicts organ system involvement in laminopathies. *Clin Genet* 2005;68:31-34.
80. Shumaker DK, Kuczmarski ER, Goldman RD. The nucleoskeleton: lamins and actin are major players in essential nuclear functions. *Current Opinion in Cell Biology* 2003;15(3):358-366.
81. Herrmann H, Aebi U. Intermediate filaments: molecular structure, assembly mechanism, and integration into functionally distinct intracellular scaffolds. *Annu Rev Biochem* 2004;73:749-789.

82. Holt I, Ostlund C, Stewart CL, Man N, Worman HJ, Morris GE. Effect of pathogenic mis-sense mutations in lamin A on its interaction with emerin in vivo. *J Cell Sci* 2003;116:3027-35.
83. Worman H, Courvalin J. How do mutations in lamins A and C cause disease? *J Clin Invest* 2004;113:349 - 351.
84. Lutz RJ, Trujillo MA, Denham KS, Wenger L, Sinensky M. Nucleoplasmic localization of prelamin A: implications for prenylation-dependent lamin A assembly into the nuclear lamina. *Proceedings of the National Academy of Sciences of the United States of America* 1992;89(7):3000-3004.
85. Bridger JM, Foeger N, Kill IR, Herrmann H. The nuclear lamina. *FEBS Journal* 2007;274(6):1354-1361.
86. Gruenbaum Y, Wilson KL, Harel A, Goldberg M, Cohen M. Review: Nuclear Lamins--Structural Proteins with Fundamental Functions. *Journal of Structural Biology* 2000;129(2-3):313-323.
87. Lammerding J, Schulze PC, Takahashi T, Kozlov S, Sullivan T, Kamm RD, Stewart CL, Lee RT. Lamin A/C deficiency causes defective nuclear mechanics and mechanotransduction. *J Clin Invest* 2004;113(3):370-8.
88. Hutchison CJ. Lamins: building blocks or regulators of gene expression? *Nat Rev Mol Cell Biol* 2002;3(11):848-858.
89. Lammerding J, Fong LG, Ji JY, Reue K, Stewart CL, Young SG, Lee RT. Lamins A and C but Not Lamin B1 Regulate Nuclear Mechanics. *The Journal Of Biological Chemistry* 2006;281(35):25768-25780.
90. Hutchison CJ, Worman HJ. A-type lamins: guardians of the soma? *Nat Cell Biol* 2004;6(11):1062-7.
91. Dechat T, Korbei B, Vaughan O, Vlcek S, Hutchison C, Foisner R. Lamina-associated polypeptide 2alpha binds intranuclear A-type lamins. *J Cell Sci* 2000;113(19):3473-3484.
92. Naetar N, Foisner R. Lamin complexes in the nuclear interior control progenitor cell proliferation and tissue homeostasis. *Cell Cycle* 2009;8:1488-1493.

93. Chen S, Martin C, Maya-Mendoza A, Tang CW, Lovric J, Sims PFG, Jackson DA. Reduced Expression of Lamin A/C Results in Modified Cell Signaling and Metabolism Coupled with Changes in Expression of Structural Proteins. *Journal of Proteome Research* 2009;8(11):5196-5211.
94. Markiewicz E, Dechat T, Foisner R, Quinlan RA, Hutchison, CJ. Lamin A/C binding protein LAP2alpha is required for nuclear anchorage of retinoblastoma protein. *Mol Biol Cell* 2002;13:4401-4413.
95. Dorner D, Vlcek, S, Foeger, N, Gajewski A, Makolm C, Gotzmann J, Hutchison CJ, Foisner R. Lamin-associated polypeptide 2alpha regulates cell cycle progression and differentiation via the retinoblastoma-E2F pathway. *J Cell Biol* 2006;173:83-93.
96. Pekovic V, Harborth J, Broers JL, Ramaekers FC, van Engelen B, Lammens M, von Zglinicki T, Foisner R, Hutchison CJ, Markiewicz E. Nucleoplasmic LAP2alpha-lamin A complexes are required to maintain a proliferative state in human fibroblasts. *J Cell Biol* 2007;176:163-172.
97. Schirmer EC, Guan T, Gerace L. Involvement of the Lamin Rod Domain in Heterotypic Lamin Interactions Important for Nuclear Organization. *The Journal of Cell Biology* 2001;153(3):479-490.
98. Izumi M, Vaughan OA, Hutchison CJ, Gilbert DM. Head and/or CaaX Domain Deletions of Lamin Proteins Disrupt Preformed Lamin A and C But Not Lamin B Structure in Mammalian Cells. *Molecular Biology of the Cell* 2000;11(12):4323-4337.
99. Lees-Miller SP. Dysfunction of lamin A triggers a DNA damage response and cellular senescence. *DNA Repair* 2006;5(2):286-289.
100. Caron M, Auclair M, Donadille B, Bereziat V, Guerci B, Laville M, Narbonne H, Bodemer C, Lascols O, Capeau J and others. Human lipodystrophies linked to mutations in A-type lamins and to HIV protease inhibitor therapy are both associated with prelamin A accumulation, oxidative stress and premature cellular senescence. *Cell Death Differ* 2007;14(10):1759-1767.
101. Dechat T, Adam SA, Taimen P, Shimi T, Goldman RD. Nuclear Lamins. *Cold Spring Harbor Perspectives in Biology* 2010;2(a000547).

102. Johnson B, Nitta R, Frock R, Mounkes L, Barbie D, Stewart C, Harlow E, Kennedy B. A-type Lamins regulate retinoblastoma protein function by promoting subnuclear localization and preventing proteasomal degradation. *PNAS* 2004;101(26).
103. Kudlow BA, Stanfel MN, Burtner CR, Johnston ED, Kennedy BK. Suppression of Proliferative Defects Associated with Processing-defective Lamin A Mutants by hTERT or Inactivation of p53. *Mol. Biol. Cell* 2008;19(12):5238-5248.
104. Yaffe MB, Schutkowski M, Shen M, Zhou XZ, Stukenberg PT, Rahfeld J-U, Xu J, Kuang J, Kirschner MW, Fischer G and others. Sequence-Specific and Phosphorylation-Dependent Proline Isomerization: A Potential Mitotic Regulatory Mechanism. *Science* 1997;278(5345):1957-1960.
105. Rozen S, Skaletsky, H. Primer3 on the WWW for general users and for biologist programmers. In: Krawetz S, Misener, S, editor. *Bioinformatics Methods and Protocols in the series Methods in Molecular Biology*: Humana Press, Totowa, NJ; 2000.
106. Moore PL, Damelin LH, Harrison TJ. ¹⁴C-methylamine-glutaraldehyde conjugation as an alternative to iodination for protein labeling *Biotechniques* 2003;35(2):379-82.
107. Avouch J, Witters, LA, Alexander MC, Bush MA. *J Biol Chem* 1978(253):4754.
108. Garrison JC, Wagner JD. *J Biol Chem* 1982;254.
109. Veronese FM, Boccu E, Fontana A. Modification of tryptophan 108 in lysozyme by 2-nitro-4-carboxyphenylsulfenyl chloride. *FEBS Letters* 1972;21(3):277-280.
110. Aebersold RH, Leavitt J, Saavedra RA, Hood LE, Kent SBH. Internal amino acids equence analysis of proteins separated by one-dimensional electrophoresis after in situ protease digestion in nitrocellulose. *Proc Natl Acad Sci USA* 1987;84:6970-6974.
111. Contor L, Lamy F, Lecocq RE. Use of electroblotting to detect and analyze phoshotyrosine containing peptides separated by two-gel electrophoresis. *Anal Biochem* 1987;160:414-420.

112. Cooper JA, Sefton BM, Hunter T. Detection and quantitation of phosphotyrosine in proteins. *Methods Enzymol* 1983;99:387-402.
113. Wing KD. *Science* 1988;241:467-469.
114. Dhadialla T, Carlson G, Le D. *Annu Rev Entomol* 1998;43:545-569.
115. Rippmann JF, Hobbie S, Daiber C, Guilliard B, Bauer M, Birk J, Nar H, Garin-Chesa P, Rettig WJ, Schnapp A. Phosphorylation-dependent Proline Isomerization Catalyzed by Pin1 Is Essential for Tumor Cell Survival and Entry into Mitosis. *Cell Growth Differ* 2000;11(7):409-416.
116. ELM Database RGC, Diella F, Via A, Puntervoll P, Gemünd C, Chabanis-Davidson S, Michael S, Sayadi A, Bryne JC, Chica C, et al.; Reference 2: Puntervoll P, Linding R, Gemünd C, Chabanis-Davidson S, Mattingdal M, Cameron S, Martin DMA, Ausiello G, Brannetti B, Costantini A, et al Reference 1: ELM: the status of the 2010 eukaryotic linear motif resource; Reference 2: ELM server: a new resource for investigating short functional sites in modular eukaryotic proteins (<http://elm.eu.org/>). *Nucleic Acids Res Ref* 1: 2010; Ref 2: 2003; Accessed July 2011; Ref 1: 38(Database issue); Ref 2: 31:Ref 1: D167-80; Ref 2: 3625-3630.
117. Li J, Ning Y, Hedley W, Saunders B, Chen Y, Tindill N, Hannay T, Subramaniam S. The Molecule Pages database. *Nature* 2002;420(6916):716-717.
118. Bateman A, Birney E, Cerruti L, Durbin R, Etwiller L, Eddy Sean R, Griffiths-Jones S, Howe KL, Marshall M, Sonnhammer ELL. The Pfam Protein Families Database. *Nucleic Acids Research* 2002;30(1):276-280.
119. Obenauer JC, Cantley LC, Yaffe MB. Scansite 2.0: proteome-wide prediction of cell signaling interactions using short sequence motifs. *Nucleic Acids Research* 2003;31(13):3635-3641.
120. Prasad TSK, Goel, R., Kandasamy, K., Keerthikumar, S.Kumar, S., Mathivanan, S., Telikicherla, D., Raju, R., Shafreen, B., Venugopal, A., et al. Human Protein Reference Database - 2009 update (<http://www.hprd.org/>). *Nucleic Acids Research*. Volume 372009 (accessed July 2011). p D767-D772.

121. Ukekawa R, Miki K, Fujii M, Hirano H, Ayusawa D. Accumulation of multiple forms of lamin A with down-regulation of FACE-1 suppresses growth in senescent human cells. *Genes to Cells* 2007;12(3):397-406.
122. Ragnauth CD, Warren DT, Liu Y, McNair R, Tajsic T, Figg N, Shroff R, Skepper J, CM S. Prelamin A acts to accelerate smooth muscle cell senescence and is a novel biomarker of human vascular aging. *Circulation* 2010;121(20):2200-10.
123. Amanchy R, Periaswamy, B., Mathivanan, S., Reddy, R., Tattikota, S. G., and Pandey, A. A compendium of curated phosphorylation-based substrate and binding motifs. *Nature Biotechnology* 2007;25:285-286.
124. Mishra G, Suresh M, Kumaran K, Kannabiran N, Suresh S, Bala P, Shivkumar K, Anuradha N, Reddy R, Raghavan TM, et al. Human Protein Reference Database - 2006 Update. *Nucleic Acids Research* 2006;34:D411-D414.
125. Peri S NJ, Amanchy R, Kristiansen TZ, Jonnalagadda CK, Surendranath V, Niranjana V, Muthusamy B, Gandhi TK, Gronborg M, et al. Development of human protein reference database as an initial platform for approaching systems biology in humans. *Genome Research* 2003;13:2363-2371.
126. Dephoure N, Zhou C, Villen J, Beausoleil SA, Bakalarski CE, Elledge SJ, Gygi SP. A quantitative atlas of mitotic phosphorylation. *Proc Natl Acad Sci U S A* 2008;105(31):10763-10767.
127. Whitfield ML, Sherlock G, Saldanha AJ, Murray JI, Ball CA, et al. Identification of genes periodically expressed in the human cell cycle and their expression in tumors. *Mol Biol Cell* 2002;13:1977-2000.
128. Beyrouthy MJ, Alexander KE, Baldwin A, Whitfield ML, Bass HW, McGee D, Hurt MM. Identification of G1-Regulated Genes in Normally Cycling Human Cells. *PLoS ONE* 2008;3(12).
129. Morgan D. Cyclin-dependent kinases: Engines, clocks, and microprocessors. *Annu Rev Cell Dev Biol* 1997;13:261-291.
130. Massague J. G1 cell cycle control and cancer. *Nature* 2004;432:298-306.

131. Dhillon N, Oki M, Szyjka SJ, Aparicio OM, Kamakaka RT. H2A.Z Functions To Regulate Progression through the Cell Cycle. *Mol. Cell. Biol.* 2006;26(2):489-501.
132. Ingenuity-Systems^R. Ingenuity Pathways AnalysisTM, Ingenuity Systems^R My Pathways Path Designer, www.ingenuity.com. 2011.
133. Belt E, Fijneman R, van den Berg E, Bril H, Delis-van Diemen P, Tijssen M, van Essen H, de Lange-de Klerk E, Belien J, Stockmann H and others. Loss of lamin A/C expression in stage II and III colon cancer is associated with disease recurrence. *Eur J Cancer* 2011;Article in Press.
134. Bock K, Kohle C. Ah receptor: Dioxin-mediated toxic responses as hints to deregulated physiologic functions. . *Biochem Pharmacol* 2006.
135. Hestermann E, Brown M. Agonist and chemopreventative ligands induce differential transcriptional cofactor recruitment by aryl hydrocarbon receptor. *Mol Cell Biol* 2003;23(21):7920-5.
136. Ge N-L, CJ CE. A direct interaction between the aryl hydrocarbon receptor and retinoblastoma protein. *J Biol Chem* 1998;273:22708-22713.
137. Puga A, Barnes SJ, Dalton TP, Chang C-y, Knudsen ES, Maier MA. Aromatic Hydrocarbon Receptor Interaction with the Retinoblastoma Protein Potentiates Repression of E2F-dependent Transcription and Cell Cycle Arrest. *Journal of Biological Chemistry* 2000;275(4):2943-2950.
138. Marlowe J, Puga A. Aryl hydrocarbon receptor, cell cycle regulation, toxicity, and tumorigenesis. *J Cell Biochem* 2005;96:1174-1184.
139. Manju K, Muralikrishna B, Parnaik VK. Expression of disease-causing lamin A mutants impairs the formation of DNA repair foci. *J Cell Sci* 2006;119(13):2704-2714.
140. MacLachlan TK, Somasundaram K, Sgagias M, Shifman Y, Muschel RJ, Cowan KH, El-Deiry WS. BRCA1 Effects on the Cell Cycle and the DNA Damage Response Are Linked to Altered Gene Expression. *Journal of Biological Chemistry* 2000;275(4):2777-2785.

141. New England Biolabs Inc. RheoSwitch (R) Mammalian Inducible Expression System Instruction Manual (RheoSwitch is a registered trademark of RheoGene, Inc.). www.neb.com, NEB, 240 County Road, Ipswich MA 01938: 2007;Instruction Manual Version 1.3.
142. Karzenowski D, Potter D, Padidam M. *BioTechniques* 2005;39:191-196.
143. Dai X, Willis L, Palli S, Theilmann D. *Protein Expr Purif* 2005;42:236-245.
144. Palli S, Kapitskaya M, Kumar M, Cress D. *Eur J Biochem* 2003;270:1308-1315.
145. Kumar M, Potter D, Hormann R, Edwards A, Tice C, Smith H, Dipietro M, Polley M, Lawless M, Wolohan P and others. *J Biol Chem* 2004;279:27211-27218.
146. Candelario J, Borrego S, Reddy S, Comai L. Accumulation of distinct prelamin A variants in human diploid fibroblasts differentially affects cell homeostasis. *Experimental Cell Research* 2010;317(3):319-329.
147. Goldman RD, Shumaker DK, Erdos MR, Eriksson M, Goldman AE, Gordon LB, Gruenbaum Y, Khuon S, Mendez M, Varga Re and others. Accumulation of mutant lamin A causes progressive changes in nuclear architecture in Hutchinsonâ€“Gilford progeria syndrome. *Proceedings of the National Academy of Sciences of the United States of America* 2004;101(24):8963-8968.
148. Cao K, Capell BC, Erdos MR, Djabali K, Collins FS. A lamin A protein isoform overexpressed in Hutchinson-Gilford progeria syndrome interferes with mitosis in progeria and normal cells. *Proceedings of the National Academy of Sciences* 2007;104(12):4949-4954.
149. GeneCards. GeneCards: The Human Gene Compendium v.3. www.genecards.org. 1997-2011 ed: Crown Human Genome Center at the Weizmann Institute of Science in Israel; 1997-2011 (Accessed August 2011).
150. NCBI, (1) Maglott DR, Ostell, Pruitt KD, Tatusova T; (2) Wheeler DL, Barrett T, Benson DA, Bryant SH, et al.; (3) Gerhard DS, Wagner L, Feingold EA, Shenmen CM, et al.; (4) Schuler GD, Epstein JA, Ohkawa H, Kans JA. (1) Entrez Gene: gene-centered information at NCBI; (2) Database resources of the National Center for Biotechnology Information; (3) The status, quality, and expansion of the NIH full-length cDNA project: the Mammalian Gene Collection (MGC); (4) Entrez: molecular biology database and retrieval system (1-2) *Nucleic*

Acids Res; (3) Genome Res; (4) Methods Enzymol. Volume (1)Database Issue:D54-8; (2)Database Issue:D39-45; (3)14:2121-7; (4)266:141-162; 2011(Accessed); 2005(1-2); 2004(3);1996(4).

151. Galderisi U, Jori FP, Giordano A. Cell cycle regulation and neural differentiation. *Oncogene* 2003;22:5208-19.
152. Hunter S, Apweiler R, Attwood TK, Bairoch A, Bateman A, Binns D, Bork P, Das U, Daugherty L, Duquenne L, Finn RD GJ, Haft D, Hulo N, Kahn D, Kelly E, Laugraud A, Letunic I, Lonsdale D, Lopez R, Madera M, Maslen J, McAnulla C, McDowall J, Mistry J, Mitchell A, Mulder N, Natale D, Orengo C, Quinn AF, Selengut JD, Sigrist CJ, Thimma M, Thomas PD, Valentin F, Wilson D, Wu CH, Yeats C InterPro: the integrative protein signature database. *Nucleic Acids Res.* 2009 ed. Volume 37 (Database Issue)2009. p D224-228.
153. Ren B, Cam H, Takahashi Y, Volkert T, Terragni J, Young RA, Dynlacht BD. E2F integrates cell cycle progression with DNA repair, replication, and G2/M checkpoints. *Genes & Development* 2002;16(2):245-256.
154. Papst PJ, Sugiyama H, Nagasawa M, et al. Cdc2-cyclin B phosphorylates p70 S6 kinase on Ser411 at mitosis. *J Biol Chem* 1998;273:15077 - 15084.
155. Long JJ, Leresche A, Kriwacki RW, et al. Repression of TFIIH transcriptional activity and TFIIH-associated cdk7 kinase activity at mitosis. *Mol Cell Biol* 1998;18:1467 - 1476.
156. Kong M, Barnes EA, Ollendorff V, Donoghue DJ. Cyclin F regulates the nuclear localization of cyclin B1 through a cyclin-cyclin interaction. *EMBO J* 2000;19(6):1378-1388.
157. Maddika S, Ande SR, Panigrahi S, Paranjothy T, Weglarczyk K, Zuse A, Eshraghi M, Manda KD, Wiechec E, Los M. Cell survival, cell death and cell cycle pathways are interconnected: Implications for cancer therapy. *Drug Resistance Updates* 2007;10(1-2):13-29.
158. Todd DE, Densham RM, Molton SA, Balmanno K, Newson C, Weston CR, Garner AP, Scott L, Cook SJ. ERK1//2 and p38 cooperate to induce a p21CIP1-dependent G1 cell cycle arrest. *Oncogene* 2004;23(19):3284-3295.

159. Zhang J, Krishnamurthy PK, Johnson GVW. Cdk5 phosphorylates p53 and regulates its activity. *Journal of Neurochemistry* 2002;81(2):307-313.
160. Dzeja PP, Chung S, Faustino RS, Behfar A, Terzic A. Developmental Enhancement of Adenylate Kinase-AMPK Metabolic Signaling Axis Supports Stem Cell Cardiac Differentiation. *PLoS ONE* 2009;6(4):e19300.
161. Collavin L, Lazarevic, D, Utrera, R, Marzinotto, S, Monte, M, Schneider, C. wt p53 dependent expression of a membrane-associated isoform of adenylate kinase. *Oncogene* 1999;18: 5879-5888.
162. Siu Y-T, Jin D-Y. CREB – a real culprit in oncogenesis. *FEBS Journal* 2007;274(13):3224-3232.
163. Green MF, Anderson KA, Means AR. Characterization of the CaMKK[beta]-AMPK signaling complex. *Cellular Signalling* 2011;In Press (July 2011), Corrected Proof.
164. Suzuki A, Kusakai G-i, Kishimoto A, Shimojo Y, Ogura T, Lavin MF, Esumi H. IGF-1 phosphorylates AMPK-[alpha] subunit in ATM-dependent and LKB1-independent manner. *Biochemical and Biophysical Research Communications* 2004;324(3):986-992.
165. Kastan M, Lim, DS. The many substrates and functions of ATM. *Nat Rev Mol Cell Biol* 2000;1:179-186.
166. Shiloh Y. ATM and related protein kinases safeguarding genome integrity. *Nat Rev Cancer* 2003;3:155-168.
167. Kurose A, Tanaka T, Huang X, Halicka HD, Traganos F, Dai W, Darzynkiewicz Z. Assessment of ATM phosphorylation on Ser-1981 induced by DNA topoisomerase I and II inhibitors in relation to Ser-139-histone H2AX phosphorylation, cell cycle phase, and apoptosis. *Cytometry Part A* 2005;68A(1):1-9.
168. Jazayeri A, Falck J, Lukas C, Bartek J, Smith GCM, Lukas J, Jackson SP. ATM- and cell cycle-dependent regulation of ATR in response to DNA double-strand breaks. *Nat Cell Biol* 2006;8(1):37-45.

169. Inoue Y, Kitagawa M, Taya Y. Phosphorylation of pRB at Ser612 by Chk1/2 leads to a complex between pRB and E2F-1 after DNA damage. *EMBO J* 2007;26(8):2083-2093.
170. Kastan MB, Onyekwere O, Sidransky D, Vogelstein B, Craig RW. Participation of p53 protein in the cellular response to DNA damage. *Cancer Res Treat* 1991;51:6304-6311.
171. Shieh SYA, J.; Tamai, K.; Taya, Y.; Prives, C. The human homologs of checkpoint kinases Chk1 and Cds1 (Chk2) phosphorylate p53 at multiple DNA damage-inducible sites. *Genes Dev* 2000;14:289-300.
172. Meek SEL, W. S.; Piwnica-Worms, H. . Comprehensive proteomic analysis of interphase and mitotic 14-3-3-binding proteins. *J Biol Chem* 2004;279:32046-32054.
173. Kastan M, Bartek, J. Cell cycle checkpoints and cancer. *Nature* 2004;432:316-323.
174. Kurki S, Peltonen K, Latonen L, Kiviharju TM, Ojala PM, Meek D, Laiho M. Nucleolar protein NPM interacts with HDM2 and protects tumor suppressor protein p53 from HDM2-mediated degradation. *Cancer cell* 2004;5(5):465-475.
175. Xiao J, Zhang Z, Chen GG, Zhang M, Ding Y, Fu J, Li M, Yun J-P. Nucleophosmin/B23 interacts with p21WAF1/CIP1 and contributes to its stability. *Cell Cycle* 2009;8(6):889-895.
176. Maignel DA, Jones L, Chakravarty D, Yang C, Carrier F. Nucleophosmin Sets a Threshold for p53 Response to UV Radiation. *Mol. Cell. Biol.* 2004;24(9):3703-3711.
177. Janssens V, Goris J. Protein phosphatase 2A: a highly regulated family of serine/threonine phosphatases implicated in cell growth and signalling. *Biochem. J.* 2001;353(3):417-439.
178. Davis AJ, Yan Z, Martinez B, Mumby MC. Protein Phosphatase 2A Is Targeted to Cell Division Control Protein 6 by a Calcium-binding Regulatory Subunit. *Journal of Biological Chemistry* 2008;283(23):16104-16114.

179. McGowan C, Russell P. Cell cycle regulation of human WEE1. *EMBO J* 1995;14(10):2166-2175.
180. Lu X, Nannenga B, Donehower LA. PPM1D dephosphorylates Chk1 and p53 and abrogates cell cycle checkpoints. *Genes & Development* 2005;19(10):1162-1174.
181. Kubbutat MH, Jones SN, Vousden KH. Regulation of p53 stability by Mdm2. *Nature* 1997;387:299-303.
182. Wade M, Wang YV, Wahl GM. The p53 orchestra: Mdm2 and Mdmx set the tone. *Trends Cell Biol* 2010;20(5):299-309.
183. Ciliberto A, Novak B, Tyson JJ. Steady states and oscillations in the p53/Mdm2 network. *Cell Cycle* 2005;4:488-493.
184. Jin Y, Lee H, Zeng SX, Dai MS, Lu H. MDM2 promotes p21waf1/cip1 proteasomal turnover independently of ubiquitylation. *EMBO J* 2003;22:6365-6377.
185. Uchida C, Miwa S, Kitagawa K, Hattori T, Isobe T, Otani S, Oda T, Sugimura H, Kamijo T, Ookawa K, Yasuda H, Kitagawa M. Enhanced Mdm2 activity inhibits pRB function via ubiquitin-dependent degradation. *EMBO J* 2005;24:160-169.
186. Brady M, Vlatkovic N, Boyd MT. Regulation of p53 and MDM2 Activity by MTBP. *Mol. Cell. Biol.* 2005;25(2):545-553.
187. Boyd MT, Vlatkovic N, Haines DS. A Novel Cellular Protein (MTBP) Binds to MDM2 and Induces a G1 Arrest That Is Suppressed by MDM2. *Journal of Biological Chemistry* 2000;275(41):31883-31890.
188. Yang W, Dicker DT, Chen J, El-Deiry WS. CARPs enhance p53 turnover by degrading 14-3-3 σ ; and stabilizing MDM2. *Cell Cycle* 2008;7(5):670-682.
189. Kawamoto RM, Caswell AH. Autophosphorylation of glyceraldehydephosphate dehydrogenase and phosphorylation of protein from skeletal muscle microsomes. *Biochemistry* 1986;25:657- 661.

190. Morgenegg G, Winkler GC, Hubscher U, Heizmann CW, Mous J, Kuenzle CC. Glyceraldehyde-3-phosphate dehydrogenase is a nonhistone protein and a possible activator of transcription in neurons. *J Neurochem* 1986;47:54-62.
191. Huitorel P, Pantaloni D. Bundling of microtubules by glyceraldehyde-3-phosphate dehydrogenase and its modulation by ATP. *Eur J Biochem* 1985;150:265-269.
192. Sioud M, Jespersen L. Enhancement of hammerhead ribozyme catalysis by glyceraldehyde-3-phosphate dehydrogenase. *J Mol Biol* 1996;257:775-789.
193. Baxi M, Vishwanatha, JK. Uracil DNA glycosylase/glyceraldehyde-3-phosphate dehydrogenase is an Ap4A binding protein. *Biochemistry* 1995;34:9700-9707.
194. Chen R-W, Saunders PA, Wei H, Li Z, Seth P, Chuang D-M. Involvement of Glyceraldehyde-3-Phosphate Dehydrogenase (GAPDH) and p53 in Neuronal Apoptosis: Evidence That GAPDH Is Upregulated by p53. *The Journal of Neuroscience* 1999;19(21):9654-9662.
195. Williamson EA, Dadmanesh F, Koeffler HP. BRCA1 transactivates the cyclin-dependent kinase inhibitor p27Kip1. *Oncogene* 2002;21:3199 -3206.
196. Jin S, Zhao H, Fan F, Blanck P, Fan W, Colchagie AB, Fornace Jr AJ, Zhan Q. *Oncogene* 2000 19:4050-4057.
197. Somasundaram K, Zhang H, Zeng Y-X, Houvras Y, Peng Y, Zhang H, Wu GS, Licht JD, Weber BL, El-Deiry WS. *Nature* 1997;389:187-190.
198. Gudmundsdottir K, Ashworth A. The roles of BRCA1 and BRCA2 and associated proteins in the maintenance of genomic stability. *Oncogene* 2006;25(43):5864-5874.
199. Boletta A. Emerging evidence of a link between the polycystins and the mTOR pathways. *PathoGenetics* 2009;2(6).
200. Bhunia AK, Piontek K, Boletta A, Liu L, Qian F, Xu P-N, Germino FJ, Germino GG. PKD1 Induces p21waf1 and Regulation of the Cell Cycle via Direct Activation of the JAK-STAT Signaling Pathway in a Process Requiring PKD2. *Cell* 2002;109(2):157-168.

201. Graziani I, Elias S, De Marco MA, Chen Y, Pass HI, De May RM, Strack PR, Miele L, Bocchetta M. Opposite Effects of Notch-1 and Notch-2 on Mesothelioma Cell Survival under Hypoxia Are Exerted through the Akt Pathway. *Cancer Research* 2008;68(23):9678-9685.
202. Bruni P, Minopoli G, Brancaccio T, Napolitano M, Faraonio R, Zambrano N, Hansen U, Russo T. Fe65, a Ligand of the Alzheimer's beta-Amyloid Precursor Protein, Blocks Cell Cycle Progression by Down-regulating Thymidylate Synthase Expression. *Journal of Biological Chemistry* 2002;277(38):35481-35488.
203. Kawai T, Nakaya T, Suzuki T. Roles of the intramolecular regions of FE65 in its trans-accumulation and in p53 stabilization in the nuclear matrix of osmotically stressed cells. *FEBS Letters* 2010;584:765-769.
204. Martinez SC, Cras-Meneur C, Bernal-Mizrachi E, Permutt MA. Glucose Regulates Foxo1 Through Insulin Receptor Signaling in the Pancreatic Islet beta-cell. *Diabetes* 2006;55(6):1581-1591.
205. Pomerance M, Carapau D, Chantoux F, Mockey M, Correze C, Francon J, Blondeau J-P. CCAAT/Enhancer-Binding Protein-Homologous Protein Expression and Transcriptional Activity Are Regulated by 3',5'-Cyclic Adenosine Monophosphate in Thyroid Cells. *Molecular Endocrinology* 2003;17(11):2283-2294.
206. Slomnicki L, and Lesniak W. A putative role of the Amyloid Precursor Protein Intracellular Domain (AICD) in transcription. *Acta Neurobiol Exp* 2008;68: 219-228.
207. Copanaki E, Schürmann T, Eckert A, Leuner K, Müller WE, Prehn JHM, Kögel D. The amyloid precursor protein potentiates CHOP induction and cell death in response to ER Ca²⁺ depletion. *Biochimica et Biophysica Acta (BBA) - Molecular Cell Research* 2007;1773(2):157-165.
208. Liu Y, Wang Y, Rusinol AE, Sinensky MS, Liu J, Shell SM, Zou Y. Involvement of xeroderma pigmentosum group A (XPA) in progeria arising from defective maturation of prelamin A. *The FASEB Journal* 2008;22(2):603-611.
209. Leung C, Sun, D, Zheng, M, Knowles, DR, Liem, RK. Microtubule actin cross-linking factor (MACF): a hybrid of dystonin and dystrophin that can interact with the actin and microtubule cytoskeletons. *J Cell Biol* 1999;147(6):1275-86.

210. Iwano T, Tachibana M, Reth M, Shinkai Y. Importance of TRF1 for Functional Telomere Structure. *Journal of Biological Chemistry* 2004;279(2):1442-1448.
211. Okamoto K, Iwano T, Tachibana M, Shinkai Y. Distinct Roles of TRF1 in the Regulation of Telomere Structure and Lengthening. *Journal of Biological Chemistry* 2008;283(35):23981-23988.
212. Diotti R, Loayza, D. Shelterin complex and associated factors at human telomeres. *Nucleus* 2011;2(2):119-135.
213. Tsai RYL. Nucleolar modulation of TRF1: A dynamic way to regulate telomere and cell cycle by nucleostemin and GNL3L. *Cell Cycle* 2009;8(18):2913-2917.
214. Xiong L, Department of Math/CS, Emory University, Zhou W, Winship Cancer Institute, School of Medicine, Emory University. Accessed 2011 PANDA Phosphor Antibody Array Data Analysis Web-Based Software, <http://www.mathcs.emory.edu/panda/>.
215. Ishida N, Kitagawa M, Hatakeyama S, Nakayama K-i. Phosphorylation at Serine 10, a Major Phosphorylation Site of p27 Kip1 , Increases Its Protein Stability. *Journal of Biological Chemistry* 2000;275(33):25146-25154.
216. Malmlöf M, Roudier E, Högberg J, Stenius U. MEK-ERK-mediated phosphorylation of Mdm2 at Ser-166 in hepatocytes. Mdm2 is activated in response to inhibited Akt signaling. *J Biol Chem* 2007;282(4):2288-96.
217. Lavin MF, Gueven N. The complexity of p53 stabilization and activation. *Cell Death Differ* 2006;13(6):941-950.
218. Fabbro M, Savage K, Hobson K, Deans AJ, Powell SN, McArthur GA, Khanna KK. BRCA1-BARD1 Complexes Are Required for p53Ser-15 Phosphorylation and a G1/S Arrest following Ionizing Radiation-induced DNA Damage. *Journal of Biological Chemistry* 2004;279(30):31251-31258.
219. Kitagawa R, Bakkenist CJ, McKinnon PJ, Kastan MB. Phosphorylation of SMC1 is a critical downstream event in the ATMâ€NBS1â€BRCA1 pathway. *Genes & Development* 2004;18(12):1423-1438.

220. Liu R, Zhou XW, Tanila H, Bjorkdahl C, Wang JZ, Guan ZZ, Cao Y, Gustafsson JA, Winblad B, Pei JJ. Phosphorylated PP2A (tyrosine 307) is associated with Alzheimer neurofibrillary pathology. *J Cell Mol Med* 2008;12(1):241-257.
221. Peng C, Graves P, Ogg S, Thoma R, Byrnes M, 3rd, Wu Z, Stephenson M, Piwnica-Worms H. C-TAK1 protein kinase phosphorylates human Cdc25C on serine 216 and promotes 14-3-3 protein binding. *Cell Growth Differ* 1998;9(3):197-208.
222. Bonnet J, Mayonove P, Morris MC. Differential phosphorylation of Cdc25C phosphatase in mitosis. *Biochemical and Biophysical Research Communications* 2008;370(3):483-488.
223. Doble BW, Woodgett JR. GSK-3: tricks of the trade for a multi-tasking kinase. *Journal of Cell Science* 2003;116(7):1175-1186.
224. Harwood A, Braga VMM. Cdc42 & GSK-3: signals at the crossroads. *Nat Cell Biol* 2003;5(4):275-277.
225. De Larco JE, Todaro, G. J. Growth factors from murine sarcoma virus transformed cells. *Proc. Natl. Acad. Sci. USA* 1978;75:4001-4005.
226. Dennler S, Goumans M-J, ten Dijke P. Transforming growth factor beta signal transduction. *Journal of Leukocyte Biology* 2002;71(5):731-740.
227. Bannister AJ, Kouzarides T. The CBP co-activator is a histone acetyltransferase. *Nature* 1996;384:641-643.
228. Goodman RH, and Smolik, S. CBP/p300 in cell growth, transformation, and development. *Genes Dev* 2000;14:1553-1577.
229. Luo RX, Dean, DC. Chromatin remodeling and transcriptional regulation. *J Natl Cancer Inst* 1999;91:1288-1294.
230. Magnaghi-Jaulin L, Ait-Si-Ali S, Harel-Bellan A. Histone acetylation in signal transduction by growth regulatory signals. *Semin Cell Dev Biol* 1999;10:197-203.

231. Grant P, Berger, SL. Histone acetyltransferase complexes. *Semin Cell Dev Biol* 1999;10:169-177.
232. Gray SG, Ekstrom, TJ. The human histone deacetylase family. *Exp Cell Res* 2001;262:75-83.
233. Poleskaya A, Naguibneva I, Fritsch L, Duquet A, Ait-Si-Ali S, Robin P, Vervisch A, Pritchard LL, Cole P, Harel-Bellan, A. CBP/p300 and muscle differentiation: no HAT, no muscle. *EMBO J* 2001;20:6816-6825.
234. Roth SY, Denu, JM, Allis, CD. Histone acetyltransferases. *Annu Rev Biochem* 2001;70:81-120.
235. Yao T-P, Oh SP, Fuchs M, Zhou N-D, Ch'ng L-E, Newsome D, Bronson RT, Li E, Livingston D M, Eckner, R. Gene dosage-dependent embryonic development and proliferation defects in mice lacking the transcriptional integrator p300. *Cell* 1998;93:361-372.
236. Nicholson KM, Anderson NG. The protein kinase B/Akt signalling pathway in human malignancy. *Cellular Signalling* 2002;14(5):381-395.
237. Brunet A, Bonni A, Zigmond MJ, Lin MZ, Juo P, Hu LS, Anderson MJ, Arden KC, Blenis J, Greenberg ME. Akt promotes cell survival by phosphorylating and inhibiting a Forkhead transcription factor. *Cell* 1999;96:857-868.
238. Brunet A, et al. 14-3-3 transits to the nucleus and participates in dynamic nucleocytoplasmic transport. *J Cell Biol* 2002;156:817-828.
239. Biggs WH, Meisenhelder J, Hunter T, Cavenee WK, Arden KC. Protein kinase B/Akt-mediated phosphorylation promotes nuclear exclusion of the winged helix transcription factor FKHR1. *Proceedings of the National Academy of Sciences* 1999;96(13):7421-7426.
240. Heald R, McKeon F. Mutations of phosphorylation sites in lamin A that prevent nuclear lamina disassembly in mitosis. *Cell* 1990;61:579-589.
241. Peter M, Nakagawa J, Doree M, Labbe JC, Nigg EA. In vitro disassembly of the nuclear lamina and M phase-specific phosphorylation of lamins by cdc2 kinase. *Cell* 1990;61:591-602.

242. Olsen JV, Vermeulen M, Santamaria A, Kumar C, Miller ML, Jensen LJ, Gnad F, Cox J, Jensen TS, Nigg EA and others. Quantitative Phosphoproteomics Reveals Widespread Full Phosphorylation Site Occupancy During Mitosis. *Sci. Signal.* 2010;3(104):ra3-.
243. HPRD PhosphoMotif Finder, Reference 1: Amanchy R, Periaswamy B, Mathivanan S, Reddy R, Tattikota SG, and Pandey, AA; Reference 2: Prasad TSK, Goel R, Kandasamy K, Keerthikumar S, Kumar S, Mathivanan S, Telikicherla, D, Raju R, Shafreen B, Venugopal A, et al. Ref 1: A compendium of curated phosphorylation-based substrate and binding motifs; Ref 2: Human Protein Reference Database - 2009 update. Ref 1: *Nature Biotechnology*; Ref 2: *Nucleic Acids Research*. Volume Ref 1: 25; Ref 2: 37Ref 1: 2007; Ref 2: 2009; Accessed July 2011. p Ref 1: 285-286; Ref 2: D767-D772.
244. Gould CM, Diella, F, Via, A, Puntervoll, P, Gemünd, C, Chabanis-Davidson, S, Michael, S, Sayadi, A, Bryne, J C, Chica, C, et al. ELM: the status of the 2010 eukaryotic linear motif resource *Nucleic Acids Res* 2010;38:D167-80.
245. Edman P, Högfeldt E, Sillén LG, Kinell P-O. Method for determination of the amino acid sequence in peptides. *Acta Chem Scand* 1950;4:283-293.
246. Lee C-P, Huang Y-H, Lin S-F, Chang Y, Chang Y-H, Takada K, Chen M-R. Epstein-Barr Virus BGLF4 Kinase Induces Disassembly of the Nuclear Lamina To Facilitate Virion Production. *J. Virol.* 2008;82(23):11913-11926.
247. Hamirally S, Kamil JP, Ndassa-Colday YM, Lin AJ, Jahng WJ, Baek M-C, Noton S, Silva LA, Simpson-Holley M, Knipe DM and others. Viral Mimicry of Cdc2/Cyclin-Dependent Kinase 1 Mediates Disruption of Nuclear Lamina during Human Cytomegalovirus Nuclear Egress. *PLoS Pathog* 2009;5(1):e1000275.
248. Lou Z, Minter-Dykhouse K, Wu X, Chen J. MDC1 is coupled to activated CHK2 in mammalian DNA damage response pathways. *Nature* 2003;421:957-961.
249. Stewart GS, Wang B, Bignell CR, Tylor AMR, Elledge SJ. MDC1 is a mediator of the mammalian DNA damage checkpoint. *Nature* 2003;421:961-966.
250. Lou Z, Chen BPC, Asaithamby A, Minter-Dykhouse K, Chen DJ, Chen J,. MDC1 regulates DNA-PK autophosphorylation in response to DNA damage. *J Biol Chem* 2004;279:46359-46362.

251. Mochan TA, Venere M, DiTullio Jr. RA, Halazonetis TD 53BP1 and NFBD1/MDC1-Nbs1 function in parallel interacting pathways activating ataxia-telangiectasia mutated (ATM) in response to DNA damage. *Cancer Res* 2003;63:8586-8591.
252. Kim JE, Minter-Dykhouse K, Chen J. Signaling networks controlled by the MRN complex and MDC1 during early DNA damage responses. *Mol Carcinog* 2006;45:403-408.
253. Jack MT, Woo RA, Hirao A, Cheung A, Mak TW, Lee PWK. Chk2 is dispensable for p53-mediated G1 arrest but required for a latent p53-mediated apoptotic response. *Proc. Natl. Acad. Sci. USA* 2002;23:9825-9829.
254. Ismail IA, Kang K-S, Lee HA, Kim J-W, Sohn Y-K. Genistein-induced neuronal apoptosis and G2/M cell cycle arrest is associated with MDC1 up-regulation and PLK1 down-regulation. *European Journal of Pharmacology* 2007;575(1-3):12-20.
255. Rai R, Phadnis A, Haralkar S, Badwe RA, Dai H, Li K, Lin S-Y. Differential regulation of centrosome integrity by DNA damage response proteins. *Cell Cycle* 2008;7(14):2225-2233.
256. Bekker-Jensen S, Lukas C, Melander F, Bartek J, Lukas J Dynamic assembly and sustained retention of 53BP1 at the sites of DNA damage are controlled by Mdc1/NFBD1. *The Journal of Cell Biology* 2005;170(2):201-211.
257. Shibata A, Barton O, Noon AT, Dahm K, Deckbar D, Goodarzi AA, Loeblich M, Jeggo PA. Role of ATM and the Damage Response Mediator Proteins 53BP1 and MDC1 in the Maintenance of G2/M Checkpoint Arrest. *Mol Cell Biol* 2010;30(13):3371-3383.
258. The UniProt Consortium. Ongoing and future developments at the Universal Protein Resource, www.uniprot.org. *Nucleic Acids Res.* Volume 39 2011 (Accessed July 2011). p D214-D219.
259. Jain E, Bairoch A, Duvaud S, Phan I, Redaschi N, Suzek BE, Martin MJ, McGarvey P, Gasteiger E. Infrastructure for the life sciences: design and implementation of the UniProt website. *BMC Bioinformatics* 2009;10(136).
260. Sudol M, Sliwa K, Russo T. Functions of WW domains in the nucleus. *FEBS Letters* 2001;490(3):190-195.

261. Liao Y, Wei Y, Zhou X, Yang J-Y, Dai C, Chen Y-J, Agarwal N, Sarbassov D, Shi D, Yu D and others. Peptidyl-prolyl *cis/trans* isomerase Pin1 is critical for the regulation of PKB/Akt stability and activation phosphorylation. *Oncogene* 2009;28(26):2436-2445
262. Liao Y, Hung M-C. Physiological regulation of Akt activity and stability. *Am J Transl Res* 2010;2(1):19-42.
263. Zhou W, Q. Yang, et al. Pin1 Catalyzes Conformational Changes of Thr-187 in p27Kip1 and Mediates Its Stability through a Polyubiquitination Process. *Journal of Biological Chemistry* 2009;284(36):23980-23988.
264. Brenkman AB, de Keizer PLJ, van den Broek NJF, van der Groep P, van Diest PJ, van der Horst A, Smits AMM, Burgering BMT. The Peptidyl-Isomerase Pin1 Regulates p27kip1 Expression through Inhibition of Forkhead Box O Tumor Suppressors. *Cancer Research* 2008;68(18):7597-7605.
265. Brenkman AB, van den Broek NJF, de Keizer PLJ, van Gent DC, Burgering BMT. The DNA damage repair protein Ku70 interacts with FOXO4 to coordinate a conserved cellular stress response. *FASEB J.* 2010:fj.10-158717.
266. Wulf GM, Liou Y-C, Ryo A, Lee SW, Lu KP. Role of Pin1 in the Regulation of p53 Stability and p21Transactivation, and Cell Cycle Checkpoints in Response to DNA Damage. *The Journal Of Biological Chemistry* 2002;277(50):47976-47979.
267. Zacchi P, Gostissa M, Uchida T, Salvagno C, Avolio F, Voliniak S, Ronai Z, Blandino G, Schneider C, Del Sal G. The prolyl isomerase Pin1 reveals a mechanism to control p53 functions after genotoxic insults. *Nature* 2002;419(24).
268. Eckerdt F, Yuan J, Saxena K, Martin B, Kappel S, Lindenau C, Kramer A, Naumann S, Daum S, Fischer G and others. Polo-like Kinase 1-mediated Phosphorylation Stabilizes Pin1 by Inhibiting Its Ubiquitination in Human Cells. *Journal of Biological Chemistry* 2005;280(44):36575-36583.
269. Crenshaw D, Yang J, Means AR, Kornbluth S. The mitotic peptidyl-prolyl isomerase, Pin1, interacts with Cdc25 and Plx1. *EMBO J* 1998;17(5):1315-1327.
270. Zhou XZ, Kops O, Werner A, Lu P-J, Shen M, Stoller G, Ilertz GK, Stark M, Fischer G, Lu KP. Pin1-Dependent Prolyl Isomerization Regulates Dephosphorylation of Cdc25C and Tau Proteins *Molecular Cell* 2000;6:873-883.

271. Xu Y-X, Hirose Y, Zhou XZ, Lu KP, Manley JL. Pin1 modulates the structure and function of human RNA polymerase II. *Genes & Development* 2003;17(22):2765-2776.
272. Nakano A, Koinuma D, Miyazawa K, Uchida T, Saitoh M, Kawabata M, Hanai J-i, Akiyama H, Abe M, Miyazono K and others. Pin1 Down-regulates Transforming Growth Factor- β^2 (TGF- β^2) Signaling by Inducing Degradation of Smad Proteins. *Journal of Biological Chemistry* 2009;284::6109-6115.
273. Lu KP, Zhou XZ. The prolyl isomerase PIN1: a pivotal new twist in phosphorylation signalling and disease. *Nat Rev Mol Cell Biol* 2007;8.
274. Kato Y, Ito M, Kawai K, Nagata K, Tanokura M. Determinants of Ligand Specificity in Groups I and IV WW Domains as Studied by Surface Plasmon Resonance and Model Building. *J Biol Chem* 2002;277(12):10173-10177.
275. Milbradt J, Webel R, Auerochs S, Sticht H, Marschall M. Novel Mode of Phosphorylation-triggered Reorganization of the Nuclear Lamina during Nuclear Egress of Human Cytomegalovirus. *Journal of Biological Chemistry* 2010;285(18):13979-13989.
276. Shen M, Stukenberg PT, Kirschner MW, Lu KP. The essential mitotic peptidyl-prolyl isomerase Pin1 binds and regulates mitosis-specific phosphoproteins *Genes & Development* 1998;12:706-720.
277. Lu KP, Hanes, SD, Hunter, TA. A human peptidylprolyl isomerase essential for regulation of mitosis. *Nature* 1996;380:544-547.
278. Lu P-J, Zhou XZ, Liou Y-C, Noel JP, Lu KP. Critical Role of WW Domain Phosphorylation in Regulating Phosphoserine Binding Activity and Pin1 Function. *Journal of Biological Chemistry* 2002;277(4):2381-2384.
279. Sewing A, Burger C, Brusselbach S, Schalk C, Lucibello FC, Muller R. Human cyclin D1 encodes a labile nuclear protein whose synthesis is directly induced by growth factors and suppressed by cyclic AMP. *Journal of Cell Science* 1993;104(2):545-555.
280. Kato J-y, Matsuoka M, Polyak K, Massague J, Sherr CJ. Cyclic AMP-induced G1 phase arrest mediated by an inhibitor (p27Kip1) of cyclin-dependent kinase 4 activation. *Cell* 1994;79(3):487-496.

281. Vadiveloo PK, Filonzi EL, Stanton HR, Hamilton JA. G1 phase arrest of human smooth muscle cells by heparin, IL-4 and cAMP is linked to repression of cyclin D1 and cdk2. *Atherosclerosis* 1997;133(1):61-69.
282. Williamson EA, Burgess GS, Eder P, Litz-Jackson S, Boswell HS. Cyclic AMP negatively controls c-myc transcription and G1 cell cycle progression in p210 BCR-ABL transformed cells: inhibitory activity exerted through cyclin D1 and cdk4. *Leukemia* 1997;11(1):73-85.
283. Sherr CJ, Roberts JM. CDK inhibitors: positive and negative regulators of G1-phase progression. *Genes & Development* 1999;13(12):1501-1512.
284. Diehl JA, Cheng M, Roussel MF, Sherr CJ. Glycogen synthase kinase-3 β regulates cyclin D1 proteolysis and subcellular localization. *Genes & Development* 1998;12(22):3499-3511.
285. Muise-Helmericks RC, Grimes HL, Bellacosa A, Malstrom SE, Tsichlis PN, Rosen N. Cyclin D Expression Is Controlled Post-transcriptionally via a Phosphatidylinositol 3-Kinase/Akt-dependent Pathway. *Journal of Biological Chemistry* 1998;273(45):29864-29872.
286. Takuwa N, Fukui Y, Takuwa Y. Cyclin D1 Expression Mediated by Phosphatidylinositol 3-Kinase through mTOR-p70S6K-Independent Signaling in Growth Factor-Stimulated NIH 3T3 Fibroblasts. *Mol. Cell. Biol.* 1999;19(2):1346-1358.
287. Ramaswamy S, Nakamura N, Sansal I, Bergeron L, Sellers WR. A novel mechanism of gene regulation and tumor suppression by the transcription factor FKHR. *Cancer cell* 2002;2(1):81-91.
288. Schmidt M, Fernandez de Mattos S, van der Horst A, Klomp maker R, Kops GJPL, Lam EW-F, Burgering BMT, Medema RH. Cell Cycle Inhibition by FoxO Forkhead Transcription Factors Involves Downregulation of Cyclin D. *Mol. Cell. Biol.* 2002;22(22):7842-7852.
289. John GB, Gallardo TD, Shirley LJ, Castrillon DH. Foxo3 is a PI3K-dependent molecular switch controlling the initiation of oocyte growth. *Developmental Biology* 2008;321(1):197-204.

290. Obsil T, Obsilova V. Structure/function relationships underlying regulation of FOXO transcription factors. *Oncogene* 2008;27(16):2263-2275.
291. Accili D, Arden, K.C. FoxOs at the crossroads of cellular metabolism, differentiation, and transformation. *Cell* 2004;117:421-426.
292. van der Horst A, Burgering, B.M. Stressing the role of FoxO proteins in lifespan and disease. *Nat Rev Mol Cell Biol* 2007;8:440-450.
293. Calnan DR, Brunet, A. The FoxO code. *Oncogene* 2008;27:2276-2288.
294. van der Vos KE, Coffey, PJ. FOXO-binding partners: it takes two to tango. 2008 *Oncogene* 2008;27:2289-2299.
295. Hedrick S. The cunning little vixen: Foxo and the cycle of life and death. *Nat Immunol* 2009;10:1057-1063.
296. Nowak K, Killmer K, Gessner C, Lutz W. E2F-1 regulates expression of FOXO1 and FOXO3a. *Biochimica et Biophysica Acta (BBA) - Gene Structure and Expression* 2007;1769(4):244-252.
297. Essaghir A, Dif N, Marbehant CY, Coffey PJ, Demoulin J-B. The Transcription of FOXO Genes Is Stimulated by FOXO3 and Repressed by Growth Factors. *Journal of Biological Chemistry* 2009;284(16):10334-10342.
298. Huang H, Tindall DJ. Dynamic FoxO transcription factors. *Journal of Cell Science* 2007;120(15):2479-2487.
299. Burgering BMT, Coffey PJ. Protein kinase B (c-Akt) in phosphatidylinositol-3-OH kinase signal transduction. *Nature* 1995;376(6541):599-602.
300. Franke TF, Yang S-I, Chan TO, Datta K, Kazlauskas A, Morrison DK, Kaplan DR, Tsichlis PN. The protein kinase encoded by the Akt proto-oncogene is a target of the PDGF-activated phosphatidylinositol 3-kinase. *Cell* 1995;81(5):727-736.
301. Burgering BMT, Kops GJPL. Cell cycle and death control: long live Forkheads. *Trends in Biochemical Sciences* 2002;27(7):352-360.

302. Rena G, et al. Two novel phosphorylation sites on FKHR that are critical for its nuclear exclusion. *EMBO J* 2002;21:2263-2271.
303. Hu M, et al. I κ B kinase promotes tumorigenesis through inhibition of forkhead FOXO3a. *Cell* 2004;117:225-237.
304. Yang J, et al. ERK promotes tumorigenesis by inhibiting FOXO3a via MDM2-mediated degradation. *Nat Cell Biol* 2008;10:138-148.
305. Asada S, Daitoku H, Matsuzaki H, Saito T, Sudo T, Mukai H, Iwashita S, Kako K, Kishi T, Kasuya Y and others. Mitogen-activated protein kinases, Erk and p38, phosphorylate and regulate Foxo1. *Cellular Signalling* 2007;19(3):519-527.
306. Rena G, Prescott, AR, Guo, S, Cohen, P, Unterman, TG. Roles of the forkhead in rhabdomyosarcoma (FKHR) phosphorylation sites in regulating 14-3-3 binding, transactivation and nuclear targeting. *Biochem J* 2001;354:605-612.
307. Brownawell AM, Kops, GJ, Macara, IG, Burgering, BM. Inhibition of nuclear import by protein kinase B (Akt) regulates the subcellular distribution and activity of the forkhead transcription factor AFX. *Mol Cell Biol* 2001;21:3534-3546.
308. Essers MA, Weijzen, S, Vries-Smits, AM, Saarloos I, de Ruiter, ND, Bos, JL, Burgering, BM. FOXO transcription factor activation by oxidative stress mediated by the small GTPase Ral and JNK. *EMBO J* 2004;23:4802-4812.
309. Yuan Z, Becker EBE, Merlo P, Yamada T, DiBacco S, Konishi Y, Schaefer EM, Bonni A. Activation of FOXO1 by Cdk1 in Cycling Cells and Postmitotic Neurons. *Science* 2008;319(5870):1665-1668.
310. Kops GJ, Dansen, TB, Polderman, PE, Saarloos, I, Wirtz, KW, Coffey, PJ, Huang, TT, Bos, JL, Medema, RH, Burgering, BM. Forkhead transcription factor FOXO3a protects quiescent cells from oxidative stress. *Nature* 2002;419.
311. van der Heide LP, Smidt MP. Regulation of FoxO activity by CBP/p300-mediated acetylation. *Trends in Biochemical Sciences* 2005;30(2):81-86.
312. Hatta M, Liu F, Cirillo LA. Acetylation curtails nucleosome binding, not stable nucleosome remodeling, by FoxO1. *Biochemical and Biophysical Research Communications* 2009;379(4):1005-1008.

313. Matsuzaki H, Daitoku H, Hatta M, Aoyama H, Yoshimochi K, Fukamizu A. Acetylation of Foxo1 alters its DNA-binding ability and sensitivity to phosphorylation. *Proceedings of the National Academy of Sciences of the United States of America* 2005;102(32):11278-11283.
314. van der Horst A, Vries-Smiths AM, Brenkman AB, et al. FOXO4 transcriptional activity is regulated by monoubiquitination and USP7/HAUSP. *Nat Cell Biol* 2006;8:1064-73.
315. Di Fiore P, Polo S, Hofmann K. When ubiquitin meets ubiquitin receptors: a signalling connection. *Nat Rev Mol Cell Biol* 2003;4:491-7.
316. Salmena L, Pandolfi P. Changing venues for tumour suppression: balancing destruction and localization by monoubiquitylation. *Nat Rev Cancer* 2007;7:409-13.
317. Dimri GP, Lee X, Basile G, Acosta M, Scott G, Roskelley C, Medrano EE, Linskens M, Rubelj I, Pereira-Smith O. A biomarker that identifies senescent human cells in culture and in aging skin in vivo. *Proceedings of the National Academy of Sciences* 1995;92(20):9363-9367.
318. Ranganathan R, Lu KP, Hunter T, Noel JP. Structural and functional analysis of the mitotic rotamase Pin1 suggests substrate recognition is phosphorylation dependent. *Cell* 1997;89:875-886.
319. Verdecia MA, Bowman ME, Lu KP, Hunter T, Noel JP. Structural basis for phosphoserine-proline recognition by group IV WW domains. *Nat Struct Biol* 2007;7:639-643.
320. Zhou XZ, Lu PJ, Wulf G, Lu KP. Phosphorylation-dependent prolyl isomerization: a novel signaling regulatory mechanism. *Cell Mol Life Sci* 1999;56:788-806.
321. Fischer G, Tradler T, Zarnt T. The mode of action of peptidyl prolyl cis/trans isomerases in vivo: binding vs. catalysis. *FEBS Letters* 1998;426:17-20.
322. Jacobs DM, Saxena K, Vogtherr M, Bernad³ P, Pons M, Fiebig KM. Peptide Binding Induces Large Scale Changes in Inter-domain Mobility in Human Pin1. *Journal of Biological Chemistry* 2003;278(28):26174-26182.

323. Myers JK, Morris DP, Greenleaf AL, Oas TG. Phosphorylation of RNA polymerase II CTD fragments results in tight binding to the WW domain from the yeast prolyl isomerase Ess1. *Biochemistry* 2001;40:8479-8486.
324. Yi P, Wu R-C, Sandquist J, Wong J, Tsai SY, Tsai M-J, Means AR, O'Malley BW. Peptidyl-Prolyl Isomerase 1 (Pin1) Serves as a Coactivator of Steroid Receptor by Regulating the Activity of Phosphorylated Steroid Receptor Coactivator 3 (SRC-3/AIB1). *Mol. Cell. Biol.* 2005;25(21):9687-9699.
325. Malhas AN, Vaux DJ. Transcription factor sequestration by nuclear envelope components. *Cell Cycle* 2009;8(7):959-964.
326. Capanni C, Mattioli E, Columbaro M, Lucarelli E, Parnaik VK, Novelli G, Wehnert M, Cenni V, Maraldi NM, Squarzoni S and others. Altered pre-lamin A processing is a common mechanism leading to lipodystrophy. *Human Molecular Genetics* 2005;14(11):1489-1502.
327. Lee K-H, Park J-W, Chun Y-S. Non-hypoxic transcriptional activation of the aryl hydrocarbon receptor nuclear translocator in concert with a novel hypoxia-inducible factor-1alpha isoform. *Nucleic Acids Research* 2004;32(18):5499-5511.
328. Nebert D, Dalton T, Okey A, Gonzalez F. Role of aryl hydrocarbon receptor-mediated induction of the CYP1 enzymes in environmental toxicity and cancer *J Biol Chem* 2004;279:23847-23850.
329. Mulero-Navarro S, Carvajal-Gonzalez J, Herranz M, Ballestar E, Fraga M, Ropero S, Esteller M, Fernandez-Salguero P. The dioxin receptor is silenced by promoter hypermethylation in human acute lymphoblastic leukemia through inhibition of Sp1 binding. *Carcinogenesis* 2006;27:1099-1104.
330. Fujii-Kuriyama Y, Mimura J. Molecular mechanisms of AhR functions in the regulation of cytochrome P450 genes. *Biochem Biophys Res Commun* 2005;338(1):311-7.
331. Oshima M, Mimura J, Sekine H, Okawa H, Fujii-Kuriyama Y. SUMO Modification Regulates the Transcriptional Repressor Function of Aryl Hydrocarbon Receptor Repressor. *J Biol Chem* 2009;284(17):11017-11026.
332. Tojo M, Matsuzaki K, Minami T, Honda Y, Yasuda H, Chiba T, Saya H, Fujii-Kuriyama Y, Nakao M. The aryl hydrocarbon receptor nuclear transporter is

- modulated by the SUMO-1 conjugation system. *J Biol Chem* 2002;277(48):46576-85.
333. Bernshausen T, Jux B, Esser C, Abel J, Fritsche E. Tissue distribution and function of the Aryl hydrocarbon receptor repressor (AhRR) in C57BL/6 and Aryl hydrocarbon receptor deficient mice. *Arch Toxicol* 2005;Oct 1-6.
 334. Klinge C, Jernigan S, Risinger K, Lee J, Tyulmenkov V, Falkner K, Prough R. Short heterodimer partner (SHP) orphan nuclear receptor inhibits the transcriptional activity of aryl hydrocarbon receptor (AHR)/AHR nuclear translocator (ARNT). *Arch Biochem Biophys* 2001;390(1):64-70.
 335. Yang X, Liu D, Murray T, Mitchell G, Hesterman E, Karchner S, Merson R, Hahn M, Sherr D. The aryl hydrocarbon receptor constitutively represses c-myc transcription in human mammary tumor cells. *Oncogene* 2005;24(53):7869-81.
 336. Safe S, Wormke M, Samudio I. Mechanisms of inhibitory aryl hydrocarbon receptor-estrogen receptor crosstalk in human breast cancer cells. *J Mammary Gland Biol Neoplasia* 2000;5(3):295-306.
 337. Ruby C, Leid M, Kerkvliet N. 2,3,7,8-Tetrachlorodibenzo-p-dioxin suppresses tumor necrosis factor-alpha and anti-CD40-induced activation of NF-kappaB/Rel in dendritic cells: p50 homodimer activation is not affected. *Mol Pharmacol* 2002;62(3):722-8.
 338. Mimura J. Biological role of AhR signaling pathway. *Seikagaku* 2004;76(4):359-63.
 339. Puga A, Ma C, Marlowe JL. The aryl hydrocarbon receptor cross-talks with multiple signal transduction pathways. *Biochem Pharmacol* 2009;77(4):713-722.
 340. Puga A, Xia Y, C CE. Role of the aryl hydrocarbon receptor in cell cycle regulation. *Chem Biol Interact* 2002;141:117-130.
 341. Marlowe JL, Knudsen ES, Schwemberger S, Puga A. The Aryl Hydrocarbon Receptor Displaces p300 from E2F-dependent Promoters and Represses S Phase-specific Gene Expression. *THE JOURNAL OF BIOLOGICAL CHEMISTRY* 2004;279(28):29013-29022.

342. Tohkin M, Fukuhara M, Elizondo G, Tomita S, Gonzalez FJ. Aryl Hydrocarbon Receptor Is Required for p300-Mediated Induction of DNA Synthesis by Adenovirus E1A. *Molecular Pharmacology* 2000;58(4):845-851.
343. Watabe Y, Nazuka N, Tezuka M, Shimba S. Aryl Hydrocarbon Receptor Functions as a Potent Coactivator of E2F1-Dependent Transcription Activity. *Biological & Pharmaceutical Bulletin* 2010;33(3):389-397.
344. Strobeck M, AF AF, Puga A, Knudsen E. Restoration of retinoblastoma mediated signaling to Cdk2 results in cell cycle arrest. *Oncogene* 2000;19:1857-1867.
345. Huang W-C, Chen C-C. Akt Phosphorylation of p300 at Ser-1834 Is Essential for Its Histone Acetyltransferase and Transcriptional Activity. *Mol. Cell. Biol.* 2005;25(15):6592-6602.
346. Dougherty MK, *et al.* . Regulation of Raf-1 by direct feedback phosphorylation. *Mol Cell* 2005;17:215-224.
347. Nitta R, Jameson S, Kudlow B, Conlan L, Kennedy B. Stabilization of the Retinoblastoma protein by A-Type Nuclear Lamins is Required for INK4-A-mediated Cell Cycle Arrest *Molecular and Cellular Biology* 2006;26(14).
348. Dyson N. The regulation of E2F by pRB-family proteins. *Genes Dev* 1998;12:2245-2262.
349. Paggi MG, Baldi A, Bonetto F, Giordano A. Retinoblastoma protein family in cell cycle and cancer: a review. *J Cell Biochem* 1996;62:418-430.
350. Chittenden T, Livingston, D. M., and DeCaprio, J. A. Cell cycle analysis of E2F in primary human T cells reveals novel E2F complexes and biochemically distinct forms of free E2F. *Mol Cell Biol* 1993;13:3975-3983.
351. Gaubatz S, Lindeman GJ, Ishida S, Jakoi L, Nevins JR, Livingston DM, Rempel RE. E2F4 and E2F5 play an essential role in pocket protein-mediated G1 control. *Mol Cell Biol* 2000;6:729-735.
352. Cobrinik D, Whyte, P., Peeper, D. S., Jacks, T., and Weinberg, R. A. Cell cycle-specific association of E2F with the p130 E1A-binding protein. *Genes Dev* 1993;7:2392-2404.

353. Moberg K, Starz MA, Lees JA. E2F-4 switches from p130 to p107 and pRB in response to cell cycle reentry. *Mol Cell Biol* 1996;16:1436-1449.
354. Ginsberg D, Vairo, G., Chittenden, T., Xiao, Z. X., Xu, G., Wydner, K. L., DeCaprio, J. A., Lawrence, J. B., and Livingston, D. M. E2F-4, a new member of the E2F transcription factor family, interacts with p107. *Genes Dev* 1994;8:2665-2679.
355. Beijersbergen RL, Kerkhoven, R. M., Zhu, L., Carlee, L., Voorhoeve, P. M., and Bernards, R. E2F-4, a new member of the E2F gene family, has oncogenic activity and associates with p107 *in vivo*. *Genes Dev* 1994;8:2680-2690.
356. Hijmans EM, Voorhoeve, P. M., Beijersbergen, R. L., van 't Veer, L. J., and Bernards, R. E2F-5, a new E2F family member that interacts with p130 *in vivo*. *Mol Cell Biol* 1995;15:3082-3089.
357. Zhu L, Xie, E., and Chang, L. S. Differential roles of two tandem E2F sites in repression of the human p107 promoter by retinoblastoma and p107 proteins. *Mol Cell Biol* 1995;15:3552-3562.
358. Chellappan SP. The E2F transcription factor: role in cell cycle regulation and differentiation. *Mol Cell Differ* 1994;2:201-220.
359. Takahashi Y, Rayman JB, Dynlacht BD. Analysis of promoter binding by the E2F and pRB families *in vivo*: distinct E2F proteins mediate activation and repression. *Genes Dev* 2000;14:804-816.
360. van den Heuvel S, Dyson NJ. Conserved functions of the pRB and E2F families. *Nat Rev Mol Cell Biol* 2008;9(9):713-724.
361. Morkel M, Wenkel J, Bannister AJ, Kouzarides T, Hagemeier C. An E2F-like repressor of transcription. *Nature* 1997;390:567-568.
362. Cartwright P, Muller H, Wagener C, Holm K, Helin K. E2F-6: a novel member of the E2F family is an inhibitor of E2F-dependent transcription. *Oncogene* 1998;17:611-623.

363. Gaubatz S, Wood JG, Livingston DM. Unusual proliferation arrest and transcriptional control properties of a newly discovered E2F family member, E2F-6. *Proc Natl Acad Sci USA* 1998;95:9190-9195.
364. Trimarchi JM, Fairchild B, Verona R, Moberg K, Andon N, Lees JA. E2F-6, a member of the E2F family that can behave as a transcriptional repressor. *Proc Natl Acad Sci USA* 1998;95:2850-2855.
365. DiStefano LM, Jensen R, Helin K. E2F7, a novel E2F featuring DP-independent repression of a subset of E2F-regulated genes. *EMBO J* 2003;22:6289-6298.
366. Maiti B, Li J, Bruin Ad, Gordon F, Timmers C, Opavsky R, Patil K, Tuttle J, Cleghorn W, Leone G. Cloning and characterization of mouse E2F8, a novel mammalian E2F family member capable of blocking cellular proliferation. *J Biol Chem* 2005;280:18211-18220.
367. Giangrande PH, Zhu W, Schlisio S, Sun X, Mori S, Gaubatz S, Nevins JR. A role for E2F6 in distinguishing G1/S- and G2/M-specific transcription. *Genes & Development* 2004;18(23):2941-2951.
368. Nahle Z, Polakoff, J., Davuluri, R. V., McCurrach, M. E., Jacobson, M. D., Narita, M., Zhang, M. Q., Lazebnik, Y., Bar-Sagi, D., and Lowe, S. W. Direct coupling of the cell cycle and cell death machinery by E2F. *Nat Cell Biol* 2002;4:859-864.
369. Bates S, Phillips, A. C., Clark, P. A., Stott, F., Peters, G., Ludwig, R. L., and Vousden, K. H. p14ARF links the tumour suppressors RB and p53. *Nature* 1998;395(6698):124-125.
370. Wang C, Hou X, Mohapatra S, Ma Y, Cress WD, Pledger WJ, Chen J. Activation of p27Kip1 Expression by E2F1. *Journal of Biological Chemistry* 2005;280(13):12339-12343.
371. Alexander K, Hinds PW. Requirement for p27KIP1 in Retinoblastoma Protein-Mediated Senescence. *Mol. Cell. Biol.* 2001;21(11):3616-3631.
372. Polyak K, Lee, M. H., Erdjument-Bromage, H., Koff, A., Roberts, J. M., Tempst, P., and Massague, J. Cloning of p27Kip1, a cyclin-dependent kinase inhibitor and a potential mediator of extracellular antimitogenic signals. *Cell* 1994;78:59-66.

373. Polyak K, Kato, J. Y., Solomon, M. J., Sherr, C. J., Massague, J., Roberts, J. M., and, Koff A. p27Kip1, a cyclin-Cdk inhibitor, links transforming growth factor-beta and contact inhibition to cell cycle arrest. *Genes Dev* 1994;8:9-22.
374. Toyoshima H, and Hunter, T. p27, a novel inhibitor of G1 cyclin-Cdk protein kinase activity, is related to p21. *Cell* 1994;78:67-74.
375. Morisaki H, Fujimoto, A., Ando, A., Nagata, Y., Ikeda, K., and Nakanishi, M. Cell cycle-dependent phosphorylation of p27 cyclin-dependent kinase (Cdk) inhibitor by cyclin E/Cdk2. *Biochem. Biophys. Res. Commun.* 1997;240:386-390.
376. Vlach J, Hennecke, S., and Amati, B. Phosphorylation-dependent degradation of the cyclin-dependent kinase inhibitor p27. *EMBO J.* 1997;16:5334-5344.
377. Masciukko V, Sgambato, A., Pacilio, C., Pucci, B., Ferrandina, G., Palazzo, J., Carbone, A., Cittadini, A., Mancuso, S., Scambia, G., and Giordano, A. . Frequent loss of expression of the cyclin-dependent kinase inhibitor p27 in epithelial ovarian cancer. *Cancer Res* 1999;59:3790-3794.
378. Nevins JR. Toward an understanding of the functional complexity of the E2F and Retinoblastoma families. *Cell Growth & Differ* 1998;9:585-593.
379. Trimarchi JM, Lees JA. Sibling rivalry in the E2F family. *Nat Rev Mol Cell Biol* 2002;3:11-20.
380. Garnovskaya MN, Mukhin YV, Vlasova TM, Grewal JS, Ullian ME, Tholanikunnel BG, Raymond JR. Mitogen-induced Rapid Phosphorylation of Serine 795 of the Retinoblastoma Gene Product in Vascular Smooth Muscle Cells Involves ERK Activation. *Journal of Biological Chemistry* 2004;279(23):24899-24905.
381. Gallo G, Giordano A. Are RB proteins a potential substrate of Pin1 in the regulation of the cell cycle? *Journal of Cellular Physiology* 2005;205(2):176-181.
382. Hasan S, Hassa PO, Imhof R, Hottiger MO. Transcription coactivator p300 binds PCNA and may have a role in DNA repair synthesis. *Nature (Lond.)* 2001;410:387-391.
383. Struhl K. Histone acetylation and transcriptional regulatory mechanisms. *Genes Dev* 1998;12:599-606.

384. Kouzarides T. Histone acetylases and deacetylases in cell proliferation. *Curr Opin Genet Dev* 1999;9:40-48.
385. Blobel GA. CREB-binding protein and p300: molecular integrators of hematopoietic transcription. *Blood* 2000;95.
386. Poizat C, Sartorelli V, Chung G, Kloner RA, Kedes L. Proteasome-mediated degradation of the coactivator p300 impairs cardiac transcription. *Mol Cell Biol* 2000;20:8643-8654.
387. Brehm A, Miska, EA, McCance, DJ, Reid, JL, Bannister, AJ, Kouzarides T. Retinoblastoma protein recruits histone deacetylase to repress transcription. *Nature (Lond.)* 1998;391:597-600.
388. Vo N, Goodman RH. CREB-binding protein and p300 in transcriptional regulation. *J Biol Chem* 2001;276:13505-13508.
389. Ait-Si-Ali S, Poleskaya A, Filleur S, Ferreira R, Duquet A, Robin P, Vervish A, Trouche D, Cabon F, Harel-Bellan A. CBP/p300 histone acetyl-transferase activity is important for the G1/S transition. *Oncogene* 2000;19: 2430-2437.
390. Felzien LK, Farrell S, Betts JC, Mosavin R, Nabel G J. Specificity of cyclin E-Cdk2, TFIIB, and E1A interactions with a common domain of the p300 coactivator. *Mol Cell Biol* 1999;19:4241-4246.
391. Ewen M. Where the cell cycle and histones meet. *Genes Dev* 2000;14.
392. Peeper DS, Shvarts A, Brummelkamp T, Douma S, Koh EY, Daley GQ, Bernards R. A functional screen identifies hDRIL1 as an oncogene that rescues RAS-induced senescence. *Nat Cell Biol* 2002;4:148-153.
393. Bandyopadhyay D, Okan NA, Bales E, Nascimento L, Cole PA, Medrano EE. Down-Regulation of p300/CBP Histone Acetyltransferase Activates a Senescence Checkpoint in Human Melanocytes. *Cancer Research* 2002;62(21):6231-6239.
394. Urnov FD, Wolffe AP. Chromatin remodeling and transcriptional activation: the cast (in order of appearance). *Oncogene* 2001;20.

395. Howard BH. Replicative senescence: considerations relating to the stability of heterochromatin domains. *Exp Gerontol* 1996;31:281-293.
396. Wade PA. Transcriptional control at regulatory checkpoints by histone deacetylases: molecular connections between cancer and chromatin. *Human Molecular Genetics* 2001;10(7):693-698.
397. Ferreira R, Naguibneva I, Pritchard LL, Ait-Si-Ali S, Harel-Bellan A. The Rb/chromatin connection and epigenetic control: opinion. *Oncogene* 2001;20:3128-3133.
398. Vandel L, Nicolas E, Vaute O, Ferreira R, Ait-Si-Ali, S, and Trouche, D. Transcriptional repression by the retinoblastoma protein through the recruitment of a histone methyltransferase. *Mol Cell Biol* 2001;21:6484-6494.
399. Nielsen SJ, Schneider R, Bauer UM, Bannister AJ, Morrison A, O'Carroll D, Firestein R, Cleary M, Jenuwein T, Herrera RE, Kouzarides T. Rb targets histone H3 methylation and HP1 to promoters. *Nature (Lond.)* 2001;412:561-565.
400. Paik J, et al. FoxOs are lineage-restricted redundant tumor suppressors and regulate endothelial cell homeostasis. *Cell* 2007;128:309-323.
401. Fu Z, Tindall DJ. FOXOs, cancer and regulation of apoptosis. *Oncogene* 2008;27(16):2312-2319.
402. Martins CP, Berns A. Loss of p27(Kip1) but not p21(Cip1) decreases survival and synergizes with MYC in murine lymphomagenesis. *EMBO J* 2008;21:3739-3748.
403. de Keizer PLJ, Packer LM, Szypowska AA, Riedl-Polderman PE, van den Broek NJF, de Bruin A, Dansen TB, Marais R, Brenkman AB, Burgering BMT. Activation of FOXO transcription factors by oncogenic BRAF promotes p21^{cip1}-dependent senescence. *Cancer Res* 2010;70(21):8526-8536.
404. Campisi J, d'Adda di Fagagna F. Cellular senescence: when bad things happen to good cells. *Nat Rev Mol Cell Biol* 2007;8(9):729-740.
405. Collado M, Blasco MA, Serrano M. Cellular senescence in cancer and aging. *Cell* 2007;130:223-233.

406. Finkel T. Redox-dependent signal transduction. *FEBS Lett* 2000;476:52-54.
407. Stone JR, Yang, S. Hydrogen peroxide: a signaling messenger. *Antioxid Redox Signal* 2006;8:243-270.
408. Chen QM, Bartholomew, JC, Campisi, J, Acosta, M, Reagan, JD, Ames, BN. Molecular analysis of H₂O₂-induced senescent-like growth arrest in normal human fibroblasts: p53 and Rb control G1 arrest but not cell replication. *Biochem J* 1998;332(Pt. 1):43-50.
409. Giorgio M, Trinei, M, Migliaccio, E, Pelicci, PG. Hydrogen peroxide: a metabolic by-product or a common mediator of ageing signals? *Nat Rev Mol Cell Biol* 2007;8:722-728.
410. Harman D. Aging: a theory based on free radical and radiation chemistry. *J Gerontol* 1956;11:298-300.
411. Nemoto S, Finkel T. Redox regulation of forkhead proteins through a p66shc-dependent signaling pathway. *Science* 2002;295:2450-2452.
412. Kenyon C CJ, Gensch E, Rudner A, Tabtiang R. A *C. elegans* mutant that lives twice as long as wild type. *Nature* 1993;366:461-464.
413. Willcox BJ, Donlon TA, He Q, Chen R, Grove JS, Yano K, Masaki KH, Willcox DC, Rodriguez B, Curb JD. FOXO3A genotype is strongly associated with human longevity. *Proc.Natl.Acad.Sci.U.S.A.* 2008;105:13987-13992.
414. Dansen TB, Burgering BMT. Unravelling the tumor-suppressive functions of FOXO proteins. *Trends in Cell Biology* 2008;18(9):421-429.
415. Yeh ES, Means AR. PIN1, the cell cycle and cancer. *Nature Reviews Cancer* 2007;7:381-388.
416. Sage J, Mulligan GJ, Attardi LD, Miller A, Chen S, Williams B, Theodorou E, Jacks T. Targeted disruption of the three Rb-related genes leads to loss of G1 control and immortalization. *Genes & Development* 2000;14(23):3037-3050.

417. Herbig U, Jobling WA, Chen BPC, Chen DJ, Sedivy JM. Telomere Shortening Triggers Senescence of Human Cells through a Pathway Involving ATM, p53, and p21CIP1, but Not p16INK4a. *Molecular Cell* 2004;14(4):501-513.
418. Maclaine NJ, Hupp TR. The regulation of p53 by phosphorylation: A model for how distinct signals Integrate into the p53 pathway *Aging Cell* 2009;1(5):490-502.
419. Pluquet O, Hainaut P. Genotoxic and non-genotoxic pathways of p53 induction. *Cancer Letters* 2001;174(1):1-15.
420. Ozaki T, Nakagawara A. p53: The Attractive Tumor Suppressor in the Cancer Research Field. *Journal of Biomedicine and Biotechnology* 2011;vol. 2011.
421. May P, May E. Twenty years of p53 research: structural and functional aspects of the p53 protein [*published erratum appears in Oncogene 2000 Mar 23;19(13):1734*]. *Oncogene* 1999;18:7621-7636.
422. Ljungman M. M. Ljungman, Dial 9-1-1 for p53: mechanisms of p53 activation by cellular stress. *Neoplasia* 2000;2:208-225.
423. Agarwal ML, Taylor WR, Chernov MV, Chernova OB, Stark GR. The p53 network. *J Biol Chem* 1998;273:1-4.
424. Prives C, Hall PA. The P53 pathway. *Journal of Pathology* 1999;187(1):112-126
425. El-Deiry WS. The role of p53 in chemosensitivity and radiosensitivity. *Oncogene* 2003;22(47): 7486-7495.
426. Saito Si, Yamaguchi H, Higashimoto Y, Chao C, Xu Y, Fornace AJ, Appella E, Anderson CW. Phosphorylation Site Interdependence of Human p53 Post-translational Modifications in Response to Stress. *Journal of Biological Chemistry* 2003;278(39):37536-37544.
427. Vousden K, Lu X. Live or let die: the cell's response to p53. *Nat Rev Cancer* 2002;2:594-604.

428. Talos F, U.M.Moll. Role of the p53 family in stabilizing the genome and preventing polyploidization. *Advances in Experimental Medicine and Biology* 2010;676:73-91.
429. Donehower LA, Harvey M, al. BLSe. Mice deficient for p53 are developmentally normal but susceptible to spontaneous tumours. *Nature* 1992;356(6366):215-221
430. Saito S, Goodarzi AA, Higashimoto Y, Noda Y, Lees-Miller SP, Appella E, Anderson CW. ATM mediates phosphorylation at multiple p53 sites, including Ser (46), in response to ionizing radiation. *J Biol Chem* 2002;277:12491-12494.
431. Boehme KA, Kulikov R, Blattner C. p53 stabilization in response to DNA damage requires Akt/PKB and DNA-PK. *Proceedings of the National Academy of Sciences* 2008;105(22):7785-7790.
432. Kubbutat MH, Jones SN, Vousden KH. Regulation of p53 stability by Mdm2. *Nature* 1997 1997;387:299-303.
433. Haupt Y, Maya R, Kazaz A, Oren M. Mdm2 promotes the rapid degradation of p53. *Nature* 1997;387:296-299.
434. Fuchs SY, Adler V, Buschmann T, Wu X, Ronai Z. Mdm2 association with p53 targets its ubiquitination. *Oncogene* 1998;17:2543-2547.
435. Fuchs SY, Adler V, Buschmann T, Yin Z, Wu X, Jones SN, Ronai Z. JNK targets p53 ubiquitination and degradation in nonstressed cells. *Genes Dev* 1998;12:2658-2663.
436. Lane DP, Hall PA. MDM2-arbiter of p53's destruction. *Trends Biochem Sci* 1997;22:372-374.
437. Oliner JD, Kinzler KW, Meltzer PS, George DL, Vogelstein B. Amplification of a gene encoding a p53-associated protein in human sarcomas. *Nature* 1992;358:80-83.
438. Tao W, Levine AJ. Nucleocytoplasmic shuttling of oncoprotein Hdm2 is required for Hdm2- mediated degradation of p53. *Proc. Natl. Acad. Sci. USA* 1999;96:3077-3080.

439. Wu X, Bayle JH, Olson D, Levine AJ. The p53-mdm-2 autoregulatory feedback loop. *Genes Dev* 1993;7:1126-1132.
440. Sionov RV, Haupt Y. The cellular response to p53: the decision between life and death. *Oncogene* 1999;18(45):6145-6157.
441. Itahana K, Dimri GP, Hara E, Itahana Y, Zou Y, Desprez P-Y, Campisi J. A Role for p53 in Maintaining and Establishing the Quiescence Growth Arrest in Human Cells. *Journal of Biological Chemistry* 2002;277(20):18206-18214.
442. Sherr CJ, Roberts JM. CDK inhibitors: positive and negative regulators of G1-phase progression. *Genes Dev* 1999;13:1501-1512.
443. Vousden KH, Ryan KM. p53 and metabolism. *Nat Rev Cancer* 2009;9:691-700.
444. Demidenko ZN, Korotchkina LG, Gudkov AV, Blagosklonny MV. Paradoxical suppression of cellular senescence by p53. *PNAS* 2010;107(21):9660-9664.
445. Feng Z, Zhang H, Levine AJ, Jin S. The coordinate regulation of the p53 and mTOR pathways in cells. *Proceedings of the National Academy of Sciences of the United States of America* 2005;102(23):8204-8209.
446. Constantinou C, Clemens MJ. Regulation of the phosphorylation and integrity of protein synthesis initiation factor eIF4G1 and the translational repressor 4E-BP1 by p53. *Oncogene* 2005;24:4839-4850.
447. Budanov AV, Karin M. p53 Target Genes Sestrin1 and Sestrin2 Connect Genotoxic Stress and mTOR Signaling. *Cell* 2008;134(3):451-460.
448. Matthew EM, Hart LS, Astrinidis A, Navaraj A, Dolloff NG, Dicker DT, Henske EP, El-Deiry WS. The p53 target Plk2 interacts with TSC proteins impacting mTOR signaling, tumor growth and chemosensitivity under hypoxic conditions. *Cell Cycle* 2009;8:4168-75.
449. Maki CG. Decision-making by p53 and mTOR. *Aging* 2010;2:324-326.
450. Stambolic V, MacPherson D, Sas D, Lin Y, Snow B, Jang Y, Benchimol S, Mak TW. Regulation of PTEN transcription by p53. *Mol Cell* 2001;8:317-325.

451. Blagosklonny MV. Cell senescence and hypermitogenic arrest. *EMBO Rep* 2003;4:358-362.
452. Demidenko ZN, Blagosklonny MV. Growth stimulation leads to cellular senescence when the cell cycle is blocked. *Cell Cycle* 2008;7:3355-33561.
453. Demidenko ZNaBM. At concentrations that inhibit mTOR, resveratrol suppresses cellular senescence. *Cell* 2009;8:1901-1904.
454. Korotchkina LG, Demidenko ZN, Gudkov AV, Blagosklonny MV. Cellular quiescence caused by the Mdm2 inhibitor Nutlin-3A. *Cell Cycle* 2009;8(22):3777-3781.
455. Korotchkina LG Leontieva OV BE, Demidenko ZN, Gudkov AV, Blagosklonny MV The choice between p53-induced senescence and quiescence is determined in part by the mTOR pathway. *Aging* 2010;2:344-352.
456. Zheng H, You H, Zhou XZ, Murray SA, Uchida T, Wulf G, Gu L, Tang X, Lu KP, Xiao ZX The prolyl isomerase Pin1 is a regulator of p53 in genotoxic response. *Nature* 2002;419:849-853.
457. Wheaton K, Muir J, Ma W, Benchimol S. BTG2 antagonizes Pin1 in response to mitogens and telomere disruption during replicative senescence. *Aging Cell* 2010;9(5):747-760.
458. Campisi J. From cells to organisms: can we learn about aging from cells in culture? *Exp Gerontol* 2001;36:607-618.
459. Bandyopadhyay D, Timchenko N, Suwa T, Hornsby PJ, Campisi J, Medrano EE. The human melanocyte: a model system to study the complexity of cellular aging and transformation in non-fibroblastic cells. *Exp Gerontol* 2001;36:1265-1275.
460. Bruston F, Delbarre E, Östlund C, Worman HJ, Buendia B, Duband-Goulet I. Loss of a DNA binding site within the tail of prelamin A contributes to altered heterochromatin anchorage by progerin. *FEBS Letters* 2010;584(14):2999-3004.
461. Xu Y-X, Manley JL. New Insights into Mitotic Chromosome Condensation: A Role for the Prolyl Isomerase Pin1. *Cell Cycle* 2007;6(23):2896-2901.

462. Xu Y-X, Manley JL. The Prolyl Isomerase Pin1 Functions in Mitotic Chromosome Condensation. *Molecular Cell* 2007;26(2):287-300.
463. Monje P, Hernández-Losa J, Lyons RJ, Castellone MD, Gutkind JS. Regulation of the Transcriptional Activity of c-Fos by ERK. *Journal of Biological Chemistry* 2005;280(42):35081-35084.
464. Saxena UH, Owens L, Graham JR, Cooper GM, Hansen U. Prolyl Isomerase Pin1 Regulates Transcription Factor LSF (TFCP2) by Facilitating Dephosphorylation at Two Serine-Proline Motifs. *Journal of Biological Chemistry* 2009;285(41):31139-31147.

APPENDICES

Appendix A. Full SABiosciences RT-qPCR Gene List/Array Data

PCR Array Catalog:

PAMM-020 (Mouse Cell Cyle)

Test Group: 24 hr/500 nM Induced L647R PreA-expressing Rheswitch 3T3 cells

Control Group: Uninduced L647R (Not Induced "NI" DMSO-treated) Rheswitch 3T3 cells

Fold Difference Cutoff: 2

p-value Cutoff: 0.05

Arrays included in Test Group: L647R PLATE1, L647R PLATE2, L647R PLATE3

Arrays included in Control Group: L647R NI-PLATE1, L647R NI-PLATE2, L647R NI-PLATE3

Position	Symbol	Fold Regulation	Status	p-value	Unigene	Refseq	Gene Name	RT2 Catalog
A01	Abl1	1.324	OKAY	0.04650	Mm.1318	NM_009594	AI325092/Abl/E430008G22Rik/MGC117749/c-Abl	PPM03439B
A02	Ak1	7.917	OKAY	0.00729	Mm.480325	NM_021515	Ak-1/B430205N08Rik	PPM27482E
A03	Apbb1	40.928	A	0.02435	Mm.38469	NM_009685	Fe65/Rir	PPM28549A
A04	Atm	4.033	OKAY	0.00036	Mm.5088	NM_007499	AI256621/C030026E19Rik	PPM03454B
A05	Brca1	19.360	OKAY	0.00109	Mm.244975	NM_009764	-	PPM03442A
A06	Brca2	14.107	OKAY	0.00032	Mm.236256	NM_009765	AI256696/AW045498/Fancd1/RAB163	PPM03704E
A07	Camk2a	13.817	A	0.00348	Mm.131530	NM_177407	CaMKII/R74975/mKIAA0968	PPM31219A
A08	Camk2b	15.190	A	0.00010	Mm.439733	NM_007595	Camk2d/MGC90738	PPM04592A
A09	Casp3	4.537	OKAY	0.00706	Mm.34405	NM_009810	A830040C14Rik/AC-3/Apopain/CC3/PPP32/Caspase-3/Lice/Yama/mlidy	PPM02922E
A10	Ccna1	6.226	A	0.04367	Mm.4815	NM_007628	MGC159139	PPM03258B
A11	Ccna2	4.464	OKAY	0.00007	Mm.4189	NM_009828	AA408589/Ccn-1/Ccn1/Ccna/CycA2/Cyca	PPM02913C
A12	Ccnb1	1.989	OKAY	0.00734	Mm.260114	NM_172301	Ccnb1-rs1/Ccnb1-rs13/CycB1/Cycb-4/Cycb-5/Cycb1-rs1/MGC18763/MGC90915	PPM02894E
B01	Ccnb2	-2.097	OKAY	0.03536	Mm.22592	NM_007630	CycB2	PPM03259E
B02	Ccnc	10.045	OKAY	0.00249	Mm.278584	NM_016746	AI451004/AU020987/CG1C	PPM02905B
B03	Ccnd1	5.836	OKAY	0.00365	Mm.273049	NM_007631	AI327039/Cyl-1/PRAD1/bcl-1/cD1	PPM02903E
B04	Ccne1	18.443	OKAY	0.00277	Mm.16110	NM_007633	AW538188/CycE1	PPM02891B
B05	Ccnf	1.106	OKAY	0.32047	Mm.77695	NM_007634	CycF/Fbxo1	PPM03260B
B06	Cdc25a	1.083	OKAY	0.24310	Mm.307103	NM_007658	D9Erttd393e	PPM03246E
B07	Cdk2	2.107	OKAY	0.00062	Mm.111326	NM_016756	A630093N05Rik	PPM02902E
B08	Cdk4	37.315	OKAY	0.00103	Mm.6839	NM_009870	Crk3	PPM02911C
B09	Cdk5rap1	8.990	OKAY	0.00064	Mm.289427	NM_025876	2310066P17Rik	PPM37671E
B10	Cdkn1a	6.313	OKAY	0.00194	Mm.195663	NM_007669	CAP20/CDKI/CIP1/Cdkn1/P21/SDI1/Waf1/mda6/p21Cip1/p21WAF	PPM02901A
B11	Cdkn1b	23.237	OKAY	0.00010	Mm.2958	NM_009875	AA408329/AI843786/Kip1/p27/p27Kip1	PPM02909B
B12	Cdkn2a	-2.471	C	0.00095	Mm.4733	NM_009877	ARF-INK4a/Arf/INK4a-ARF/Ink4a/Arf/MTS1/Pctr1/p16/p16(INK4a)/p16INK4a/p19<ARF>/p19ARF	PPM02906E
C01	Chek1	22.136	OKAY	0.00070	Mm.16753	NM_007691	C85740/Chk1/rad27	PPM03253A

Continued next page

Appendix A (Continued)

Position	Symbol	Fold Regulation	Status	p-value	Unigene	Refseq	Gene Name	RT2 Catalog
C02	Cks1b	1.638	OKAY	0.32036	Mm.3049	NM_016904	2410005G18Rik/2610005D03Rik/AA407784/Cks1/sid1334	PPM03255B
C03	Ddit3	4.579	OKAY	0.00076	Mm.110220	NM_007837	CHOP-10/CHOP10/chop/gadd153	PPM03736A
C04	Dnajc2	-1.564	OKAY	0.01399	Mm.266312	NM_009584	AU020218/MIDA1/Zrf1/Zrf2	PPM36067E
C05	Dst	25.369	OKAY	<0.00001	Mm.478284	NM_134448	2310001O04Rik/A830042E19Rik/AW554249/BP230/BPA G1-n/Bpag/Bpag1/Macf2/ah/athetoid/dt/mKIAA0728/nmf339	PPM05185F
C06	E2f1	6.357	OKAY	0.00158	Mm.18036	NM_007891	E2F-1/KIAA4009/mKIAA4009	PPM02892E
C07	E2f2	3.494	OKAY	0.23644	Mm.307932	NM_177733	9230110J10/E130207A07	PPM03463A
C08	E2f3	2.825	OKAY	0.00083	Mm.268356	NM_010093	E2F3b/E2f3a/mKIAA0075	PPM03263B
C09	E2f4	9.613	OKAY	0.00157	Mm.34554	NM_148952	2010111M04Rik/AI427446	PPM03464A
C10	Gadd45a	-1.158	OKAY	0.35949	Mm.72235	NM_007836	AA545191/Ddit1/GADD45	PPM02927B
C11	Gpr132	-1.916	OKAY	0.00644	Mm.20455	NM_019925	G2a	PPM04846E
C12	Hus1	3.754	OKAY	0.00366	Mm.42201	NM_008316	mHus1	PPM03266B
D01	Inha	7.021	OKAY	0.00137	Mm.1100	NM_010564	AW555078	PPM04412E
D02	Itgb1	9.613	OKAY	0.00003	Mm.263396	NM_010578	4633401G24Rik/AA409975/A960159/CD29/ENSMUSG0000051907/FnrB/Gm9863/gp1la	PPM03668B
D03	Macf1	9.770	OKAY	0.00121	Mm.402299	NM_001199	ABP620/Acf7/Aclp7/MACF/R74989/mACF7/mKIAA0465	PPM24961A
D04	Mad2l1	2.704	OKAY	0.00231	Mm.485053	NM_019499	AA673185/MAD2/MGC113763	PPM03267A
D05	Mcm2	17.651	OKAY	0.00351	Mm.16711	NM_008564	AA959861/AW476101/BM28/CDCL1/Mcmd2/mKIAA0030	PPM03268B
D06	Mcm3	-1.264	OKAY	0.06021	Mm.4502	NM_008563	AL033361/C80350/Mcmd/P1/p1.m	PPM03269E
D07	Mcm4	1.380	OKAY	0.03367	Mm.1500	NM_008565	19G/AI325074/AU045576/Cdc21/KIAA4003/Mcmd4/mKIAA4003/mcdc21	PPM03270A
D08	Mdm2	2.097	OKAY	0.00418	Mm.22670	NM_010786	1700007J15Rik/AA415488/Mdm-2	PPM02929B
D09	Mki67	1.279	OKAY	0.00944	Mm.4078	NM_001081	D630048A14Rik/Ki-67/Ki67	PPM03457A
D10	Mre11a	6.269	OKAY	0.00068	Mm.149071	NM_018736	Mre11/Mre11b	PPM03445B
D11	Msh2	-1.044	OKAY	0.30323	Mm.4619	NM_008628	AI788990	PPM04993E
D12	Mtbp	17.529	OKAY	0.00147	Mm.390829	NM_134092	AI429604/MDM2BP	PPM05073B
E01	Myb	-2.471	C	0.00095	Mm.52109	NM_010848	AI550390/M16449/MGC18531/c-myb	PPM05270C
E02	Nek2	15.581	OKAY	0.00051	Mm.33773	NM_010892	AA617254/C77054	PPM28098A
E03	Nfatc1	5.534	OKAY	0.00079	Mm.329560	NM_016791	2210017P03Rik/AI449492/AV076380/NF-ATc/NFAT2/NFATc/Nfatcb	PPM04560F
E04	Notch2	10.691	OKAY	0.00009	Mm.254017	NM_010928	AI853703/N2	PPM05137B
E05	Npm2	16.545	A	0.00051	Mm.347749	NM_181345	MGC123506/MGC123507	PPM41992B
E06	Pcna	-1.352	OKAY	0.06326	Mm.7141	NM_011045	-	PPM03456E
E07	Pes1	-1.191	OKAY	0.03433	Mm.28659	NM_022889	-	PPM27335E
E08	Pkd1	4.590	OKAY	0.00007	Mm.290442	NM_013630	FLJ00285/MGC118471/PC1/mFLJ00285	PPM37759E
E09	Pmp22	-1.838	OKAY	0.01359	Mm.1237	NM_008885	22kDa/Gas-3/HNPP/Tr/trembler	PPM05053E
E10	Ppm1d	4.302	OKAY	0.00394	Mm.45609	NM_016910	AV338790/Wip1	PPM04992A
E11	Ppp2r3a	20.464	A	0.00137	Mm.271249	NM_001161	3222402P14Rik/A730042E07/MGC29057	PPM36321E
E12	Ppp3ca	2.838	OKAY	0.02059	Mm.331389	NM_008913	2900074D19Rik/AI841391/AW413465/CN/Caln/Calna/CnA/MGC106804	PPM05007B
F01	Prm1	2.660	B	0.59979	Mm.42733	NM_013637	Prm-1	PPM28989D
F02	Rad17	1.137	OKAY	0.26549	Mm.248489	NM_011233	9430035O09Rik/MmRad24	PPM03276E

Continued next page

Appendix A (Continued)

Position	Symbol	Fold Regulation	Status	p-value	Unigene	Refseq	Gene Name	RT2 Catalog
F03	Rad21	2.381	OKAY	0.00060	Mm.182628	NM_009009	MGC150311/MGC150312/SCC1/mKIAA0078	PPM32537B
F04	Rad51	-1.539	OKAY	0.53383	Mm.471596	NM_011234	AV304093/Rad51a/Reca	PPM03278B
F05	Rad9	5.420	OKAY	0.00248	Mm.277629	NM_011237	Rad9a	PPM03279E
F06	Ran	-1.894	OKAY	0.00684	Mm.297440	NM_009391	-	PPM05257E
F07	Rbl1	11.458	OKAY	0.00075	Mm.244671	NM_011249	AW547426/PRB1/p107	PPM02898B
F08	Rbl2	2.517	OKAY	0.01196	Mm.235580	NM_011250	Rb2/p130	PPM02896B
F09	Sesn2	5.496	OKAY	0.00070	Mm.23608	NM_144907	HI95/MGC11758/SEST2/Ses2	PPM26463A
F10	Sfn	25.252	A	0.00053	Mm.44482	NM_018754	Er/Mme1/Ywhas	PPM03467A
F11	Shc1	5.959	OKAY	0.00036	Mm.86595	NM_011368	Shc/ShcA/p66/p66shc	PPM04024B
F12	Skp2	3.968	OKAY	0.00511	Mm.35584	NM_013787	FBXL1/MGC102075/MGC11668	PPM02915B
G01	Slfn1	1.851	B	0.38371	Mm.10948	NM_011407	AV316259	PPM25636A
G02	Smc1a	19.540	OKAY	0.00074	Mm.482095	NM_019710	5830426124Rik/KIAA0178/SMC-1A/Sb1.8/Smc1/Smc1alpha/Smc111/Smcb/mKIAA0178	PPM26876A
G03	Stag1	2.359	OKAY	0.00140	Mm.42135	NM_009282	AU045003/SA-1/Scs3	PPM28956E
G04	Sumo1	1.008	OKAY	0.89002	Mm.362118	NM_009460	GMP1/MGC103203/PIC1/SENTRIN/SMT3/SMT3H3/SMT3/SUMO-1/Smt3C/Ubl1	PPM03281E
G05	Taf10	2.540	OKAY	0.00455	Mm.285771	NM_020024	30kDa/AU041226/TAFII30/Taf2h	PPM37466A
G06	Terf1	3.360	OKAY	0.00019	Mm.4306	NM_009352	Pin2/Trbf1/Trf1	PPM04758A
G07	Tfdp1	2.806	OKAY	0.00137	Mm.925	NM_009361	Dp1/Drtf1	PPM03468E
G08	Psmg2	3.007	OKAY	0.00115	Mm.150701	NM_134138	1700017117Rik/AW545363/Clastr3/Tnfsf5ip1	PPM31670A
G09	Trp53	2.806	OKAY	0.00060	Mm.222	NM_011640	Tp53/bbl/bfy/bhy/p44/p53	PPM02931B
G10	Trp63	1.321	B	0.87605	Mm.20894	NM_011641	A1462811/Ket/MGC115972/P51/P63/P63/P73/Trp63/Trp53rp1	PPM03458A
G11	Tsg101	1.247	OKAY	0.10884	Mm.241334	NM_021884	A1255943/CC2	PPM34493F
G12	Wee1	24.905	OKAY	0.00016	Mm.287173	NM_009516	Wee1A	PPM04998E
H01	Gusb	1.908	OKAY	0.02722	Mm.3317	NM_010368	A1747421/Gur/Gus/Gus-r/Gus-s/Gus-t/Gus-u/Gut/asd/g	PPM05490B
H02	Hprt	-1.034	OKAY	0.59453	Mm.299381	NM_013556	C81579/HPGRT/Hprt1/MGC103149	PPM03559E
H03	Hsp90ab1	1.034	OKAY	0.55713	Mm.2180	NM_008302	90kDa/AL022974/C81438/Hsp84/Hsp84-1/Hsp90/Hspcb/MGC115780	PPM04803E
H04	Gapdh	17.570	OKAY	0.00004	Mm.343110	NM_008084	Gapd/MGC102544/MGC102546/MGC103190/MGC103191/MGC105239	PPM02946E
H05	Actb	14.843	OKAY	0.00183	Mm.328431	NM_007393	Actx/E430023M04Rik/beta-actin	PPM02945A
H06	MGDC	-2.471	C	0.00095	N/A	SA_00106	MIGX1B	
H07	RTC	-2.925	OKAY	0.08167	N/A	SA_00104	RTC	
H08	RTC	-3.099	OKAY	0.08341	N/A	SA_00104	RTC	
H09	RTC	-2.832	OKAY	0.15561	N/A	SA_00104	RTC	
H10	PPC	-2.618	OKAY	0.00107	N/A	SA_00103	PPC	
H11	PPC	-2.540	OKAY	0.00068	N/A	SA_00103	PPC	

Set as reference (“housekeeping”) gene

p-value >0.05, not considered as highly statistically relevant for the purposes of this study.

Less than 2-fold expression change, not considered as highly statistically relevant for the purposes of this study.

RT-qPCR assay specific controls, data are relatively meaningless on this “expression fold change” scale, controls met comparison standards in relevant statistical evaluations.

Continued next page

Appendix A (Continued)

Comments:

A: This gene's average threshold cycle is relatively high (> 30) in either the control or the test sample, and is reasonably low in the other sample (< 30).

These data mean that the gene's expression is relatively low in one sample and reasonably detected in the other sample suggesting that the actual fold-change value is at least as large as the calculated and reported fold-change result.

This fold-change result may also have greater variations if p value > 0.05 ; therefore, it is important to have a sufficient number of biological replicates to validate the result for this gene.

B: This gene's average threshold cycle is relatively high (> 30), meaning that its relative expression level is low, in both control and test samples, and the p -value for the fold-change is either unavailable or relatively high ($p > 0.05$).

This fold-change result may also have greater variations; therefore, it is important to have a sufficient number of biological replicates to validate the result for this gene.

C: This gene's average threshold cycle is either not determined or greater than the defined cut-off value (default 35), in both samples meaning that its expression was undetected, making this fold-change result erroneous and un-interpretable.

Fold Change & Fold Regulation:

Fold-Change ($2^{(-\Delta\Delta Ct)}$) is the normalized gene expression ($2^{(-\Delta Ct)}$) in the Test Sample divided the normalized gene expression ($2^{(-\Delta Ct)}$) in the Control Sample.

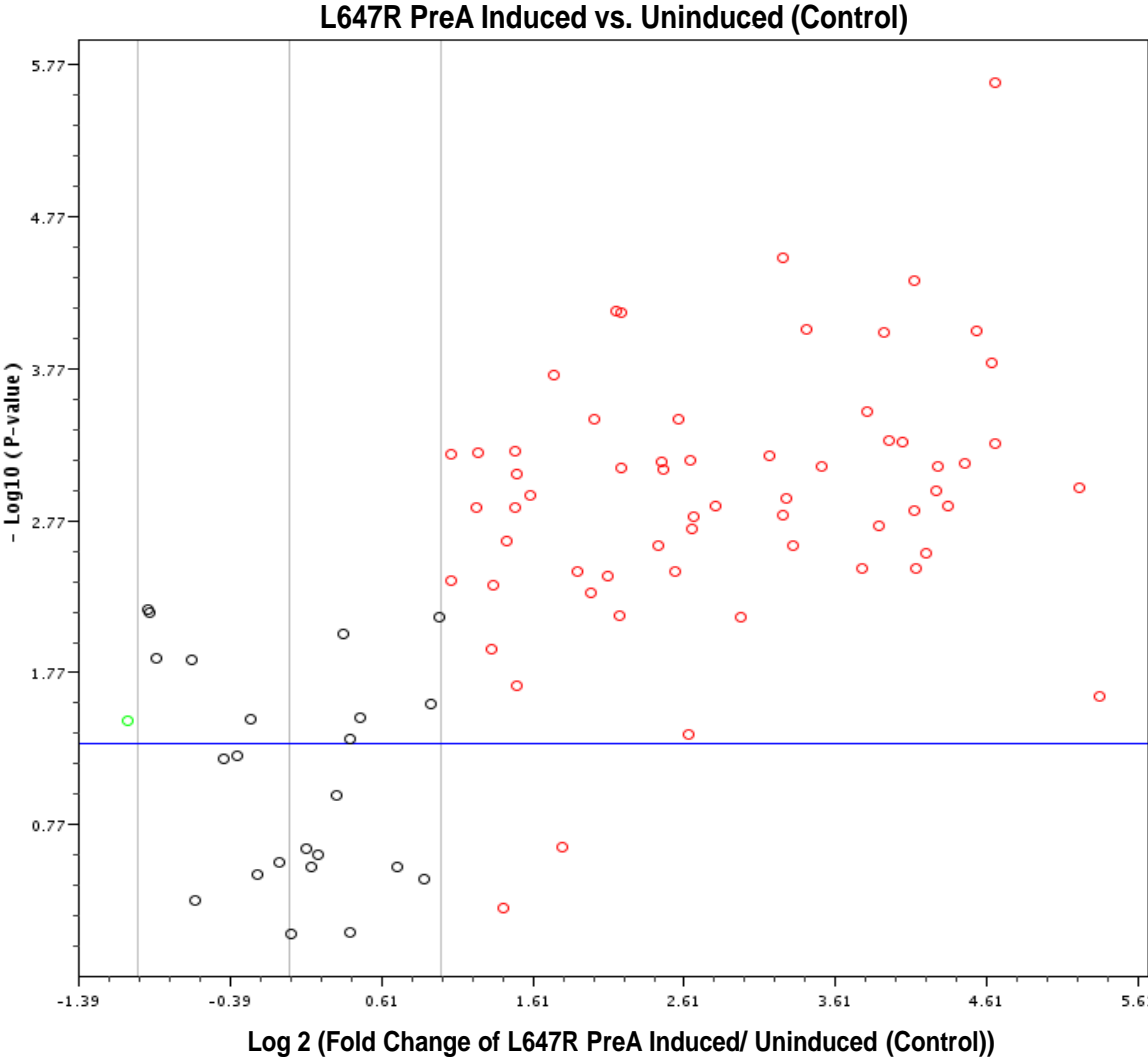
Fold-Regulation represents fold-change results in a biologically meaningful way. Fold-change values greater than one indicate a positive- or an up-regulation, and the fold-regulation is equal to the fold-change.

Fold-change values less than one indicate a negative or down-regulation, and the fold-regulation is the negative inverse of the fold-change.

p-value:

The p values are calculated based on a Student's t -test of the replicate $2^{(-\Delta Ct)}$ values for each gene in the control group and treatment groups, and p values less than 0.05 are indicated in red.

Appendix B. Volcano Plot of RT-qPCR Data (Corresponding to Genes in Appendix A)



Appendix C. Supplemental Motif Analysis Data
 HPRD Survey of Kinase Substrate Sites in Lamin A Peptide Sequence

Position in Query Protein	Sequence in Query Protein	Corresponding Motif Described in the Literature (Phosphorylated Residues In Red)	Features of Motif Described in the Literature
2 - 4	ETP	X[pS/pT]P	GSK-3, ERK1, ERK2, CDK5 substrate motif
2 - 5	ETPS	[E/D]XX[pS/pT]	Casein Kinase I substrate motif
2 - 6	ETPSQ	[E/D][pS/pT]XXX	b-Adrenergic Receptor kinase substrate motif
4 - 6	PSQ	XpSQ	DNA dependent Protein kinase substrate motif
4 - 6	PSQ	P[pS/pT]X	DNA dependent Protein kinase substrate motif
4 - 9	PSQRRRA	X[pS/pT]XXX[A/P/S/T]	G protein-coupled receptor kinase 1 substrate motif
5 - 6	SQ	pSQ	ATM kinase substrate motif
5 - 7	SQR	[pS/pT]X[R/K]	PKA kinase substrate motif
5 - 7	SQR	[pS/pT]X[R/K]	PKC kinase substrate motif
7 - 10	RRAT	RXX[pS/pT]	Calmodulin-dependent protein kinase II substrate motif
7 - 10	RRAT	[R/K]XX[pS/pT]	PKC kinase substrate motif
7 - 10	RRAT	[R/K][R/K]X[pS/pT]	PKA kinase substrate motif
7 - 10	RRAT	[R/K][R/X]X[pS/pT]	PAK2 kinase substrate motif
8 - 10	RAT	[R/K]X[pS/pT]	PKA kinase substrate motif
8 - 10	RAT	[R/K]X[pS/pT]	PKC kinase substrate motif
11 - 16	RSGAQA	X[pS/pT]XXX[A/P/S/T]	G protein-coupled receptor kinase 1 substrate motif
17 - 19	SST	pSX[E/pS*/pT*]	Casein Kinase II substrate motif
17 - 22	SSTPLS	X[pS/pT]XXX[A/P/S/T]	G protein-coupled receptor kinase 1 substrate motif
18 - 20	STP	X[pS/pT]P	GSK-3, ERK1, ERK2, CDK5 substrate motif
18 - 22	STPLS	pSXXX[pS/pT]	MAPKAPK2 kinase substrate motif
18 - 22	STPLS	pSXXXpS*	GSK3 kinase substrate motif
19 - 22	TPLS	[pS/pT]XX[S/T]	Casein Kinase I substrate motif
19 - 22	TPLS	[pS/pT]XX[E/D/pS*/pY*]	Casein Kinase II substrate motif
20 - 23	PLSP	PXpSP	GSK-3, ERK1, ERK2, CDK5 substrate motif
20 - 23	PLSP	XXpSP	GSK-3, ERK1, ERK2, CDK5 substrate motif
20 - 23	PLSP	PX[pS/pT]P	ERK1, ERK2 Kinase substrate motif
20 - 25	PLSPTR	PL[pS/pT]PX[R/K/H]	CDK4 kinase substrate motif
21 - 23	LSP	X[pS/pT]P	GSK-3, ERK1, ERK2, CDK5 substrate motif
22 - 23	SP	pSP	ERK1, ERK2 Kinase substrate motif
22 - 24	SPT	pSX[E/pS*/pT*]	Casein Kinase II substrate motif
22 - 25	SPTR	[pS/pT]PX[R/K]	CDK1, 2, 4, 6 kinase substrate motif
22 - 25	SPTR	[pS/pT]PX[R/K]	Growth associated histone H1 kinase substrate motif
22 - 25	SPTR	[pS/pT]PX[R/K]	Cdc2 kinase substrate motif
22 - 26	SPTRI	pSPX[R/K]X	CDK kinase substrate motif

Appendix C (Continued)

Position in Query Protein	Sequence in Query Protein	Corresponding Motif Described in the Literature (Phosphorylated Residues in Red)	Features of Motif Described in the Literature
23 - 25	PTR	P <p>[pS/pT]</p> X	DNA dependent Protein kinase substrate motif
24 - 27	TRIT	<p>[pS/pT]</p> XX[S/T]	Casein Kinase I substrate motif
25 - 27	RIT	[R/K]X <p>[pS/pT]</p>	PKA kinase substrate motif
25 - 27	RIT	[R/K]X <p>[pS/pT]</p>	PKC kinase substrate motif
46 - 51	IDRVRS	[M/I/L/V]X[R/K]XX <p>[pS/pT]</p>	Chk1 kinase substrate motif
46 - 51	IDRVRS	[M/I/L/V/F/Y]XRXX <p>[pS/pT]</p>	Calmodulin-dependent protein kinase IV substrate motif
46 - 52	IDRVRS	[M/I/L/V/F/Y]XRXX <p>[pS/pT]</p> [M/I/L/V/I]	Calmodulin-dependent protein kinase II alpha substrate motif
46 - 53	IDRVRSLE	[M/V/L/I/F]X[R/K]XX <p>[pS/pT]</p> XX	Calmodulin-dependent protein kinase II substrate motif
48 - 51	RVRS	RXXpS	Calmodulin-dependent protein kinase II substrate motif
48 - 51	RVRS	RXXpS	PKA kinase substrate motif
48 - 51	RVRS	RXX <p>[pS/pT]</p>	Calmodulin-dependent protein kinase II substrate motif
48 - 51	RVRS	[R/K]XX <p>[pS/pT]</p>	PKC kinase substrate motif
51 - 53	SLE	pSX[E/ <p>[pS*/pT*]</p>]	Casein Kinase II substrate motif
51 - 54	SLET	<p>[pS/pT]</p> XX[S/T]	Casein Kinase I substrate motif
51 - 54	SLET	pSXX[E/ <p>[pS*/pT*]</p>]	Casein Kinase II substrate motif
52 - 55	LETE	XX <p>[pS/pT]</p> E	G protein-coupled receptor kinase 1 substrate motif
53 - 57	ETENA	[E/D] <p>[pS/pT]</p> XXX	b-Adrenergic Receptor kinase substrate motif
61 - 70	LRITSEEVV	[M/V/L/I/F][R/K/H]XXX <p>[pS/pT]</p> XXX[I/L/I/F]	AMP-activated protein kinase substrate motif
62 - 64	RIT	[R/K]X <p>[pS/pT]</p>	PKA kinase substrate motif
62 - 64	RIT	[R/K]X <p>[pS/pT]</p>	PKC kinase substrate motif
62 - 65	RITE	XX <p>[pS/pT]</p> E	G protein-coupled receptor kinase 1 substrate motif
64 - 67	TESE	<p>[pS/pT]</p> XX[E/D]	Casein Kinase II substrate motif
64 - 67	TESE	<p>[pS/pT]</p> XX[E/D/ <p>[pS*/pY*]</p>]	Casein Kinase II substrate motif
64 - 67	TESE	<p>[pS/pT]</p> XX[E/D]	Casein Kinase II substrate motif
65 - 69	ESEEV	[E/D] <p>[pS/pT]</p> XXX	b-Adrenergic Receptor kinase substrate motif
66 - 68	SEE	pSX[E/ <p>[pS*/pT*]</p>]	Casein Kinase II substrate motif
68 - 71	EVVS	[E/D]XX <p>[pS/pT]</p>	Casein Kinase I substrate motif
70 - 75	VSREVS	[M/I/L/V]X[R/K]XX <p>[pS/pT]</p>	Chk1 kinase substrate motif
70 - 75	VSREVS	X <p>[pS/pT]</p> XXX[A/P/S/T]	G protein-coupled receptor kinase 1 substrate motif
70 - 75	VSREVS	[M/I/L/V/F/Y]XRXX <p>[pS/pT]</p>	Calmodulin-dependent protein kinase IV substrate motif
70 - 77	VSREVSGI	[M/V/L/I/F]X[R/K]XX <p>[pS/pT]</p> XX	Calmodulin-dependent protein kinase II substrate motif
71 - 73	SRE	pSX[E/ <p>[pS*/pT*]</p>]	Casein Kinase II substrate motif
71 - 75	SREVS	pSXXX <p>[pS/pT]</p>	MAPKAPK2 kinase substrate motif
71 - 75	SREVS	pSXXXpS*	GSK3 kinase substrate motif
72 - 75	REVS	RXXpS	Calmodulin-dependent protein kinase II substrate motif
72 - 75	REVS	RXXpS	PKA kinase substrate motif
72 - 75	REVS	RXX <p>[pS/pT]</p>	Calmodulin-dependent protein kinase II substrate motif
72 - 75	REVS	[R/K]XX <p>[pS/pT]</p>	PKC kinase substrate motif

Appendix C (Continued)

Position in Query Protein	Sequence in Query Protein	Corresponding Motif Described in the Literature (Phosphorylated Residues in Red)	Features of Motif Described in the Literature
72 - 75	REVS	R[K/E/R]XpS	PKC epsilon kinase substrate motif
89 - 91	RKT	[R/K]X[pS/pT]	PKA kinase substrate motif
89 - 91	RKT	[R/K]X[pS/pT]	PKC kinase substrate motif
90 - 94	KTLD	KXXX[pS/pT]	PKA kinase substrate motif
91 - 94	TLDS	[pS/pT]XX[S/T]	Casein Kinase I substrate motif
91 - 94	TLDS	[pS/pT]XX[E/D/pS*/pY*]	Casein Kinase II substrate motif
93 - 97	DSVAK	[E/D][pS/pT]XXX	b-Adrenergic Receptor kinase substrate motif
117 - 121	KARNT	KXXX[pS/pT]	PKA kinase substrate motif
119 - 121	RNT	[R/K]X[pS/pT]	PKA kinase substrate motif
119 - 121	RNT	[R/K]X[pS/pT]	PKC kinase substrate motif
119 - 123	RNTKK	[R/K]X[pS/pT]X[R/K]	PKC kinase substrate motif
121 - 123	TKK	[pS/pT]X[R/K]	PKA kinase substrate motif
121 - 123	TKK	[pS/pT]X[R/K]	PKC kinase substrate motif
121 - 124	TKKE	[pS/pT]XX[E/D]	Casein Kinase II substrate motif
121 - 124	TKKE	[pS/pT]XX[E/D/pS*/pY*]	Casein Kinase II substrate motif
121 - 124	TKKE	[pS/pT]XX[E/D]	Casein Kinase II substrate motif
142 - 147	NSKEAA	X[pS/pT]XXX[A/P/S/T]	G protein-coupled receptor kinase 1 substrate motif
143 - 145	SKE	pSX[E/pS*/pT*]	Casein Kinase II substrate motif
148 - 153	LSTALS	X[pS/pT]XXX[A/P/S/T]	G protein-coupled receptor kinase 1 substrate motif
149 - 153	STALS	pSXXX[pS/pT]	MAPKAPK2 kinase substrate motif
149 - 153	STALS	pSXXXpS*	GSK3 kinase substrate motif
150 - 153	TALS	[pS/pT]XX[S/T]	Casein Kinase I substrate motif
150 - 153	TALS	[pS/pT]XX[E/D/pS*/pY*]	Casein Kinase II substrate motif
151 - 154	ALSE	XX[pS/pT]E	G protein-coupled receptor kinase 1 substrate motif
153 - 155	SEK	[pS/pT]X[R/K]	PKA kinase substrate motif
153 - 155	SEK	[pS/pT]X[R/K]	PKC kinase substrate motif
153 - 158	SEKRTL	[pS/pT]XXX[S/T][M/L/V/I/F]	Casein Kinase I substrate motif
154 - 157	EKRT	[E/D]XX[pS/pT]	Casein Kinase I substrate motif
155 - 157	KRT	[R/K]X[pS/pT]	PKA kinase substrate motif
155 - 157	KRT	[R/K]X[pS/pT]	PKC kinase substrate motif
196 - 199	RLQT	RXX[pS/pT]	Calmodulin-dependent protein kinase II substrate motif
196 - 199	RLQT	[R/K]XX[pS/pT]	PKC kinase substrate motif
196 - 201	RLQTMK	[R/K]XX[pS/pT]X[R/K]	PKC kinase substrate motif
199 - 201	TMK	[pS/pT]X[R/K]	PKA kinase substrate motif
199 - 201	TMK	[pS/pT]X[R/K]	PKC kinase substrate motif
199 - 202	TMKE	[pS/pT]XX[E/D]	Casein Kinase II substrate motif
199 - 202	TMKE	[pS/pT]XX[E/D/pS*/pY*]	Casein Kinase II substrate motif
199 - 202	TMKE	[pS/pT]XX[E/D]	Casein Kinase II substrate motif
208 - 212	KNIYS	KXXX[pS/pT]	PKA kinase substrate motif
210 - 213	IYSE	XX[pS/pT]E	G protein-coupled receptor kinase 1 substrate motif

Appendix C (Continued)

Position in Query Protein	Sequence in Query Protein	Corresponding Motif Described in the Literature (Phosphorylated Residues in Red)	Features of Motif Described in the Literature
212 - 214	SEE	pSX[E/pS*/pT*]	Casein Kinase II substrate motif
216 - 218	RET	[R/K]X[pS/pT]	PKA kinase substrate motif
216 - 218	RET	[R/K]X[pS/pT]	PKC kinase substrate motif
216 - 220	RETKR	[R/K]X[pS/pT]X[R/K]	PKC kinase substrate motif
217 - 221	ETKRR	[E/D][pS/pT]XXX	b-Adrenergic Receptor kinase substrate motif
218 - 220	TKR	[pS/pT]X[R/K]	PKA kinase substrate motif
218 - 220	TKR	[pS/pT]X[R/K]	PKC kinase substrate motif
221 - 224	RHET	RXX[pS/pT]	Calmodulin-dependent protein kinase II substrate motif
221 - 224	RHET	[R/K]XX[pS/pT]	PKC kinase substrate motif
223 - 227	ETRLV	[E/D][pS/pT]XXX	b-Adrenergic Receptor kinase substrate motif
236 - 239	EFES	[E/D]XX[pS/pT]	Casein Kinase I substrate motif
238 - 242	ESRLA	[E/D][pS/pT]XXX	b-Adrenergic Receptor kinase substrate motif
263 - 268	LEKTYS	[M/I/L/V]X[R/K]XX[pS/pT]	Chk1 kinase substrate motif
263 - 270	LEKTYSAK	[M/V/L/I/F]X[R/K]XX[pS/pT]XX	Calmodulin-dependent protein kinase II substrate motif
265 - 268	KTYS	KXX[pS/pT]	PKA kinase substrate motif
265 - 268	KTYS	[R/K]XX[pS/pT]	PKC kinase substrate motif
265 - 270	KTYSAK	[R/K]XX[pS/pT]X[R/K]	PKC kinase substrate motif
268 - 270	SAK	[pS/pT]X[R/K]	PKA kinase substrate motif
268 - 270	SAK	[pS/pT]X[R/K]	PKC kinase substrate motif
275 - 277	RQS	RXpS	PKA kinase substrate motif
275 - 277	RQS	[R/K]X[pS/pT]	PKA kinase substrate motif
275 - 277	RQS	[R/K]X[pS/pT]	PKC kinase substrate motif
277 - 279	SAE	pSX[E/pS*/pT*]	Casein Kinase II substrate motif
279 - 282	ERNS	[E/D]XX[pS/pT]	Casein Kinase I substrate motif
280 - 282	RNS	RXpS	PKA kinase substrate motif
280 - 282	RNS	[R/K]X[pS/pT]	PKA kinase substrate motif
280 - 282	RNS	[R/K]X[pS/pT]	PKC kinase substrate motif
296 - 301	RIRIDS	RXRXX[pS/pT]	Akt kinase substrate motif
296 - 301	RIRIDS	[R/K]XRXXpS	MAPKAPK1 kinase substrate motif
296 - 302	RIRIDSL	[R/K]XRXX[pS/pT][M/L/V/I]	p70 Ribosomal S6 kinase substrate motif
296 - 302	RIRIDSL	RXRXX[pS/pT][F/L]	Akt kinase substrate motif
298 - 301	RIDS	RXXpS	Calmodulin-dependent protein kinase II substrate motif
298 - 301	RIDS	RXXpS	PKA kinase substrate motif
298 - 301	RIDS	RXX[pS/pT]	Calmodulin-dependent protein kinase II substrate motif
298 - 301	RIDS	[R/K]XX[pS/pT]	PKC kinase substrate motif
300 - 303	DSL	[E/D]XX[pS/pT]	Casein Kinase I substrate motif
300 - 304	DSL	[E/D][pS/pT]XXX	b-Adrenergic Receptor kinase substrate motif
301 - 303	SLS	pSX[E/pS*/pT*]	Casein Kinase II substrate motif
302 - 307	LSAQLS	X[pS/pT]XXX[A/P/S/T]	G protein-coupled receptor kinase 1 substrate motif

Appendix C (Continued)

Position in Query Protein	Sequence in Query Protein	Corresponding Motif Described in the Literature (Phosphorylated Residues in Red)	Features of Motif Described in the Literature
303 - 307	SAQLS	pSXXX[pS/pT]	MAPKAPK2 kinase substrate motif
303 - 307	SAQLS	pSXXXpS*	GSK3 kinase substrate motif
306 - 308	LSQ	XpSQ	DNA dependent Protein kinase substrate motif
307 - 308	SQ	pSQ	ATM kinase substrate motif
325 - 329	DSLAR	[E/D][pS/pT]XXX	b-Adrenergic Receptor kinase substrate motif
329 - 334	RERDTS	RXRXX[pS/pT]	Akt kinase substrate motif
329 - 334	RERDTS	[R/K]XRXXpS	MAPKAPK1 kinase substrate motif
330 - 333	ERDT	[E/D]XX[pS/pT]	Casein Kinase I substrate motif
330 - 337	ERDTSRRL	XRXX[pS/pT]XRX	PKC kinase substrate motif
331 - 333	RDT	[R/K]X[pS/pT]	PKA kinase substrate motif
331 - 333	RDT	[R/K]X[pS/pT]	PKC kinase substrate motif
331 - 334	RDTs	RXXpS	Calmodulin-dependent protein kinase II substrate motif
331 - 334	RDTs	RXXpS	PKA kinase substrate motif
331 - 334	RDTs	RXX[pS/pT]	Calmodulin-dependent protein kinase II substrate motif
331 - 334	RDTs	[R/K]XX[pS/pT]	PKC kinase substrate motif
331 - 335	RDTSR	[R/K]X[pS/pT]X[R/K]	PKC kinase substrate motif
331 - 336	RDTsRR	[R/K]XX[pS/pT]X[R/K]	PKC kinase substrate motif
332 - 336	DTSRR	[E/D][pS/pT]XXX	b-Adrenergic Receptor kinase substrate motif
333 - 335	TSR	[pS/pT]X[R/K]	PKA kinase substrate motif
333 - 335	TSR	[pS/pT]X[R/K]	PKC kinase substrate motif
388 - 390	RLS	RXpS	PKA kinase substrate motif
388 - 390	RLS	[R/K]X[pS/pT]	PKA kinase substrate motif
388 - 390	RLS	[R/K]X[pS/pT]	PKC kinase substrate motif
388 - 391	RLSP	XXpSP	GSK-3, ERK1, ERK2, CDK5 substrate motif
389 - 391	LSP	X[pS/pT]P	GSK-3, ERK1, ERK2, CDK5 substrate motif
389 - 394	LSPSPT	X[pS/pT]XXX[A/P/S/T]	G protein-coupled receptor kinase 1 substrate motif
390 - 391	SP	pSP	ERK1, ERK2 Kinase substrate motif
390 - 392	SPS	pSX[E/pS*/pT*]	Casein Kinase II substrate motif
390 - 394	SPSPT	pSXXX[pS/pT]	MAPKAPK2 kinase substrate motif
390 - 394	SPSPT	pSPXX[pS*/pT*]	Casein Kinase I substrate motif
391 - 393	PSP	P[pS/pT]X	DNA dependent Protein kinase substrate motif
392 - 393	SP	pSP	ERK1, ERK2 Kinase substrate motif
392 - 395	SPTS	[pS/pT]XX[S/T]	Casein Kinase I substrate motif
392 - 395	SPTS	pSXX[E/pS*/pT*]	Casein Kinase II substrate motif
392 - 395	SPTS	[pS/pT]XX[E/D/pS*/pY*]	Casein Kinase II substrate motif
394 - 396	TSQ	XpSQ	DNA dependent Protein kinase substrate motif
395 - 396	SQ	pSQ	ATM kinase substrate motif
395 - 397	SQR	[pS/pT]X[R/K]	PKA kinase substrate motif
395 - 397	SQR	[pS/pT]X[R/K]	PKC kinase substrate motif
397 - 402	RSRGRA	X[pS/pT]XXX[A/P/S/T]	G protein-coupled receptor kinase 1 substrate motif

Appendix C (Continued)

Position in Query Protein	Sequence in Query Protein	Corresponding Motif Described in the Literature (Phosphorylated Residues in Red)	Features of Motif Described in the Literature
399 - 404	RGRASS	RXRXX[pS/pT]	Akt kinase substrate motif
399 - 404	RGRASS	[R/K]XRXXpS	MAPKAPK1 kinase substrate motif
401 - 403	RAS	RXpS	PKA kinase substrate motif
401 - 403	RAS	[R/K]X[pS/pT]	PKA kinase substrate motif
401 - 403	RAS	[R/K]X[pS/pT]	PKC kinase substrate motif
401 - 404	RASS	RXXpS	Calmodulin-dependent protein kinase II substrate motif
401 - 404	RASS	RXXpS	PKA kinase substrate motif
401 - 404	RASS	RXX[pS/pT]	Calmodulin-dependent protein kinase II substrate motif
401 - 404	RASS	[R/K]XX[pS/pT]	PKC kinase substrate motif
403 - 406	SSHS	[pS/pT]XX[S/T]	Casein Kinase I substrate motif
403 - 406	SSHS	pSXX[E/pS*/pT*]	Casein Kinase II substrate motif
403 - 406	SSHS	[pS/pT]XX[E/D/pS*/pY*]	Casein Kinase II substrate motif
403 - 407	SSHSS	pSXXX[pS/pT]	MAPKAPK2 kinase substrate motif
403 - 407	SSHSS	pSXXXpS*	GSK3 kinase substrate motif
404 - 406	SHS	pSX[E/pS*/pT*]	Casein Kinase II substrate motif
406 - 408	SSQ	XpSQ	DNA dependent Protein kinase substrate motif
407 - 408	SQ	pSQ	ATM kinase substrate motif
407 - 409	SQT	pSX[E/pS*/pT*]	Casein Kinase II substrate motif
414 - 416	SVT	pSX[E/pS*/pT*]	Casein Kinase II substrate motif
416 - 418	TKK	[pS/pT]X[R/K]	PKA kinase substrate motif
416 - 418	TKK	[pS/pT]X[R/K]	PKC kinase substrate motif
420 - 423	KLES	KXX[pS/pT]	PKA kinase substrate motif
420 - 423	KLES	[R/K]XX[pS/pT]	PKC kinase substrate motif
420 - 424	KLEST	KXXX[pS/pT]	PKA kinase substrate motif
422 - 426	ESTES	[E/D][pS/pT]XXX	b-Adrenergic Receptor kinase substrate motif
423 - 425	STE	pSX[E/pS*/pT*]	Casein Kinase II substrate motif
423 - 426	STES	[pS/pT]XX[S/T]	Casein Kinase I substrate motif
423 - 426	STES	pSXX[E/pS*/pT*]	Casein Kinase II substrate motif
423 - 426	STES	[pS/pT]XX[E/D/pS*/pY*]	Casein Kinase II substrate motif
423 - 428	STESRS	X[pS/pT]XXX[A/P/S/T]	G protein-coupled receptor kinase 1 substrate motif
425 - 428	ESRS	[E/D]XX[pS/pT]	Casein Kinase I substrate motif
426 - 428	SRS	pSX[E/pS*/pT*]	Casein Kinase II substrate motif
427 - 429	RSS	RXpS	PKA kinase substrate motif
427 - 429	RSS	[R/K]X[pS/pT]	PKA kinase substrate motif
427 - 429	RSS	[R/K]X[pS/pT]	PKC kinase substrate motif
428 - 431	SSFSS	[pS/pT]XX[S/T]	Casein Kinase I substrate motif
428 - 431	SSFSS	pSXX[E/pS*/pT*]	Casein Kinase II substrate motif
428 - 431	SSFSS	[pS/pT]XX[E/D/pS*/pY*]	Casein Kinase II substrate motif
429 - 431	SFS	pSX[E/pS*/pT*]	Casein Kinase II substrate motif
430 - 432	FSQ	XpSQ	DNA dependent Protein kinase substrate motif

Appendix C (Continued)

Position in Query Protein	Sequence in Query Protein	Corresponding Motif Described in the Literature (Phosphorylated Residues in Red)	Features of Motif Described in the Literature
431 - 432	SQ	pSQ	ATM kinase substrate motif
435 - 437	RTS	RXpS	PKA kinase substrate motif
435 - 437	RTS	[R/K]X[pS/pT]	PKA kinase substrate motif
435 - 437	RTS	[R/K]X[pS/pT]	PKC kinase substrate motif
435 - 439	RTSGR	[R/K]X[pS/pT]X[R/K]	PKC kinase substrate motif
436 - 441	TSGRVA	X[pS/pT]XXX[A/P/S/T]	G protein-coupled receptor kinase 1 substrate motif
437 - 439	SGR	[pS/pT]X[R/K]	PKA kinase substrate motif
437 - 439	SGR	[pS/pT]X[R/K]	PKC kinase substrate motif
453 - 458	RLRNKS	RXRXX[pS/pT]	Akt kinase substrate motif
453 - 458	RLRNKS	[R/K]XRXXpS	MAPKAPK1 kinase substrate motif
455 - 458	RNKS	RXXpS	Calmodulin-dependent protein kinase II substrate motif
455 - 458	RNKS	RXXpS	PKA kinase substrate motif
455 - 458	RNKS	RXX[pS/pT]	Calmodulin-dependent protein kinase II substrate motif
455 - 458	RNKS	[R/K]XX[pS/pT]	PKC kinase substrate motif
457 - 463	KSNEDQS	XpSXXDXX	Pyruvate dehydrogenase kinase substrate motif
458 - 460	SNE	pSX[E/pS*/pT*]	Casein Kinase II substrate motif
458 - 461	SNED	pSXX[E/D]	Casein kinase II substrate motif
458 - 461	SNED	[pS/pT]XX[E/D]	Casein Kinase II substrate motif
458 - 461	SNED	[pS/pT]XX[E/D/pS*/pY*]	Casein Kinase II substrate motif
458 - 461	SNED	[pS/pT]XX[E/D]	Casein Kinase II substrate motif
460 - 463	EDQS	[E/D]XX[pS/pT]	Casein Kinase I substrate motif
479 - 484	LTYRFP	X[pS/pT]XXX[A/P/S/T]	G protein-coupled receptor kinase 1 substrate motif
480 - 482	TYR	[pS/pT]X[R/K]	PKA kinase substrate motif
480 - 482	TYR	[pS/pT]X[R/K]	PKC kinase substrate motif
486 - 488	KFT	[R/K]X[pS/pT]	PKA kinase substrate motif
486 - 488	KFT	[R/K]X[pS/pT]	PKC kinase substrate motif
486 - 490	KFTLK	[R/K]X[pS/pT]X[R/K]	PKC kinase substrate motif
488 - 490	TLK	[pS/pT]X[R/K]	PKA kinase substrate motif
488 - 490	TLK	[pS/pT]X[R/K]	PKC kinase substrate motif
495 - 500	VTIWAA	X[pS/pT]XXX[A/P/S/T]	G protein-coupled receptor kinase 1 substrate motif
504 - 509	ATHSPP	X[pS/pT]XXX[A/P/S/T]	G protein-coupled receptor kinase 1 substrate motif
505 - 508	THSP	XXpSP	GSK-3, ERK1, ERK2, CDK5 substrate motif
506 - 508	HSP	X[pS/pT]P	GSK-3, ERK1, ERK2, CDK5 substrate motif
507 - 508	SP	pSP	ERK1, ERK2 Kinase substrate motif
507 - 510	SPPT	[pS/pT]XX[S/T]	Casein Kinase I substrate motif
507 - 510	SPPT	pSXX[E/pS*/pT*]	Casein Kinase II substrate motif
509 - 511	PTD	P[pS/pT]X	DNA dependent Protein kinase substrate motif
515 - 519	KAQNT	KXXX[pS/pT]	PKA kinase substrate motif
524 - 529	NSLRTA	X[pS/pT]XXX[A/P/S/T]	G protein-coupled receptor kinase 1 substrate motif
525 - 527	SLR	[pS/pT]X[R/K]	PKA kinase substrate motif

Appendix C (Continued)

Position in Query Protein	Sequence in Query Protein	Corresponding Motif Described in the Literature (Phosphorylated Residues in Red)	Features of Motif Described in the Literature
525 - 527	SLR	[pS/pT]X[R/K]	PKC kinase substrate motif
525 - 528	SLRT	[pS/pT]XX[S/T]	Casein Kinase I substrate motif
525 - 528	SLRT	pSXX[E/pS*/pT*]	Casein Kinase II substrate motif
526 - 528	LRT	LRpT	LKB1 Kinase substrate motif
533 - 536	STGE	pSXX[E/D]	Casein kinase II substrate motif
533 - 536	STGE	pSXX[E/pS*/pT*]	Casein Kinase II substrate motif
533 - 536	STGE	[pS/pT]XX[E/D]	Casein Kinase II substrate motif
533 - 536	STGE	[pS/pT]XX[E/D/pS*/pY*]	Casein Kinase II substrate motif
533 - 536	STGE	[pS/pT]XX[E/D]	Casein Kinase II substrate motif
542 - 546	KLVR	KXXX[pS/pT]	PKA kinase substrate motif
543 - 548	LVRSVT	[M/I/L/V]X[R/K]XX[pS/pT]	Chk1 kinase substrate motif
543 - 548	LVRSVT	[M/I/L/V/F/Y]XRXX[pS/pT]	Calmodulin-dependent protein kinase IV substrate motif
543 - 549	LVRSVTV	[M/I/L/V/F/Y]XRXX[pS/pT][M/I/L/Y]	Calmodulin-dependent protein kinase II alpha substrate motif
543 - 550	LVRSVTVV	[M/V/L/I/F]X[R/K]XX[pS/pT]XX	Calmodulin-dependent protein kinase II substrate motif
545 - 548	RSVT	RXX[pS/pT]	Calmodulin-dependent protein kinase II substrate motif
545 - 548	RSVT	[R/K]XX[pS/pT]	PKC kinase substrate motif
546 - 548	SVT	pSX[E/pS*/pT*]	Casein Kinase II substrate motif
548 - 551	TVVE	[pS/pT]XX[E/D]	Casein Kinase II substrate motif
548 - 551	TVVE	[pS/pT]XX[E/D/pS*/pY*]	Casein Kinase II substrate motif
548 - 551	TVVE	[pS/pT]XX[E/D]	Casein Kinase II substrate motif
567 - 572	GSHCSS	X[pS/pT]XXX[A/P/S/T]	G protein-coupled receptor kinase 1 substrate motif
568 - 571	SHCS	[pS/pT]XX[S/T]	Casein Kinase I substrate motif
568 - 571	SHCS	pSXX[E/pS*/pT*]	Casein Kinase II substrate motif
568 - 571	SHCS	[pS/pT]XX[E/D/pS*/pY*]	Casein Kinase II substrate motif
568 - 572	SHCSS	pSXXX[pS/pT]	MAPKAPK2 kinase substrate motif
568 - 572	SHCSS	pSXXXpS*	GSK3 kinase substrate motif
571 - 573	SSS	pSX[E/pS*/pT*]	Casein Kinase II substrate motif
571 - 577	SSSGDPA	XpSXXDXX	Pyruvate dehydrogenase kinase substrate motif
572 - 575	SSGD	pSXX[E/D]	Casein kinase II substrate motif
572 - 575	SSGD	[pS/pT]XX[E/D]	Casein Kinase II substrate motif
572 - 575	SSGD	[pS/pT]XX[E/D/pS*/pY*]	Casein Kinase II substrate motif
572 - 575	SSGD	[pS/pT]XX[E/D]	Casein Kinase II substrate motif
582 - 585	RSRT	RXX[pS/pT]	Calmodulin-dependent protein kinase II substrate motif
582 - 585	RSRT	[R/K]XX[pS/pT]	PKC kinase substrate motif
583 - 585	SRT	pSX[E/pS*/pT*]	Casein Kinase II substrate motif
589 - 594	GTCGQP	X[pS/pT]XXX[A/P/S/T]	G protein-coupled receptor kinase 1 substrate motif
596 - 599	DKAS	[E/D]XX[pS/pT]	Casein Kinase I substrate motif
597 - 599	KAS	[R/K]X[pS/pT]	PKA kinase substrate motif

Appendix C (Continued)

Position in Query Protein	Sequence in Query Protein	Corresponding Motif Described in the Literature (Phosphorylated Residues in Red)	Features of Motif Described in the Literature
597 - 599	KAS	[R/K]X[pS/pT]	PKC kinase substrate motif
597 - 601	KASAS	KXXX[pS/pT]	PKA kinase substrate motif
598 - 603	ASASGS	X[pS/pT]XXX[A/P/S/T]	G protein-coupled receptor kinase 1 substrate motif
599 - 601	SAS	pSX[E/pS*/pT*]	Casein Kinase II substrate motif
599 - 603	SASGS	pSXXX[pS/pT]	MAPKAPK2 kinase substrate motif
599 - 603	SASGS	pSXXXpS*	GSK3 kinase substrate motif
611 - 616	SSGSS	X[pS/pT]XXX[A/P/S/T]	G protein-coupled receptor kinase 1 substrate motif
612 - 615	SSGS	[pS/pT]XX[S/T]	Casein Kinase I substrate motif
612 - 615	SSGS	pSXX[E/pS*/pT*]	Casein Kinase II substrate motif
612 - 615	SSGS	[pS/pT]XX[E/D/pS*/pY*]	Casein Kinase II substrate motif
612 - 616	SSGSS	pSXXX[pS/pT]	MAPKAPK2 kinase substrate motif
612 - 616	SSGSS	pSXXXpS*	GSK3 kinase substrate motif
613 - 615	SGS	pSX[E/pS*/pT*]	Casein Kinase II substrate motif
615 - 620	SSASSV	[pS/pT]XXX[S/T][M/L/V/I/F]	Casein Kinase I substrate motif
616 - 618	SAS	pSX[E/pS*/pT*]	Casein Kinase II substrate motif
616 - 619	SASS	[pS/pT]XX[S/T]	Casein Kinase I substrate motif
616 - 619	SASS	pSXX[E/pS*/pT*]	Casein Kinase II substrate motif
616 - 619	SASS	[pS/pT]XX[E/D/pS*/pY*]	Casein Kinase II substrate motif
618 - 623	SSVTVT	X[pS/pT]XXX[A/P/S/T]	G protein-coupled receptor kinase 1 substrate motif
619 - 621	SVT	pSX[E/pS*/pT*]	Casein Kinase II substrate motif
619 - 623	SVTVT	pSXXX[pS/pT]	MAPKAPK2 kinase substrate motif
623 - 626	TRSY	[pS/pT]XX[E/D/pS*/pY*]	Casein Kinase II substrate motif
625 - 627	SYR	[pS/pT]X[R/K]	PKA kinase substrate motif
625 - 627	SYR	[pS/pT]X[R/K]	PKC kinase substrate motif
625 - 628	SYRS	[pS/pT]XX[S/T]	Casein Kinase I substrate motif
625 - 628	SYRS	pSXX[E/pS*/pT*]	Casein Kinase II substrate motif
627 - 632	RSVGGGS	X[pS/pT]XXX[A/P/S/T]	G protein-coupled receptor kinase 1 substrate motif
628 - 632	SVGGGS	pSXXX[pS/pT]	MAPKAPK2 kinase substrate motif
628 - 632	SVGGGS	pSXXXpS*	GSK3 kinase substrate motif
632 - 637	SGGGSF	[pS/pT]XXX[S/T][M/L/V/I/F]	Casein Kinase I substrate motif
635 - 641	GSFGDNL	XpSXXDXX	Pyruvate dehydrogenase kinase substrate motif
636 - 639	SFGD	pSXX[E/D]	Casein kinase II substrate motif
636 - 639	SFGD	[pS/pT]XX[E/D]	Casein Kinase II substrate motif
636 - 639	SFGD	[pS/pT]XX[E/D/pS*/pY*]	Casein Kinase II substrate motif
636 - 639	SFGD	[pS/pT]XX[E/D]	Casein Kinase II substrate motif
643 - 646	TRSY	[pS/pT]XX[E/D/pS*/pY*]	Casein Kinase II substrate motif
650 - 653	NSSP	XXpSP	GSK-3, ERK1, ERK2, CDK5 substrate motif
650 - 655	NSSPRT	X[pS/pT]XXX[A/P/S/T]	G protein-coupled receptor kinase 1 substrate motif
651 - 653	SSP	X[pS/pT]P	GSK-3, ERK1, ERK2, CDK5 substrate motif
651 - 655	SSPRT	pSXXX[pS/pT]	MAPKAPK2 kinase substrate motif

Appendix C (Continued)

Position in Query Protein	Sequence in Query Protein	Corresponding Motif Described in the Literature (Phosphorylated Residues in Red)	Features of Motif Described in the Literature
652 - 653	SP	pSP	ERK1, ERK2 Kinase substrate motif
652 - 654	SPR	[pS/pT]P[R/K]	Growth associated histone H1 kinase substrate motif
652 - 654	SPR	[pS/pT]X[R/K]	PKA kinase substrate motif
652 - 654	SPR	[pS/pT]X[R/K]	PKC kinase substrate motif
652 - 655	SPRT	[pS/pT]XX[S/T]	Casein Kinase I substrate motif
652 - 655	SPRT	pSXX[E/pS*/pT*]	Casein Kinase II substrate motif
654 - 657	RTQS	RXXpS	Calmodulin-dependent protein kinase II substrate motif
654 - 657	RTQS	RXXpS	PKA kinase substrate motif
654 - 657	RTQS	RXX[pS/pT]	Calmodulin-dependent protein kinase II substrate motif
654 - 657	RTQS	[R/K]XX[pS/pT]	PKC kinase substrate motif
655 - 658	TQSP	XXpSP	GSK-3, ERK1, ERK2, CDK5 substrate motif
656 - 658	QSP	X[pS/pT]P	GSK-3, ERK1, ERK2, CDK5 substrate motif
657 - 658	SP	pSP	ERK1, ERK2 Kinase substrate motif

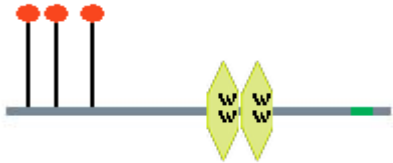




Absent in mature LA; Absent in del50/Progerin (in addition to all sequence absent from LA, except residues 657-661, which are absent from mature LA but present in del50/Progerin)

Appendix D. Supplemental Motif Analysis Data: HPRD Survey of Kinase-Dependent Protein Motif-Binding Sites in Lamin A Peptide Sequence


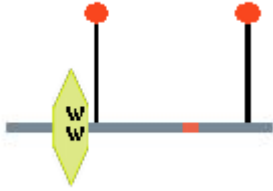
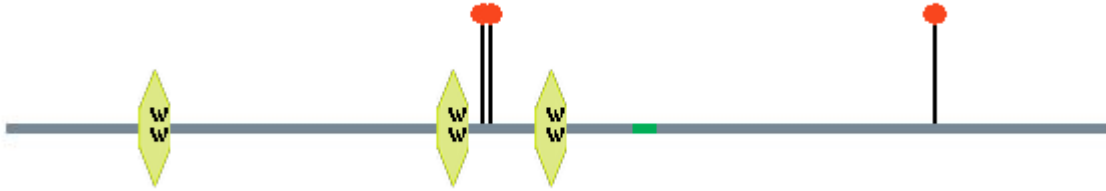


	Position in Query Protein	Sequence in Query Protein	Corresponding Motif Described in the Literature (Phosphorylated Residues in Red)	Features of Motif Described in the Literature
1	3 - 4	TP	[pS/pT]P	WW domain binding motif
2	17 - 19	SST	S[pS/pT]X	MDC1 BRCT domain binding motif
3	17 - 19	SST	S[pS/pT]X	Plk1 PBD domain binding motif
4	19 - 20	TP	[pS/pT]P	WW domain binding motif
5	22 - 23	SP	[pS/pT]P	WW domain binding motif
6	48 - 51	RVRS	RXXpS	14-3-3 domain binding motif
7	72 - 75	REVS	RXXpS	14-3-3 domain binding motif
8	149 - 151	STA	S[pS/pT]X	MDC1 BRCT domain binding motif
9	149 - 151	STA	S[pS/pT]X	Plk1 PBD domain binding motif
10	298 - 301	RIDS	RXXpS	14-3-3 domain binding motif
11	331 - 334	RDTs	RXXpS	14-3-3 domain binding motif
12	390 - 391	SP	[pS/pT]P	WW domain binding motif
13	392 - 393	SP	[pS/pT]P	WW domain binding motif
14	401 - 404	RASS	RXXpS	14-3-3 domain binding motif
15	403 - 405	SSH	S[pS/pT]X	MDC1 BRCT domain binding motif
16	403 - 405	SSH	S[pS/pT]X	Plk1 PBD domain binding motif
17	406 - 408	SSQ	S[pS/pT]X	MDC1 BRCT domain binding motif
18	406 - 408	SSQ	S[pS/pT]X	Plk1 PBD domain binding motif
19	423 - 425	STE	S[pS/pT]X	MDC1 BRCT domain binding motif
20	423 - 425	STE	S[pS/pT]X	Plk1 PBD domain binding motif
21	428 - 430	SSF	S[pS/pT]X	MDC1 BRCT domain binding motif
22	428 - 430	SSF	S[pS/pT]X	Plk1 PBD domain binding motif
23	455 - 458	RNKS	RXXpS	14-3-3 domain binding motif
24	507 - 508	SP	[pS/pT]P	WW domain binding motif
25	533 - 535	STG	S[pS/pT]X	MDC1 BRCT domain binding motif
26	533 - 535	STG	S[pS/pT]X	Plk1 PBD domain binding motif
27	571 - 573	SSS	S[pS/pT]X	MDC1 BRCT domain binding motif
28	571 - 573	SSS	S[pS/pT]X	Plk1 PBD domain binding motif
29	612 - 614	SSG	S[pS/pT]X	MDC1 BRCT domain binding motif
30	612 - 614	SSG	S[pS/pT]X	Plk1 PBD domain binding motif
31	615 - 617	SSA	S[pS/pT]X	MDC1 BRCT domain binding motif
32	615 - 617	SSA	S[pS/pT]X	Plk1 PBD domain binding motif
33	618 - 620	SSV	S[pS/pT]X	MDC1 BRCT domain binding motif
34	618 - 620	SSV	S[pS/pT]X	Plk1 PBD domain binding motif
35	651 - 653	SSP	S[pS/pT]X	MDC1 BRCT domain binding motif
36	651 - 653	SSP	S[pS/pT]X	Plk1 PBD domain binding motif
37	652 - 653	SP	[pS/pT]P	WW domain binding motif
38	654 - 657	RTQS		14-3-3 domain binding motif
39	657 - 658	SP	[pS/pT]P	WW domain binding motif

Absent in mature LA; Absent in del50/Progerin (in addition to all sequence absent from LA, except residues 657-661, which are absent from mature LA but present in del50/Progerin)




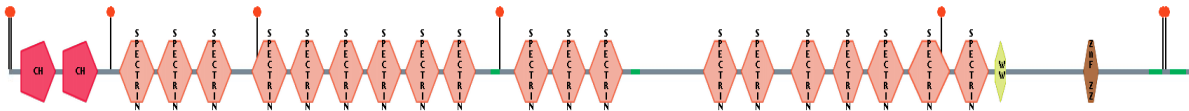

Appendix E. WW Domain-Containing Nuclear Proteins (HPRD)

1	<p>Name : WW domain containing protein, 45KD</p>  <p>Number of Interactions : 3</p>	<p>Molecule Function : Transcription regulator activity</p>
2	<p>Name : NEDD4</p>  <p>Number of Interactions : 37</p>	<p>Molecule Function : Ubiquitin-specific protease activity</p>
3	<p>Name : Amyloid beta A4 precursor protein binding family B, member 1</p>  <p>Number of Interactions : 16</p>	<p>Molecule Function : Receptor signaling complex scaffold activity</p>
4	<p>Name : Amyloid beta (A4) precursor protein binding family B member 3</p> <p>Number of Interactions : 3</p> 	<p>Molecule Function : Receptor signaling complex scaffold activity</p>
5	<p>Name : Pin1</p>  <p>Number of Interactions : 55</p>	<p>Molecule Function : Isomerase activity</p>

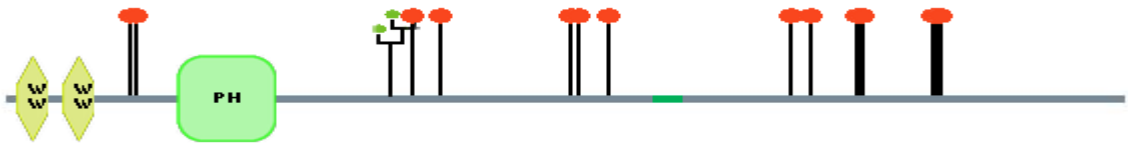
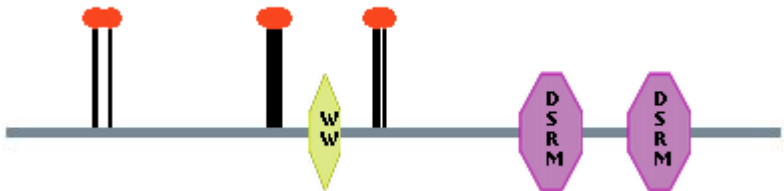
Appendix E (Continued)

6	Name : WW domain containing oxidoreductase	Molecule Function : Oxidoreductase activity
 <p>Number of Interactions : 7</p>		
7	Name : Polyglutamine binding protein 1	Molecule Function : Transcription regulator activity
 <p>Number of Interactions : 12</p>		
8	Name : Transcription elongation regulator 1	Molecule Function : Transcription factor activity
 <p>Number of Interactions : 25</p>		
9	Name : FNBP4	Molecule Function : Molecular function unknown
 <p>Number of Interactions : 6</p>		
10	Name : MAGI-3	Molecule Function : Molecular function unknown
 <p>Number of Interactions : 12</p>		

Appendix E (Continued)

11	Name : Smad ubiquitination regulatory factor 2	Molecule Function : Ubiquitin-specific protease activity
 <p>Number of Interactions : 66</p>		
12	Name : SMAD specific E3 ubiquitin protein ligase 1	Molecule Function : Ubiquitin-specific protease activity
 <p>Number of Interactions : 76</p>		
13	Name : DNA mismatch repair protein Mlh3	Molecule Function : Protein binding
 <p>Number of Interactions : 3</p>		
14	Name : Utrophin	Molecule Function : Cytoskeletal anchoring activity
 <p>Number of Interactions : 14</p>		
15	Name : WW domain containing protein 1	Molecule Function : Ubiquitin-specific protease activity
 <p>Number of Interactions : 20</p>		

Appendix E (Continued)

16	Name : PEPP2	Molecule Function : Receptor signaling complex scaffold activity
 <p>The diagram shows a horizontal grey bar representing the PEPP2 protein. From left to right, it features: two yellow diamond-shaped domains labeled 'W'; a green rounded rectangle labeled 'PH'; a cluster of three black vertical stems with red circular heads; a pair of black vertical stems with red circular heads; a small green segment; another pair of black vertical stems with red circular heads; and finally, two pairs of black vertical stems with red circular heads.</p>		
Number of Interactions : 2		
17	Name : DiGeorge syndrome critical region gene 8	Molecule Function : Molecular function unknown
 <p>The diagram shows a horizontal grey bar representing the protein. From left to right, it features: a pair of black vertical stems with red circular heads; a single black vertical stem with a red circular head; a yellow diamond-shaped domain labeled 'W'; another pair of black vertical stems with red circular heads; and two purple hexagonal domains labeled 'DSRM'.</p>		
Number of Interactions : 1		

VITA

CHRISTINA N. BRIDGES

Education: East Tennessee State University, J.H. Quillen College of Medicine, Johnson City, TN, Biomedical Sciences, Ph.D., 2012

Western Carolina University, Cullowhee, NC, Clinical Laboratory Sciences, B.S., Minor: Chemistry, *Magna Cum Laude* Honors, 1998

University of North Carolina-Asheville, Asheville, NC, Biology, Transfer Prerequisites, University Scholars Scholarship Program; Honors Program; Dean's List, 1992-1996

Professional

Experience: Staff Scientist; Coordinator: WNC Maternal Serum Screening Program, Fullerton Genetics Laboratory, Asheville, NC, 2011-Present

Molecular Genetics Technologist, Fullerton Genetics Laboratory, Asheville, NC, 2000-2011

Medical Technologist: Clinical Chemistry, Hematology, Serology, Mission Hospitals Laboratory, Asheville, NC, 1999-2002

Microbiologist/Parasitologist; Educational Program Coordinator, Genova Diagnostic Laboratories, Asheville, NC, 1997-2001

Professional

Certifications: Medical Laboratory Specialist/ Medical Technologist, American Society for Clinical Pathology, MLS/MT(ASCP)^{CM}, 1998

Clinical Laboratory Specialist: American Society for Clinical Pathology/National Credentialing Agency for Laboratory Personnel, Molecular Biology, MB(ASCP)^{CM}, CLSp(MB) (NCA), 2004

Abstracts/

Presentations: Kalman L, Leonard J, Gerry N, Tarleton J, **Bridges C**, Gastier-Foster JM, Pyatt RE, Stonerock E, Johnson M, Richards S, Schrijver I, Rangel Miller V, Adadevoh Y, Furlong P, Beiswanger C, and Toji L. "QUALITY ASSURANCE FOR DUCHENNE MUSCULAR DYSTROPHY GENETIC TESTING: DEVELOPMENT OF A GENOMIC DNA REFERENCE MATERIAL PANEL." Association for Molecular Pathology 2010 Annual Meeting, San Jose CA (November 17-20)

Kalman L, Toji L, Tarleton J, **Bridges C**, Gerry N, Beiswanger C, Gastier-Foster J, and Leonard J. "QUALITY ASSURANCE FOR DUCHENNE MUSCULAR DYSTROPHY GENETIC TESTING: FIRST STEPS IN THE DEVELOPMENT OF A GENOMIC DNA REFERENCE MATERIAL PANEL." American College of Medical Genetics 2010 Annual Clinical Genetics Meeting Honolulu, HI (March 26-30, 2010)

Bridges C, Sinensky M, Lerner L, Rusiñol A. "PRELAMIN A AFFECTS DIFFERENTIAL GENE EXPRESSION AND REGULATION OF CELL CYCLE." 2009 Appalachian Student Research Forum, Johnson City TN (April, 2009)

Kalman L, Buller A, Caggana M, Highsmith WE, Rohlf EM, Tarleton J, **Bridges C**, Toji L, Barker S, Pratt VM. "DEVELOPMENT OF GENOMIC DNA REFERENCE MATERIALS FOR CYSTIC FIBROSIS GENETIC TESTING." Association for Molecular Pathology 2008 Annual Meeting, Grapevine, TX (October 29-November 2, 2008) **AND** American College of Medical Genetics 2009 Annual Clinical Genetics Meeting Tampa, Florida (March 25-29, 2009)

Sinensky M, Rusiñol A, **Bridges C**, "REGULATION OF PRELAMIN A ACCUMULATION BY THE ZMPSTE24 ENDOPROTEASE DURING CELLULAR QUIESCENCE." American Society of Cell Biology Annual Meeting, San Francisco, CA (December 13-17, 2008).

Bridges, C & Rusiñol, A. "COMPARISON OF THE ACTIVITY AND EXPRESSION OF THE ZMPSTE24 ENDOPROTEASE IN CELLULAR QUIESCENCE." 2008 Appalachian Student Research Forum, Johnson City, TN (April-2-3, 2008).

Publications: Pratt VM, Caggana M, **Bridges C**, Buller AM, DiAntonio L, Highsmith WE, Holtegaard LM, Muralidharan K, Rohlf EM, Tarleton J, Toji L, Barker SD, Kalman LV. Development of Genomic Reference Materials for Cystic Fibrosis Genetic Testing. The Journal of Molecular Diagnostics. May 2009;11(3)

Kalman L, Leonard J, Gerry N, Tarleton J, **Bridges C**, Gastier-Foster JM, Pyatt RE, Stonerock E, Johnson M, Richards S, Schrijver I, Ma T, Rangel Miller V, Adadevoh Y, Furlong P, Beiswanger C, and Toji L. Quality Assurance for Duchenne and Becker Muscular Dystrophy Genetic Testing: Development of a genomic DNA reference material panel, Journal of Molecular Diagnostics, March, 2011;13(2).

Manuscripts

in Progress: Bridges CN, Sinensky MS, Lerner, LR, Rusiñol AR. "Prelamin A regulates a program of gene expression in cell cycle control" (running title), Bridges CN, Rusiñol AR. Pin 1 prolyl isomerase mediates Lamin A isoform-specific regulation of cell cycle progression (running title).

Bridges CN, Rusiñol AR. Histone modification involving variant H2A.Z is a mechanism for Prelamin A cell cycle regulatory control (running title).

Professional Affiliations/

Society Memberships: American Association of Bioanalysts (AAB); American Society for Clinical Pathology (ASCP); American Society of Human Genetics (ASHG); Association of Genetic Technologists (AGT); American Association for the Advancement of Science (AAAS); International Society for Advancement of Cytometry (ISAC); Clinical Cytometry Society (CCS); American Society for Investigative Pathology (ASIP); American Association for Clinical Chemistry (AACC); Association for Molecular Pathology (AMP)